CALIBRATION OF ORIFICE PLATES WITH SPECIAL EMPHASIS ON EDGE SHARPNESS AND ECCENTRICITY

I. LEBI

SEPTEMBER 1979

Submitted to the University of Cape Town in fulfilment for the degree of Master of Science in Engineering.

The University of Cape Town has been given the right to reproduce this thesis in whole or in part. Copyright is held by the author.

University of Cape Town

The copyright of this thesis vests in the author. No quotation from it or information derived from it is to be published without full acknowledgement of the source. The thesis is to be used for private study or non-commercial research purposes only.

Published by the University of Cape Town (UCT) in terms of the non-exclusive license granted to UCT by the author.

University of Cape Town

ABSTRACT

A general review of the literature pertaining to flow measurement with orifice plates is presented. Special emphasis is laid on the factors influencing the coefficient of discharge of orifice plates and on the difference between the various engineering standards. Particular consideration is given to the effect on the discharge coefficient of rounding the upstream edge of the orifice plate and of changes in plate eccentricity. Various methods to calibrate orifice plates and to measure the edge roundness of orifice plates are discussed.

Orifice plates with area ratios ranging from 0,1 to 0,55 were tested in order to evaluate variations in the coefficient of discharge with changes in:

a) the upstream edge radius;
b) the plate concenctricity.

The calibration tests were conducted with apparatus based on a system of weighing the working fluid which accumulates in a tank over an accurately determined time interval. In order to measure the upstream edge radius of an orifice plate, a lead foil holder was designed. Using the holder, accurate imprints of the edge profile were obtained in the lead foil.

The apparatus used and the method of calibration is described in detail. Attention is drawn to the precautions required for accurate calibration. The method of calibration used was complicated by fluctuations in the differential pressure. It was found that the mean of twelve randon pressure differential readings at a specific flow rate did not vary by more than $\pm$ 0,05 mm of mercury. Increasing the number of pressure

readings taken did not improve upon the accuracy of the calculated mean pressure reading.

When the validity of the results are considered the following factors must be remembered:

a) The calibrations were performed in a pipe of 100 mm diameter.
b) The repeatability of the upstream edge radius measurement is between $\pm$ 2 and $\pm$ 5 per cent depending on the edge radius.

The results indicate that an increase in the coefficient of discharge of up to 0,5 per cent arises due to a change in the position of the upstream pressure tapping from D to D + 0,035D and of the downstream pressure from D/2- 0,02D to D/2 + 0,047D. This shows that the tolerance quoted in the British Standard for the positioning of the D and D/2 tappings is to high for accurate flow measurement.

The coefficient of discharge obtained for the sharp edged concentric orifice plates were compared with the various engineering standards. The comparison showed that the experimentally determined coefficients were within the tolerance limit quoted by the British standard but some were outside the tolerance limits of ASME and I.S.O. If the correction factor determined in this thesis for orifice plates whose edge sharpness is not 0,0004 is applied to the coefficients of discharge of the orifice plates tested, then an improvement in agreement with the various standards results.

The author's results showed that the coefficient of discharge of square edged orifice plates did not remain constant at high Reynolds numbers. Thus they agreed with the specifications of ASME and not with those of the British Standard.

The results indicate that the coefficient of discharge is dependent on the sharpness ratio and on the area ratio of an

orifice plate. The discharge coefficient of the orifice plate with an area ratio of 0,1 was more affected by changes in the sharpness ratio than that of the other plates.

The experimental results for effect of edge sharpness were compared with Herning's result. Agreement to within 0,2 per cent was found. From Hernings and the authors results correction curves for effect of edge sharpness were deduced.

The author recommends the use of three different correction curves: one for orifice plates with sharpness ratios varying between 0,0002 and 0,0006; one for orifice plates with sharpness ratios larger than 0,0006 and area ratios greater than 0,2; and one for orifice plates with sharpness ratios greater than 0,0006 and area ratios less than 0,2.

The results showed increasing or decreasing the sharpness ratio of an orifice plate above or below 0,0004 caused a corresponding increase or decrease in the value of the discharge coefficient. It was found that small changes in the upstream edge radius of an orifice plate caused considerable changes in the value of the discharge coefficient. The specifications of ASME and ISO for the upstream edge sharpness of an orifice plate proved to be completely inadequate.

The specifications of both the German and the British Standards were satisfactory only if errors in the coefficient of discharge of $\pm$ 0,5 per cent were acceptable.

It was found that the change in the coefficient of discharge was a function of eccentricity and of the area ratio. The relationship between the coefficient of discharge and the eccentricity ratio can be expressed by an equation of the following form:

$$C_D = A\, e^{(E/D-d)B}$$

The larger the area ratio of an orifice plate the larger is the effect of eccentricity. Adherence to the specifications for maximum allowable eccentricity as given by the various engineering standards, was found not to cause such an error in the value of the specified coefficients that they would lie outside their tolerance limits. It was also found that improvement in the accuracy of the standard coefficients would result if the specifications for maximum allowable eccentricity would be given by equation 2

$$\frac{100\,E}{D-d} < 3{,}55 - 1{,}69\,m \quad \ldots\ldots 2$$

If the specifications of equation 2 are used then the maximum error in the coefficient of discharge due to eccentricity will be less than 0,1 per cent.

The specifications of the British standard and AGA concerning eccentricity of an orifice plate are not as stringent as those given by this equation, although the ISO specifications compare well with the experimental findings.
The data obtained for the effect of eccentric location correlates well with results obtained by other researchers in this field. Further research is required to prove conclusively the validity of equation 1 and 2.

ACKNOWLEDGEMENTS

The author wishes to express his thanks and appreciation to

1) Professor R.K. Dutkiewicz for his active interest, guidance and advice.

2) The academic and workshop staff of the Mechanical Engineering Department of the University of Cape Town for their advice and assistance in building the experimental equipment.

3) The Council for Scientific and Industrial Research, Pretoria for their financial assistance.

4) All others who made the completion of this thesis possible.

Finally, the author wishes to thank his family for their moral and financial support.

CONTENTS

APPENDIX

LIST OF FIGURES

LIST OF TABLES

NOMENCLATURE

		Units
a	Pipe radius	metres
a_o	radius at point o.	metres
C_c	Contraction coefficient	
C_D	Coefficient of discharge	
C_v	Velocity coefficient	
d	orifice diameter	metres
D	pipe diameter	metres
e	thickness of the orifice edge	millimetres
E	eccentricity of the orifice plate	metres
F	eccentricity of the orifice plate/ pipe diameter	
h	pressure difference	millimetres of water
K	overall coefficient of discharge	
l	distance from upstream face of the orifice plate to the centre of the pressure tappings	metres
L	straight length of pipe before and after the orifice plate	metres
m	area ratio $\left(\frac{d}{D}\right)^2$	
M	eccentricity ratio $\frac{E}{D-d}$	
P_1	pressure at the upstream tap	millimetre of water
P_2	pressure at the downstream tap	millimetre of water

q	mass rate of flow	kilograms
r	upstream edge radius of the orifice plate	millimetre
Re_d	Reynolds number based on the orifice diameter	
Re_D	Reynolds number based on the pipe diameter	
t	thickness of the orifice plate	millimetre
V_1	velocity of the water at the upstream tap	millimetres
V_2	velocity of the water at the down-stream tap	millimetres
u	velocity at a point	millimetres
U	average velocity	millimetres
Y	coefficient of expansion	
$\bar{\alpha}$	coefficient of friction	
β	diameter ratio	
η	coefficient of size	
λ	lamda friction factor	
μ	dynamic viscosity	
$\bar{\mu}$	coefficient of contraction	
ρ	density of the fluid	kilograms/ cubic metre

GLOSSARY

Area ratio - The ratio obtained by dividing the area of the orifice by the area of the pipe.

Coefficient of discharge - An empirical factor obtained by dividing the actual mass rate of flow by the theoretical mass rate of flow.

Diameter ratio - The ratio obtained by dividing the orifice diameter by the pipe diameter.

Eccentricity ratio - The ratio obtained by dividing the eccentricity of an orifice plate by the difference between the pipe diameter and the orifice diameter.

Fully eccentric orifice plate - An orifice plate which is so positioned that one side of the circular opening is flush with the inside wall of the pipe.

An oversharp orifice plate - An orifice plate whose sharpness ratio is less than 0,0004.

Sharpness ratio - The ratio obtained by dividing the upstream edge radius of an orifice plate by the orifice diameter.

CHAPTER ONE

INTRODUCTION

1.1 BRIEF HISTORY OF ORIFICE METERING

It is known that man has been metering water by some means or another since ancient times. The first record of orifice plate usage appears in a book written by Lentus Frontinus the Water Commissioner of Rome. In his book entitled "De Aquaeductu Urbis Romae" he describes a comprehensive system of water metering employed during the first century A.D. (1).

Towards the end of the 19th century Professor Robinson of the Ohio State University designed an orifice meter which was used to measure the flow rate of gas (2). Later in 1903 Thomas R. Weymouth (3) performed experiments with square edged, concentric orifice plates. He used the results of these experiments to determine empirical coefficients which he correlated with the ratio of the orifice diameter to the pipe diameter. His experiments were performed with flange taps. In 1913 Hickstein (4) conducted similar tests from which he developed empirical coefficients for orifice plates with pipe taps. Professor Horace Judd (5) presented a paper at a meeting of A.S.M.E. in 1916 on the use of orifice plates with Vena Contracta taps.

Beitler (6&7) did much research on orifice plates between 1924 - 1935. The results of his work formed the basis of the joint A.S.M.E. and A.G.A. report (8) of 1935 which itself forms the basis of the A.S.M.E. (9, 10, 11) and A.G.A. (12,13,14) standards. The work of R. Witte (15, 16, 17) was adopted by I.S.A. (18, 19, 20) and D.I.N. (21, 22). Although these standards are continually being revised, the basic orifice design remains that of these two researchers. To widen the use of orifice plates, researchers designed special type of orifice plates. In 1916 Judd published

his findings on tests conducted with eccentric orifice plates. Later he initiated research into segmental orifice plates. Masson (23) continued with work in this field. Today the American Standards give actual values for the coefficients of discharge of these plates. The use of a semicircular edged orifice plate was first suggested by Professor Smidt. In 1933 Giese (24) tested quadrant edge orifice plates while later Koennecke (25 & 26) recommended values for the ratio of the edge-radius to the pipe diameter (r/d) to be used for these plates. Recently tests by Ramamoorthy and Seetharamiah (27 & 28) have shown that these plates can be used in the range of Reynolds numbers from 20 000 to 600 000. To improve on the sensitivity of the orifice plate to disturbances in the upstream flow conditions, the Royal Aircraft Establishment investigated the use of annular orifices. Howell (29) found that these plates are less sensitive to swirl and other upstream flow conditions than the sharp square edged orifice plate.

In industry today the orifice plate is the most common flow measuring device. Spencer (30) found that orifice plates are used more often than any other flow meter in Great Britain while Caldwell (31) states that most high pressure, large volume gas streams within the United States are measured with orifice meters. In the petroleum industry approximately 90% of all flow measurement is done with orifice plates. The quantities of fluid measured to day are high and therefore high accuracies in measurement are required. For example a petroleum plant pumps as much as thirty million cubic meters of fuel a day into tankers and here a 1% error is equivalent to 300 000 cubic meters (32) while in the natural gas transmission industry 1% of annual sales amounts to ten million dollars (33). Similarly in large power stations because of the quantities involved errors of 1% are considered unacceptable.

Since orifice plates are so widely used and because higher accuracies are continually required, research into orifice plates is continually taking place especially with respect to factors affecting their coefficients of discharge. These factors are discussed in Chapter 2.

1.2 THE ORIFICE PLATE

The orifice plate is a pressure differential device used for measuring the flow rate of a fluid in a closed conduit. It consists of a thin flat plate containing a circular hole as shown in figure 1. The plate is usually clamped between flanges at a joint in the pipeline. The plane is perpendicular to the axis of the pipe and the hole is concentric with the pipe. The upstream edge of the plate is square as this ensures complete contraction of the fluid stream within the orifice. The cylindrical entrance piece (e) is kept short so as to maintain jet stability and to avoid re-attachment of the jet. The bevel angle is there to ensure that no interference takes place with the natural expansion of the jet in the downstream vicinity of the orifice plate.

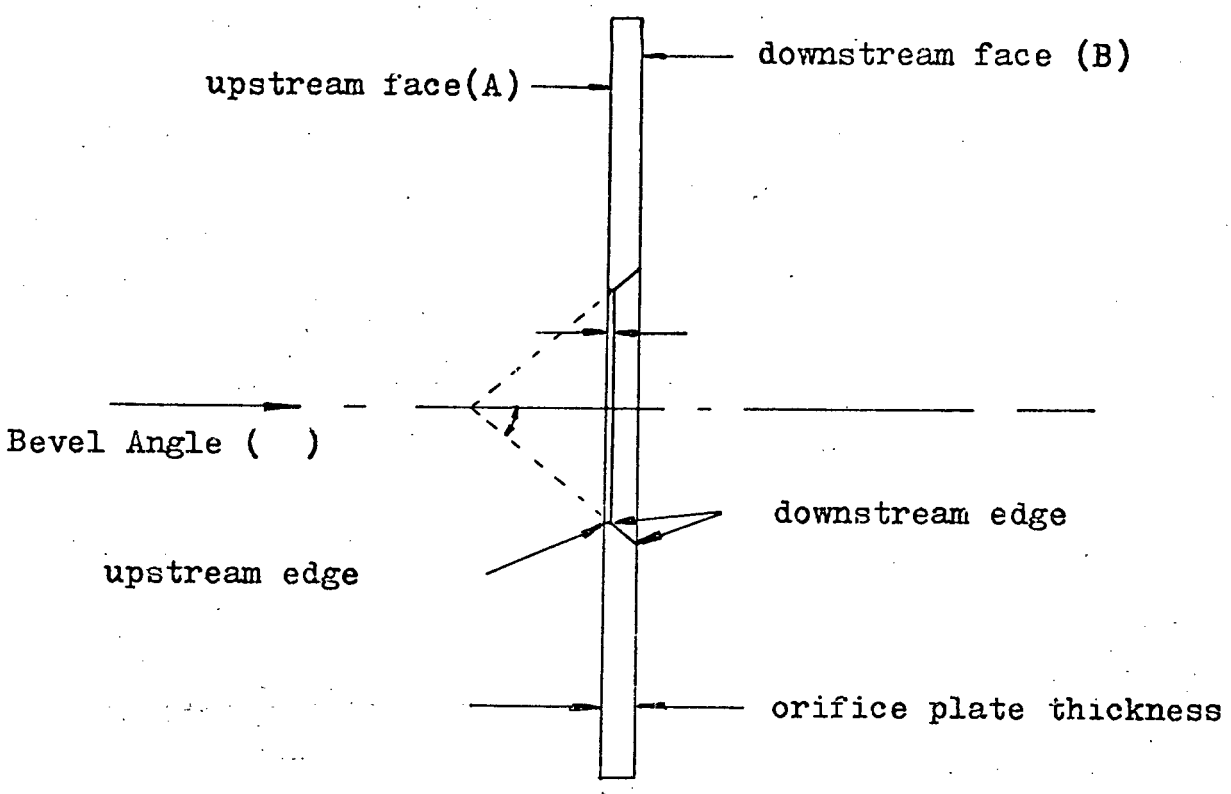

Figure 1. A standard orifice plate.

From the above discription it is evident that the orifice plate is a very simple device. It creates a change in the static pressure while the fluid passes through it and this change in pressure is proportional to the flow rate. Often in industry the manometer or the pressure measuring device is calibrated directly in flow units

A review of the the advantages of the orifice plates illustrates why they are so commonly used. It's advantages are:-

1. No moving parts.
2. Simple to construct.
3. Cheap to manufacture, install, operate and maintain.
4. Highly accurate with good repeatability.
5. Able to effect a highly localized pressure drop with a small overall throttling effect.
6. Reasonably insensitive to viscosity changes over a large range of flow rates.
7. Usually installed with the pressure tappings in close proximity to the meter. Thus errors due to temperature variations are minimised.

It's main disadvantages with respect to other flow meters are:-

1. Relatively high pressure loss.
2. Can not be used with any certainty for flows where the throat Reynolds number is below 10 000 or above 10 000 000 although with slight modifications it can be used outside this range. (34).
3. Most affected by upstream flow conditions.

To ensure high accuracy, engineering standards have been published which stipulate installation and metering conditions. Since the orifice plate is so sensitive to upstream flow conditions the overall accuracy which can be expected if the plate is installed to any of the engineering standards is only in the order of $\pm$ 1.5 percent. If the orifice plate is calibrated an accuracy of $\pm$ 0,1 percent can be achieved.

1.3 ENGINEERING STANDARDS AND CODES RELATING TO FLOW MEASUREMENT WITH ORIFICE PLATES

To avoid the necessity of calibrating every orifice plate, standards on flow measurement have been drawn up by various engineering bodies. In the standards details are specified regarding the design, the manfacture and the precautions to be adopted in the installation and use of orifice plates.

If the standard specifications are adhered to, then the specified coefficients are applicable. The calculated flowrate corrected by using the relevant equations and coefficient is correct within certain tolerance limits. Those limits as given by A.S.M.E., I.S.O. and the British standards are reproduced in Table 2. In the I.S.O. code the tolerance limit is expressed in equation form for corner tapped orifice plates.

These tolerance limits only apply if the value of the pipe diameter, diameter ratio and Reynolds number are accurately known.

The flow codes most frequently referred to in practice are:-

1. The British Standards BS 1042:1964.
2. The American Society of Mechanical Engineers, ASME flow code.
3. The German DIN code.
4. The International Standard Organisation, ISO Recommendations.
5. The American Gas Association, AGA Report.

A small difference in the value of the calculated flowrate results if the specifications given by the various codes are used for the

TABLE 1

Basic measuring tolerances as given by the various standards

TYPE OF ORIFICE	FLUID METERS (ASME)	ISO	B.S. 1042:1964
CORNER TAPPED	$D \geq 50$ $0{,}70 \geq \beta \geq 0{,}20$ $R_D \geq 7000D$	Tolerance $= \pm 0{,}25 \times \left\| 1 + 2\beta^4 + 100\,(r_{Re} - 1) + \beta^2\,(\log Re_D - 6)^2 + \frac{50}{D} \right\|$	$D \geq 50$ $0{,}5 \geq m \geq 0$ $R_d \geq 20\,000$
	Tolerance +/- 0,55 %		Tolerance = +/- 0,50%
D & D/2	$D \geq 50$ $0{,}70 \geq \beta \geq 0{,}20$ $R_D \geq 4000D$	Vena Contracta taps $0{,}7 \geq \beta \geq 0{,}2$ $6000 \leq Re_D \leq 10^7$	$D \geq 50$ $0 \geq 40\ m \geq 0{,}05$ $R_d \geq 20{,}000$
	Tolerance = +/- 0,50%	Tolerance = +/- 0,25%	Tolerance = +/- 0,75%
Flange Taps		$D \geq 50$ $0{,}7 \geq \beta \geq 0{,}2$ $8000 \leq Re_d \leq 10^7$	$D \geq 50$ $0{,}48 \geq m \geq 0.04$ $10 \geq R_d \geq 100{,}000$
	Not Specified	Tolerance = +/- 0,30%	Tolerance = +/- 0,6%

NOTE: In ASME for references of R_D, x.D, D is measured in inches and x is any number

calculations, The resultant variation is due to minor differences between the standards. These differences therefore require further discussion.

1.3.1 The Difference between the Standard Specifications

The difference in specifications regarding the design of the orifice plate, the precautions regarding installation and the effect of Reynolds number on the coefficient of discharge are discussed.

1.3.1.1 The Design of the Orifice Plate (Figure 2)

The specifications relating to the design, the size and the shape of an orifice plate are given in Table 2. From Table 2 it is evident that real differences exist in the specifications of the different codes regarding the shape, size and surface finish of an orifice plate. A discussion on some of these follows.

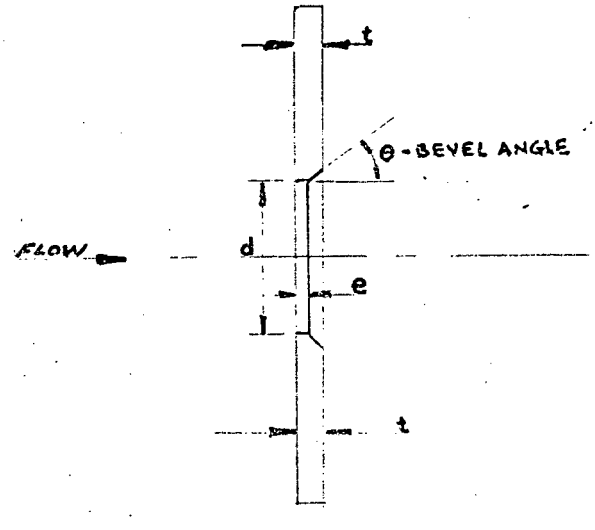

Fig.2 . A Square-edged Orifice Plate

a) Edge sharpness. The edge sharpness of an orifice plate affects the flow conditions and this affects the value of the coefficient of discharge and that of the calculated flowrate. The definition of the edge sharpness given by the ASME and ISO codes is vague. The British Standard and the DIN code specify the maximum edge radius. The minimum edge radius is not specified by any of the codes. The following questions regarding the edge sharpness of an orifice plate need to be answered:

1. At what value of the edge radius is the standard coefficient correct?
2. Does a relationship exist between the edge sharpness and the coefficient of discharge and, if so, how are they related?
3. If the edge is sharper than specified by the British Standard, what is the effect on the coefficient?

b) Thickness. The thickness of the orifice plate (t) and of its upstream edge (e) is not fully specified by some of the codes. The British Standard does not specify the minimum allowable thickness for an orifice plate, while the ASME and AGA codes do not specify the maximum allowable.

For practical purposes the advice of T.H.Redding (36) should be followed. He states: "The criterion governing the minimum orifice-plate thickness is that it should be sufficient to withstand, without distortion, any difference in pressure that may be established between its faces, including any transient pressure difference due to water hammer or other cause of surging pressure. The maximum plate thickness must not, however, be so great as to affect the flow pattern in the upstream and downstream proximity of the orifice which contain the various pressure tappings". He suggests that the minimum thickness used should be that given by ASME & AGA while the maximum thickness should be equal to that specified by ISO & B.S. 1042.

c) Orifice Edge Thickness. The latest ISO code (37) specifies both the minimum and maximum value of the orifice edge thickness (e) and that of the orifice plate (t).

d) Bevel Angle. The bevel angle is specified by ASME & AGA as equal to 45 degrees while the British and ISO standards allow this angle to vary between 30 and 45 degrees.

e) Circularity. The ASME and AGA standards do not specify circularity of the orifice bore and the extent to which the bore has to be parallel. There is a difference of 0,05% between the specification given by ISO and by the British Standards concerning the circularity of the orifice bore of an orifice plate with diameter ratios less than 0,67.

f) Surface Finish. The surface finish of the upstream face of the orifice plate is fully specified by BS 1042, while the other standards simply specify a finish as good as that of good commercial rolled stock.

Any difference in shape, size and surface finish results in a change in the flow conditions, thereby affecting the pressure difference readings which in turn affect the accuracy of the calculated flow rate.

1.3.1.2 Installation of the Orifice Plate

a) Straight length of approach piping required

Most of the errors attributed to inadequate straight length of approach piping are a result of swirl, eddying and vortices. The errors caused can be considerable and therefore the minimum approach length is of

TABLE 2

The specifications of the various engineering standards regarding the design of orifice plates

ITEM OF INTEREST	ASME	ISO	B.S.
ORIFICE PLATE THICKNESS (t)	No maximum limit is specified for D < 100 t > 1,7 for 0 < D < 100 3 < t < 6 for D > 100	0,05D > t ≥ e The values of "t" should not differ among themselves by more than 0,005D	t < 0, 1D for β ≤ 0,67 t < 0, 05D for β>0,67
ORIFICE EDGE THICKNESS (e)	e < 1/30 D e < 1/8 d e < $\frac{D-d}{8}$ The lowest value obtained should be used	0,005D≤e≤0,02D If β≤0,2 then 0,005D≤e≤0,1d If β> 0,7 then e/t≃1/3 The values of "e" should not differ among themselves by more than 0,001D	e < 0,1d for β ≤ 0,2 e < 0,02D for β > 0,2
BEVEL ANGLE (θ)	If t > e then θ - 45 If t = e then θ = 0°	If t > e then 30°<θ< 45° If t ≤ 0,02D then θ = 0°	If t > e then 30°<θ<45° If t≤ θ_e, then 45° = 0°
DIAMETER OF ORIFICE (d)	If D < 38 then 0,7 >ρ> 0,25 If 50>D738 then 0,8>ρ>0,20	0,1D < d < 0,8D	If D<50 then 6<d<0,707D If D>50 then d<0,837D.
THE UPSTREAM EDGE	It must be sharp. It is considered sharp if, when viewed with the naked eye it does not seem to reflect a beam of light		r/d < 0,0004

TABLE 2 (Continued)

ITEM OF INTEREST	ASME	ISO	B.S.
CIRCULARITY OF THE ORIFICE	Must be circular	It must be circular so that: $d = d +/- 0,0005d$	Circular at the upstream face so that: If $\beta < 0,67$, $d = d +/- 0,001d$ If $\beta > 0,67$. $d = d +/- 0,0005d$
BORE OF THE ORIFICE	It must be perpendicular to the upstream face of the orifice plate.		It must be parallel within $0,5^{o}$
FLATNESS AND SMOOTHNESS OF THE UPSTREAM FACE A	It shall be flat over a circle of diameter, D. concentric with the orifice such that if any two points are joined by a straight line the perpendicular distance between plate and straight line shall not be greater than one per cent of distance between the points.		
	The upstream face should be at least as smooth as good commercial rolled stock.	It should be smooth to within 0,0003d (peak-to-hollow height) within a circle whose diameter is not less than 1,5d	If $m \leq 0,67$ then the upstream face A should be smooth to within 0,0003 d (peak-to-hollow height) within a circle whose diameter is not less than 1,5d while if $\beta > 0,67$ than within a circle of diameter not less than 1,0d
DOWNSTREAM FACE OF THE ORIFICE PLATE	No specifications given	It shall be flat and parallel with the upstream face. The downstream face does not	No restrictions on flatness and roughness. Must be parallel to the upstream face to within $0,5^{o}$.

TABLE 2 (continued)

DOWNSTREAM FACE OF THE ORIFICE PLATE (Continued)		have to have the same quality surface finish as the upstream face. The flatness and surface conditions are judged by visual inspection.	

importance for accurate measurement. Comparing the minimum approach lengths as specified by the different national standards shows large differences (Fig. 3, 4, 5, 6). For example: The difference in the approach length after one 90 degree elbow as specified by ISO and by ASME for anorifice plate with a diameter ratio of 0,6 is over 100%. (ISO, 18 pipe diameters; ASME 8 pipe diameters). In all cases the straight length of approach piping required for measurement of flow with a small diameter ratio orifice plate is considerably less than for orifice plates with large diameter ratios.

b) The use of flow straighteners

In many commercial installations it is not possible to use the stipulated straight length of approach piping and therefore flow straighteners are introduced.

The various engineering standards differ in their recommendations relating to the use of flow straighteners. Both the American standards (ASME & AGA) allow for their use, while the British standard is non-committal and the German one is against their utilisation.

The British standard recommends the use of two or three perforated plates spaced one pipe diameter apart, rather than flow straighteners of the honeycomb or nest type. If any flow straightener is used, it is recommended that a minimum of 10 pipe diameters of straight approach piping is used.

c) The condition of the upstream and downstream piping (Table3)

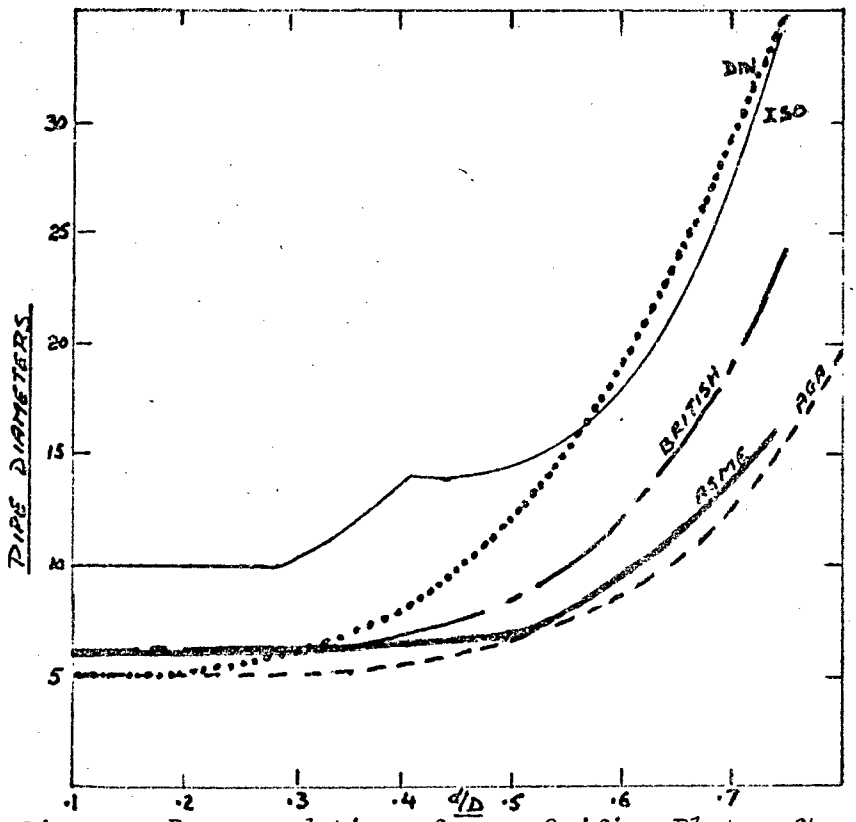

Fig. 3
Installation Distance Recommendations for an Orifice Plate after a 90° Elbow

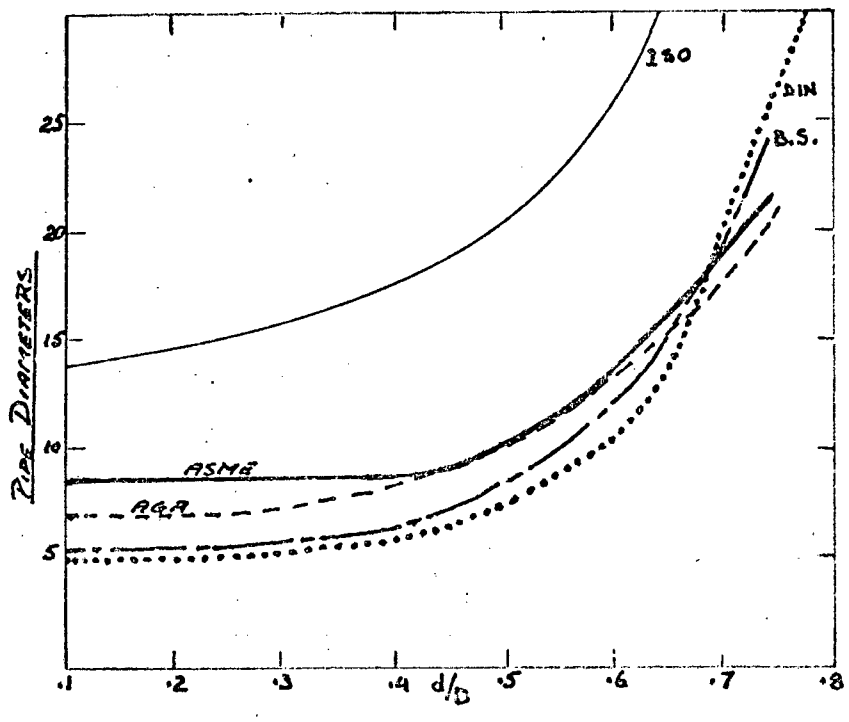

Fig. 4
Installation Distance Recommendations for an Orifice Plate after Two 90 Degree Elbows in Same Plane

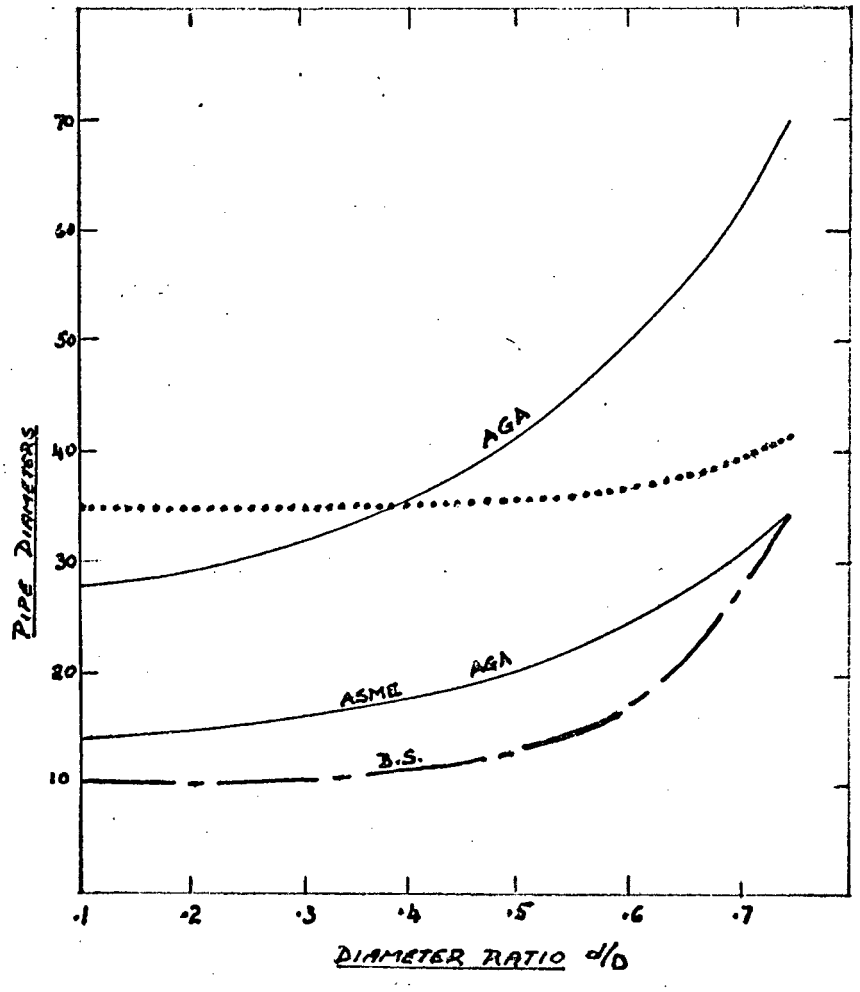

Fig. 5 *Spacing Recommendations for an Orifice Plate After Three 90 Degree Elbows in Two Planes*

Note: *Upper A.G.A. curve, when first two are in different planes.*

Lower A.G.A. curve, when first two are in same plane

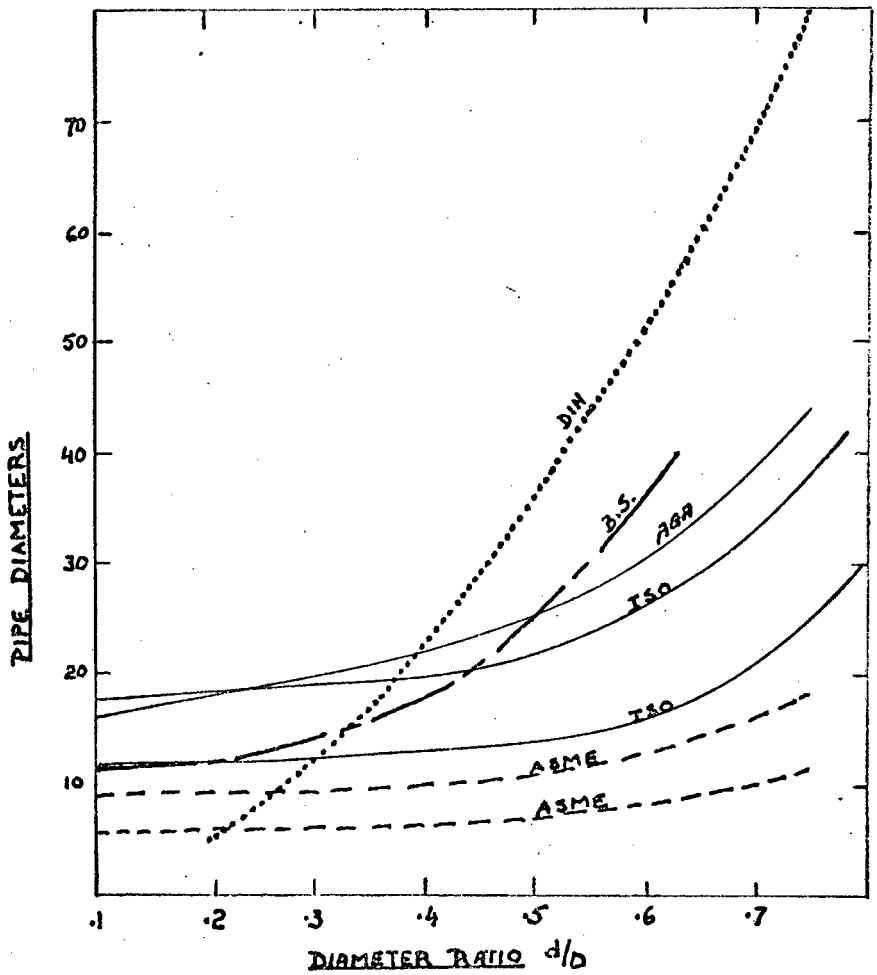

Fig. 6 Spacing Recommendations for an Orifice Plate After a Valve.

Note: Upper A.S.M.E. & I.S O. curve for a globe valve.

Lower A.S.M.E. & I.S.O. curve for a gate valve.

TABLE 3

The specifications of ISO and of the British Standards regarding the condition of upstream and downstream piping.

ITEM OF INTEREST	ISO	BS(1042)
Surface and condition of approach piping	Inside surface must be clean, free from pitting and deposit and not encrusted. Factors for different surface finished pipes is given	Correction factors are given for various size pipes made from various materials
+ lower limit for pipe size	Dmin = 50mm	25mm for all tapings except for a flange taping for which Dmin = 50mm
+ upper limit for pipe size	Dmax = 750mm	no upper limit
Pipe circularity	D - D +/- 0,003D for L > 2D. It is considered circular if it appears so by mere visual inspection.	If L < 2D then $D = D +/- \left[\frac{2(1-m)}{100}\right] D$
Protrusions into the pipe	No protrusions, obstructions or branch corrections	If L < 2D no projections into upstream pipe allowed. If L > 2D then the projection length is given by $\frac{(1-m)(2,5L/D-4)D}{100}$
Thermometer Pocket	It should be placed at least 5D after plate (downstream). If it is placed upstream then it is the same as for B.S. (1042)	Pocket diameter is $\leq$ 0,03D if 20D < L > 5D and 0,13D if L > 20D
Downstream Pipe	Same diameter as the upstream pipeline within +/- 2%.	No fittings installed at a distance less than 3 pipe diameters.

+ NOTE - Upper and lower limits of pipe sizes are imposed by the availability of data and does not imply an inherent limitation on the lower and upper limit of pipe size for the different types of orifices.

Small differences exist between these specifications. The British standards are more specific in their requirements.

* It is interesting to note that the standards do not specify a specific surface finish to the upstream pipe just before the orifice plate. Work done by Clark and other researchers (see Chapter 2) has shown that the surface roughness of the upstream pipe just before the orifice plate affects the coefficient of discharge and thereby the accuracy of the flow measurement.

d) Concentricity of orifice plate axis with that of the pipe

The orifice plate has to be concentric with the pipe. The maximum distance (eccentricity) between the axis of the orifice plate and that of the pipe is specified by the standards (see Table 4).

TABLE 4

Specifications of the standards regarding the maximum allowable eccentricity of an orifice plate

Standard			
ASME	AGA	BS	ISO
0,8 mm	0,03D	$\pm 0{,}005(1-\beta)D$	$0{,}015D(\frac{1}{\beta}-1)$

The difference in the allowable eccentricity according to the various standards is great. For example if in a one hundred millimetre pipe line an orifice plate with diameter ratio of 0,5 is installed, then according to AGA a three millimetre eccentricity is allowed; while

according to BS 1042, the maximum eccentricity should not exceed 0,25 millimeters.

e) Squareness of the plate

The British standards and the ISO codes stipulate that the upstream face of the plate must be perpendicular to the axis of the pipe within two percent and one percent respectively.

f) Gasket size.

The gasket inner diameter on either side of the orifice plate must be greater than the pipe diameter. The above statement can be found in both the British and the ISO standards. The British standard qualifies the above statement further by specifying the maximum size of the inner diameter of the gasket to be less than 3 per cent greater than the pipe diameter.

g) The pressure taps

The specifications regarding condition, size and shape of the pressure tap holes are given in Table 5 below. It can be seen that very small differences exist in the specifications regarding the size, shape and conditions of pressure taps with the exception of ASME which allows for the use of larger diameter pressure tap holes.

TABLE 5

The Specifications regarding the shape, size, finish and location of the pressure taps.

Sphere	ASME	ISO	BS 1042
Type of tap	Single or multiple taps may be used		
Location of pressure taps	The location of the taps is dependent on the choice of tappings.(i.e.flange taps, vena contracta taps, etc.		
diameter of pressure holes, "δ"	D<50;9,5>δ>3,2 75>D>50;12,7>δ>6,4 200>D>100;19,0>δ>9,5 D>250;25,4>δ>12,7	$\delta \leq 0,8D$ and preferably between 6 & 12 mm.	$\delta \leq 0,1D$ No restriction is placed on the minimum diameter but it must be kept large enough for no accidental blockage of these holes.
		The upstream and downstream taps must have the same diameters.	
* Minimum length of pressure taps	No change in tap hole diameter for a distance of at least 2,5 times the hole diameter, as measured from the inner surface of the pipe. A distance of 3δ to 5δ is recommended if possible	No change in pressure tap diameter for a distance of not less than two diameters (δ), before expanding into pressure pipe	
Finish of pressure holes	No wire edges of projecting burrs into the pipeline are allowed at the pressure holes		
Radius of the hole edge rounding, "ℓ"	If D<50;$\ell \approx 0,4$ If 200>D>50;$\ell \leq 0,8$ If D>250;$\ell \leq 1,6$	$\ell \leq 0,1\delta$	$\ell \leq 0,1\delta$

1.3.1.3. Reynolds Number

The coefficient of discharge is dependent on the Reynolds number. An increase or a decrease in the Reynolds number results in significant changes in the value of the coefficient of discharge.

The codes are not unanimous as to the effect the Reynolds number has on the value of the discharge coefficient. The variation of code flow coefficients with the square root of the reciprocal of the Reynolds number is shown in Figure 7.

It is stated in the ASME code that a linear relationship exists between the square root of the reciprocal of the Reynolds number and the coefficient of discharge. According to the British standard the coefficient of discharge increases with increasing Reynolds number until a limiting value is reached above which it is independent of the Reynolds number and therefore remains constant. The ISO and DIN codes show a continuous change of coefficient with the Reynolds number.

The dependence of the discharge coefficient on the Reynolds number increases with increasing area ratio. Further comparison shows that the ISO, AGA, ASME and BS coefficients differ most when the pipe diameter is small and the area ratio is large.

1.3.2. The Significance of the Difference between the Engineering Codes

From the above discussion it can be seen that the codes are not unanimous as to the value of the discharge coefficient and therefore, under the same conditions, the calculated flow based on the different codes will result in a variety of answers. The difference in the calculated flowrate according to the different codes can exceed $\pm$ 1½%. This percentage is outside the allowable tolerance given by any of the codes.

1.4 OBJECTIVES

Due to modern industrial demands the accurate measurement of the flow rate in closed conduits is of utmost importance. A number of flow measuring devices are available of which the square edge orifice plate is the most popular. The advantages of the orifice plate are numerous but the accuracy within which the flow rate can be measured with an uncalibrated orifice plate is $\pm$ 1,5 percent. In many cases this level of accuracy is satisfactory, but as already shown, a greater degree of accuracy is often required.

In order to obtain greater accuracies in flow measurement using orifice plates, more stringent specifications than those called for by any of the engineering standards are required. Spencer and Harrison (38) at NEL and West (39) at ESCOM have proved that the flow rate in a pipeline can be measured using an orifice plate to an accuracy of $\pm$ 0,1%. Herning and other researchers (See Chapter 2) have shown that minor imperfections in the upstream edge of an orifice plate, and blunting of this edge, cause significant errors in the measured flow rate. Similarly the roughness of the upstream pipe, the position of the orifice plate relative to the pressure taps and to the centre of the pipe will affect the accuracy of the obtained measurement. The work done by various researchers thus shows that there is a need for experiments which will lead towards a better understanding of the effect on the coefficient of discharge of minor imperfections in the shape of the orifice plate and of small errors in the installation of the plate. The difference in the specifications of the various engineering standards further highlights the need for the above experiments.

Due to the above findings the author decided to conduct experiments with the object of determining the effect on the co-efficient of discharge of:

(a) varying the sharpness of the upstream edge, and

(b) varying the eccentric location of the orifice plate.

It is hoped that the results of these experiments will lead towards a better understanding of flow measurement with orifice plates.

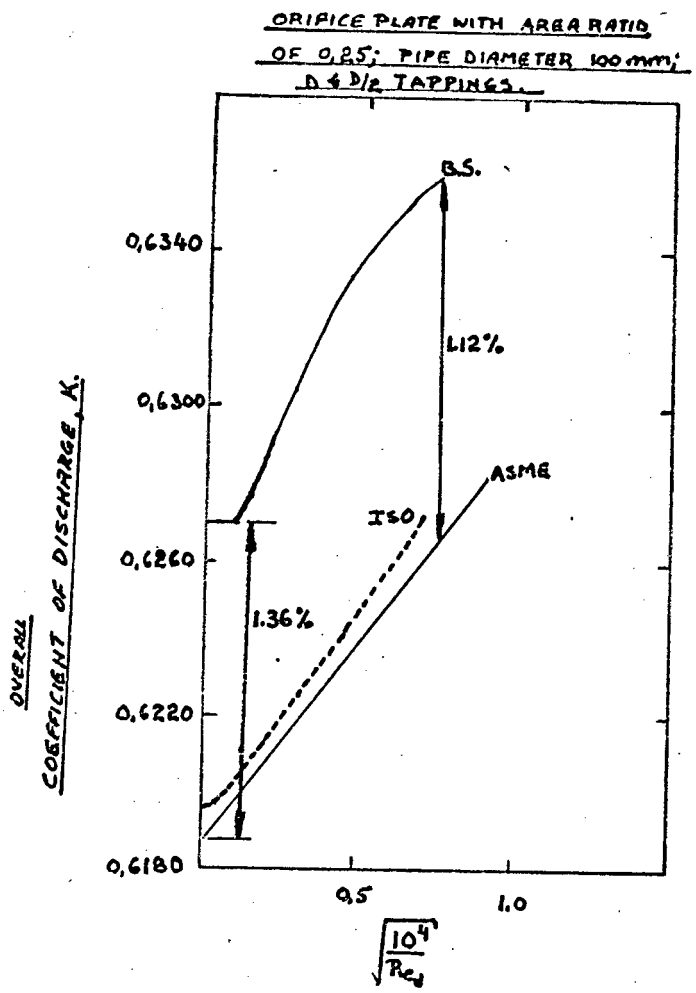

Fig. 7 The Variation in the Coefficient of Discharge as specified by various Engineering Standards with the Reynolds number

CHAPTER TWO

LITERARY SURVEY ON THE THEORY OF ORIFICE METERING

2.1 GENERAL FLOW EQUATION FOR ORIFICE PLATES

The theoretical equation for determining the rate of flow is given by

$$q = \frac{\pi d^2}{4} \left(\frac{2\rho \ (P_1 - P_2)}{1 - \left(\frac{d}{D}\right)^4} \right)^{\frac{1}{2}} \qquad (1)$$

A number of idealized assumptions are made to derive equation 1. (See Appendix A). This leads to a discrepancy between the actual and theoretical flow rate. To account for this difference an empirical factor called the "coefficient of discharge" is introduced and equation 1 can be written as

$$q = \left(\frac{\pi d^2}{4}\right) \frac{C_D}{\sqrt{1 - \left(\frac{d}{D}\right)^4}} \ \{2\rho \ (P_1 - P_2)\}^{\frac{1}{2}} \qquad (2)$$

The coefficient of discharge, C_D is defined by the following expression:

$$C_D = \frac{\text{actual mass flow rate}}{\text{theoretical mass flow rate}}$$

Numerous experiments have been conducted over the years to determine the value of this coefficient. Different engineering bodies have drawn up standards which are based on the results of these experiments. Using the values given by the various standards, the actual flow rate can be calculated.

2.2 METHODS OF EXPRESSING THE OVERALL COEFFICIENT OF DISCHARGE

Equation 2 can be written in the following form:

$$q = \frac{\pi d^2}{4} \cdot K \cdot \{2\rho (P_1 - P_2)\}^{\frac{1}{2}} \qquad (3)$$

where K is the overall coefficient of discharge.

This coefficient can be expressed in the following ways:

1) $$K = \frac{C_D}{\sqrt{1 - (\frac{d}{D})^4}}$$

In this case K is expressed in terms of a single coefficient and this coefficient accounts for all the modifications introduced into equation 1. It is influenced by:

1) the diameter ratio
2) the Reynolds number
3) the pipe diameter
4) the position of the pressure tappings
5) the viscosity
6) compressibility
7) the positioning of the plate relative to the pipe.
8) the flatness and thickness of the plate
9) the shape of the velocity profile
10) the squareness and sharpness of the upstream edge
11) the surface roughness of the pipe and plate
12) swirl and turbulence

This is the most popular way of expressing this coefficient but it helps little towards explaining why it varies with the above factors. Calculation of the flow rate is quick and simple if this overall coefficient

is used. (See Appendix D).

2) $$K = C_v C_c / \{1 - C_v^2 C_c^2 (\tfrac{d}{D})^4\}^{\frac{1}{2}}$$

Engel, F.A. (40,41,42) prefers to use this method of expressing the overall coefficient of discharge. In the above equation C_c and C_v represent the coefficients of contraction and velocity respectively.

ASME (10) states that no practical advantage is derived from expressing the discharge coefficient as a function of separate factors. Engel, (40,42,43,44) however, believes that if one crucial phenomenon after the other were to be eliminated then a better understanding could be obtained of the flow conditions which determine the characteristics of the discharge coefficient.

The erroneous assumption that the velocity at the downstream pressure tap is related to that at the upstream pressure tap, as the area of the orifice to that of the inlet pipe, can be avoided by introducing the contraction coefficient. This coefficient is equal to the ratio of the area of the jet at the vena contracta to that at the orifice. Since the area of the jet at the vena contracta varies with the diameter ratio and the properties of the fluid, the coefficient of contraction and that of discharge will vary accordingly. The coefficient of contraction is the primary factor affecting the overall coefficient (in the order of 0,96 X K).

The velocity coefficient is introduced to correct the assumption in equation 2 that the velocity is uniform across a cross-section of the pipe. Engel has found that the velocity profile and the lambda-friction

2.3 FACTORS AFFECTING THE COEFFICIENTS OF DISCHARGE

In section 2.2.1 the factors influencing the value of the overall discharge coefficient, K, are listed. These factors can be expressed by the following equation:

$$K = f(Re_d, \frac{L_1}{D}, \frac{L_2}{D}, \beta, \frac{r}{d}, \frac{e}{D}, \frac{t}{D}, \frac{\ell_1}{D}, \frac{\ell_2}{D}, \frac{\delta}{D}, \frac{\theta}{D}, D) \qquad (6)$$

where Re_d is the Reynolds number based on the orifice diameter, $\frac{L_1}{D}$ and $\frac{L_2}{D}$ are the ratios of the straight lengths of the approach and exit pipes, to the pipe diameter.

β is the diameter ratio $\frac{d}{D}$

r is the radius of the upstream edge

e is the thickness of the orifice edge

t in the thickness of the orifice plate

ℓ_1 & ℓ_2 are the distances to the centre of the pressure tappings from the upstream face of the orifice.

δ is the diameter of the pressure tappings

Θ is the roughness of the pipe wall (size of the surface granules)

2.3.1 The Effect of Varying the Straight Length of Pipe Immediately Before and After the Orifice Plate

For the overall coefficient of discharge to remain constant with varying pipe lengths, fully developed flow free of abnormal swirl and vortices with the fluid streams uniformly distributed across the pipe, is required.

For the flow to become fully developed a certain straight length of piping is necessary (See Figure 8).

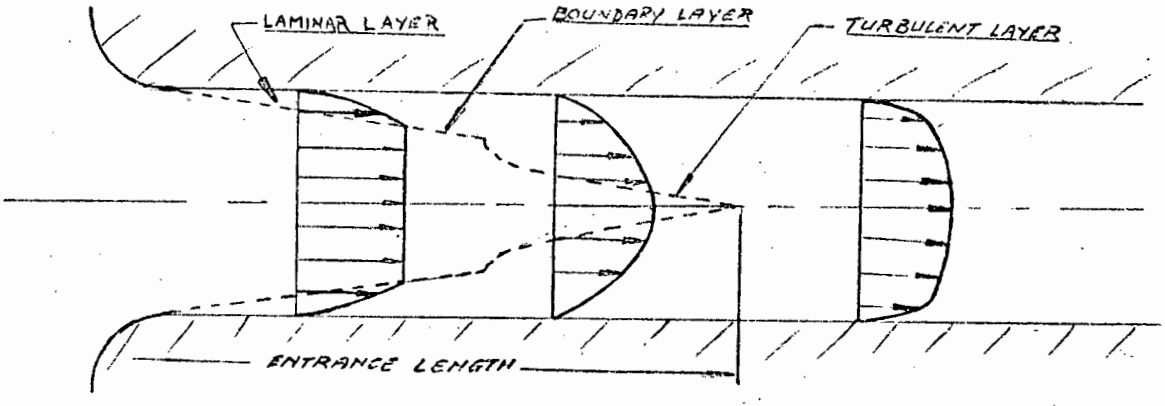

Fig. 8. Development of Velocity Profile From the Entrance of a Pipe

Pipe fittings which cause swirl such as valves, bends, T-pieces, diffusers, transition pieces and other irregularities will affect the velocity profile, and thereby the total straight length of piping required for fully developed flow at the orifice.

The various engineering standards stipulate the minimum length of straight pipe required after any such disturbance and therefore the effect of $\frac{L_1}{D}$ and $\frac{L_2}{D}$ can be considered constant.

In practical applications there is sometimes insufficient space available, and a shorter length of straight pipe must be installed than stipulated in the standards. This has the effect of increasing the value of the discharge coefficient.

Murdock and his fellow researchers (47) found that the error caused by having a globe valve a short distance upstream from an orifice plate is less that 2%. Sasiadek (48) has found that using a double orifice is preferable when the minimum length of straight pipe is not avaiable. Herning and Bellenberg (49) have found that at least 30 diameters are required for fully developed velocity profile to be achieved.

Sprenkle and Courtright (50) have shown that if any flow straightener is used then the straight length of pipe upstream of the orifice plate can be considerably shorter than required by the standards without significant errors being introduced. They found that the perforated plate flow straightener was better than the honeycomb one for this application. Zanker (51) has designed a flow straightener which requires only five pipe diameters after it for accurate measurement.

2.3.2 The Effect of the Orifice Edge Thickness

The width of the orifice edge can not be made too large with respect to the pipe diameter as with increasing edge thickness re-attachment of the jet can occur. This causes a decrease in the jet contraction which results in an increase in the flow coefficient, K.

The American standards stipulate that the ratio of the edge thickness to the pipe diameter (e/D) must not be greater than 1/30. To be able to compare the data of one researcher with that of another this limitation must be adhered to. Although this stipulation has dampened research interest in the effect of edge thickness, some characteristics have emerged: Beitler's experiments showed that for orifice plates with diameter ratios less than 0,1 the edge thickness could be increased till it was equal to 0,2 of the orifice diameter(52) . If the diameter ratio is greater than 0,1 then the edge thickness has to be less than 0,02 pipe diameters. Ruppel (53) confirmed the above but he found that if the diameter ratio is greater than 0,7 then e/D can be increased to 0,04.

Thrasher (54) found that if the edge thickness is greater than 1/40 of the pipe diameter then the discharge coefficient increases; such

increase being greater at lower Reynolds numbers.

2.3.3 The Effect of Plate Thickness

With a thick orifice plate re-attachment of the jet occurs at the walls of the cylindrical portion of the orifice and normal contraction does not occur. The jet is enlarged resulting in an increase in the flow coefficient. To avoid this occurringthe cylindrical edge, "e",is kept thin (within standard specifications) and the outlet corner of the orifice is beveled at an angle of 45 degrees to the face of the orifice plate (see Figure 9). Different values for the plate thickness are specified by the various standards. (Section 1.5).

Very little research work has been done to investigate the effect of plate thickness on the discharge coefficient. In 1930 Marks L.S. (55) pointed out the difference in flow pattern through a thick and a thin cylinder. Grace and Lapple (56) showed that the thin plate orifice is more consistent in performance than the thick plate orifice.

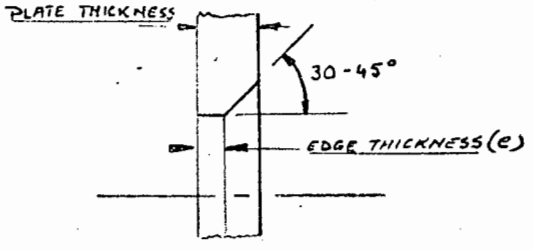

Fig. 9 The edge thickness and bevel angle of an orifice plate

2.3.4 The Effect of Pressure Tap Location

If the general flow pattern through an orifice plate is studies an understanding for the precise positioning of pressure taps results.

Figure 10 illustrates the general flow pattern of the streamlines across an orifice plate. The pressure varies along the pipe wall as shown in Figure 11. It can be seen that the pressure difference between the taps depends on the position of these taps relative to the orifice itself.

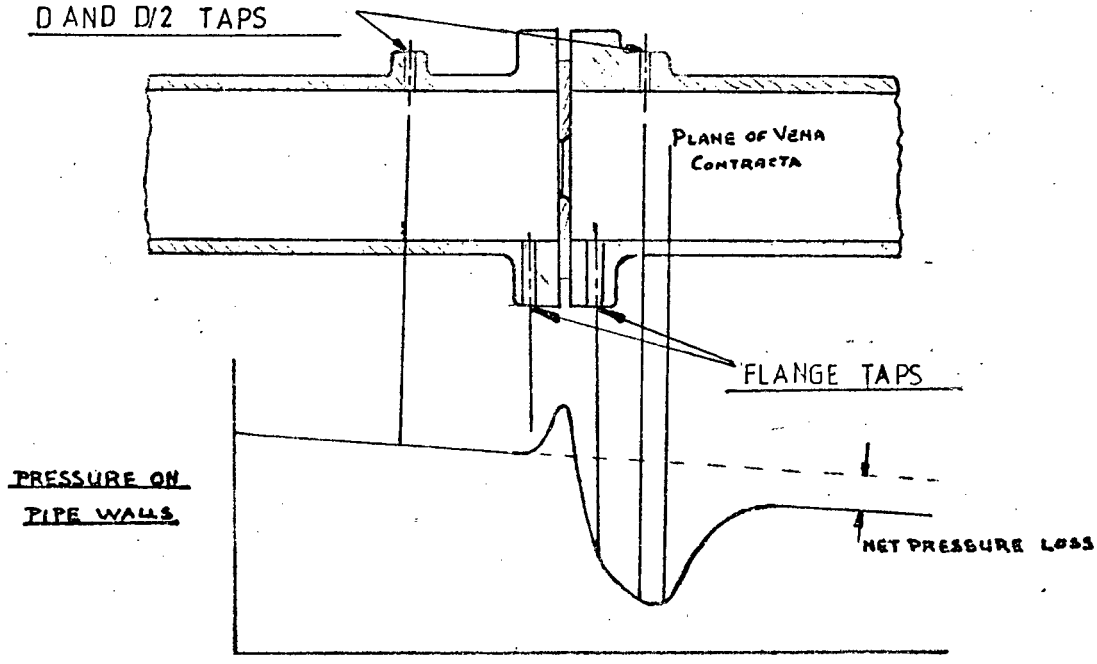

Fig. 10. General Flow Pattern of Stream Lines Across an Orifice Plate.

As the fluid flows through the upstream pipe towards the orifice plate, the pressure on the pipe wall decreases very slowly due to the dissipation of energy as heat in frictional losses. (These losses are exaggerated in figure 11). In the absence of the orifice plate the pressure would continue to fall as indicated by the dotted line. Immediately in front of the orifice plate there is a small increase in the pressure on the pipe walls due to the impact pressure on the plate. As the fluid enters the orifice its velocity increases very rapidly and the pressure on the pipe wall decreases sharply. The jet continues to contract until the vena contracta, where the streamlines are parallel and both the pressure and cross sectional area of the jet are at a minimum. Downstream from the vena contracta the jet expands, causing the pressure on the pipe walls to increase until maximum recovery has taken place. This occurs about eight diameters downstream from the orifice. Here the velocity of the fluid falls back to its initial value. The pressure, however, never reaches the value that it would have had in the absence of the orifice plate. The difference is known as the "net pressure loss" (See figure 11). This loss is due to the dissipation of some of the energy as heat in the damping of turbulent

eddies by internal friction.

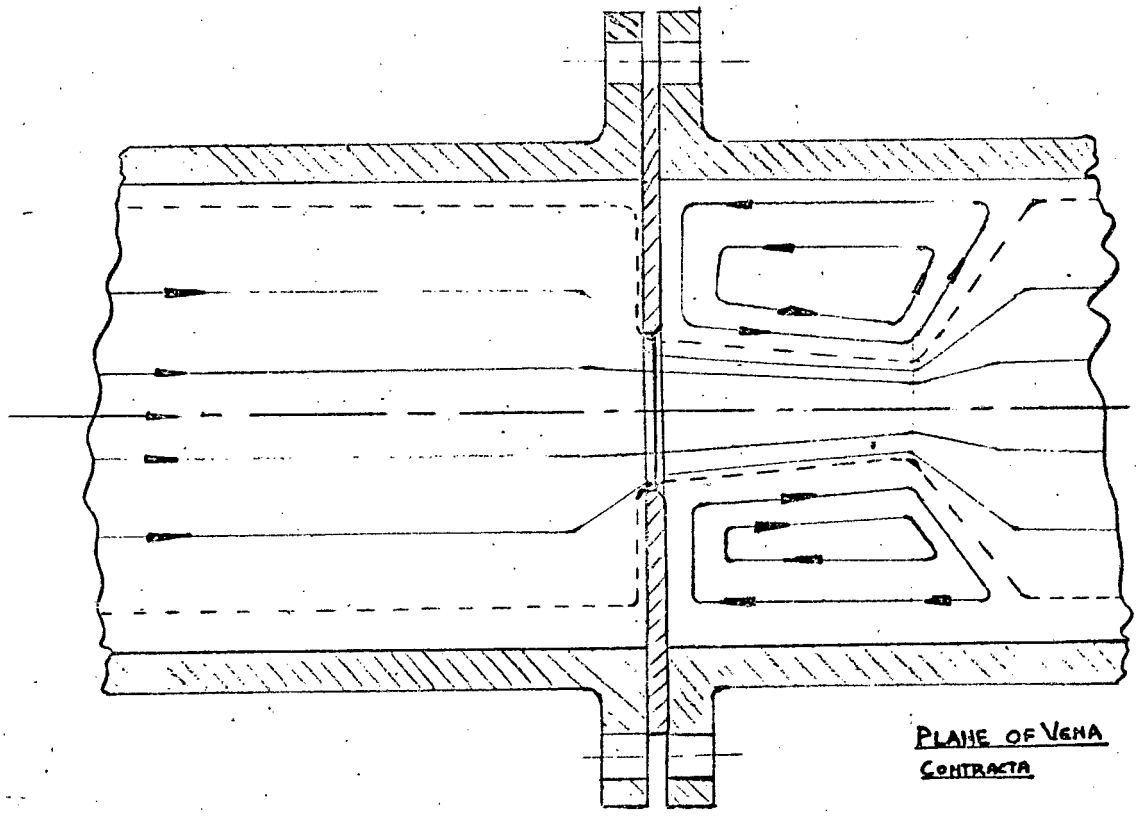

Fig. 11. Section of Square-Edged Orifice Plate showing Variation of Pressure along the Pipe Wall.

From the above it can be seen that the location of the pressure taps will affect the pressure difference measured across the orifice and therefore the coefficient of discharge. A number of standard positions have been adopted for pressure tap location. A description of those specified in the standards and those used in industry follows:

(a) Vena-Contracta Taps

The upstream connecting hole is located one pipe diameter from the upstream face of the orifice plate and the centre of the downstream connecting hole at the position of the vena contracta. The mean position of the vena contracta is given by ASME (11) and by ISO (20).

(b) Radius or D and D/2 Taps

This tapping is favoured by the British. The upstream tap is located one pipe diameter from the upstream face of the orifice while the downstream taps are located half a pipe diameter from the upstream face.

When compared with the vena contracta taps, the pressure readings are

slightly less stable due to eddying and diverging flows downstream of the orifice.

(c) Flange Taps

The upstream and downstream pressure tapping holes are both positioned one inch away from the orifice plate faces. These and corner taps are used when it is difficult or undesirable to make tappings in the pipe wall.

(d) Corner Taps

Both taps are located immediately adjacent to the plate faces. The pressure holes open in the corner formed by the pipe wall and the orifice plate.

(e) Pipe or Full Flow Taps

The upstream tap is located 2.5 pipe diameters from the face of the orifice, while the downstream tap is 8 pipe diameters from the same face. This arrangement is mainly used in the United States. It has been designed to effect a lower working pressure drop for any given flowrate. It is therefore useful when dealing with very large flowrates, especially when the area ratio is already at its maximum permissible value of 0.7 (as given by the standards). A disadvantage of using these taps is that their flow coefficients are very dependent on pipe roughness.

2.3.5 The Effect of Varying the Diameter of the Pressure Taps

The diameter of the pressure tap holes must be so small that their size will not affect the pressure observed at them. They must be free of burrs so that suction effects and changes to the velocity profile will be kept to a minimum.

Rayle R.E. (57) found that drilling burrs cause errors of up to 30% of the dynamic head, and that for sharp-edged holes, an increase in the hole diameter from 0,01 to 0,12 inches results in a 1% change in the readings. Variations in the shape of the edge do not cause errors greater than 1% in the pressure readings. The work of Zanker and Fellerman (58) confirms Rayle's findings. They show that over a range of diameters from 0,005D to 0,04D the measured coefficient increases by only 1%.

2.3.6 The Effect of Pipe Roughness

Pipe surface roughness will affect the velocity profile in the following manner:

1) A rough pipe surface gives rise to a highly centralised velocity profile and therefore an increase in the discharge coefficient (See Figure 12).

2) A smooth pipe surface gives rise to a flat velocity profile which causes a decrease in the discharge coefficient.

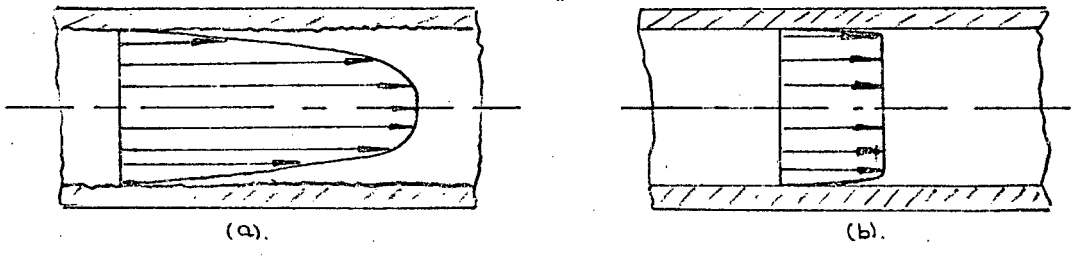

Figure 12. The Shape of Velocity Profile in (a) rough pipe (b) smooth pipe.

P.H. Oosthuizen (59) derived an equation (on the same principles as that in Appendix A 4) which can be used to predict theoretically the effect of velocity profile on the discharge coefficient.

Schag, A. (60) stated that no definite rules based on actual roughness are available. This experiment showed that the value of K was least affected if D & D/2 tappings were used. Abramaritz (61) was the first to study the effect of artificially roughened walls. He used wire meshing glued to the surface of the pipe. Results showed that if the wire mesh is ended two pipe diameters from the face of the orifice plate, then an error of 1% is introduced (λ = 0,08; rough pipe) and 2% when λ = 0,13 (very rough pipe). If the mesh is ended 0,125 pipe diameters from the plate, then the error increases to 6% in both cases.

Clark W.J. (62) performed the most thorough investigation to date in this field. He found that downstream incrustations had no significant effects. The error introduced by upstream incrustations varies with the degree of roughness, pipe diameter, area ratio and the Reynolds number. His major finding showed that clearing a rough pipe for a short distance before an orifice plate will reduce the errors to within standard specifications. This is surprising, as the coefficient of discharge varies with the velocity profile just upstream of the orifice plate, and it seems unlikely that this will have changed in the short distance of two diameters. His results were conclusive. This shows that the present explanation for the effect of pipe roughness is not totally adequate. The practical application of his findings is that the orifice plate can be installed in a separate length of smooth pipe, six diameters long, which can be conveniently removed for periodic inspection. Thibessard, G (63) has developed a linear equation which can be used to

determine the correction coefficient for pipe roughness effects if corner taps are used. Herning and Wolowski (64) have shown that to use correction factors based on pipe diameter only is inadequate and therefore the friction factor should also be taken into consideration. Spencer and fellow researchers at NEL have found that the effect of pipe roughness is greater for large area ratio orifices (65)

2.3.7 The Effect of Orifice Surface Roughness

The effect of orifice surface roughness is similar to that of pipe roughness. The effect was considered negligible until 1954 when Dall (66) showed that this is not true. He suggested that a quantitative rather than qualitative definition for the surface roughness of the plate be included in the future codes.

2.3.8 Effect of Pipe Diameter, D

The contraction of the jet is affected by the proximity of the pipe walls. The discharge coefficient of small pipes is greater than that of large pipes.

In the British standards (67) correction factors for the combined effect of pipe size and roughness are given. (See Figure 13).

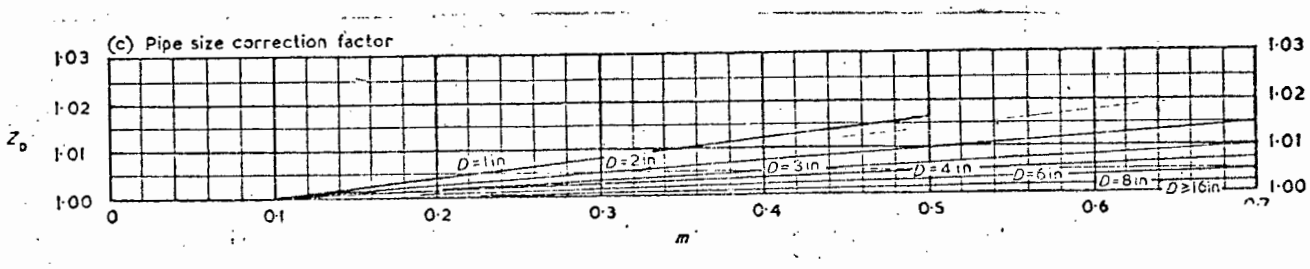

Fig. 13. Pipe size correction factor for an orifice plate with D & D/2 tappings as given by BS 1042:1964

Spencer (68) states that conclusive evidence showing that there is a size effect in addition to a Reynolds number effect does not exist. Experimental results suggest that a size effect does exist, and therefore, the above theoretical explanation is correct.

This uncertainty is due to the fact that all the separate factors which affect the discharge coefficient are interdependent and therefore difficult to determine.

2.3.9 The Effect of Diameter Ratio d/D

For the same pressure differential and fluid, the inward radial velocity of the fluid particles close to the wall increases with decreasing diameter ratio. The increased radial velocity results in:

1) increased contraction of the jet

2) higher turbulence and eddying (thus higher losses).

The overall coefficient of discharge, K, therefore decreases with decreasing diameter ratio.

Much work has been done in this field, in which the general trend has been to find how the contraction coefficient varies with the diameter ratio. Kirchoff, Trefftz, Von Mises and others developed equations according to which the value of C_c is between 0,60 and 0,62.

The practical experiments of Engel (69) showed that the coefficient of discharge is related to the diameter ratio. Beitler (70) found that a linear relationship existed between K and β if β is less than 0,7.

2.3.10 The Effect of Reynolds Number, Re_d

a) Significance of Reynolds Number

According to ASME (10) mechanical similarity is realized when the ratio of the forces acting on a fluid particle in one flow is the same as the ratio of the forces acting at a corresponding point in the other flow.

The Reynolds number is the ratio of the inertia forces to the viscous forces. It is expressed by the following equation:

$$Re = \frac{\rho v L}{\mu}$$

where ρ = density of the fluid

v = average velocity of the fluid

L = characteristic length

μ = dynamic viscosity

For orifice plates the characteristic length, L, is taken to be equal to the orifice diameter, d, and therefore

$$Re_d = \frac{\rho v d}{\mu}$$

If the Reynolds number for flow through two orifices is the same then mechanical similarity is achieved.

b) Variation of the Coefficient of Discharge with the Reynolds number

If the shape of the orifice and the specifications for the installation are according to the standards, then the overall coefficient of the orifice meter will be a function of the diameter ratio and the Reynolds number only.

$$K = f(\beta, Re_d)$$

The effect of varying the diameter ratio has been discussed earlier. For a specific orifice plate in a specific installation the coefficient K is dependent on the Reynolds number only, since the velocity distribution, jet contraction and shear are dependent on the inertia and the viscous forces.

The relationship between the coefficient, K, and the Reynolds number, Re_d, is illustrated in Figure 14.

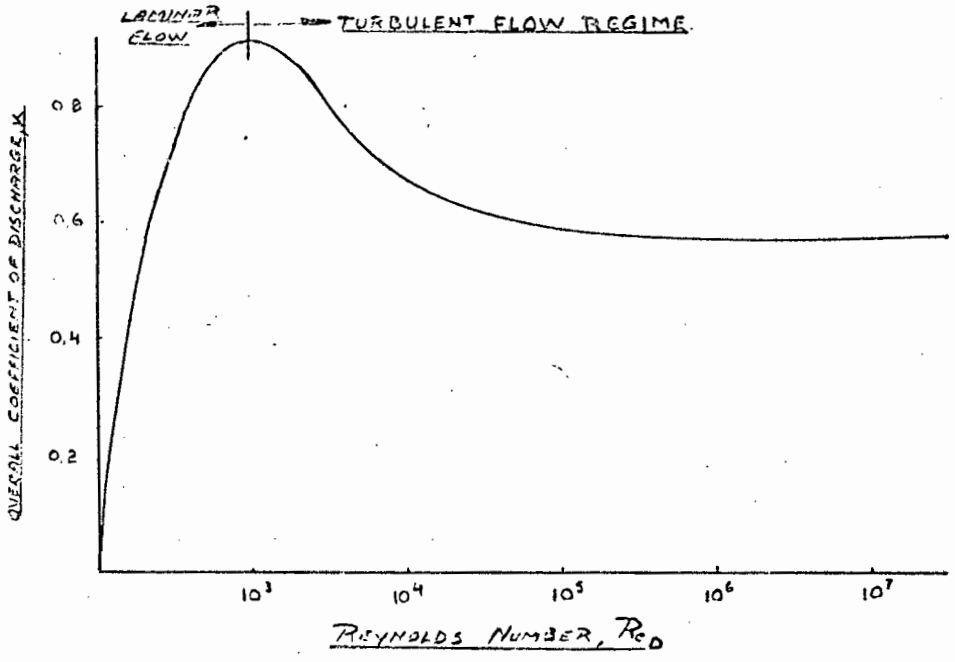

Fig.14. The relationship between the Coefficient of discharge & the Reynolds number

It can be seen that different relationships exist for the two main regions of flow (i.e. (1) Laminar (2) turbulent).

(1) Laminar Flow

Johansen (71) observed and photographed the flow pattern through orifice plates at low Reynolds numbers. At Reynolds numbers equal to 15, complete laminar flow existed, but a jet began to form with a stagnant region adjacent to the downstream face of the orifice.

The flow followed the contour of the orifice plate as shown in the Figure 15 below.

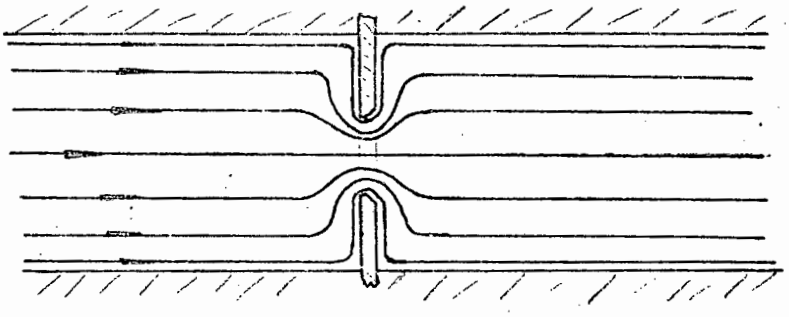

Fig. 15 *Flow at* $Re_d = 5$

As the Reynolds number increased to 100, a laminar flow back-eddy formed with a slight contraction of the jet issuing from the orifice. The laminar back-eddying increased in length along the tube with further increases in the Reynolds number. At a Reynolds number of about 230 the jet issuing from the orifice became unstable due to the formation of ripples along the boundary of the jet. These ripples were spaced (near the orifice) at regular intervals of 0.1 orifice diameters apart (See Fig. 16).

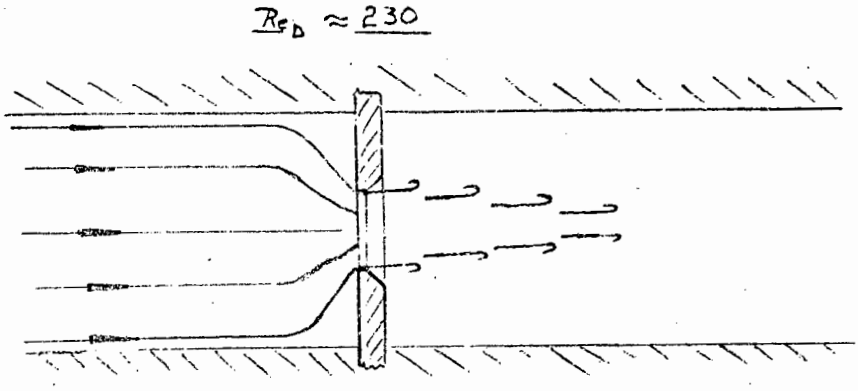

Fig. 16 *The Formation of the Bernard von Karman eddy streets when using orifice plates*

At higher Reynolds numbers, completely coiled vortex rings spaced at intervals of about one diameter are formed.

This condition prevailed until Re_d of 2000 was reached after which turbulence set in. The laminar regime terminated when the discharge coefficient reached its maximum value. The maximum value of the coefficient is dependent on the diameter ratio. Johansen (71) measured the frequency of the vortex rings and correlated the Reynolds number with the Strouhal number. The application of the Strouhal number as an "intermittence factor" (for the explanation of the onset of turbulence) is due to Rotta (72).

Iverson (73) derived the following equation for laminar flow through an orifice plate:

$$q = KA\sqrt{2gh} \qquad (7)$$

where K is equal to $\frac{Re_d}{B}$ and B is a constant determined experimentally. In laminar flow the Reynolds number is directly proportional to the mean velocity and therefore to the drop in the piezometric pressure. Therefore equation 7 can be written as

$$q = FA2gh \qquad (8)$$

where F is a constant equal to 1/B.

For laminar flow the friction head-loss coefficient, C_f, is equal to $16/Re_d$ * and therefore K is related to C_f.

Iverson (73), Millar and Nemecek (74) and other researchers have found

* *NOTE This value for the friction factor is commonly used in Britain. The Americans use a friction factor equal to four times this value. The equations used for overall head loss in the two countries differ by a factor of four.*

both analytically, and by experiment, that for full laminar flow, the friction coefficient is inversely proportional to the Reynolds number. The constant, F, is a function of the length to the diameter ratio of the orifice. Small variations in the upstream and downstream flow conditions and in the plate dimensions cause substantial changes in the laminar velocity profile and in the shear stress pattern and thus in the meter coefficient. Giese (75) and more recently Marxman and Burlage (76), demonstrated the importance of the effect of small variations in the shape of the orifice plates when used in laminar flow measurement. Their findings showed that variations of up to 10% occured in the coefficient of discharge whenever small changes were introduced in the shape of the orifice plate. As the Reynolds number increases, the laminar flow considerations become small compared to inertia influences, and the exact geometry of the plate plays a less important role.

(2) Turbulent Flow

The overall effect of the Reynolds number on the coefficient is a result of changes in the contraction of the jet and in the friction. The effects are opposing and the resultant curve is as seen in Figure 14. The above can be explained if the overall coefficient K is expressed as:
(See Appendix A 2 for derivation)

$$K = \frac{C_v \, C_c}{\left[1 - Cc^2 \, Cv^2 \, (\frac{d}{D})^4\right]^{\frac{1}{2}}}$$

The velocity coefficient, C_v, accounts for changes in velocity due to friction, $\left(\text{i.e. } C_v = \frac{V \text{ actual}}{V \text{ ideal}}\right)$

The contraction coefficient, C_c, accounts for the contraction of the jet $\left(\text{i,e,} \quad C_c = \frac{\text{Area of jet at tapping}}{\text{Orifice area}}\right)$

The variation of the discharge coefficient, K, with the Reynolds number, Re_d is due mainly to the action of the turbulent viscous forces. The viscous forces increase with a decrease in the Reynolds number. This results in a decrease in the velocity coefficient and an increase in the contraction coefficient. In turbulent flow the change in contraction coefficient is greater than that in the velocity coefficient. As the Reynolds number decreases the effect of the velocity coefficient increases and in laminar flow it becomes predominant. At very low Reynolds numbers no more contraction occurs and the change in the contraction coefficient is due to the change in the velocity coefficient (See Laminar Flows).

If two fluids are metered, the fluid with a higher viscosity will have the higher coefficient of discharge. For example, for the same jet velocity, the discharge coefficient for a medium oil is higher than that of water.

The relationship between the Reynolds number and the coefficient of discharge has been expressed in a number of ways. Witte (77) presented his results by plotting K against log Re_d. (See Figure 17).

Beitler (78) found that plotting the coefficient against the reciprocal of the Reynolds number results in a linear relationship for a wide range of flow rates. In 1935, after his results were already presented, he suggested the use of $1/\sqrt{Re_d}$. as abscissa instead of $1/Re_d$. (79). A

better linear relationship is obtained if this plot is used. Marchetti (80,81) discovered the same relationship. (See Figure 18)

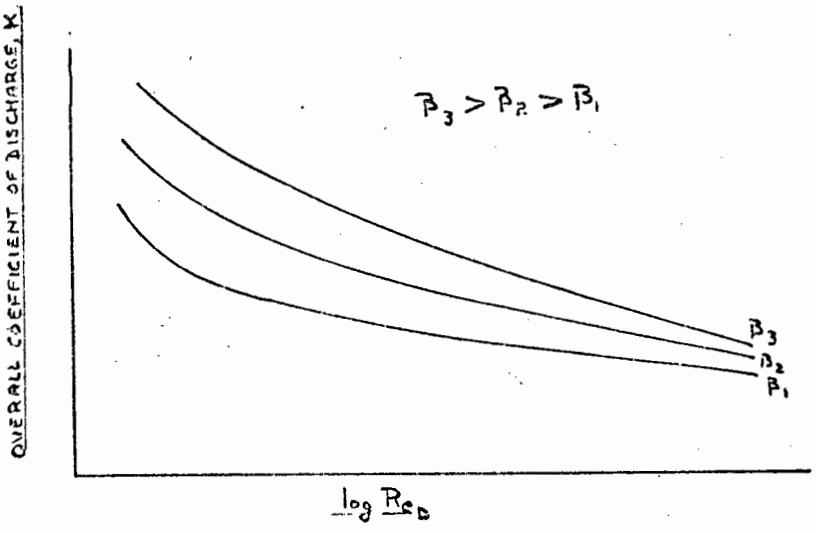

Fig. 17. Characteristic Curves of K plotted against corresponding values of log Re_d. Similar curves can be found in ISA (bulletin 12) and in VDI

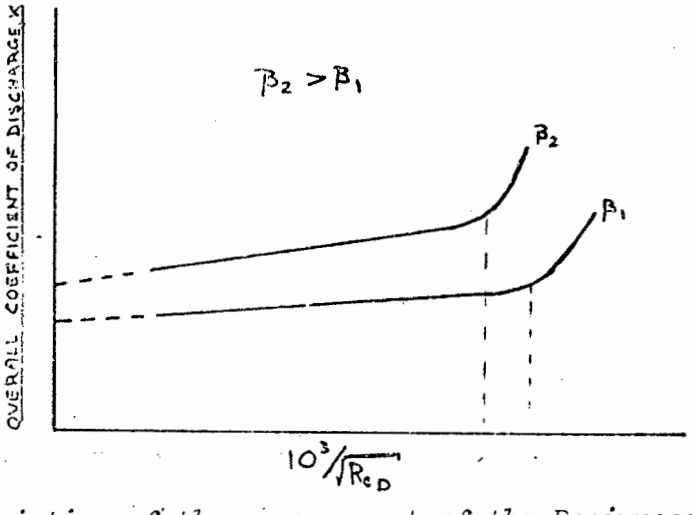

Fig. 18. Variation of the square root of the Reciprocal of the Reynolds number with the Discharge Coefficient

Beitler and Marchetti independently came to the conclusion that the discharge coefficient could be expressed mathematically for Reynolds number greater than 54 000 β^2 by the following general equation *(82)*

$$K = K_0 + b \frac{10^3}{\sqrt{Re_d}}$$

The value of K_o and of b are functions of the diameter ratio and the pipe diameter. A number of equations have been determined by different researchers.

Buckingham suggested the following equation for D & D/2 tappings (83)

$$K_o = \left[(0,6014 - 0,01352D^{-\frac{1}{4}})\right] + \left[(0,3760 + 0,07257D^{-\frac{1}{4}})\left(\frac{0,00025}{D^2\beta^2 + 0,0025D} + \beta^4 + 1,5\beta^{16}\right)\right]$$

and

$$b = \left[(0,0002 + \frac{0,0011}{D}\right] + \left[(0,00038 + \frac{0,0004}{D})\ (\beta^2 + \{16,5 + 5D\}\ \beta^{16})\right]$$

Marchetti's results (84) are expressed by the following equations:

$$K_o = 0,6031 + 0,34\beta^4 + 0,62(\beta - 0,7)^{5/3}$$

and

$$b = (0,026\beta^4 + 0,002)K_o$$

These experiments were performed with orifice plates with corner taps.

R.B. Dowdell and Yu-lin Chen (85) have done statistical analyses on the results of a number of researchers and have suggested that the following equations are more realistic for D & D/2 taps:

$$C_D = 0,59557 - 0,00061D + 0,00427D\beta + 0,03622\beta^2 - 0,00567D\beta^2 - (317,5 - 211,3D - 2988,5\beta + 1367,5D\beta + 2961,1\beta^2 - 1708D\beta^2)\ /Re_d$$

The International Standards Organisation (ISO) presents the value of the coefficient in the following form:

$$\alpha = \alpha'(1 + \frac{\beta A}{Re_D})$$

where

$$\alpha' = \alpha_e(\frac{10^6 d}{10^6 d + 381A})$$

and

$$\alpha_e = 0{,}5993 + \frac{0{,}1778}{D} + (0{,}364 + \frac{0{,}3830}{\sqrt{D}})^4 + 0{,}4(1{,}6 - \frac{25{,}40}{D})^5 +$$

$$\left|(0{,}07 + \frac{12{,}70}{D}) - \beta\right|^{5/2} - (0{,}009 + \frac{0{,}8636}{D})(0{,}5-\beta)^{3/2} +$$

$$(\frac{41935}{D^2} + 3)(\beta - 0{,}7)^{5/2}$$

and

$$A = 0{,}03937d(830 - 5000\,\beta + 9000\,\beta^2 - 4200\,\beta^3 + \frac{2671}{\sqrt{D}})$$

Marchetti found that linear relationships existed between K and $10^3/\sqrt{Re_d}$ for Reynolds numbers greater than $54000\,\beta^2$. As the diameter ratio increased the departure from linear relationship occurred at lower and lower values of $10^3/\sqrt{Re_d}$.

Marchetti found that the location of the region where a critical change took place (namely where the curve deviates from a straight line) changes with diameter ratio. He thought that the orifice edge sharpness also affected the range over which linear relationship existed. Scimemi's experiments (86) showed that a critical change took place even with orifices which had rounded edges. Buckingham and Bean (87,88) have found that for turbulent flow, the limiting values of the coefficient, K_o are sensibly linear with respect to β^4 over the range of β values from about 0,2 to 0,7.

The British Standards corrects for the effects of the Reynolds number by introducing a correction factor Z_r. (See Figure 19 below.)

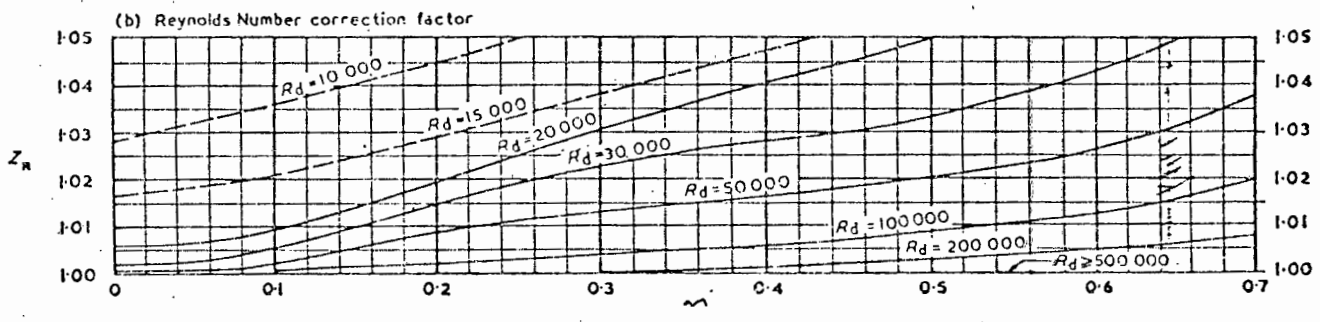

Fig. 19 Reynolds number Correction Factor as given by BS 1042 : 1964

A lot of research has been done on the effect of the Reynolds number for numbers between 20 000 - 500 000. For Reynolds numbers greater than this the different engineering standards do not agree. Insufficient experimental evidence exists to prove any of the standards correct.

2.3.11 The Effect of Eccentricity

If the centre of the orifice does not coincide with axis of the pipe then the orifice plate is said to be eccentric. The flow coefficient of an eccentric orifice plate differs from that of a concentric one. This difference is due to a change in the flow pattern. (See Figure20 below)

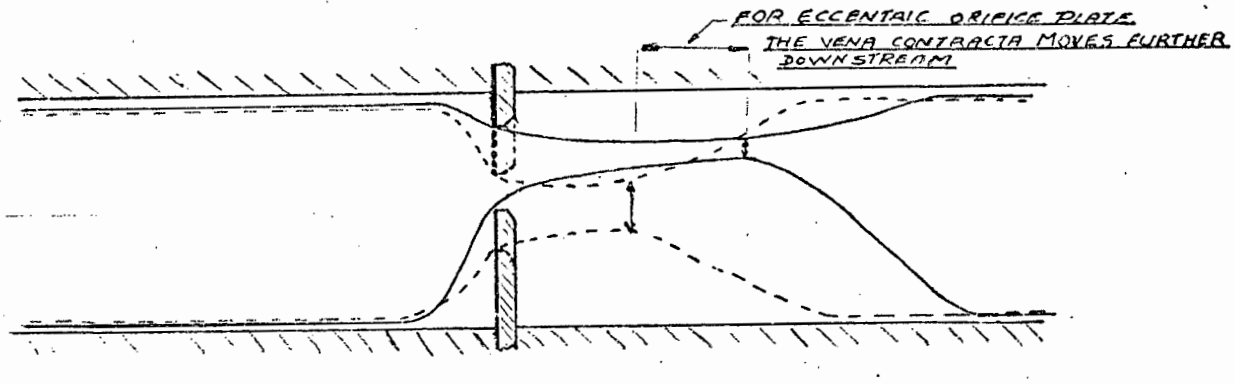

Fig. 20. Difference in flow pattern between a concentric and eccentric orifice

The vena contracta moves further downstream from the plate, resulting

in a smaller pressure difference across the plate at fixed tappings; hence an increase in the discharge coefficient.

The area of the jet is reduced less on one side than on the other since one side of the orifice is closer to the pipe than the other. The position of the pressure tapping with respect to the eccentricity of the orifice plate therefore influences the discharge coefficient.

Beitler (89) conducted experiments which led to the determination of the flow coefficient for fully eccentric orifice plates. These coefficients have been adopted by ASME (10).

Limited data is available on the actual effect that eccentricity has on the flow coefficient. Miller and Kneisel (90) have found that for all area ratios the error increased with increasing eccentricity towards the taps. They stated that for all the tests the coefficient for an eccentrically positioned plate was higher than for the same plate positioned concentrically. They suggested that using multiple tappings (a piezometric ring) will reduce errors due to directional effects. In later tests (91) they found that the change in flow coefficient is a function of the magnitude and direction of the eccentricity. Hinz, Scofield, Casale and Edwards (92) developed empirical equations for determining the flow coefficient, K_a, for orifice plates which are eccentrically located. These equations are:

$$K_a = K\left[1+f\ \left(F - \frac{0,06D}{D-d}\right)\right] \quad \text{for } 0 \leqslant F < 0,35 \qquad (8)$$

$$K_a = K\left[1+f\ (0,70-F)(0,04715)\right] \quad \text{for } 0,35 \leqslant F < 0,70 \qquad (9)$$

$$K_a = K\left[1+f\ (F - 0,70)0,06396\right] \quad \text{for } 0,70 \leqslant F \leqslant 1,0 \qquad (10)$$

where F is the distance between the centre of the orifice and the axis of the pipe, divided by the pipe radius.

K is the flow coefficient determined from the equation given by Beitler (See section 23.10.2).

They found that three definite regions existed which can be expressed by the above equations. In the region where F is greater than 0,35 and less than 0,70, large pressure fluctuations occur due to extreme turbulence. For F greater than 0,70 stability in pressure readings is again restored. These findings contradict that of Miller and Kneisel who state: "The relationship between these quantities is not readily discernible .... There appears to be no straightforward way to explain the phenomenon of eccentricity other than by graphical presentation of flow calibration data. Because of this, the projection of these results into other line sizes, Beta ratios, eccentricities, pipe roughness, etc. would not be recommended."

Bean (93) defined the eccentricity ratio as:

$$M = 2E/[D(1-\beta)] \qquad (11)$$

He found that if the eccentricity ratio is equal to or less than 0,05 then the discharge coefficient will not vary by more than 0,2% for flange taps and diameter ratios up to 0,7.

West (94) represented graphically the variation in the coefficient with the motion of the centre of the plate towards and away from the tappings. He found that for an orifice plate of 0,7 diameter ratio, which is 0,05D eccentric to the pipe axis, the flow coefficient is increased by 3,5%.

Spink (95) has presented graphically the variation in the correction factor which is to be applied for a fully eccentric orifice. The different engineering standards stipulate the maximum allowable eccentricity for an orifice plate for which the standard coefficients still apply. The equations given by the various standards differ, and this difference is discussed in Chapter 1.

2.3.12 The Effect of Edge Sharpness

The upstream edge of the sharp square-edged orifice is the only place where the flow lines touch the orifice plate. Hence rounding of the edge will affect the jet issuing from the plate. Figure 21 below shows the shape of the stream lines for a sharp square-edged orifice and for an orifice with a rounded upstream edge.

From this sketch it is apparent that the area of the jet increases as a result of rounding the upstream edge. An increase in the discharge coefficient results. If the edge radius is increased a stage will be reached where no contraction of the jet will occur and in this case the orifice plate will act as a flow nozzle. Further increases in the radius would cause separation at the edge.

In 1948 Collacott (96) stated that although it was known that the discharge efficients of chamfered orifices are higher than for square-edged ones, little work had been done to study this effect.

He tested a number of orifices whose edges were chamfered from 30 to 120 degrees and found that by increasing the bevel angle from 55 to 68 degrees and reducing the head from 20 inches to 4 inches of water, the

maximum discharge coefficient increased almost linearly from 0,87 to 0,907.

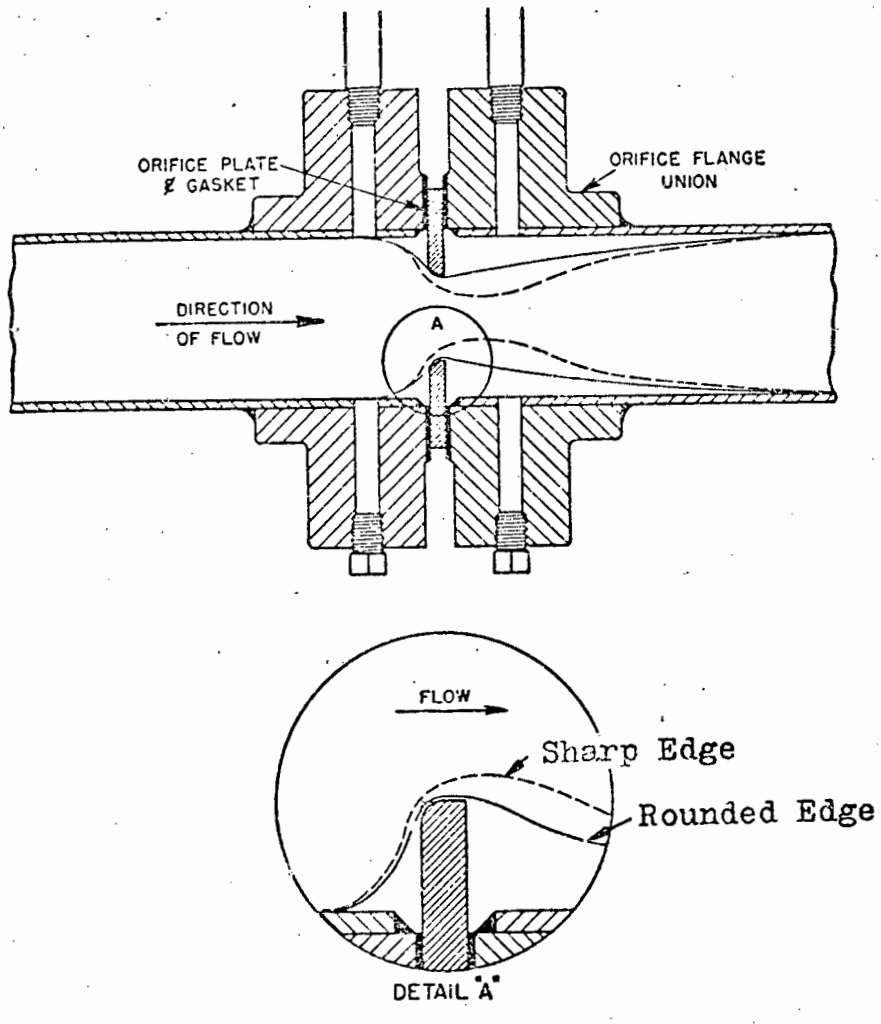

Fig. 21. Flow Lines Showing Effect of Dulling Upstream Orifice Edge
This figure is a direct copy from Spink, L.K. (97)

The 1943 edition of the British standards does not give a quantitive value for the edge radius of a standard orifice plate. The edge is considered to be sharp when a beam of light directed onto it will not be reflected. Since 1943 much research has been done on the effects of rounding the edge of an orifice plate. Spink (97) states that rounding the edge of an orifice by 0,025 mm has the same effect as increasing its diameter by 0,05 mm.

Herning (98) has developed a method of measuring the sharpness of the upstream edge of an orifice plate. He took impressions of the edge by pressing lead foil onto it. These impressions were magnified and the edge radius measured. From his experimental results he derived a multiplying correction factor for basic discharge coefficients. The correction factor is dependent on the ratio of the upstream edge radius to that of the pipe diameter r/D and on the area ratio. An error of 3,9% occurs for an orifice plate with area ratio of 0,1 and edge radius of 0,02 millimeters, while with the same edge radius an error of 1,76% occurs if the area ratio is equal to 0,4. Hence the effect of rounding the edge has a smaller effect on the discharge coefficients of orifice plates with large area ratios.

In a later article written in cooperation with Wolowski (99) they found that for standard orifices the discharge coefficient correction factor is the same for the same sharpness ratio. *

A graphical representation of their findings can be seen in Figures 22 and 23.

Herning found that the German standard on orifice plates (DIN 1952) was correct for orifice plates whose upstream edge radius is equal to 0,06 mm (See Figure 24).

Howard L. Bean (100) showed that errors up to 8% occur due to rounding the edge of orifices of 0,31, 0,50 and 0,69 diameter ratios. This occurred in a 100 mm line with ratios of radius of curvature of the

NOTE: * *Sharpness ratio is defined as the ratio of the upstream edge radius divided by the orifice internal diameter.*

inlet corner to the radius of the orifice bore ranging from 0,001 to 0,050.

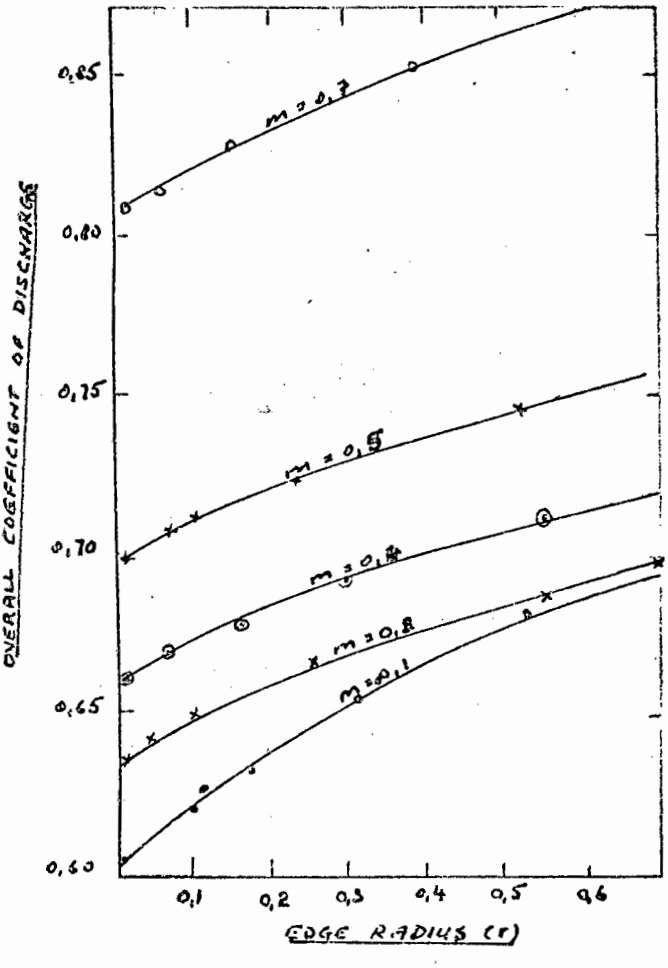

Fig22 . Herning's Results Presented Graphically

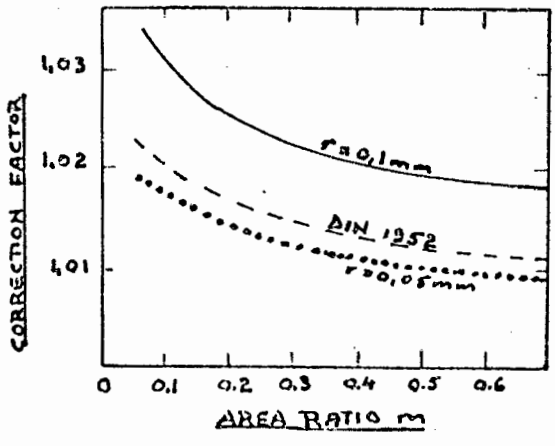

Fig. 24. Correction Factor which would have to be applied to Orifice Plates with Rounded Upstream Edge Radii

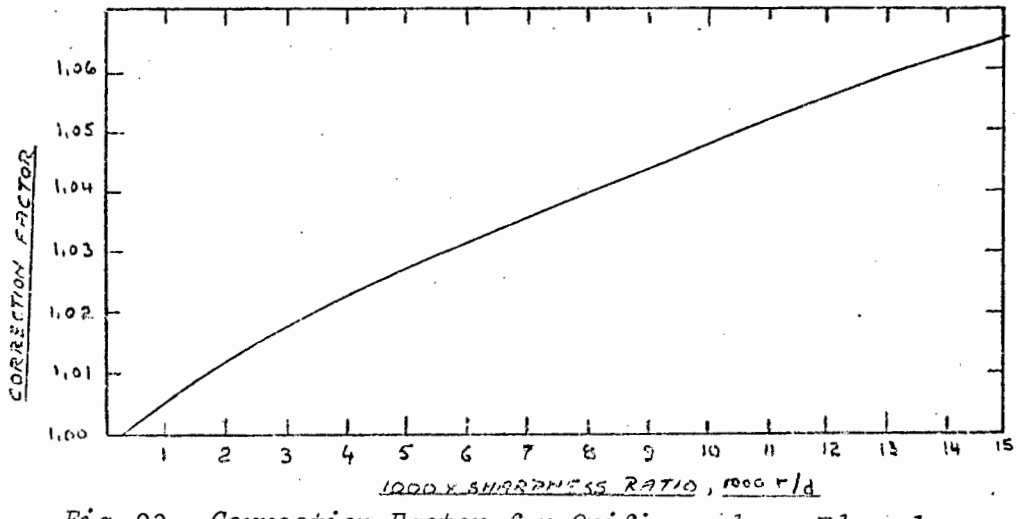

Fig. 23 Correction Factor for Orifices whose Edges have been rounded

K.A. Crockett and E.L. Upp (101) conducted experiments whose results correlated well with that of Herning and Wolowski. Similar experiments were carried out in England. Spencer, Calame and Singer (112) individually carried out experiments on the same set of orifice plates. The orifice plates were made to conform to the specifications of the German Flow Measurement Standard DIN 1952. These experiments were conducted respectively at the University of Stuttgart, at the London Laboratory of Electroflo Meters Co. Ltd., and at NEL, East Kilbride, Scotland.

Their results showed that the coefficient of discharge of an orifice plate with area ratio of 0,09 was one percent above the value given by the British and the German standards. This error occurred because of microscopic imperfections at the edge of the orifice. Work done by West (103) substantiated Spencer's findings. He stated that the effect of the orifice edge geometry on the discharge coefficient was more serious than originally believed.

The British standards have adopted Herning's suggestion that an orifice plate be considered sharp if the ratio of the upstream edge-radius to the orifice diamter is less than or equal to 0,0004. Gallacher (104) developed a new method of indirect measurement of edge sharpness. An impression of the orifice edge is obtained by first forming a negative casting which is then used as a mould for the positive cast. The positive cast is then used for viewing the edge. A thin slice from it is polished and used for measuring the edge sharpness.

In 1975 Benedict, Wyler and Brandt (105) published the results of their experiments. They found that the change in the flow coefficient due to

rounding the upstream edge of an orifice is expressed by the following empirical equation:

$$\frac{\Delta C_D}{C_D} = 0{,}85 \ln \left(\frac{r}{d} \times 10^3 \right) + 1{,}74 \qquad (12)$$

During the discussion on the above paper Head V.P. (106) suggested the use of the following equation instead:

$$C = 0{,}6015 + 0{,}37 Re_d^{0{,}5} + 0{,}018(1-e^{-850r/d}) \qquad (13)$$

The use of this equation eliminates inconsistent results for perfectly sharp plates as given by the previous equation.

An optical method for measuring the edge sharpness was proposed by Aschenbrenner (107) whereby the projection of a fine beam of light directed at the orifice edge is observed. The profile of the distorted image of the upstream face of the orifice and its bore is photographed. By a geometric equation, together with a reticle, the radius of curvature of the orifice edge is obtained. Upp (108) and more recently Jepson and Johnson (109) have improved on the design of the apparatus used by Herning. Brain and Reid (110) compared the three methods and came to the conclusion that for quick and accurate results the lead foil method was the most suitable.

Upp (108) suggested that to determine the actual relationship between the edge radius and the discharge coefficient required further investigation.

CHAPTER THREE

EXPERIMENTAL APPARATUS AND PROCEDURE

The major object of this thesis is to determine the effect that eccentricity and edge sharpness have on the coefficient of discharge of orifice plates.

In order to attain these objectives a test facility was designed which could be used to calibrate the orifice plates. From the results of these calibrations the discharge coefficient of each plate was determined. To determine the effect of edge sharpness, the edge radius of each plate was increased after each calibration and the coefficient of discharge of each plate was determined. To determine the effect of eccentricity similar tests were performed but the eccentric positioning of the orifice plate was varied.

Small changes in the coefficient of discharge were expected and therefore the minimum overall calibrating accuracy of the test equipment had to be ± 0,2 percent. Other criteria which the test equipment had to meet were:

a) To maintain a constant flow rate for the duration of any test.
b) To allow for the eccentric positioning of an orifice plate and for the accurate repositioning of the orifice plate during a calibration.
c) To allow for the calibration of orifice plates with varying edge sharpness.

d) To utilize the one hundred millimeter pipe line installed.

e) To use water as a working agent.

f) To comply with the most stringent specifications of the various engineering standards.

In addition to accurate flow measurement a method for the measurement of the upstream edge of an orifice plate was required. This could be achieved by reproducing the contour of the upstream edge of the orifice plate and then measuring the edge radius.

Finally a visual aid was required to obtain a better understanding of the changes in flow conditions which occur as a result of varying such parameters as edge sharpness, area ratio, eccentricity and Reynolds number.

3.1 CALIBRATING EQUIPMENT

To calibrate an orifice plate, constant flow in a pipe line is measured with the orifice plate and with a reference meter whose accuracy and repeatability is well known. The measured flowrates are compared and the orifice plate coefficient is determined. The accuracy of the overall system is slightly lower than that of the reference meter.

A wide variety of methods are used to calibrate orifice plates. Some of the more widely used ones are:

a) A Volumetric or Gravimetric Tank in the Standing-Start and Finish Mode.

A simple calibrating system of this type is shown in Figure 25. This system is based on comparing the volume or weight of working fluid passed through the test meter with the volume added to the tank during the period of calibration. The gravimetric system is preferred when calibrating with water or with high viscosity oils, while the volumetric method is generally used for calibrating with low viscosity hydrocarbons. This method is better suited to the calibration of quantity meters than to flow rate meters.

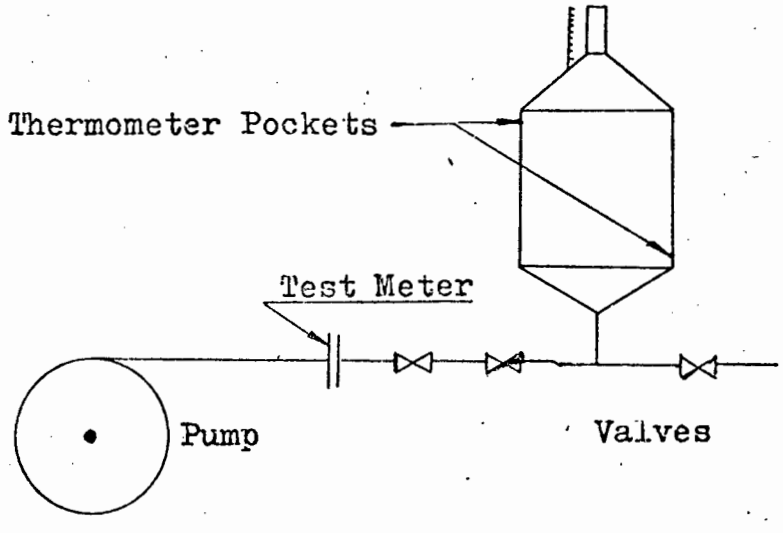

Fig.25. Method of Calibrating an Orifice with a volumetric tank in the standing-start & finish mode.

b) Gravimetric Flying Start and Finish Method with Dynamic Weighing

The calibrating equipment consists of a test meter, a timer and a weigh tank which has a dump valve at its base. The calibrating procedure is as follows: When the water in the tank reaches a preset weight a timer is set into operation until another preset weight is reached when the timer is switched off and the dump valve is opened. This method is suitable for calibrating at moderate flowrates, as at high flowrates inertia effects cause substantial errors.

c) Pipe Provers

A pipe prover consists of a hollow synthetic rubber sphere which is filled with water at a high pressure so that the diameter of the sphere is about two percent larger than that of the pipe from which the prover is constructed. The sphere is forced into the pipe so that it acts as a seal and as a piston which travels round corners. When calibrating, the fluid passes through the test meter, then through the prover and in so doing it takes the sphere from one end of the prover to the other. The time taken over a specified distance is recorded and the flowrate is calculated.

Pipe provers are expensive to install, but once installed they are reliable, rapid in operation, have a low operating cost and are highly accurate to ± 0,1 percent.

d) Gravimetric Flying Start and Finish Method with Static Weighing

This method of calibration is used successfully at NEL and ESCOM (111, 112). In this system the fluid passes through the meter, a control valve and then a fishtail, from where it emerges as a fan-shaped jet. The jet of fluid is then diverted into a reservoir (sump) or into a weigh tank. A switch connected to an electronic timer is operated by the diverter. In this way the time required to fill the weigh tank and also the mass of the water is measured.

This method is widely used where flowrate meters have to be calibrated with water.

3.1.1 The Design of the Calibrating Equipment

The calibrating equipment used in the experiments is similar to that used by the National Engineering Laboratory at East Kilbride in Scotland and by the Electricity Supply Commission at Rosherville Johannesburg in the Republic of South Africa.

This equipment was chosen for the following reasons:

1. The existing calibrating facility at U.C.T. is based on the above system and therefore only minor modifications were required.
2. The overall accuracy of the NEL and ESCOM calibrating facility is ±0,1 percent and thus it was assumed that similar accuracy could be achieved with similar equipment at U.C.T.
3. It is the most suitable equipment for calibrating orifice plates with water at medium flowrates (Re_d 10^5 - 5 x 10^5) in a laboratory.

3.1.1.1 General Layout of the Equipment

The general layout of the equipment is illustrated in Figure 26. The apparatus consists of a centrifugal pump which pumps the water from the sump into a constant head tank and from there through a flow straightener into the test section where the flowrate is measured with an orifice plate and this measurement is compared with that obtained with the reference meter. The reference meter is situated after the test section and it consists of a fishtail and a diverter. The diverter, which is pneumatically activated, diverts the water into the sump or into the weigh tank. During a calibration, an electronic timer is activated by the diverter so that the time during which the weigh tank is being filled is recorded. Thus from these readings the actual flowrate can be calculated.

Fig. 26 General Layout of the Experimental Equipment

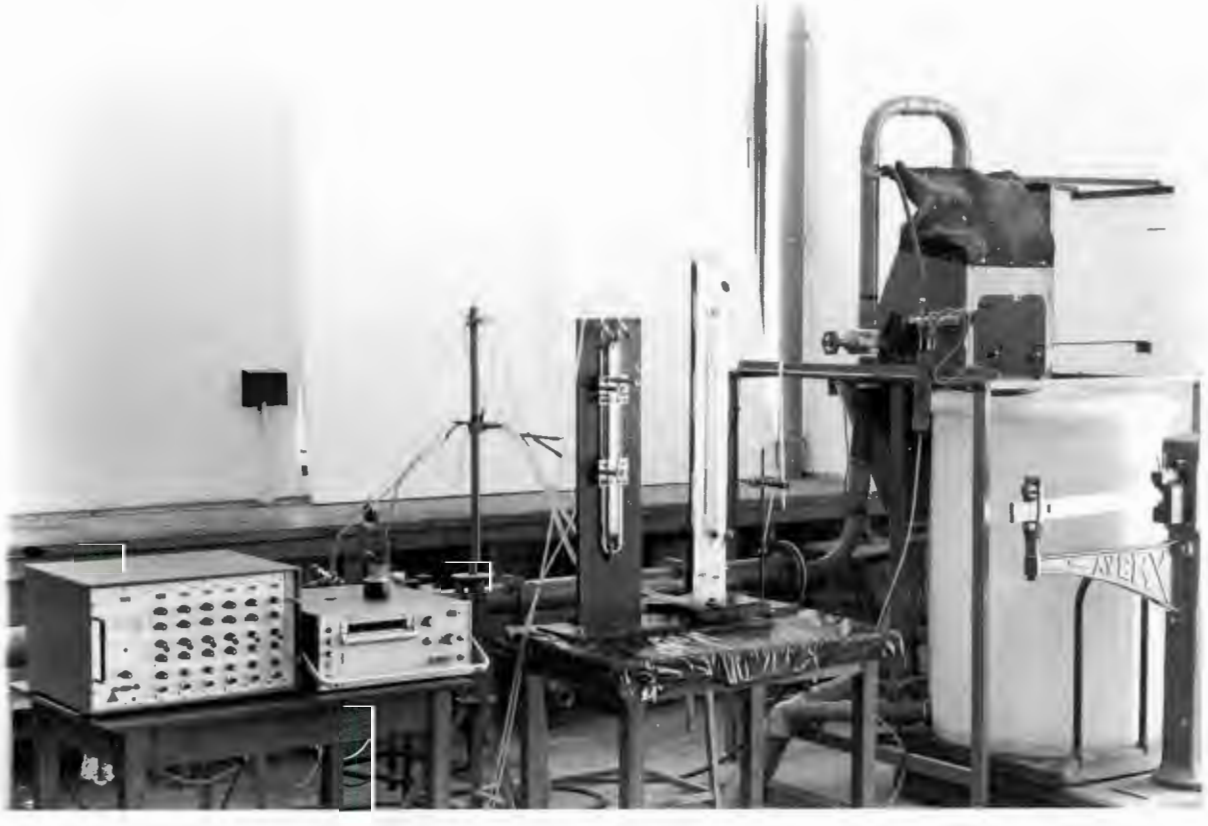

3.1.2 Detailed Description of the Calibrating Equipment

The apparatus consisted of the following parts:

a) Working Fluid

Water was chosen as the working fluid as it is incompressible, its properties are well known and it is readily available.

b) Apparatus to supply water to the Constant Head Tank

The water from the sump was delivered by a suction pump to the constant head tank. In order to ensure that no excessive rise in the water temperature would occur during a test due to the water being re-circulated the capacity of the sump was made to be five times that of the tank. Furthermore, the depth and length of the sump ensured that no vortex entrainment of air occurred at the pump and that no air bubbles were introduced at the point where the return water from the system and from the tank overflow were discharged into the sump.

To keep the water in the system free from large size solid impurities, it was strained by a coarse mesh filter before the pump and it was filtered by a combined medium and fine mesh filter after the tank.

c) The Constant Head Tank

As swirl and pulsating flow affect the accuracy of the orifice plate, direct pumping to the test line was not considered and a constant head tank was used to supply the test line with water. To ensure that no

large fluctuations in the height of the free surface occured, the tank was fitted with a weir. The excess water flowed over the weir into the overflow and back to the sump.

The flow to the tank could be adjusted with a valve which was positioned after the pump. By correctly adjusting the flow to the tank, fluctuations in the head which occurred as a result of a varying flow over the weir were limited to ten millimeters. The tank was 25 meters above the test line and thus the maximum pressure fluctuations in the test line did not exceed 0,04 percent.

d) The Test Section

The test section was supplied with water from the constant head tank via a flow straightener. The flow straightener was introduced to reduce the swirl and the eddying in the test section.

The test section was made from one hundred millimeter smooth commercial P.V.C. pipe. To ensure fully developed flow at the orifice plate the test section consisted of a straight length of round pipe over a distance of forty-seven pipe diameters upstream and fifteen pipe diameters downstream from the orifice plate. The orifice plate and the test section complied with the requirements of BS 1042:1964.

The orifice plate was installed between specially designed flanges which allowed for the eccentric installation of these plates and for the accurate repositioning of a plate during testing. The plates used were round or rectangular depending upon whether tests for either edge sharpness or eccentricity were being conducted. The flowrate was set by the

use of a valve which was situated in the fifty millimetre pipe line after the test section.

e) The Diverter

The water flowed through the test section into the diverter via a "fish tail" which was introduced to change the circular jet issuing from the pipe into a thin rectangular one.

The diverter frame was pivoted above its centre of gravity so that the water could be diverted to the measuring tank or to the collecting trough. The collecting trough was connected to the sump. To avoid spillage of water due to splashing at high flowrates, the diverter top and bottom arms were covered with rubber sheeting (Figure 27).

The time taken for the flow to be diverted into the measuring tank was measured ~~in milliseconds~~ by means of a crystal-controlled electronic timer which was actuated by a photo-electric cell mounted adjacent to the rear of the diverter. A brass plate was fitted to the rear of the diverter and when the diverter was actuated this brass plate cut across the light emitted by the photo-electric cell and so actuated the electronic timer.

The diverter was actuated by a double-acting pneumatic cylinder to which air was supplied by means of a "Hydrovane" compressor. The diversion was started by pressing a spring return valve,which actuated the pneumatic cylinder, thus effecting the diversion. Thus the complete operation of the diverter and of the timer was controlled by this valve.

Fig.27. The Diverter, the Measuring Tank, Weighing Scale and the Diverter Actuator and Timing Mechanism

The rectangular jet issuing from the "fish tail" was of finite thickness and therefore it took a finite time for it to be diverted. Due to this fact the diversion of the jet had to be as fast as possible, the velocity of traverse had to be equal in both directions and the brass plate which acuated the timer had to be so positioned that the electronic timer was started and stopped when the diversion plate crossed and recrossed the mid-point of the jet. To ensure equal velocity of traverse of the diverter in the two directions, a restrictor was introduced into the pneumatic circuit. The speed of traverse of the diverter was set by adjusting the delivery pressure of the compressor.

f) The Measuring Tank

A large capacity measuring tank was used so as to allow for the accurate determination of the mean flow rate. The level of the water in the measuring tank could be observed through the sight glass which was fitted into the side of the tank. The tank was covered so that no losses due to splashing would occur.

The measuring tank was placed on a measuring scale so that the mass of the tank and its contents could be determined at all times. To ensure the accurate determination of the mass of the tank the measuring scale was calibrated regularly against assized weights.

g) The temperature measurement

The temperature of the water in the tank as well as in the test section was measured in order that the density of the water could be accurately determined.

To measure the temperature in the test section, measurements both upstream and downstream of the orifice plate had to be taken. For this purpose thermometer pockets were fitted into the pipe. In order to avoid any disturbance in the flow at the orifice plate as a result of the insertion of the thermometer pockets, these pockets were placed forty six pipe diameters upstream and fifteen pipe diameters downstream from the orifice plate and were allowed to protrude only thirty millimeters into the pipe.

To measure the temperature of the water in the test section and in the tank, mercury thermometers were used. These thermometers were calibrated against a standard thermometer.

To accurately determine the density of the mercury in the manometer the temperature of the atmosphere surrounding the manometer was measured.

h) The Pressure Measurement

D & D/2 taps were chosen as they are commonly used in industry. Some of the other factors which were considered when the choice of taps was made were:

a) that the downstream tap lies in the vicinity of the vena contracta for orifice plates with a wide range of area ratios and for a wide range of flows, resulting in stable pressure readings and in large pressure drops being recorded.

b) that the coefficient of discharge for orifice plates fitted into installations with D & D/2 tappings is specified in a number of engineering standards.

To obtain reliable average pressure differential readings four D & D/2, tappings were connected by a ring chamber (Figure 28).

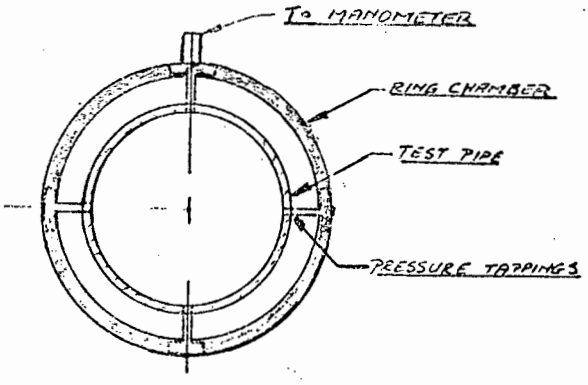

Fig. 28. The Ring Chamber at one of the Tapping Positions

The pressure differential was measured with a water-mercury and a water-air inverted manometer. The mercury manometer was specially designed for this experiment (See Appendix B for details). Some of the features of this manometer were: a least count of 0,05 millimeters; valves allowing for the purging of the manometer from air; and valves which allow for the flow to the manometer to be shut off instantaneously and thus for accurate instantaneous pressure differential readings.

To determine the magnitude and the frequency of fluctuations in the differential pressure and the cause of these fluctuations, a pressure differential transducer was installed between the ring chambers. The transducer output was amplified and recorded by means of an ultra violet recorder. In order to obtain accurate readings the transducer was calibrated against a dead weight pressure gauge calibrator. Thus with this apparatus continuous recording of the differential pressure across the orifice plate was possible.

3.1.3 Some Factors Affecting the Method of Calibration

1. Pressure Differential Fluctuations

Although the static pressure in the test line was kept constant to within 0,04 percent, due to turbulence in the line, small fluctuations in the flow occurred resulting in fluctuations in the pressure difference readings. The magnitude of the fluctuations was dependent on the flow rate. Using the high speed pressure differential transducer, it was found that the fluctuations at the maximum flow rate across the orifice plate were in the order of ± 4 per cent.

The magnitude of the pressure fluctuations when measured with the mercury manometer was lower than when measured with the pressure transducer. For example, when using the mercury manometer, the meniscus fluctuations were in the order of 0,3 per cent at low flow rates and 0,7 per cent at high ones.

To determine what caused the pressure fluctuations in the test line, the fluctuations as measured with the pressure transducer were recorded with an ultra violet recorder. The recordings showed that the variations in the pressure differential were random and thus these fluctuations were expected to be caused by natural turbulence. To prove that these pulsations were not due to such factors as water hammer or "chatter" * (113) an investigation was conducted. Calculations showed that the pulsations were not due to either of these factors and thus it was concluded that they were due to natural turbulence.

Even though fluctuation in pressure occurred, the mean pressure differential reading was expected to remain constant if it were to be determined

* *Note: CHATTER is defined in Reference 122 as being similar in characteristic to water hammer but it is a result of elasticity in the fluid system. For example, aeration or air entrainment could cause chatter. Chatter can be detected by the axial oscillation of the fluid system.*

from a number of readings taken at random intervals of time. Tests to determine how many readings had to be taken with the mercury manometer so that the average readings would remain constant to within ± 0,05 millimeters of mercury, were conducted. It was found that a minimum of twelve readings were required at high flow rates while at low flow rates eight readings were sufficient. To keep the experimental procedure as simple as possible it was decided to take twelve pressure readings irrespective of the flow rate.

2. Mechanical Vibrations

It was observed that during its operation the diverter caused the frame on which it was mounted to vibrate. Since the pipe joining the test section to the "fish tail" was fixed to this frame, the lateral vibrations were transmitted to the test section.

To reduce the amplitude of the transmitted vibrations a rubber pipe was introduced into the system. It was positioned between the test section and the control valve. After the introduction of the rubber pipe no vibrations in the test section were observed.

Tests to determine whether the operation of the diverter would affect the pressure differential readings were conducted. The following procedure was followed: The diverter was operated on a number of occasions with no flow in the test section. The pressure difference was measured with the pressure transducer. Zero reading was recorded on each occasion and therefore it was concluded that the operation of the diverter did not affect the pressure differential readings. Further tests showed that the vibration of the frame did not cause any change

or spillage in the diverted flow.

3. Pipe Diameter

The various engineering standards specify that the pipe must be round within certain limits in the vicinity of the orifice plate. In order to ensure that the requirements of these standards were adhered to, the diameter of the pipe was measured in a number of places in the vicinity of the orifice plate. The positions where the measurements were taken is shown in Figure 29. Six readings around the circumference of the pipe were taken at every position. From those measurements the diameter of the pipe was determined. Radial expansion in the P.V.C. pipe was expected with increasing flow rate and temperature. Such expansion could not be detected during any test by means of the vernier calipers used. These calipers could be read to ± 0,025 millimeters. From the results obtained it was concluded that the pipe diameter should be considered constant for calculation purposes.

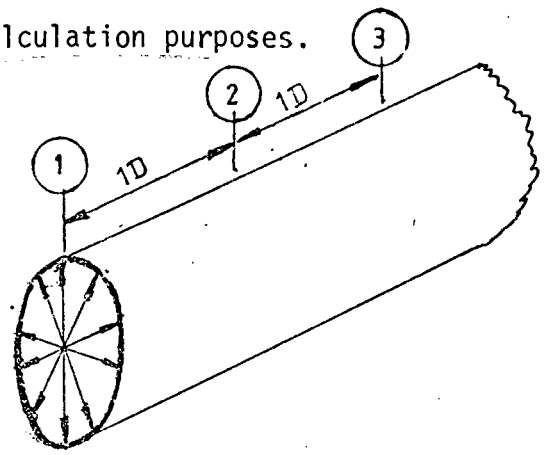

Fig. 29. The position where the diameter of the pipe was measured

4. The Orifice Diameter

The orifice plate was made from brass. Since the coefficient of thermal expansion of brass is high, the change in orifice plate diameter with

change in the water temperature should have been significant. Assuming that the temperature of the plate was equal to that of the water flowing through it, the maximum temperature variation from 18 degrees Celsius was ± 10 degrees Celsius. The largest orifice plate would have increased or decreased in diameter by 0,02 millimetres. This variation in the diameter of the orifice plate was considered significant and was taken into consideration in the calculations.

5. The Density of the Water

To ensure that the coefficient of discharge of any orifice plate would be determined to an accuracy of±0,1 per cent, the density of the water was determined experimentally at various temperatures to within ±0,01 per cent. Since the density of the water had to be known accurately, small changes in its value due to factors other than temperature had to be considered. For example particles of dust and dirt could have collected over a period of time in the sump and they could have dissolved in the water. To ensure that no change in the density other than that predicted by the temperature variation occurred, tests were conducted monthly. The findings showed that the density at a specific temperature remained constant with time.

6. The Buoyancy of the Air

The mass of air displaced from the tank by the water during a particular test was taken into account. It was found that if this factor was neglected an error of 0,1 per cent would result.

7. Equal Velocity of Traverse of the Diverter in both Directions

When the forward diversion into the measuring tank took place some water (volume A) passed into the measuring tank before the timer started and some water (volume B) passed into the sump after the timer had started (See Figure 30). The two volumes had to be equal and self-compensating for zero error. Similarly, when the return diversion out of the measuring tank and into the sump occurred, some water passed into the sump before the timer stopped and some water passed into the measuring tank after the timer had stopped. Thus, to ensure zero error the following criteria had to be fulfilled:

a) Equal velocity of traverse in both directions was required so that any error introduced during the forward diversion would be compensated for by an equal and opposite error during the return diversion.

b) The shape of the flowing jet had to be symmetrical, the timer switch had to be placed at the geometrical centre of the diverter and the centre of the jet had to coincide with that of the diverter so that during the forward or during the return diversion the volumes A & B described above would be equal and self-compensating.

c) A high velocity of traverse is required so as to minimize any possible error which could be introduced during a diversion.

To ensure equal velocity of traverse in the two directions, the following experiment was performed periodically: The timing plate was replaced by a small plate which could be mounted in such a manner that it would be symmetrical about the diverter plate. The diversion time in either direction was measured and the restrictor in the pneumatic line was reset until equal diversion time in the two directions was achieved. The diversion time in either direction was seventy seven milliseconds which time was achieved when the compressor operating pressure was set at 689,5 kN/m^2.

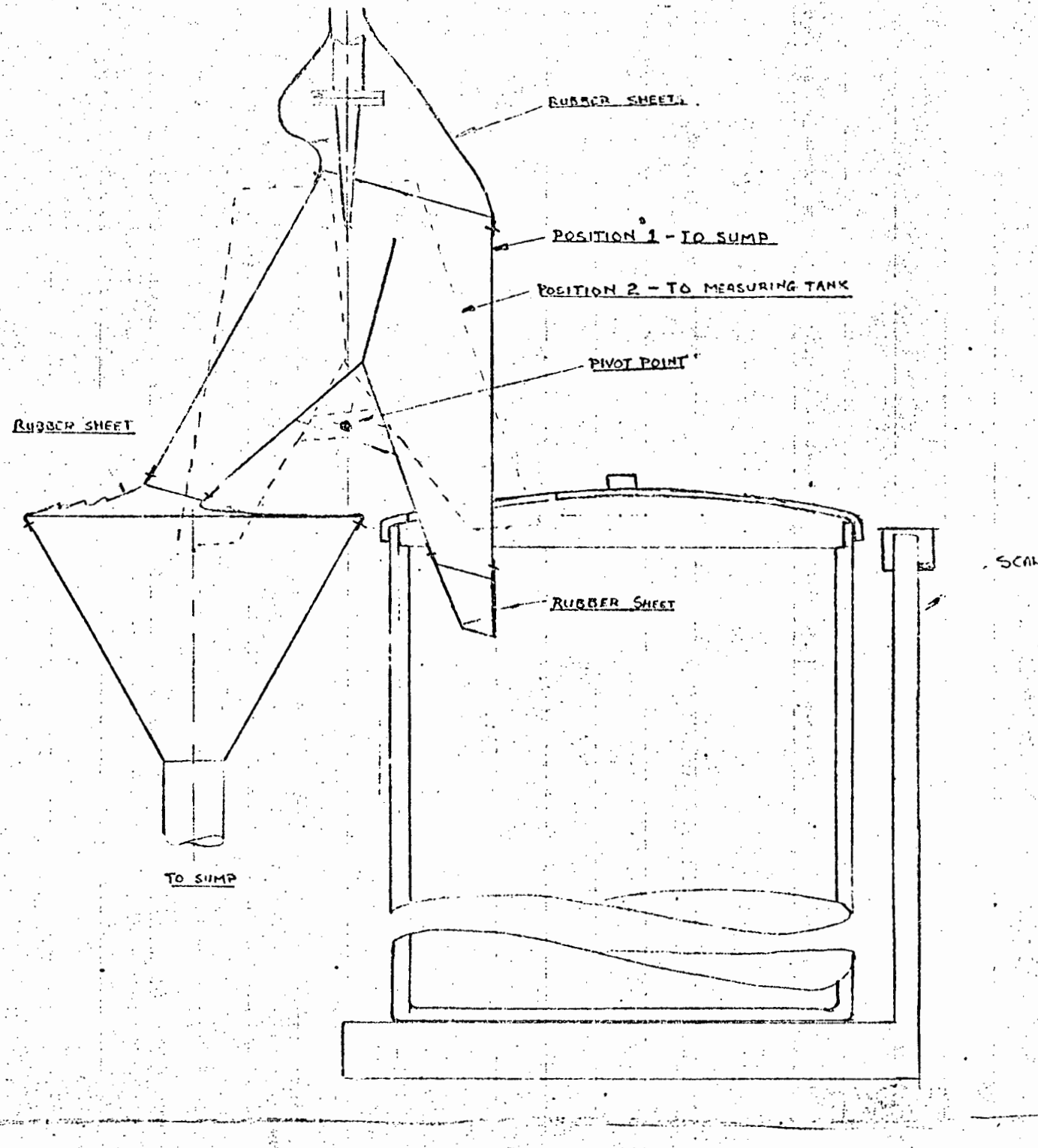

Fig.30. Positions of the Diverter

8. The Condition of the Orifice Plate

The orifice plate and the test section were designed to conform to the specifications of BS 1042:1964. The British standard on flow measurement

was chosen as at the time of the design of the orifice plates only this engineering standard was available in the library and its specifications were considered to be as relevant as that of any other recognized engineering standard.

To ensure that the orifice plates which were made by the department's workshops conformed to the required specifications, the following checks were made:

a) The upstream sharpness of each plate was measured by the lead foil method described in section 3.2. The sharpness ratio (edge radius/ orifice diameter) of the sharp orifice plates was found to be less than 0,0004. The only orifice plate with a sharpness ratio greater than 0,0004 was plate number one whose area ratio was equal to 0,1 (i.e. the plate with the smallest orifice diameter).

b) The surface roughness of the orifice plates was measured with a "Talysurf" meter. To ensure that the worst condition of the surface of the orifice plates was recorded, measurements were taken at positions where major blemishes or major imperfections in the surface of the plate were detected. Thus the average surface roughness of the plate was better than the recorded one. The measurements obtained showed that the surface of the plates was smooth and was equivalent to a ground finish.

c) The dimensions of the plate, the flatness and the straightness of the plate were also measured. The plates conformed to the requirements of BS 1042:1964.

3.1.4 General Method of Calibrating an Orifice Plate

a) Start up Procedure

Before starting to calibrate an orifice plate the following procedure was followed:

If an orifice plate was mounted between the flanges, then it was checked in order to ensure that the correct orifice plate would be calibrated. Before installing an orifice plate care was taken to check the condition of the plate. After the plate was installed the test section was straightened and levelled by adjusting the pipe supports. The pump was then primed and started. The control valve was turned until the desired flow rate was achieved. To ensure that the level in the constant head tank remained constant and that the temperature of the circulated water would not rise excessively, the rate of overflow was adjusted until a slow, steady rate was achieved.

Before starting the calibrating procedure the manometers were levelled and the manometer line was purged of the air which was entrapped in it. The manometer leads which were open to the atmosphere were then clamped. The oil level in the thermometer pockets was then checked. This procedure was necessary to ensure that correct instrument readings would be achieved.

b) Calibrating Procedure

After the start-up procedure was completed the calibrating of the orifice plates could begin. The calibrating procedure was as follows:

Five pressure differential readings were taken before preparation for the first diversion was started. The preparation for the first and second diversion entailed the closing of the drain valve of the measuring tank, the weighing of this tank, the switching on of the electronic timer and of the

photo-electric cell and the starting up of the compressor. The diverter was then actuated. While the tank was filling up, the temperature was taken of the water in the test section, in the tank and of the atmosphere. The pressure difference across the orifice plate was measured. When the measuring tank was nearly full the diverter was actuated and then the mass of the measuring tank was noted. The time taken to fill the measuring tank was then read off from the digital display of the electronic timer.

Before the second diversion was started the measuring tank was drained and four more pressure differential readings were taken. The procedure followed during a diversion was repeated. After twelve pressure readings had been taken and the procedure for the second diversion was completed the flow rate was increased and the overflow was readjusted.

The procedure described above was then repeated until tests over twenty-four flow rate readings over the full range of flow was completed.

c) Tests for Repeatability

The procedure which is described above for calibrating an orifice plate at a specific flow rate was adhered to. The difference lay in the fact that at each flow rate setting eight readings were taken. The flow rate settings at which tests for repeatability were conducted were as follows:

1. low flow rate (about 4 kg/s)
2. medium flow rate (about 8 kg/s)
3. high flow rate (about 10 kg/s)
4. maximum flow rate (about 13 kg/s)

The above tests were performed with an orifice plate with an area ratio of

0,3 and the object of these tests was to prove the repeatability of any reading at a particular flow rate.

The next day the orifice plate was replaced with one which had an area ratio of 0,55. This plate was used as it had the largest area ratio of the plates which were to be calibrated and thus the pressure difference across this plate would be low even at high flow rates and therefore repeatability under the worst conditions would be proved.

The plate was calibrated over the full range of flow. As described in the calibrating procedure each orifice plate was calibrated at twenty four flow rate settings. These flow rate settings varied from maximum to minimum and for this experiment they were increased or decreased from reading to reading at random. The above procedure was repeated four times during the following four days. Before repeating the procedure the orifice plate was first removed and then reinstalled between the flanges. The object of the above procedure was to prove the repeatability of a set of readings at any time under all operating conditions.

Similar tests were performed with the orifice plate whose area ratio was 0,15. These tests were conducted as the pressure difference across this orifice plate had to be measured with both the mercury manometer at high flow rates and with the inverted water manometer at low flow rates.

3.1.5 Tests for the Effect of Eccentric Location of an Orifice Plate

For these experiments specially designed rectangular orifice plates with area ratios of 0,15; 0,45 and 0,55 were used. These orifice plates could be moved vertically up or down from the centre position by means of the

adjusting handle. The centre position was defined as the position where the centre of the pipe coincided with the centre of the orifice and it was possible to locate this position by means of a dowel pin.

The procedure followed for calibrating each plate was similar to that described in section 3.1.2 with the exception that initially each plate was calibrated in the central position and then in various eccentric positions. Before each calibration was started the eccentricity of the orifice plate was measured with the dial gauge, which was fitted to the flange, and the reading obtained was noted.

3.1.6 The Procedure Followed to Determine the Effect of Rounding the Upstream Edge of an Orifice Plate

These experiments were performed with orifice plates of area ratios of 0,1; 0,2; 0,3; 0,4 and 0,5. The same procedure as described in section 3.1.2 for calibrating an orifice plate was followed. Before a plate was calibrated, its upsteam edge radius was measured and any blemishes or imperfections visible at these edges were noted. After the calibration was complete the upstream edge radius of the plate was increased and measured. When the required edge sharpness was achieved the orifice plates were recalibrated. This procedure was repeated until sufficient data was available on the effect on the coefficient of discharge of varying the edge sharpness of a particular orifice plate. In general an orifice plate at five different edge radii was calibrated. When all the experimental readings were completed then calibration curves for each plate were drawn.

3.2 UPSTREAM EDGE RADIUS MEASUREMENT

To achieve the objectives of this thesis it was important to develop a way or means by which the upstream edge radius of an orifice plate could be measured accurately.

The problem facing other researchers in this field was how to measure the upstream radius of the orifice plate without damaging or destroying the plate itself. This problem has been overcome in recent times by the development of the following three methods:

1. The casting method.
2. The lead foil method.
3. The optical method.

Method 1 uses the orifice plate as a mould for casting a replica of the edge from a cold forming plastic. The resultant cast follows the contour of the plate closely but a number of disadvantages or problems exist with this method. These are:

(a) The operator has to be highly skilled to produce a good casting which is free from air bubbles and is not distroted during shrinkage.

(b) The time taken for a complete measurement is more than twenty four hours.

Method 2 which was initially developed by Herning was based on the idea of obtaining an impression of the upstream edge of the orifice by pressing a very thin lead foil onto it. The problem with this method was that sometimes a fragment of lead jutted out into the radius of the remaining impression which rendered measurement impossible.

In the Optical Method a fine beam of light was projected onto the orifice edge and the image obtained was photographed. Using geometric equations the edge radius of the orifice plate was then calculated. The disadvantage of this method was the lower accuracy obtained for any measurement.

The above methods, their advantages and uses were discussed in detail in Appendix B.

3.2.1 Apparatus Used

In order to help decide which method to use for measuring the edge sharpness of the orifice plates tested a short experiment was performed (see Appendix B for detail). The experiment consisted of measuring the upstream edge of an orifice plate at a specific point by using both the casting and the lead foil methods. The optical method was not tried as Brain and Reid stated that "this method was the least reliable of the casting, lead-foil and optical methods". The casting method proved to be laborious and the obtained radius was not measurable. This was due to the fact that Technovit and Epikote 816 which were recommended by Gallacher for use in the casting method were not available and silastic had to be used instead. To obtain a thin and straight slice of silastic was difficult and thus photographs obtained showed a double edge thus making it difficult to measure accurately the upstream edge radius.

The lead foil method proved to be quick. A measurement could be completed in a few minutes and reasonable repeatability was achieved. The extent to which the imprint in the lead followed the edge was not known, but it was known that Brain and Reid found that good agreement exists between the measurement obtained by the casting method and by the lead foil method. Based on the above findings the lead foil method was adopted.

To ensure repeatable and accurate measurements of the upstream edge radius of an orifice plate a lead foil holder was designed (see Figure 31). The criteria for the design of a holder were the following:

(a) It should be capable of clamping the orifice plate in a position such that if an impression of its upstream edge were to be taken, then such impression would be along a diameter of the orifice plate.

(b) The orifice plate when clamped in the holder would have to be perpendicular to it and the approach of the lead foil to the holder would have

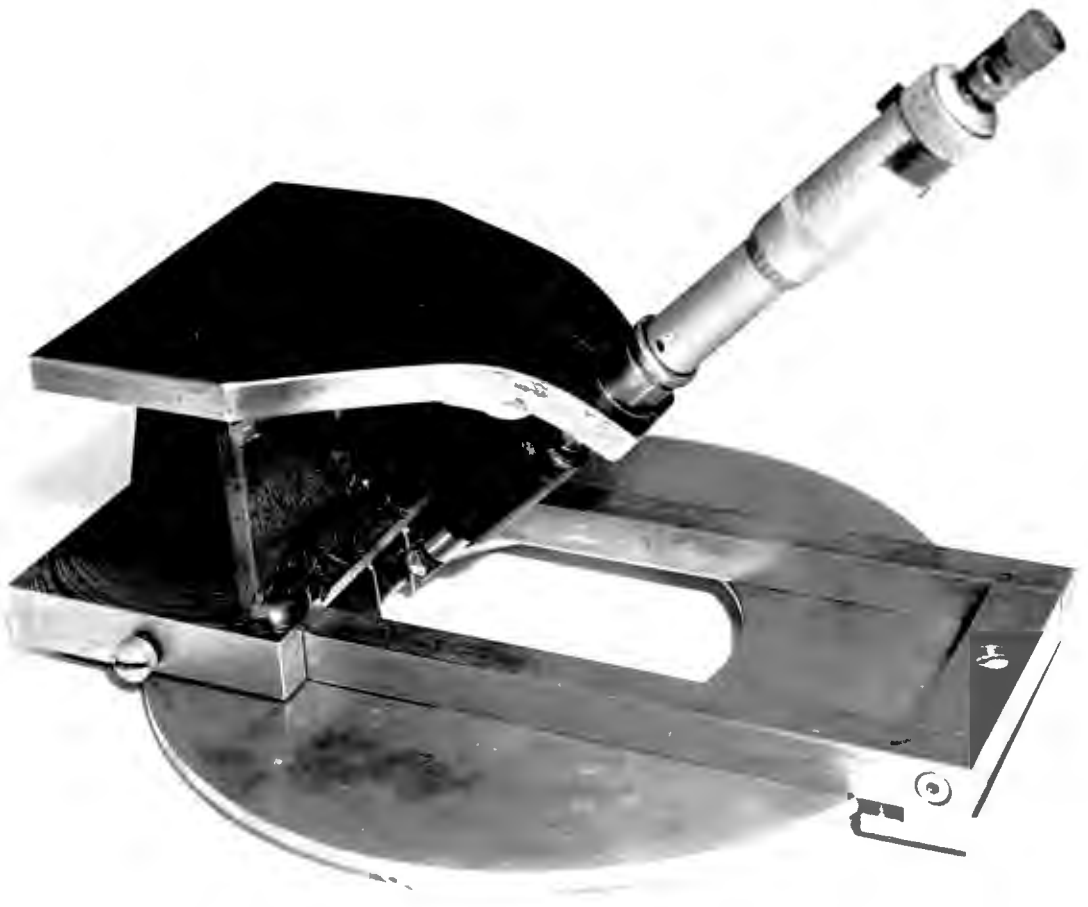

Fig.31 . Lead Foil Holder Designed to Measure the Upstream Edge Radius of an Orifice Plate

to be perpendicular to it and the approach of the lead foil to the holder would have to be at an angle of forty-five degrees to the upstream face of the plate.

(c) The depth of each impression taken would have to be the same for each and every measurement.

The lead foil holder designed fulfilled the above criteria with the exception that the depth of the impression was controlled by a micrometer screw and therefore the operator had to ensure that the depth of each impression was the same. An additional feature of the holder, not regarded as one of the pre-requisite design criteria listed above, was the facility for lifting the lead foil from the orifice edge without distorting the imprint which it contained. This was achieved by means of a spring assisted return device for the retraction of the lead foil from the orifice edge.

3.2.2 Method of Measurement

Six positions where impressions were taken of the upstream edge were marked onto the orifice plate with a "koki" pen. The orifice plate was then clamped into the holder in such a manner that the impression taken was at one of the marked positions. The lead foil was clamped into the holder so that a thin edge of about 1,5 millimetres deep projected from the end of the clamp as illustrated in Figure 32. The micrometer arm was turned until the depth of the imprint was one millimetre, after which the direction in which the micrometre had been turned, was reversed. When the arm which held the lead foil was lifted clear of the plate, the lead foil was removed by means of a pair of tweezers and transferred onto a transparent negative which bore the image of a scale graduated accurately in half millimetres. The lead foil was held in position on the film by a small piece of tape and then the film was placed into a slide holder.

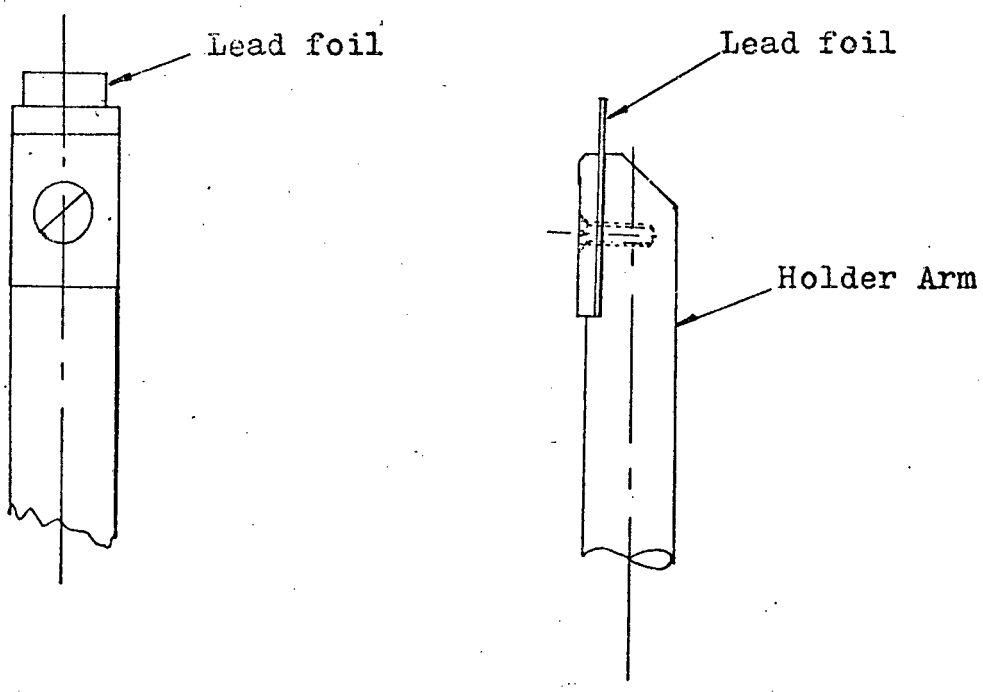

Fig. 32. Method of Clamping of Lead Foil into the Holder.

The slide was then examined under a small microscope. If the radius was measurable then the slide was placed into an enlarger and the enlarged image obtained on a screen was photographed. Some of the photographic prints obtained, showing the imprint of the orifice edge magnified three hundred times, can be seen in Figure 33a. From these photographs the radius of the upstream edge of the orifice plate was measured with a template or a radius curve. For each orifice plate the average edge radius measured at the six different positions was assumed to be the edge radius of that particular plate.

3.2.3 Tests to Prove Repeatability of Edge Sharpness Readings

In order to prove the repeatability of edge sharpness measurement when the measurements are conducted as described in section 3.2.2, the following experiment was performed. An orifice plate was clamped to

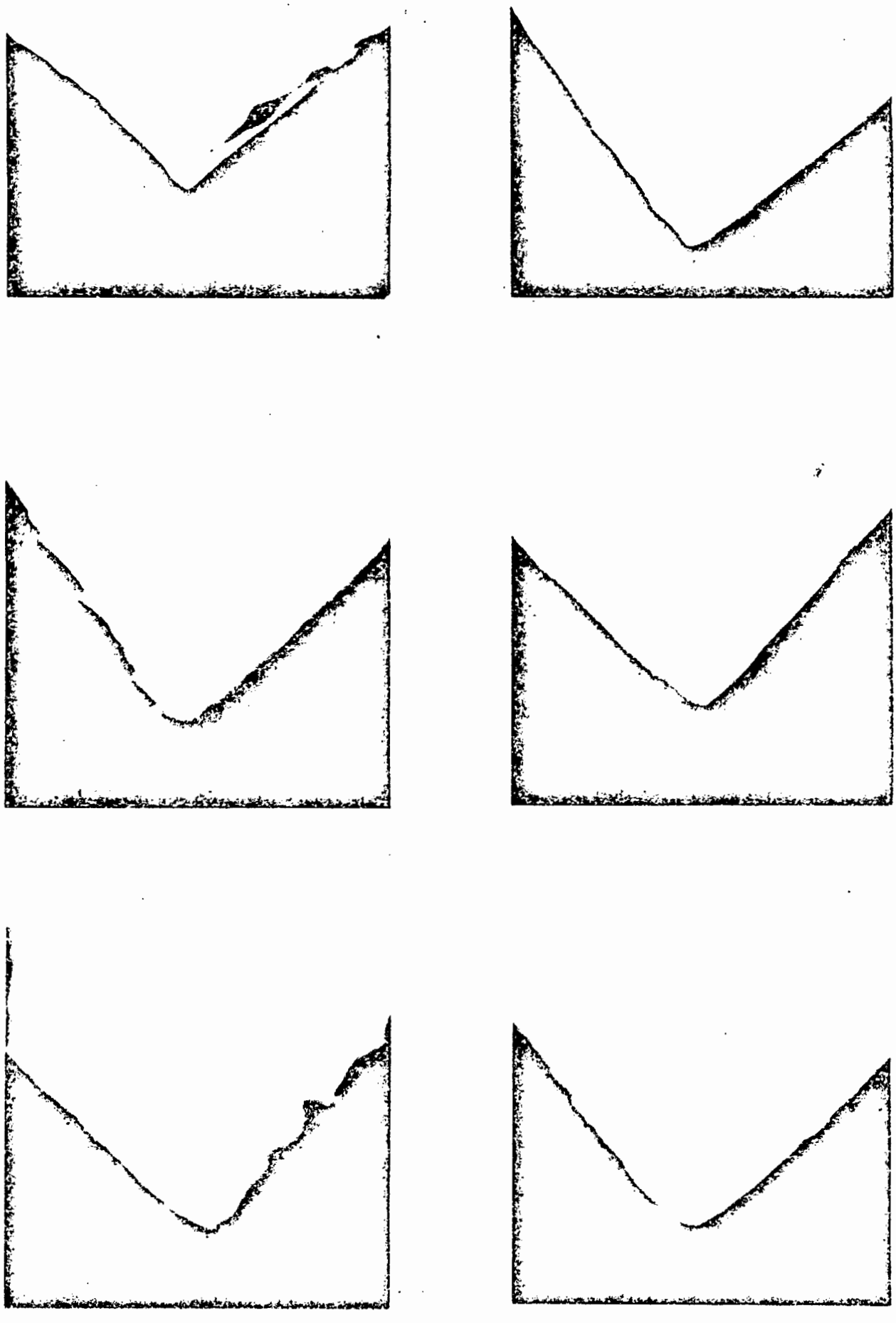

Fig.33a. Photograph of the image of the imprints obtained in the lead foil when measuring the edge sharpness of an orifice plate (magnification 300).

the holder and six consecutive impressions of the same edge were taken. The plate was then rotated through 45 degrees and six impressions of the edge of the plate at these positions were again taken. The resultant measurements of a specific edge were then compared. Similar tests were then conducted to show repeatability of measurements of the edges of plates with comparatively large edge radii.

3.2.4 THE METHOD OF INCREASING THE EDGE RADIUS OF A PLATE

The orifice plates and the flanges which held the orifice plates were made with the aid of a jig. This jig ensured that the centre of the orifice coincided with that of the flanges whose centre coincided with that of the pipe. To increase the edge radius of an orifice plate, the plate was placed into the jig which was placed in the appropriate lathe. Using fine emery paper rolled onto a ten millimeter brass tube, the upstream edge of the orifice plate was rounded. To ensure that the edge radius was made approximately equal around the circumference of the orifice, the edge was initially inspected with a magnifying glass and later using the lead foil technique, it was measured in six different positions around the circumference of the orifice.

3.2.5 PROPLEMS ENCOUNTERED IN MEASURING THE EDGE RADIUS

The repeatability of the edge sharpness reading varied from $\pm$ 2 percent to $\pm$ 5 percent depending on the sharpness of the edge. The factors which caused the low repeatability of a reading are discussed below.

The extent to which the imprint in the lead foil followed the upstream edge profile is not known and therefore the accuracy of the measurements is unknown. When the imprint in the lead is made, elastic and plastic deformation in the lead occurs and the possibility of errors due to elasticity can not be ignored.

Although the lead foil holder was designed to ensure that no distortion during the retraction of the foil from the edge would occur, on a number of occasions distortion of the edge occured. On these occasions double edges were observed on the photographs. Improvement to the spring retraction mechanism in the apparatus

helped to avoid this occuring. Distortion during the removal of the foil from the holder was another problem which could only be avoided by careful handling. The above shows that for accurate measurements using the lead foil method requires a skilled operator.

The accurate determination of the magnification of the edge profile was difficult with the apparatus used. This was due to the thickness of the scale markings when magnified three hundred times. The measurement of the distance between the scale markings was open to personal interpretation. The maximum error that could have occurred in the determination of the magnification was $\pm$ 1 percent.

The method of measuring the edge radius of an orifice from the magnified imprints with a template is shown in figure 33b. It was difficult to determine the correct edge radius as the upstream edge of the orifice plate was not always perfectly round and because the diameter of the templates available increased in one millimetre intervals. The limited sizes in which the templates were available could have caused a maximum error of $\pm$ 2,5 percent.

On a number of occasions the profile of the orifice edge was not perfectly round and its shape was similar to that shown in figure 33c. This lack of roundness was due to a lack of control in machining the size and shape of the edge profile while the edge radius was increased. To measure the edge radius of an orifice plate whose edge was not perfectly round was very difficult. In these cases the roundness of the edge was estimated.

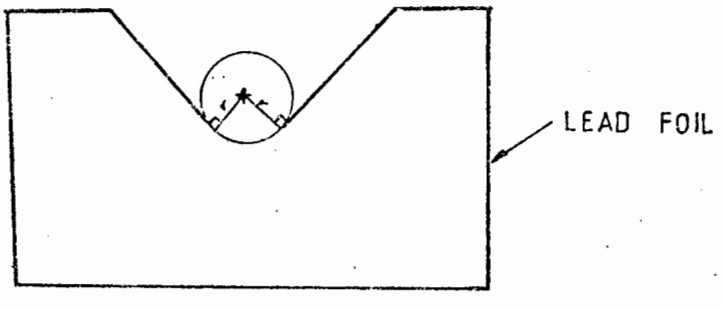

Fig. 33b. The Method of Measuring the Edge Sharpness with a Template.

On a number of occasions fragments of lead jutted out into the radius thus making measurement impossible. This problem occurred frequently especially when very sharp edges were measured. This occurrence was due to curling up of the displaced lead onto the sides of the imprint. (Fig. 33d). This factor could have caused the double edges and the undefined edges of the imprints observed in some of the photographs. Examples of problematic prints are shown in figure 33e. In all these cases new imprints had to be taken.

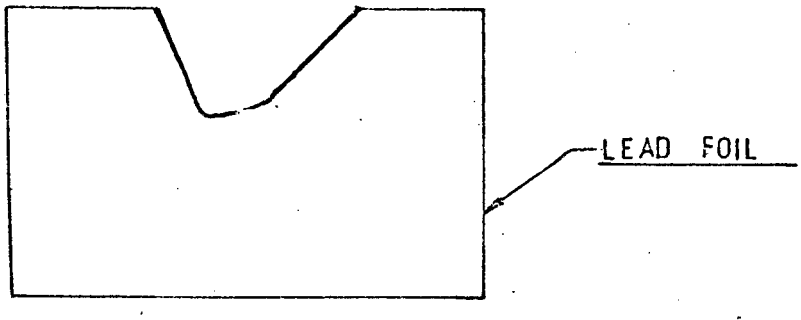

Fig.33c. A sample of the Shape of the Edges of some of the Orifice plates.

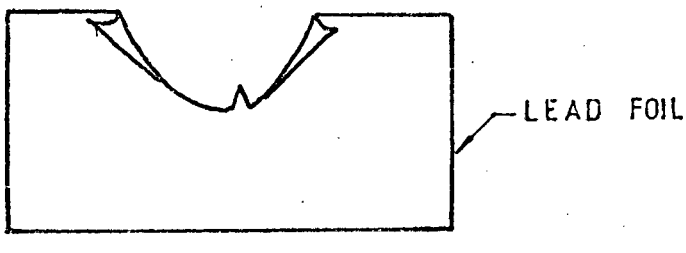

Fig.33d. Curling up of the displaced lead onto the sides of the imprint.

Upp and Crokett had encountered similar difficulties using the lead foil method. They had found that from eight measurements of the same edge, one was not measurable and the other seven were within $\pm$ 1,5% of the mean. The difference in repeatability between their measurements and the experimental ones was due to a difference in the technique and the apparatus used. This emphasised the skill which was required to obtain accurate measurements using the lead foil method.

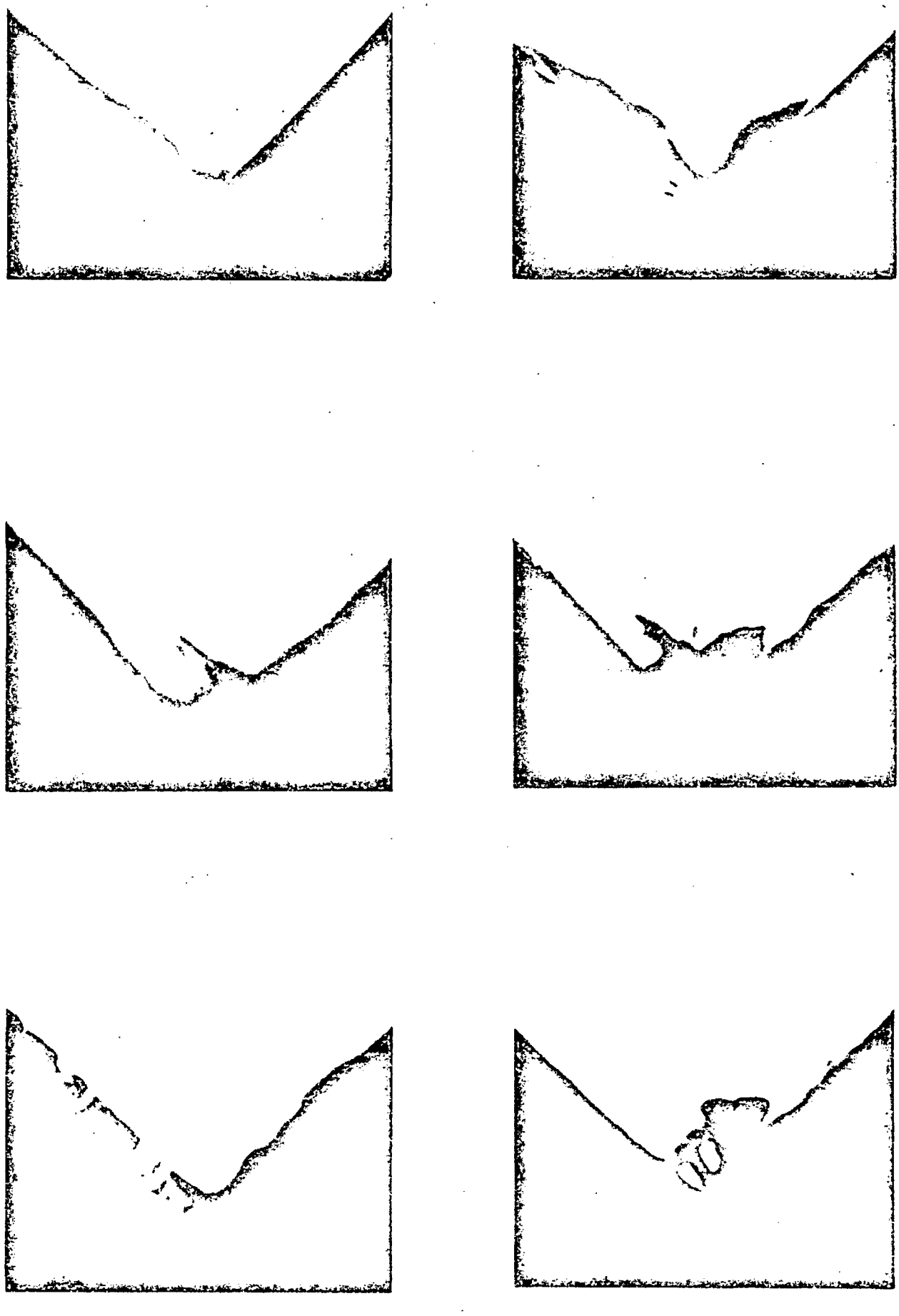

Fig33e Examples of Problematic imprints obtained.
(magnification equals 300)

3.3 APPARATUS USED FOR FLOW VISUALIZATION

In order to achieve a better understanding of flow through an orifice plate, separate tests were conducted utilising a smoke tunnel to simulate the flow through an orifice plate:

(a) whose edge radius was gradually increased; and

(b) which was positioned eccentrically to the pipe line.

The pipe walls and orifice plate were built from thirty millimetre thick wood which was sanded in order that a smooth finish would be obtained. This structure was then fitted into the smoke tunnel (See Figure 34). The smoke tunnel was fitted with a small variable speed fan which allowed for the control of the speed of the smoke which was blown through the tunnel. Photographs of some of the flow patterns obtained are shown in Figure 35.

Fig.34. Smoke Tunnel Used for Flow Visualization.

Fig.35a. Upstream edge of Orifice Plate slightly Rounded. Low Flow Rate

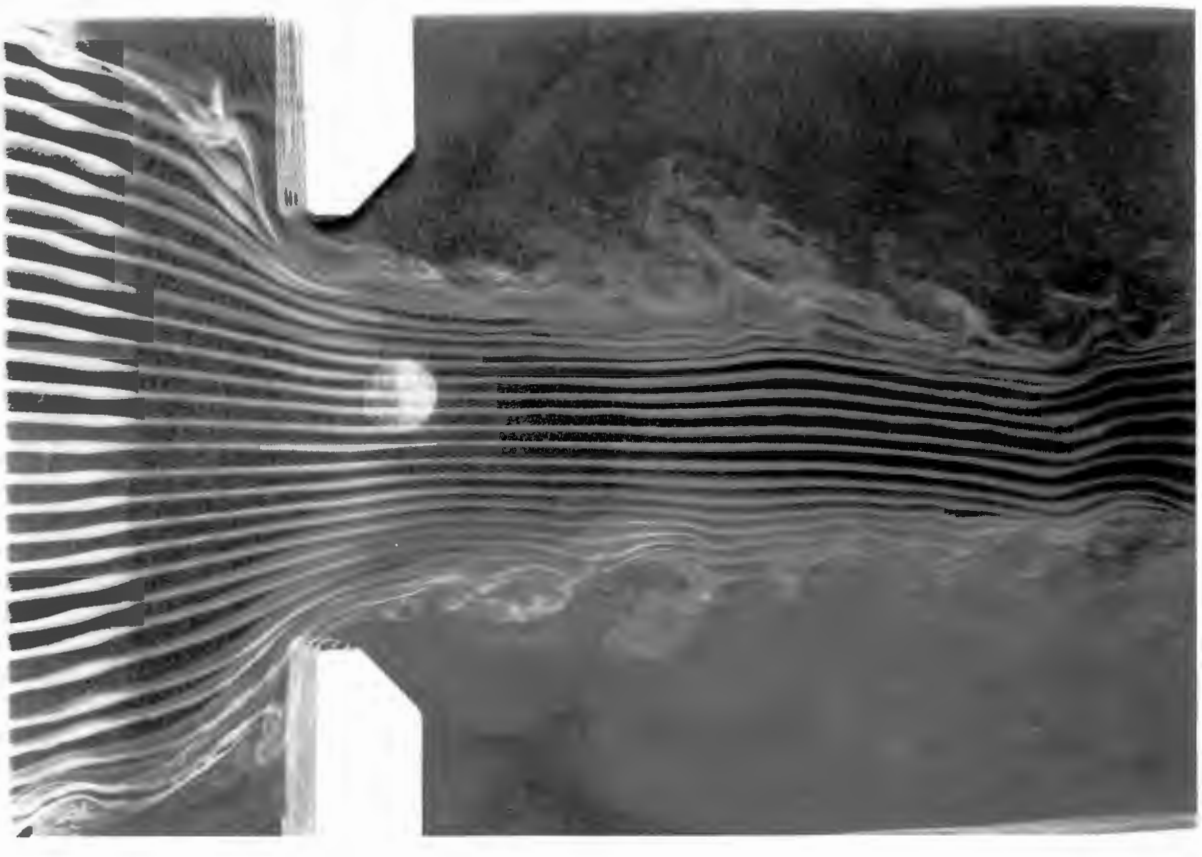

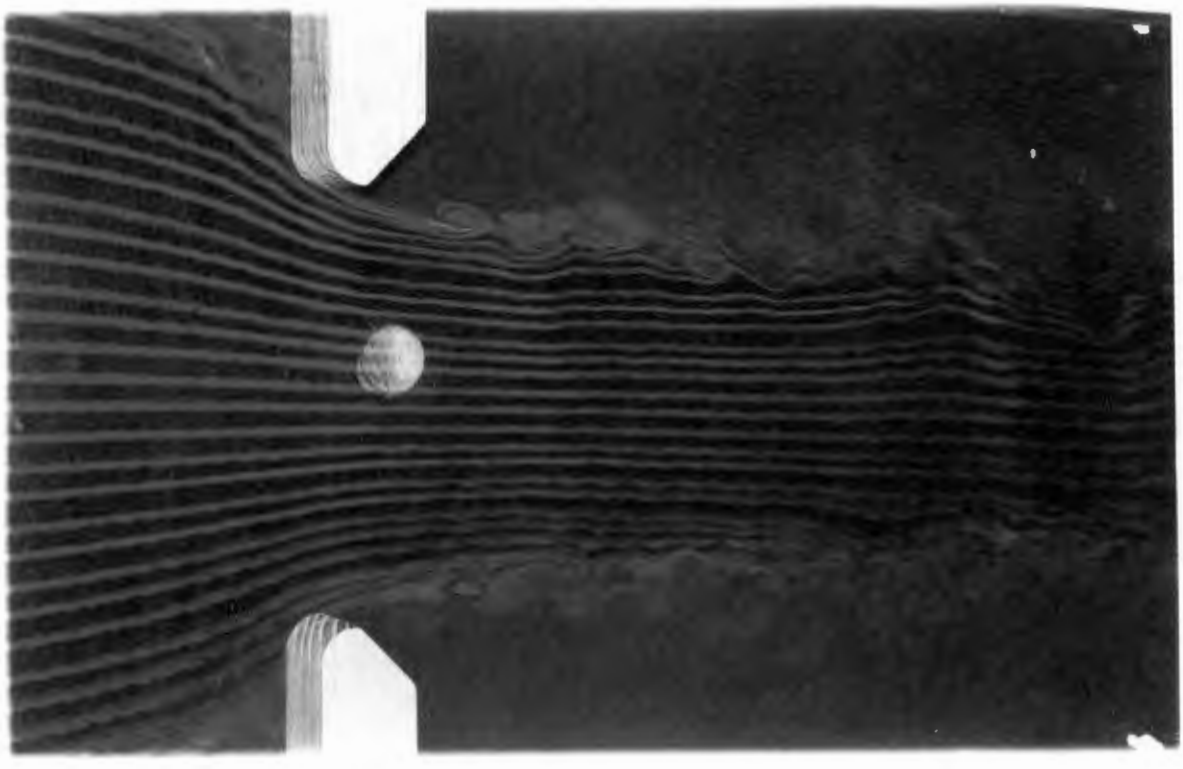

Fig.35b. Large Upstream Edge Radius. Low Flow Rate.

Fig.35c. Large Upstream Edge Radius. High Flow Rate.

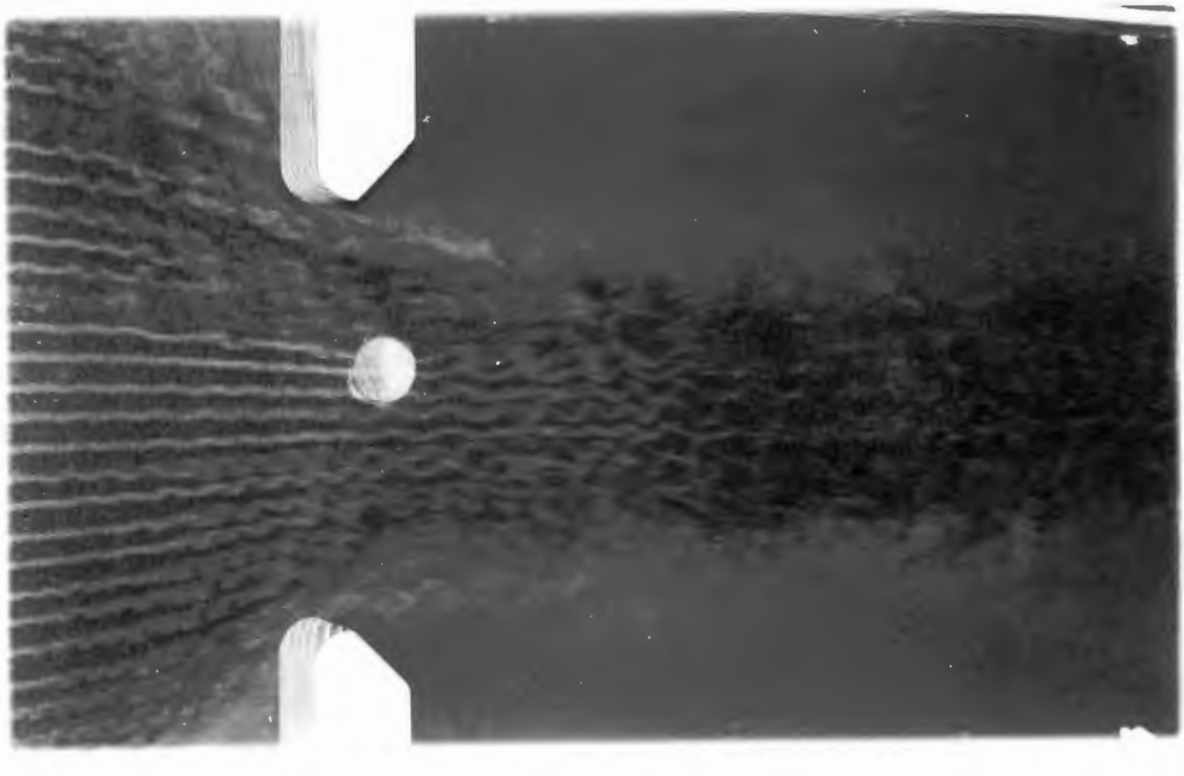

Fig.35. Change in Flow Pattern with Increasing Upstream Edge Radius of an Orifice Plate and Increasing Flow Rate

CHAPTER FOUR

R E S U L T S

4.1 REPEATABILITY OF EXPERIMENTAL READINGS

4.1.1 Repeatability of the Reference Meter

The overall tolerance, within the 95 per cent confidence limit, to which the flowrate can be determined with the reference meter is equal to $\pm$ 0,12% at maximum flowrate and $\pm$ 0,05% at low flowrates.

The tolerances quoted above were derived with the aid of an error analysis (See Appendix F).

The repeatability of individual flowrate readings was determined experimentally and it was found that at the maximum constant flowrate, the measured flowrate varied by $\pm$ 0,095% from the mean. Similarly at minimum flowrate the repeatability of a reading was $\pm$ 0,03%. The repeatability of flowrate measurements taken between these two limits was found to be between the above values.

4.1.2 Repeatability of the value of the experimentally determined discharge coefficient

Experimental tests showed that the repeatability of the determined coefficient of discharge of an orifice plate with an area ratio of 0,3 at a constant flow rate of 12,9402 kg/s was $\pm$ 0,095 per cent In the above tests eight calibrations at each flow rate were undertaken

Further tests were conducted over the full range of flow with orifice plates of area ratio equal to 0,15 and 0,55. The value of the coefficient of discharge obtained from each of the tests was plotted against the Reynolds number.

(See figure 36 and 37). It can be seen that for an orifice plate with an area ratio of 0,55, the repeatability of an individual reading varies from ± 0,19 per cent to ± 0,15 per cent depending on the Reynolds number while for the orifice plate with area ratio of 0,15 the repeatability of the determined coefficient of discharge varies from ± 0,19 per cent to ± 0,08 per cent.

A polynomial of the fourth order was drawn through the set of points obtained from one complete calibration and the value of the coefficient of discharge at any particular Reynolds number was determined from the curves obtained. If this procedure was followed for each set of data then the variation from the mean in the value of the coefficient of discharge for the orifice plate with area ratio of 0,55 is ± 0,065 per cent at a reynolds number of 100 000 and ± 0,09 per cent at a Reynolds number of 200 000 (See Figure 38)

TABLE 6

Variation in the coefficient of Discharge of an orifice plate with an area ratio of 0,55 as determined from four sets of readings

Set of reading	Reynolds number			
	100 000	150 000	200 000	225 000
1	0,6168	0,6147	0,6137	0,6146
2	0,6160	0,6148	0,6146	0,6142
3	0,6162	0,6151	0,6148	0,6151
4	0,6160	0,6156	0,6146	0,6146
Mean Coefficient	0,6163	0,6151	0,6144	0,6146
Max % Variation from mean	±0,065	±0,073	±0,090	±0,073

If a similar procedure is followed to determine the value of the discharge coefficient of the orifice plate with an area ratio of 0,15, then the variation in the value of the coefficient of discharge is $\pm$ 0,08 per cent at a Reynolds number of 100 000 and it is $\pm$ 0,01 per cent at a Reynolds number of 225 000 (See Figure 39 and Table 7)

TABLE 7

Variation in the coefficient of Discharge of an Orifice plate with an area ratio of 0,15 as determined from three set of readings

Set of reading	Reynolds number			
	100 000	150 000	200 000	225 000
1	0,6073	0,6051	0,6044	0,6044
2	0,6080	0,6054	0,6046	0,6045
3	0 6072	0,6052	0,6046	0,6045
Mean Coefficient	0,6075	0,6052	0,6045	0,6045
Max % Variation from mean	0,082	0,033	0,017	0,011

From these results it can be concluded that the repeatability of the coefficient of discharge as determined in the experiment will at worst be equal to $\pm$ 0,09 per cent.

4.1.3 Repeatability of the Edge Radius Measurement

The edge sharpness at a particular position of an orifice plate was measured six times. It was found that if a very sharp edge was measured ($r \approx 0,01$ millimetres) then the repeatability of a measurement was $\pm$ 5 per cent. If the edge was rounded

(r = 0,33 millimetres) then the repeatability of a reading increased to ± 2 per cent. The photographs taken of the lead indentations of the edge of the plate whose edge radius was 0,33 millimetres can be seen in Figure 40.

4.2 COEFFICIENTS FOR STANDARD SQUARE EDGE ORIFICE PLATES IN A 100 MILLIMETRE PIPE LINE

4.2.1 The Variation of the coefficient of discharge with the Reynolds number

The coefficient of discharge was plotted against the Reynolds number, the reciprocal of the Reynolds number and the square root of the reciprocal of the Reynolds number (Figure 41, 42 and 43 respectively).

From the plot of the coefficient of discharge versus the Reynolds number the following observations can be made:

a) In the region where the Reynolds number based on the orifice diameter was greater than 50 000 and less than 125 000 the coefficient of discharge decreased rapidly with a small increase in the Reynolds number. The boundaries of this region varied depending on the area ratio of the plate, but within the boundary quoted above, this tendency in the relationship between the discharge coefficient and the Reynolds number was apparent irrespective of the area ratio.

b) In the region where the Reynolds number was greater than 125 000 no distinct relationship between the Reynolds number and the coefficient of discharge was observed. By the expression "no distinct relationship" is meant that it was impossible from the available data to determine whether the coefficient would remain constant with increasing Reynolds number or whether it would continue to decrease at a very low rate.

To see if more information could be extracted from the data

available the coefficient of discharge was plotted against the reciprocal of the Reynolds number. From this graph it was evident that the coefficient of discharge decreased with increasing Reynolds numbers. The relationship between the reciprocal of the Reynolds number and the coefficient of discharge could be approximated by a straight line for Reynolds numbers greater than 100 000.

Plotting the coefficient of discharge against the square root of the reciprocal of the Reynolds number showed that the coefficient of discharge decreases with increasing Reynolds numbers. For Reynolds numbers greater than 100 000 this plot yielded a straight line with a higher correlation coefficient than did the plot of discharge coefficient versus the reciprocal of the Reynolds number.

It was clear from the above that the coefficient of discharge decreases with increasing Reynolds numbers in the turbulent flow region.

4 2.2. Variation of the coefficient of Discharge of Orifice Plates with the Area Ratio of the Plates

The coefficient of discharge of all the standard concentric orifice plates was plotted against the Reynolds number. A polynomial of the fourth order was fitted to the data and from the obtained curve the coefficient of discharge of each plate was determined at a Reynolds number of 100 000, 150 000 and 200 000. The determined coefficient of discharge of each plate at a particular Reynolds number was plotted against the area ratio. Curves similar to those shown in Figures 44 and 45 were obtained. The maximum scatter of individual experimental values about the curves obtained were as follows:

R_{e_d}	Maximum Scatter	At Area Ratios of
100 000	.3%	0,15; 0,4 & 0,5
150 000	.3%	0,15 & 0,45
200 000	.15%	0,15, 0,45 & 0,55

From Figures 44 and 45 it is evident that the coefficient of discharge of orifice plates increases with increasing area ratio. It is also evident that the scatter of individual points about the curves obtained decreases with increasing Reynolds numbers.

4.3 THE EFFECT OF ECCENTRIC POSITIONING OF AN ORIFICE PLATE

4.3.1 General

During the tests it was observed that the fluctuations in the mercury manometer reading initially increased with increasing eccentricity, reached a peak and then decreased until fully eccentric positioning was achieved. The magnitude of the variation in the instantaneous pressure difference across the orifice plate with increasing eccentricity was measured with the pressure differential transducer and the results were plotted in Figure 46. From Figure 46 it is evident that the magnitude of the pressure fluctuations is dependent on the area ratio of the plate and the eccentricity of the plate. The lower the area ratio the smaller the pressure fluctuations which occur and therefore the higher is the certainty in the experimental readings. It is also evident that for highly repeatable measurements the eccentricity ratio should be lower than 0,1 or greater than 0,9 irrespective of the area ratio of the plate.

4.3.2. The Effect of Eccentricity on the Coefficient of Discharge

Plotting the coefficient of discharge against the Reynolds number for an orifice plate initially located centrally and then in different eccentric positions, results in curves similar to those shown in Figure 47. From Figure 47 it is evident that the coefficient of discharge increases with increasing eccentricity.

The value of the coefficient of discharge at a Reynolds number of 100 000, 150 000 and 200 000 of the orifice plates tested was plotted against the eccentricity ratio (Figure 48). From the

resultant figure it can be seen that for each orifice plate the curves obtained for the variation of the eccentricity ratio with the coefficient of discharge at the various constant Reynolds numbers are parallel and therefore the results obtained apply at any given Reynolds number. Since the experimentally determined coefficients are more accurate at high Reynolds numbers, the Reynolds number at which the effect of eccentricity is determined and discussed is 200 000.

The coefficient of discharge at a Reynolds number of 200 00 was plotted against the following:

a) eccentricity, E, (Fig. 49)
b) eccentricity/orifice diameter, E/d (Fig. 50)
c) eccentricity/area ratio, E/m (Fig. 51)
d) eccentricity ratio, 2E/D-d (Fig. 52)

It was found that a logarithmic relationship exists between the coefficient of discharge and any of the above variables. The relationship between the coefficient of discharge and any of the above variables can be expressed by an equation of the form

$$Y = Ae^{xB}$$

In this equation A and B are constants.

The curve obtained from the plot of discharge coefficient versus eccentricity ratio had the highest correlation coefficient and therefore should be used to best represent the results. From the above plots it is evident that the effect of eccentricity on the coefficient of discharge is related to the area ratio and the magnitude of the eccentricity. The gradient of the curves increases with increasing area ratio. The larger the area ratio the greater the effect of eccentric location on the coefficient of discharge. This can best be seen from Figure 53 in which the percentage change in the value of the coefficient of discharge is plotted against the area ratio of the different orifice plates at various eccentricity ratios. From this figure it can also

be seen that when the plate is fully eccentric, the percentage change in the coefficient of discharge varies from 6,2 per cent to 8,5 per cent for plates with area ratios varying from 0,15 to 0,55 Furthermore, the effect of small positional changes for an eccentric orifice is much greater than for a concentric one.

For further analysis of the results, the percentage change in the coefficient of discharge of the orifice plates tested is plotted against the eccentricity ratio. (See Figure 54). From the resultant curves one can see that if the eccentricity ratio is less than five per cent then the percentage change in the value of the coefficient of discharge does not exceed 0,1 per cent for any of the plates tested. Since initially such large variations in the eccentricity of an orifice plate causes such small changes in the value of the coefficient of discharge there is no reason why the effect of eccentricity on the coefficient of discharge of orifice plates used in practice today cannot be kept under 0,1 per cent. To do this the standards would have to specify maximum allowable eccentricities equal to those determined below.

From Figure 54 the value of the eccentricity ratio at a change in the coefficient of discharge of 0,1 per cent is read off and then this value is plotted against the area ratio, as in Figure 55. From Figure 55 it is evident that a linear relationship exists between this allowable eccentricity and the area ratio of an orifice plate. The allowable eccentricity for the error in the coefficient of discharge to be less than 0,1 per cent can be calculated from equation 1.

For the error in the coefficient of discharge to be less than 0,1 per cent

$$\frac{100\ E}{D - d} \quad 3{,}55 - 1{,}69\ m \quad \ldots\ldots \quad 1$$

From equation 1 the allowable eccentricity for the plate with area ratio of 0,15 is 2,03 millimetres, while for the plate with area ratio of 0,55 it is 0,68 millimetres. This shows

conclusively that the coefficient of discharge of large area ratio orifice plates is more affected by error in eccentric location than are small area ratio orifice plates.

4.4 EFFECT OF ROUNDING THE EDGE OF A SQUARE EDGE ORIFICE PLATE

4.4.1 Variation of the coefficient of discharge with the Reynolds number for orifice plates of various Edge Radii

A typical experimental curve of the coefficient of discharge versus the Reynolds number for various edge radii can be seen in Figure 56. It is evident that at high Reynolds numbers the curves are approximately parallel and thus the curves derived from these results at any constant high Reynolds number (greater than 100 000) will be similar. This fact is well illustrated in Figure 57 where the coefficient of discharge is plotted against the edge radius for orifice plates of area ratios of 0,1 and 0,5 at various constant Reynolds numbers. Similar curves are obtained for the orifice plates of area ratios of 0,2; 0,3; and 0,4.

Further analysis of the results is at a Reynolds number of 200 000 as this is the highest Reynolds number at which all the plates were tested. As the curves in Figure 57 are parallel, the analysis of the results at a Reynolds number of 200 000 applies at any Reynolds number as long as turbulent flow exists.

4.4.2 The Relationship between the Edge-roundness and the discharge Coefficient

The value of the coefficient of discharge of each orifice plate was determined at a Reynolds number of 200 000 and then it was plotted in Figure 58 against the edge radius (r). From Figure 58 it can be seen that the coefficient of discharge increases with increasing edge radius and the relationship between these two variables can be expressed by a quadratic equation. The equation which represents the relationship between

the discharge coefficient and the edge radius of one orifice plate differs from that representing the same relationship for another orifice plate. This difference is due to the plates having different area ratios and therefore it can be concluded that the effect on the coefficient of discharge of varying the edge sharpness of an orifice plate is dependent on both the area ratio and the magnitude of the edge radius.

Plotting the coefficient of discharge of the orifice plates tested against the sharpness ratio results in curves which can be expressed by a quadratic equation. (See Figure 59). From figure 59 it is evident that a small increase in the sharpness ratio of a sharp orifice plate affects the discharge coefficient more than a similar increase in the sharpness ratio of a plate whose upstream edge is already rounded.

To determine the correction factor which should be applied to an orifice plate whose sharpness ratio is not 0,0004, the coefficient of discharge of each plate at this sharpness ratio was read off from figure 59. The sharpness ratio of 0,0004 was chosen as a reference as the British and the German Standards define a sharp plate as one whose sharpness ratio is equal to or less than 0,0004. The percentage deviation in the coefficient of discharge of each plate from that of a sharp plate was calculated and then it was plotted against the edge radius and the sharpness ratio of the orifice plates tested (See Figures 60 and 61 respectively)

From Figure 60 it is evident that the orifice plate with an area ratio of 0,1 is most affected by a change in the upstream edge radius of the plate. The other orifice plates with area ratios between 0,2 and 0,5 have correction factors which lie within a small band which widens with increasing

edge radius. From Figure 60 it can be seen that the effect on the coefficient of discharge of an initial small increase in the edge radius is greater than that of subsequent increases. For an orifice plate whose edge radius is greater than 0,1 millimetres, the increase in the percentage change in the coefficient of discharge is linear with increase in the edge radius.

The percentage change in the coefficient of discharge increases with increasing sharpness ratio. The most affected is the orifice plate with an area ratio of 0,5. From Figure 61 it can be seen that the coefficient of discharge of orifice plates whose sharpness ratio is less than 0,0004 are as badly affected by a change in the sharpness ratio as are those whose sharpness ratio is greater than 0,0004. This shows the inadequacy of the standards regarding the specification for sharp orifice plates if highly accurate measurement is required with an uncalibrated standard orifice plate.

It is also evident that a single correction curve for orifice plates of various sharpness ratios will result in errors in the coefficient of discharge of up to $\pm$ 1 per cent. Due to the above, for accurate flow measurement a simple correction curve for all area ratio orifice plates is not recommended.
A single correction curve can only be recommended for orifice plates whose sharpness ratio varies between 0,0002 and 0,0006. This correction curve is determined from Figure 61 and is plotted against the sharpness ratio in Figure 62. Using the correction curve specified in Figure 62 the coefficient of discharge of any orifice plate can be corrected for the effect of edge roundness to within $\pm$ 0,1 per cent. Although this correction factor applies only to orifice plates whose sharpness ratio is between 0,0002 and 0,0006 it is very useful as most orifice plates bored out on a lathe have a sharpness ratio which lies within these boundaries.

FIGURE NO. 36

TESTS FOR REPEATABILITY OF INDIVIDUAL CALIBRATIONS IN THE TEST INSTALLATION FOR AN ORIFICE PLATE WITH AREA RATIO OF 0.55

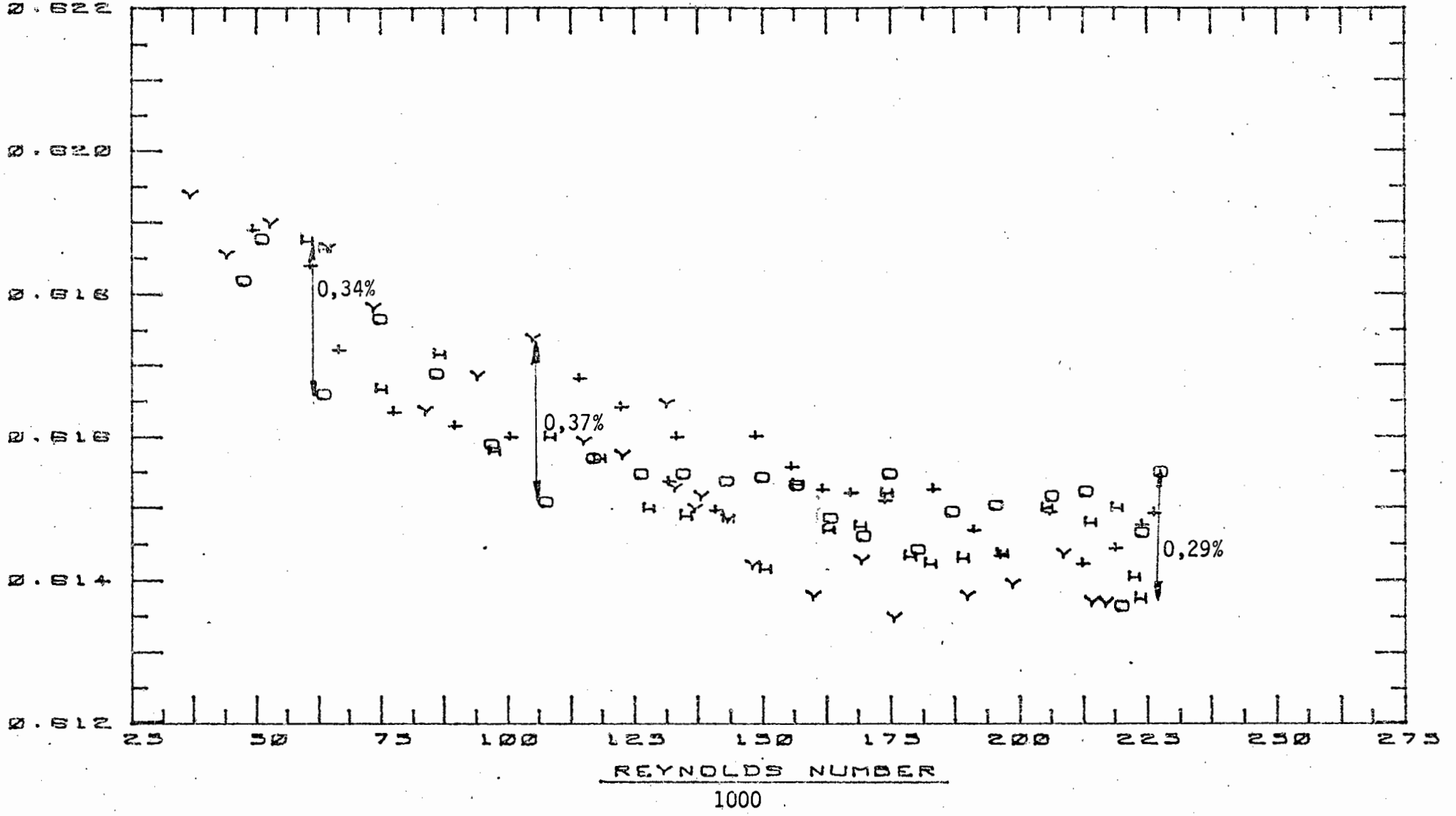

FIGURE NO. 37

TESTS FOR REPEATABILITY OF INDIVIDUAL CALIBRATIONS IN THE TEST INSTALLATION FOR AN ORIFICE PLATE WITH AREA RATIO OF 0.15

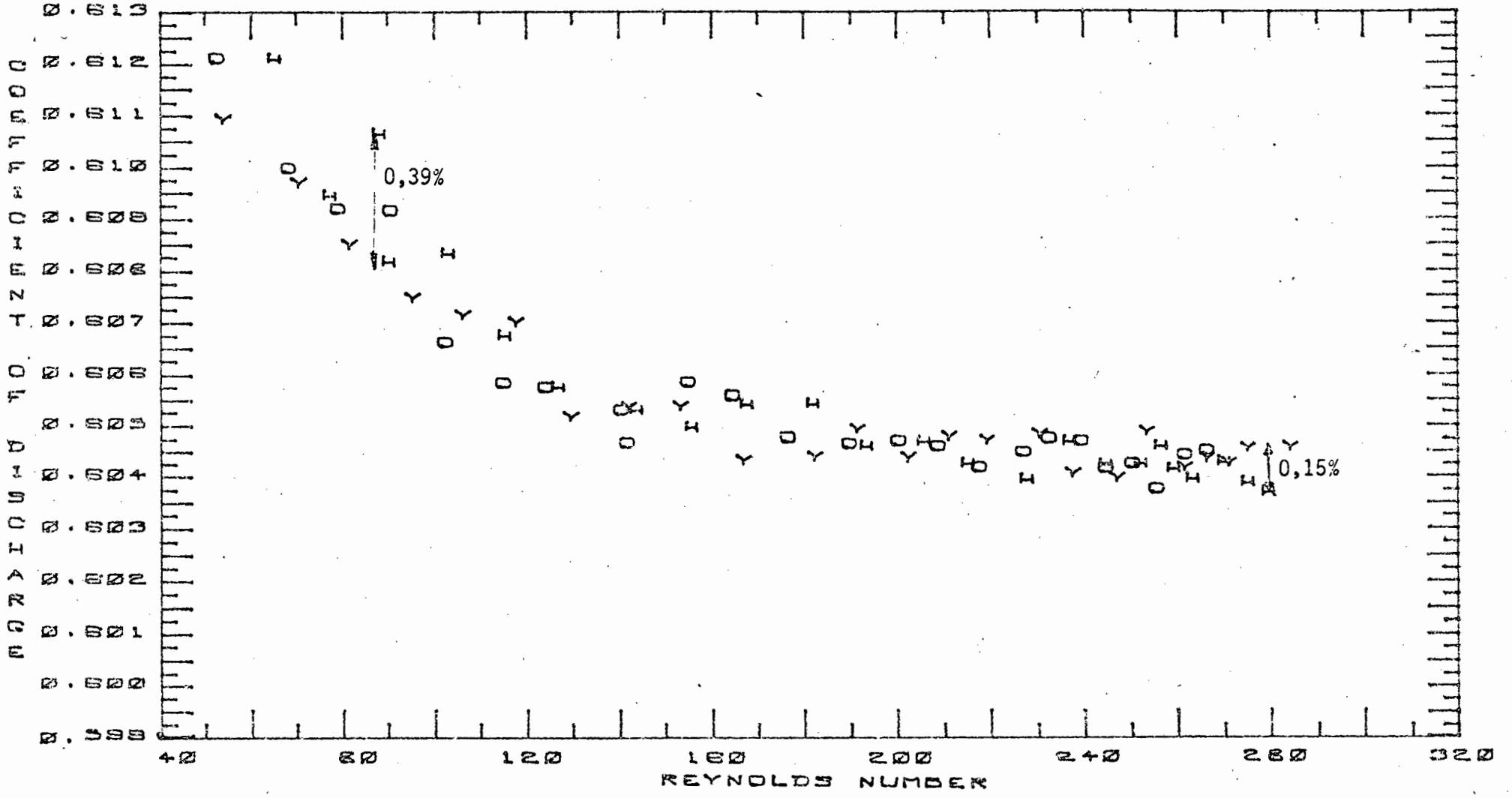

FIGURE NO. 38

TESTS FOR REPEATABILITY OF THE COEFFICIENT OF DISCHARGE OF AN ORIFICE PLATE WITH AREA RATIO OF 0.55 TESTED IN THE TEST INSTALLATION

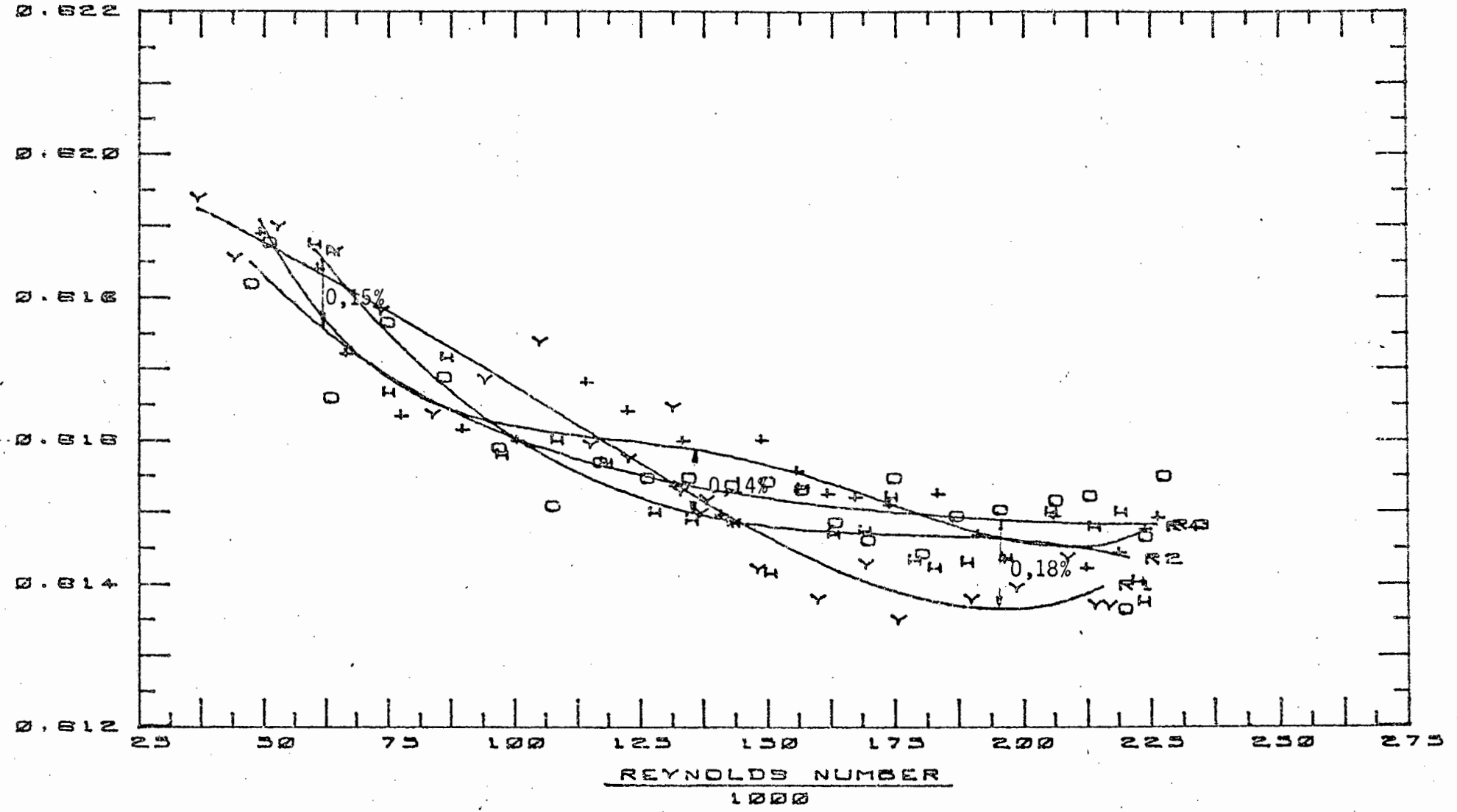

FIGURE NO. 39

TESTS FOR REPEATABILITY OF THE DISCHARGE COEFFICIENT OF AN ORIFICE PLATE WITH AREA RATIO OF 0.15 TESTED IN THE TEST INSTALLATION

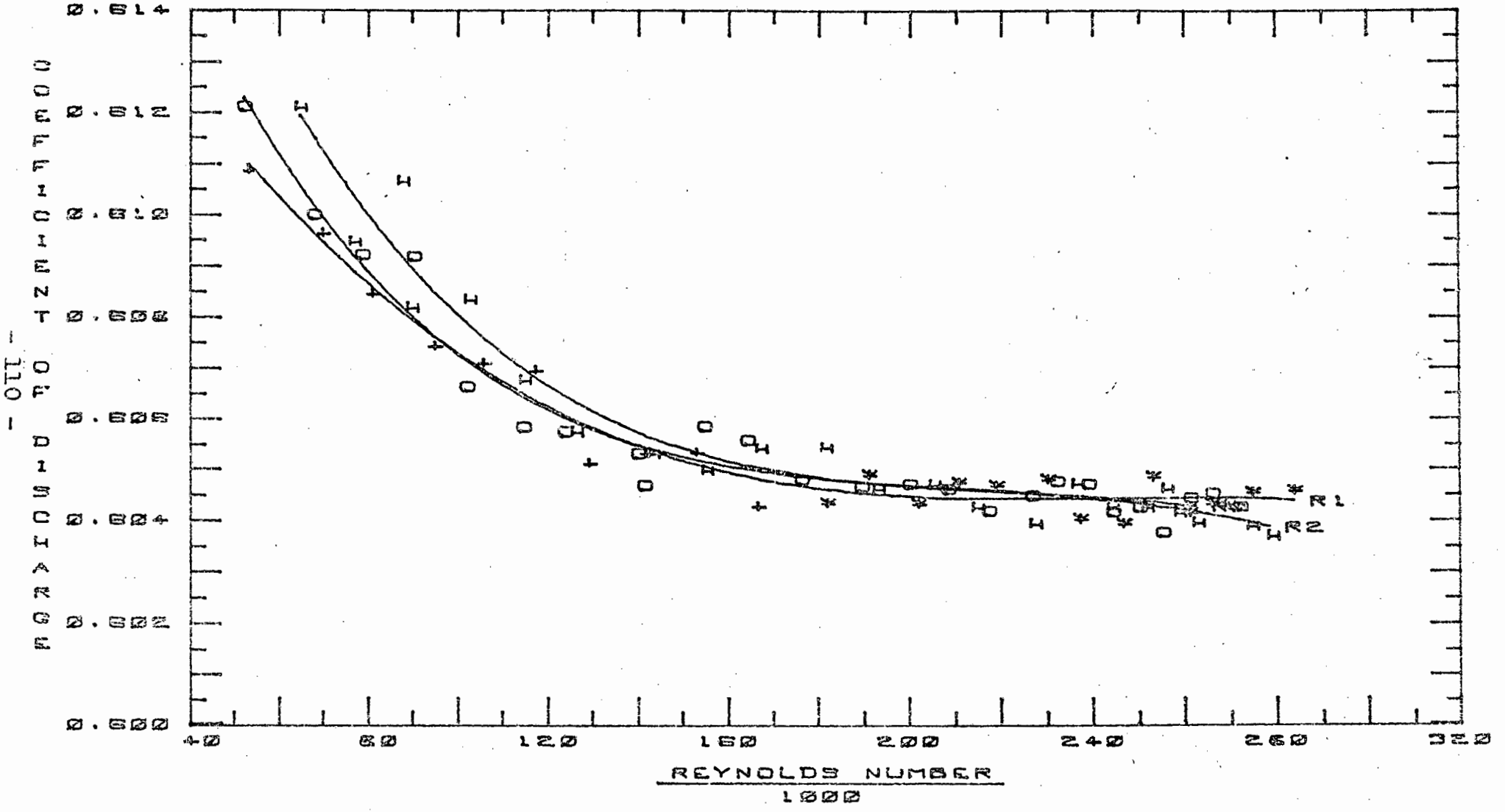

Fig.40 Repeatability of Edge Sharpness Measurement Using the Lead Foil Method (Edge Radius of 0,33 mm)

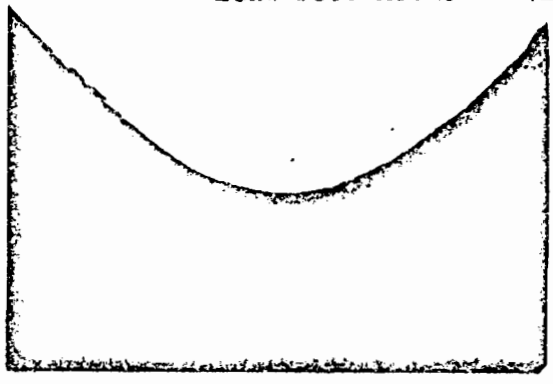
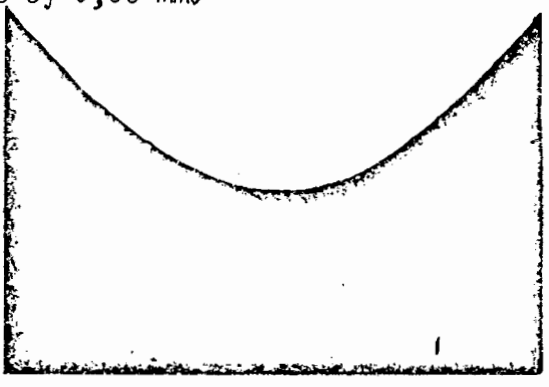
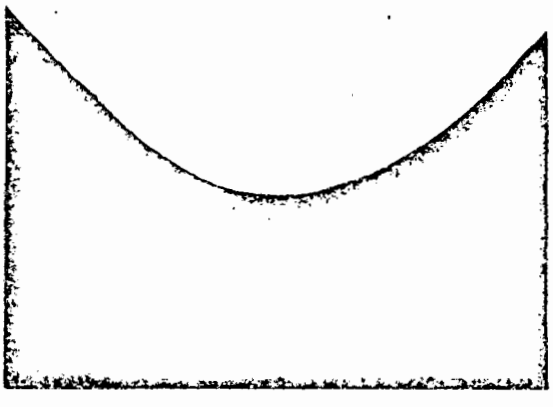
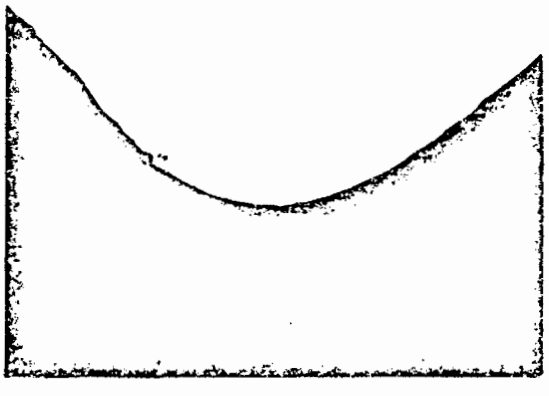
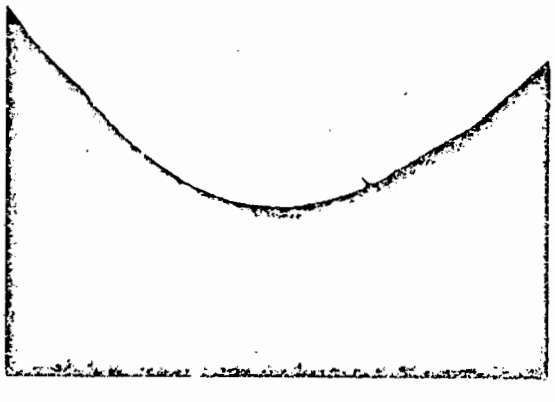
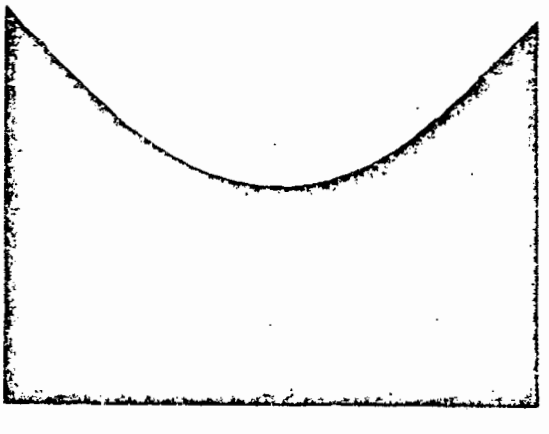

FIGURE NO. 41

THE VARIATION IN THE DISCHARGE COEFFICIENT WITH THE REYNOLDS NUMBER FOR AN ORIFICE PLATE WITH AN AREA RATIO OF 0,0985

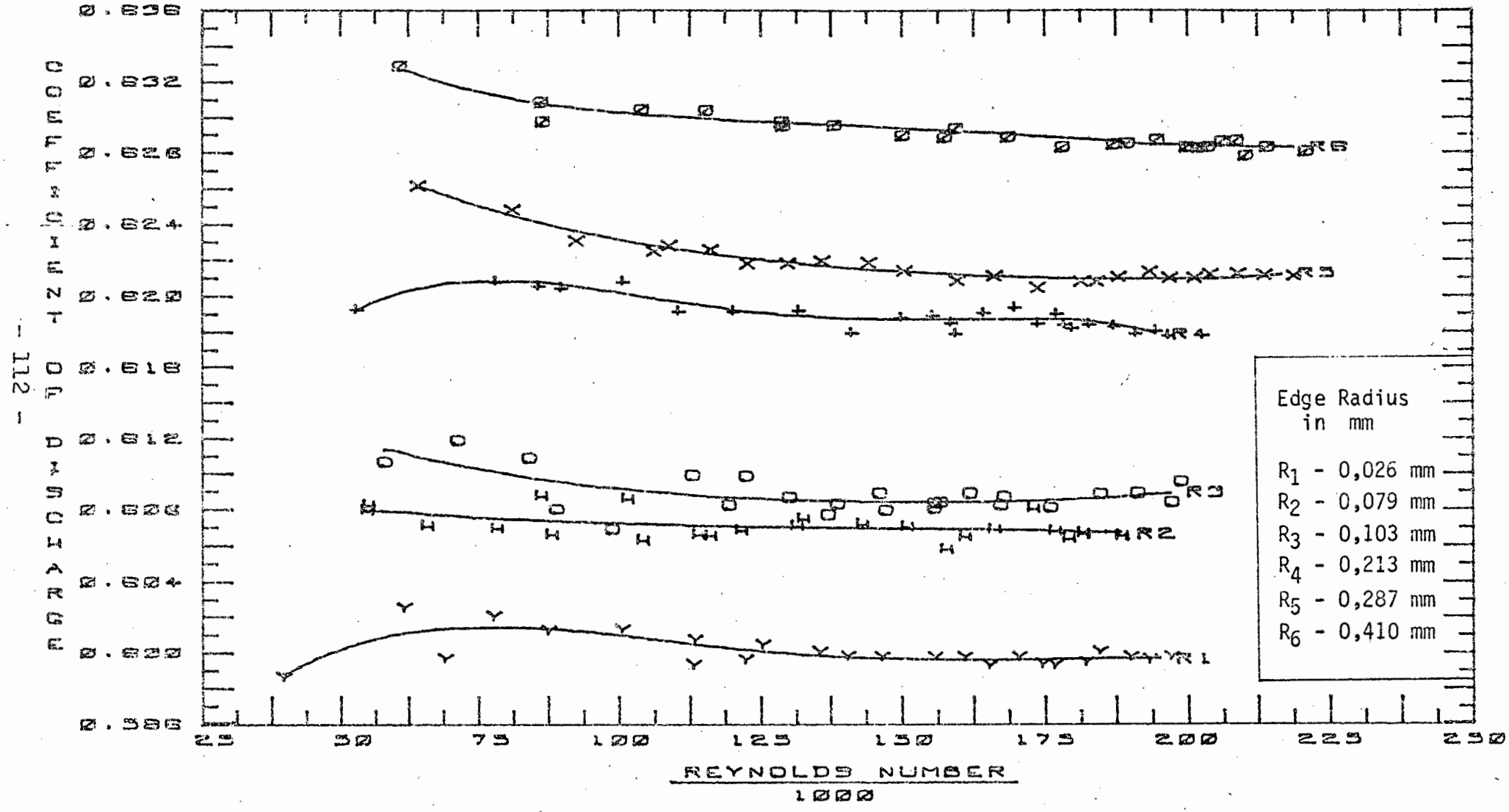

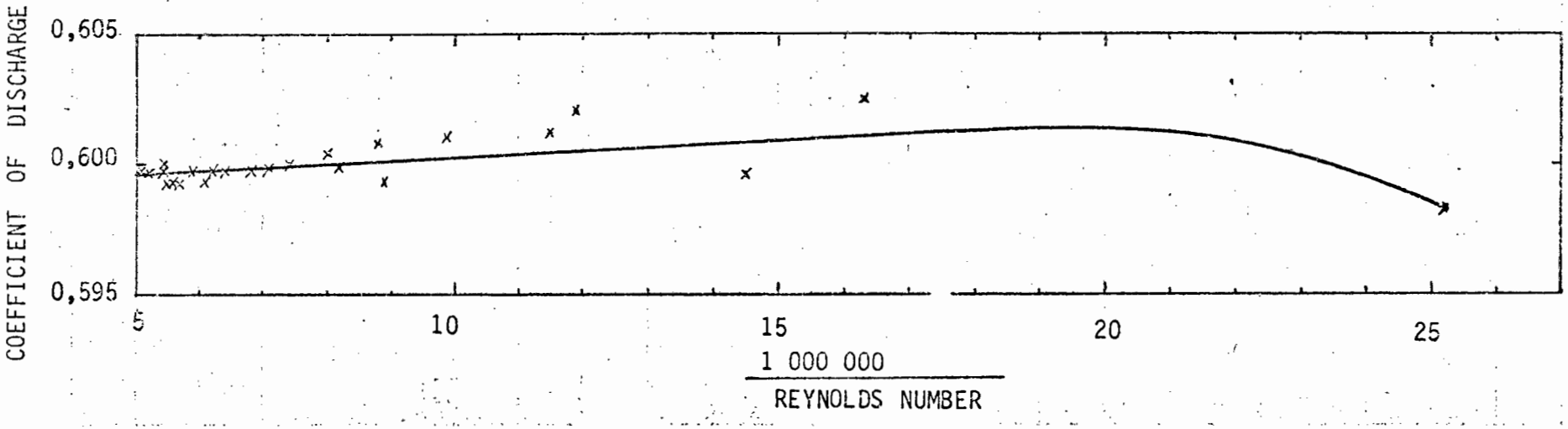

Fig. 42 The Variation in the Discharge Coefficient with the Reciprocal of the Reynolds Number for an Orifice Plate with Area Ratio of 0,0985

FIGURE NO. 43

THE VARIATION IN THE DISCHARGE COEFFICIENT WITH THE RECIPROCAL OF THE SQUARE ROOT OF THE REYNOLDS NUMBER.

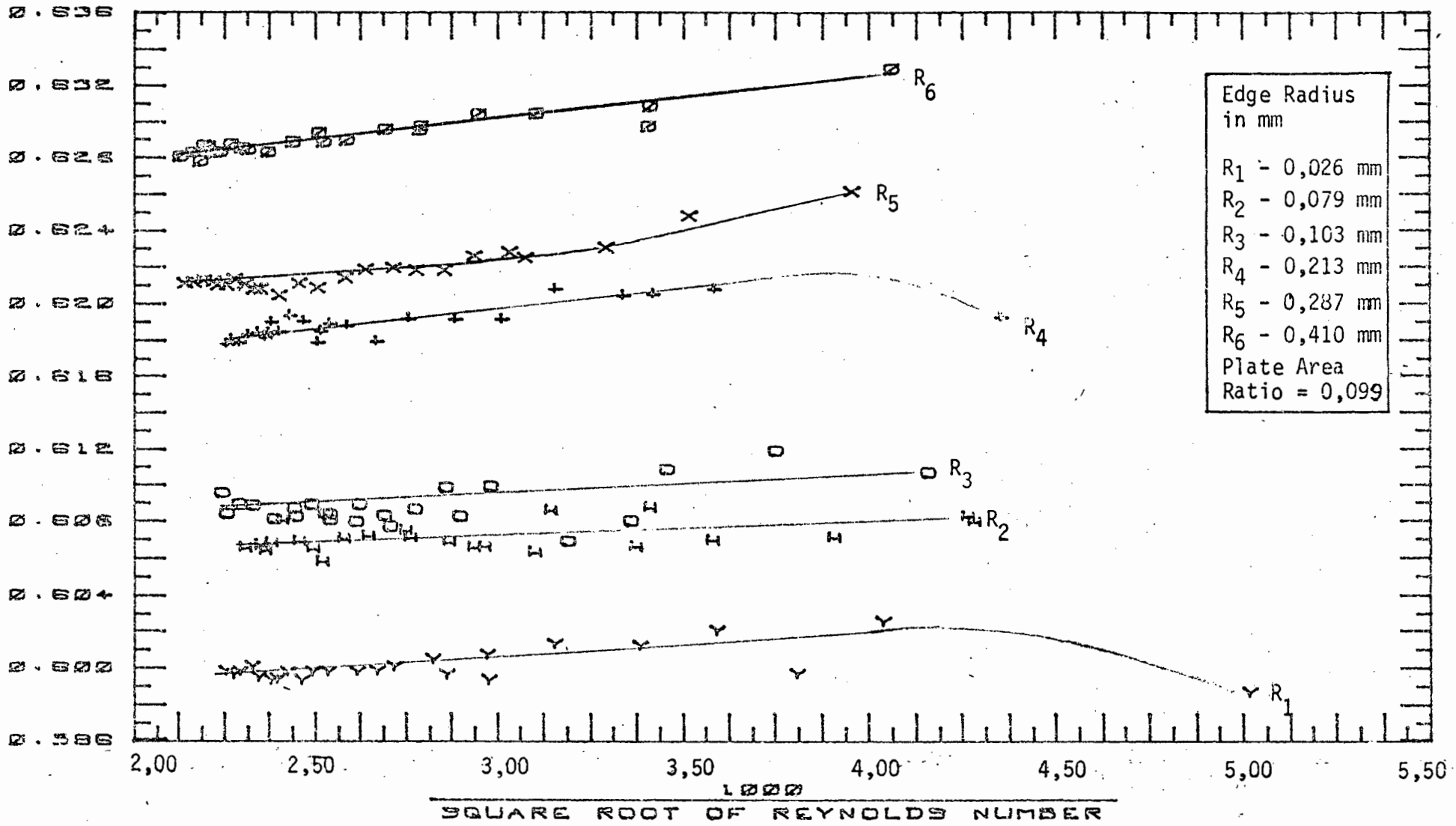

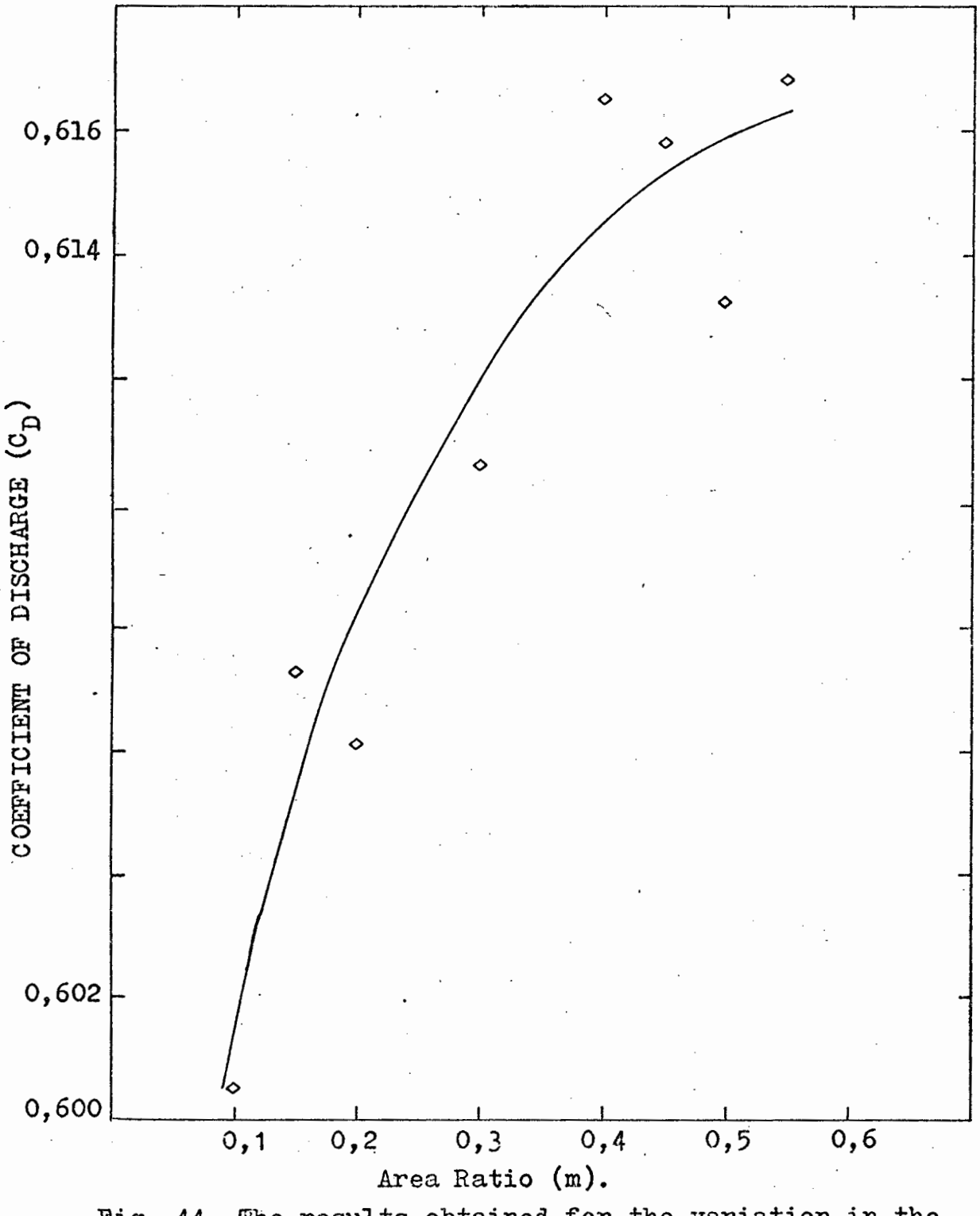

Fig. 44 The results obtained for the variation in the Discharge Coefficient with the Area Ratio at a constant Reynolds Number of 100 000.

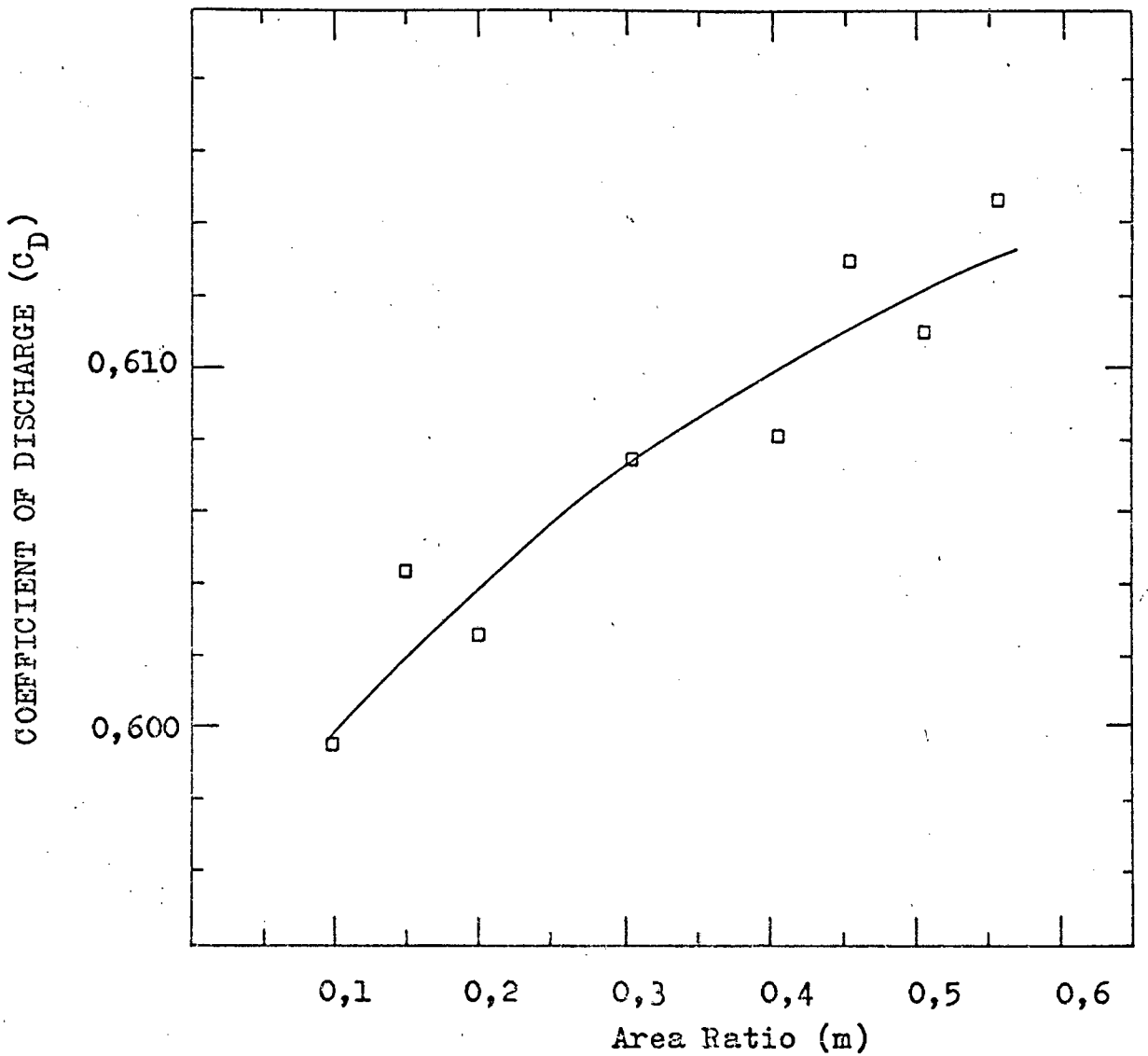

Fig. 45. The results obtained for the variation in the Discharge Coefficient with the Area Ratio at a constant Reynolds Number of 200 000.

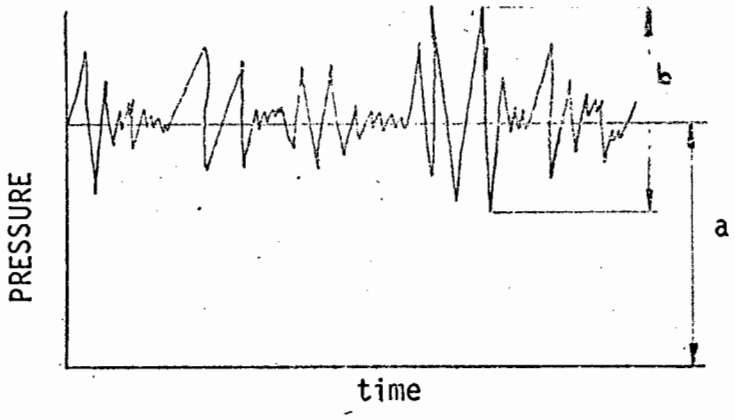

PERCENTAGE FLUCTUATION ABOUT THE MEAN PRESSURE = $\frac{b}{a} \times 100$

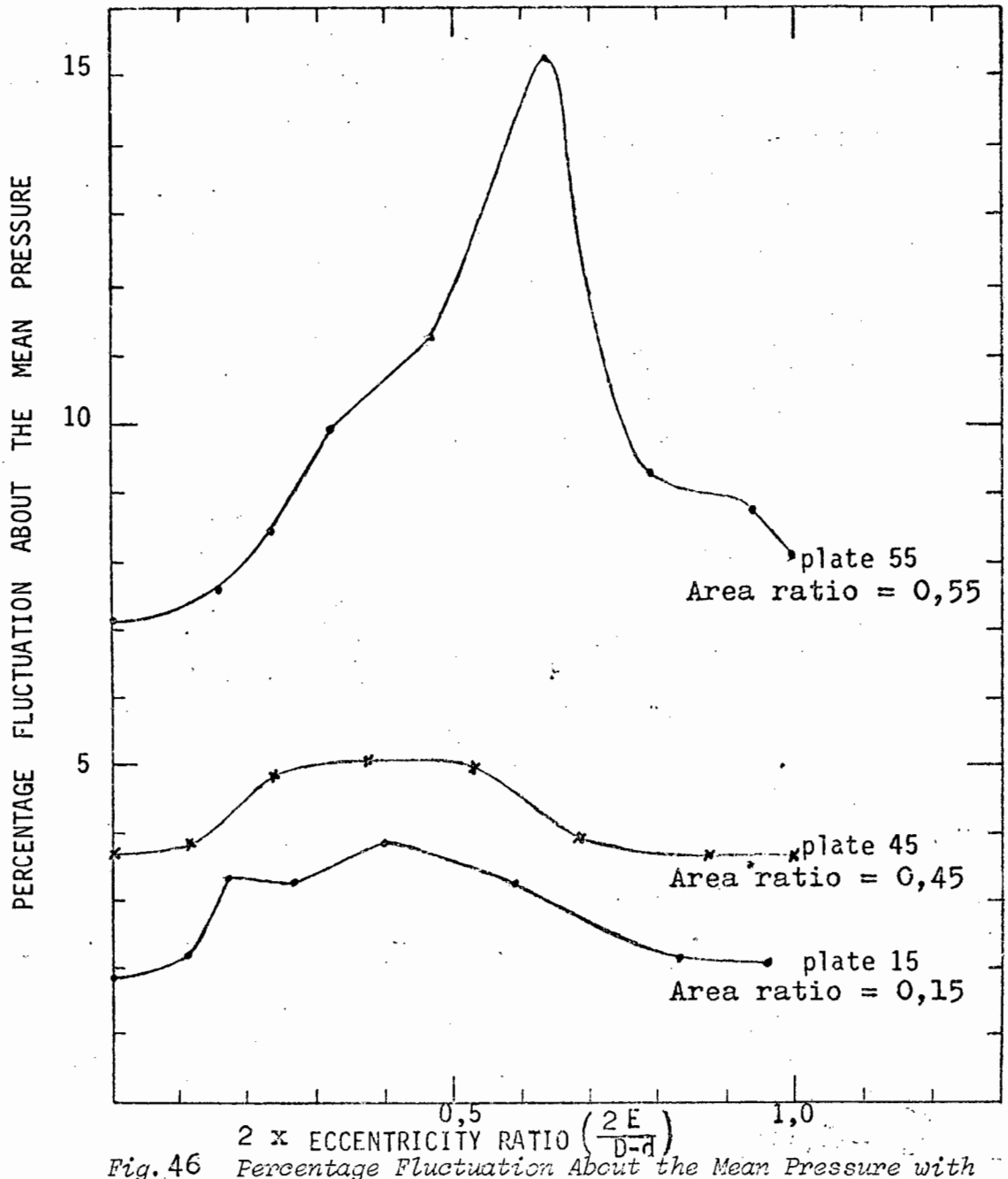

Fig. 46 *Percentage Fluctuation About the Mean Pressure with Increasing Eccentricity Ratio for Flow Measurement with Orifice Plates with area Ratios of 0,15; 0,45 and 0,55.*

FIGURE NO. 47

THE EFFECT ON THE COEFFICIENT OF DISCHARGE OF POSITIONING ECCENTRICALLY AN ORIFICE PLATE WITH AN AREA RATIO OF 0,55

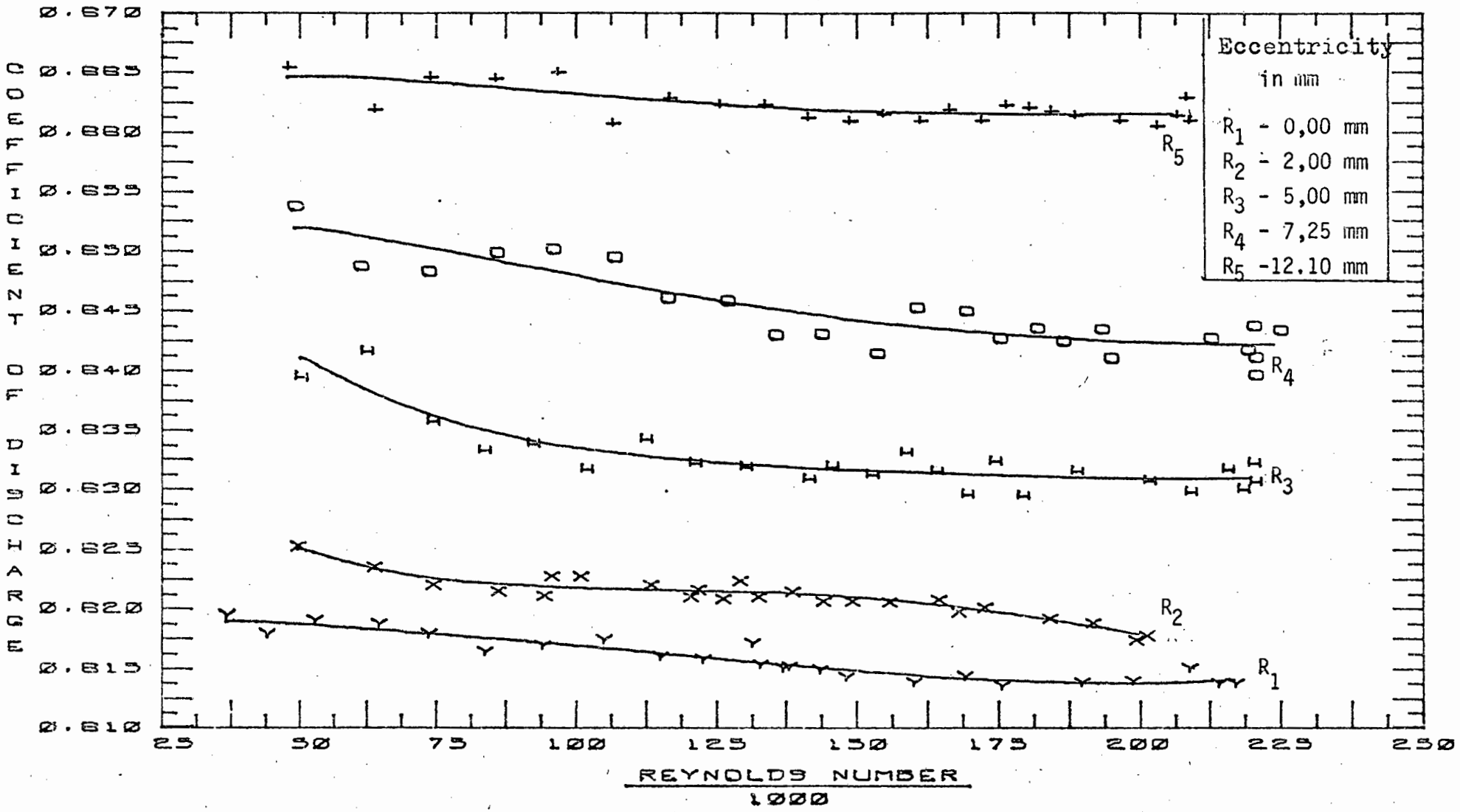

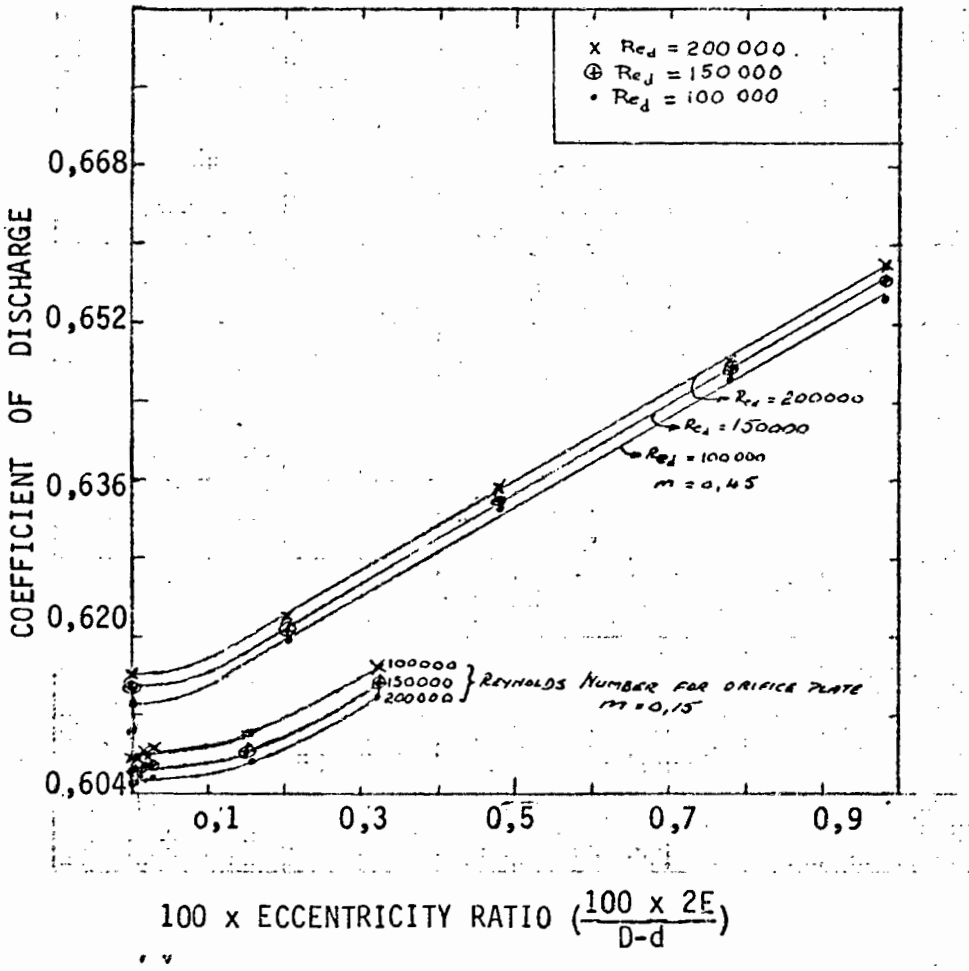

Fig. 48 The effect on the Coefficient of Discharge of increasing the eccentricity of the plate at a constant Reynolds number

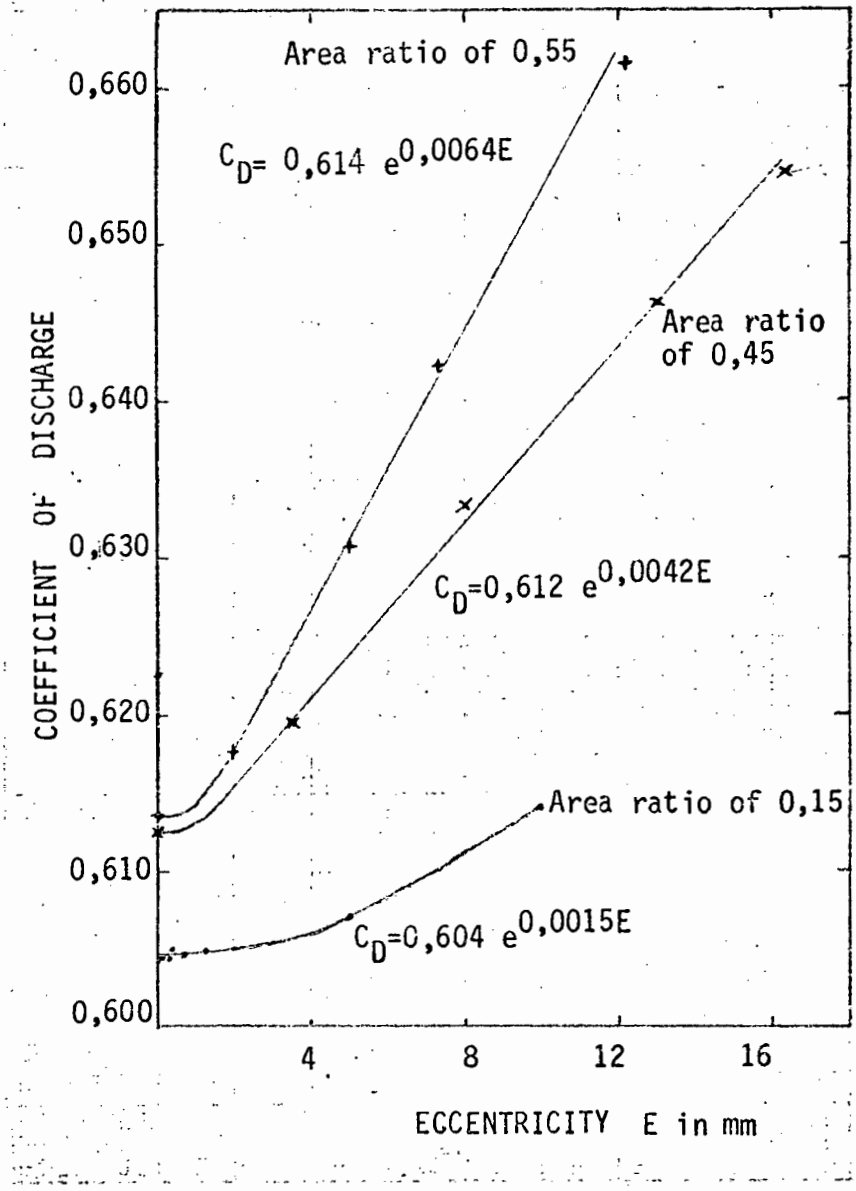

Fig. 49 The Effect on the Coefficient of Discharge of increasing the eccentricity of an orifice plate. The Coefficient of discharge was determined at a Reynolds number of 200 000

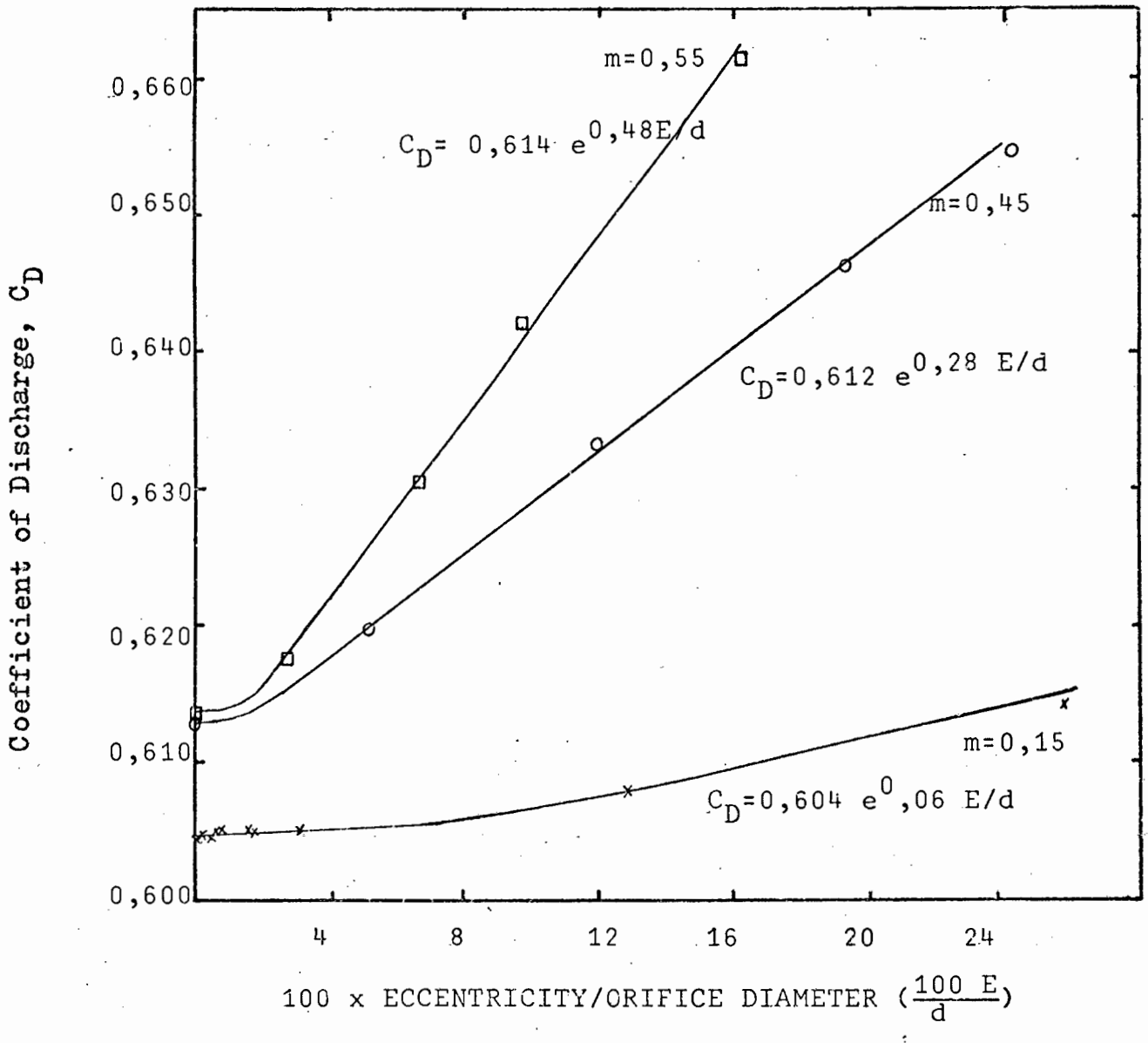

Fig. 50. The Effect on the Coefficient of Discharge of increasing the ratio of eccentricity/orifice diameter. The Coefficient of Discharge was determined at a Reynolds number of 200 000.

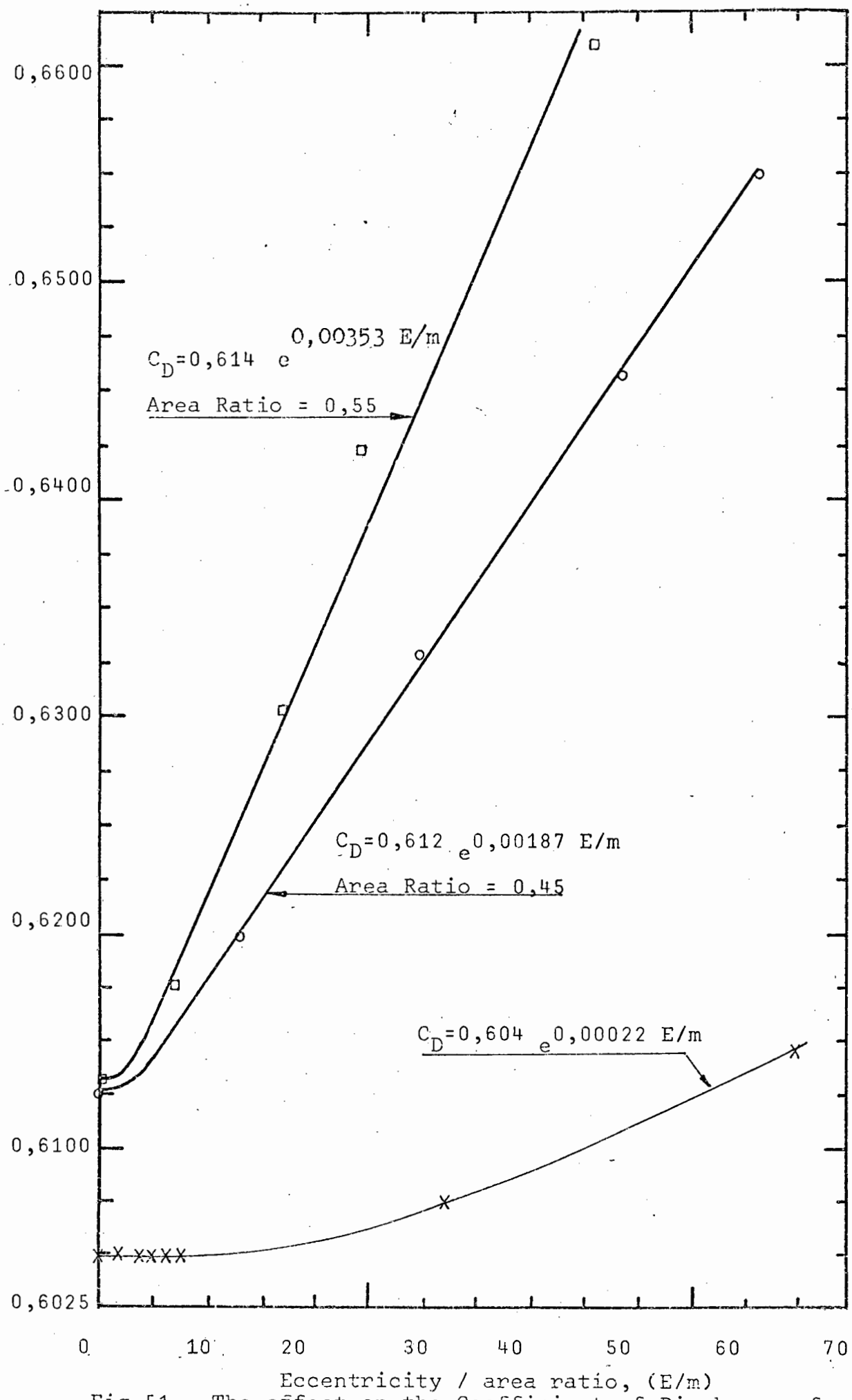

Fig.51. The effect on the Coefficient of Discharge of increasing the ratio of eccentricity/area ratio. The Coefficient of Discharge was determined at a Reynolds number of 200 000.

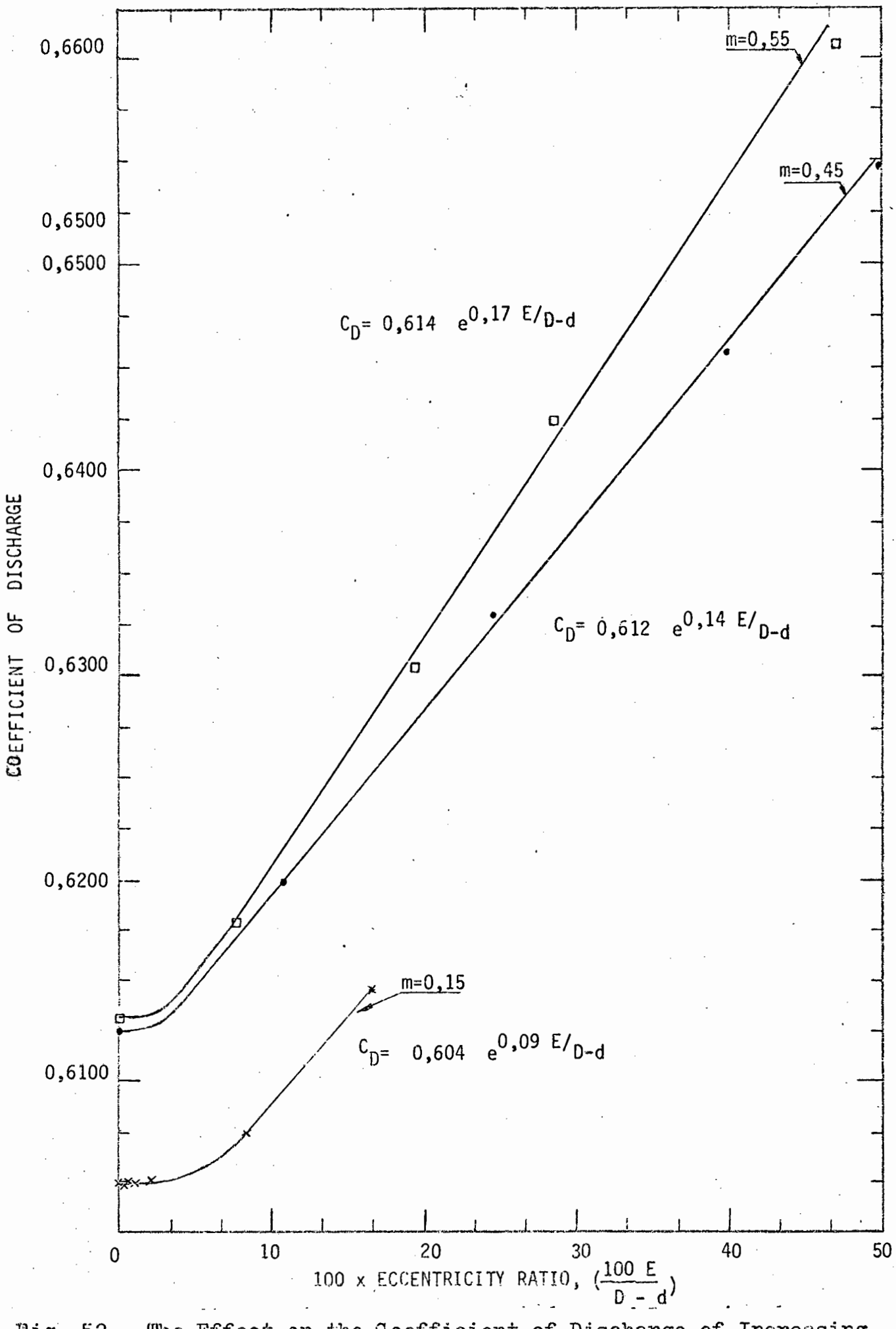

Fig. 52. The Effect on the Coefficient of Discharge of Increasing the Eccentricity ratio of an Orifice Plate. The Coefficient of Discharge was determined at a Reynolds number of 200 000

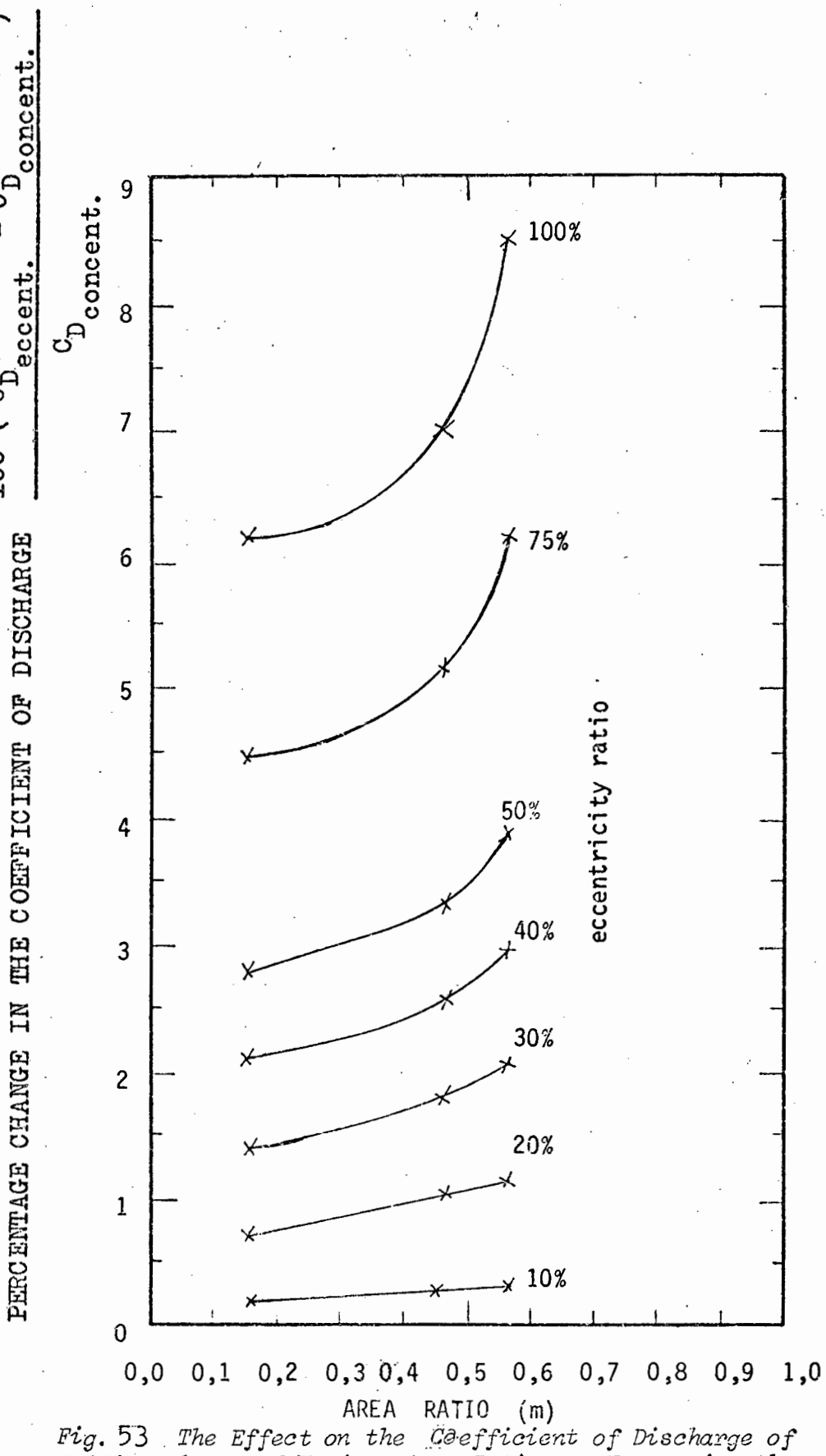

Fig. 53 The Effect on the Coefficient of Discharge of Orifice Plates of Various Area Ratios on Increasing the Eccentricity of the Plate

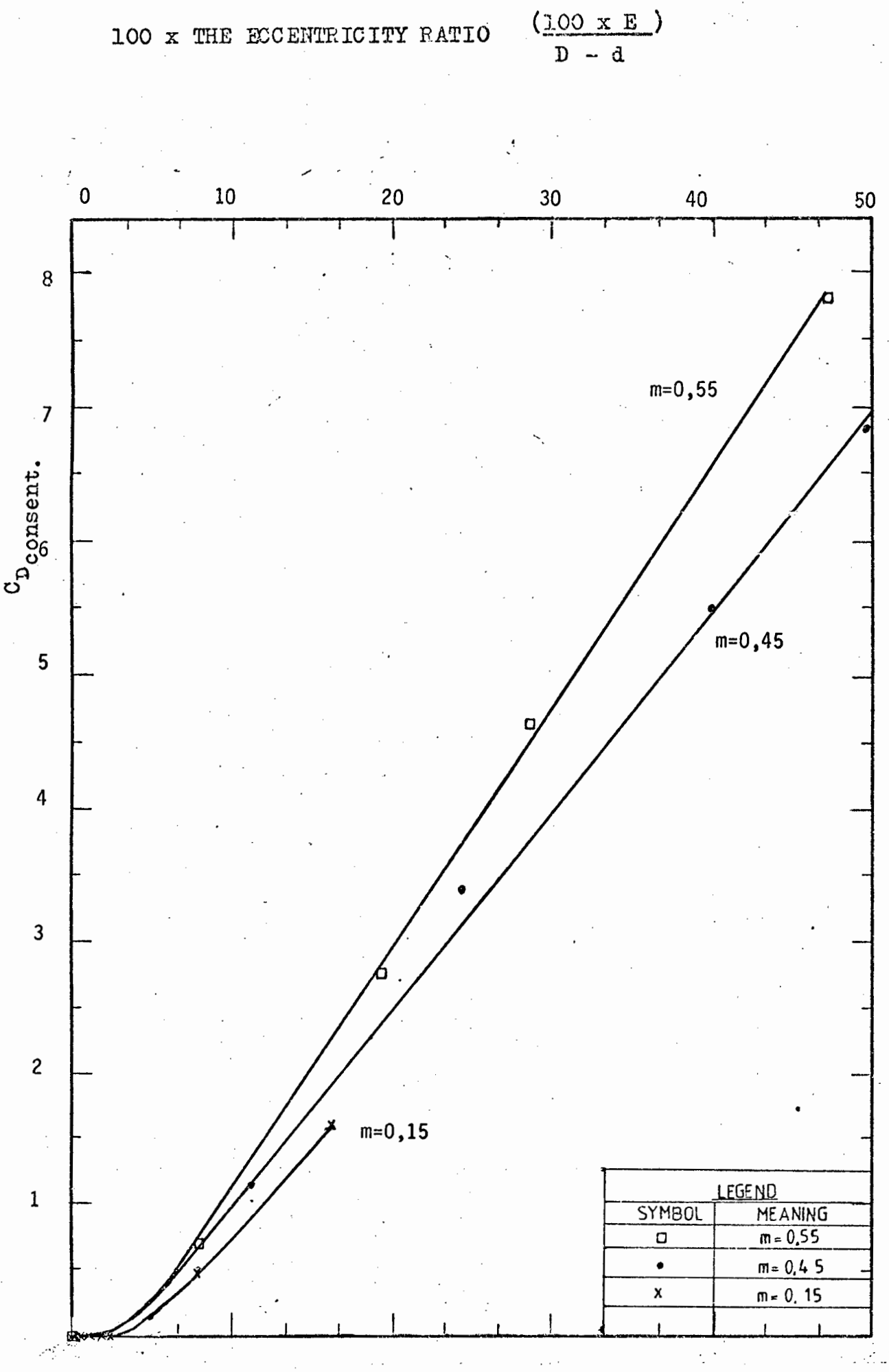

Fig. 54. The Percentage Change in the Coefficient of Discharge of an Orifice Plate with Increasing Eccentricity ratio.

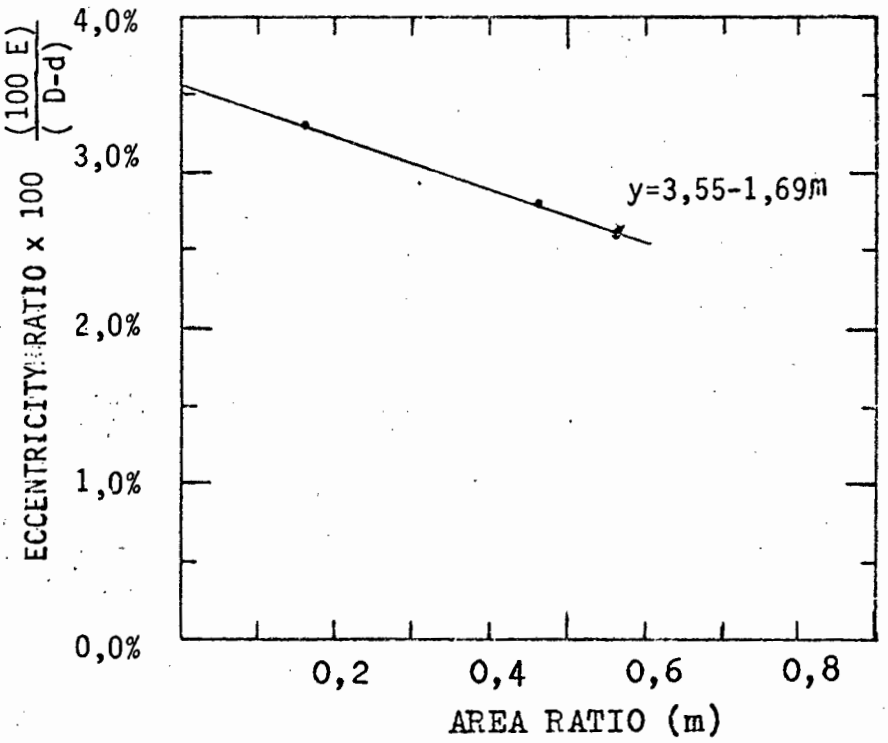

Fig. 55. The Eccentricity Ratio allowable for Orifice Plates in order that the Change in the Coefficient of Discharge due to Eccentricity will be under 0,1%.

FIGURE NO. 56

THE EFFECT OF ROUNDING THE UPSTREAM EDGE OF AN ORIFICE PLATE WITH AN AREA RATIO OF 0.0885 PLACED IN A SMOOTH P.V.C. LINE

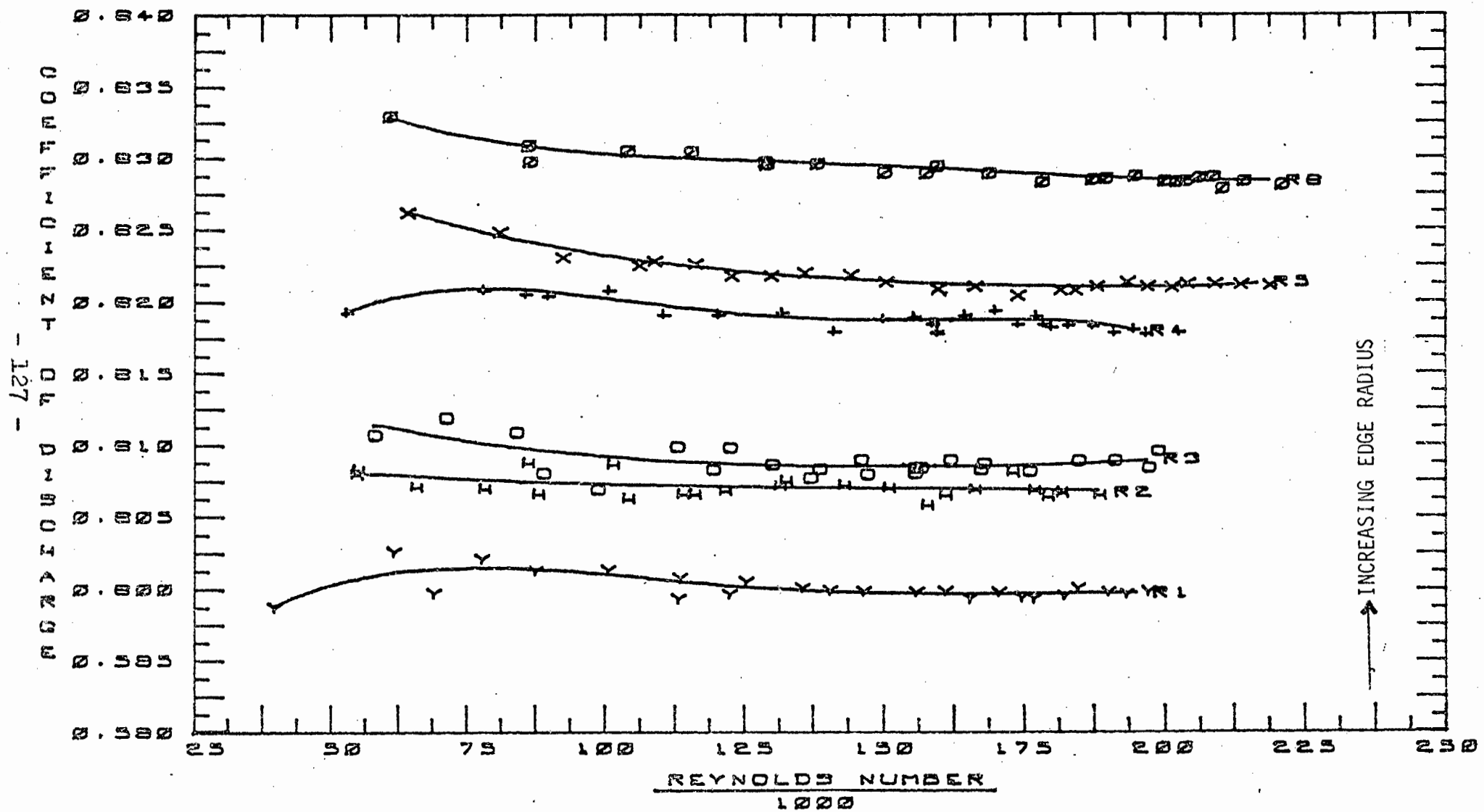

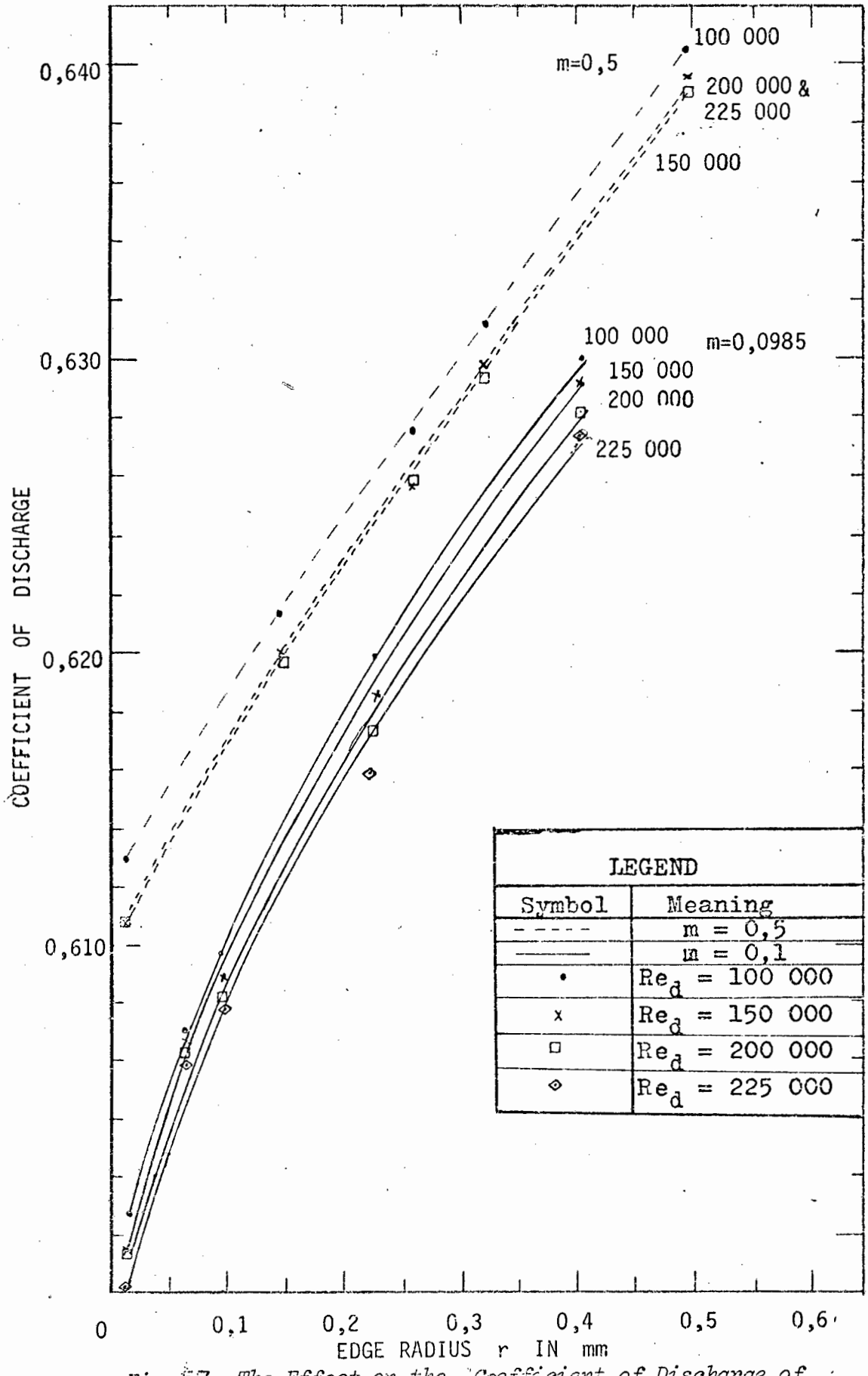

Fig. 57 The Effect on the Coefficient of Discharge of Orifice Plates of Increasing the Upstream Edge Roundness of the Plate at constant Reynolds Numbers.

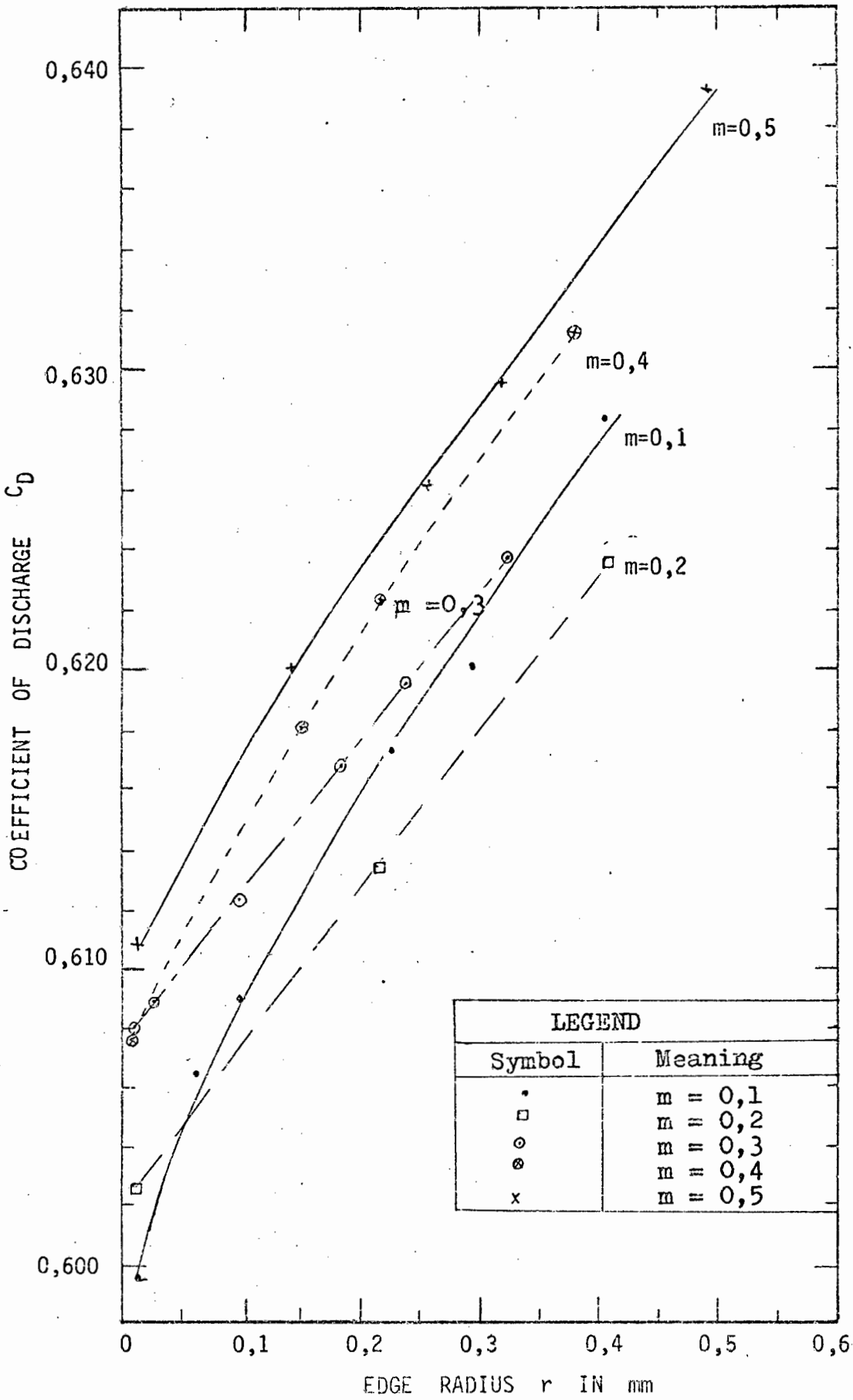

Fig.66. The Effect on the Coefficient of Discharge of Orifice Plates of Increasing the Upstream Edge Radius of a Plate

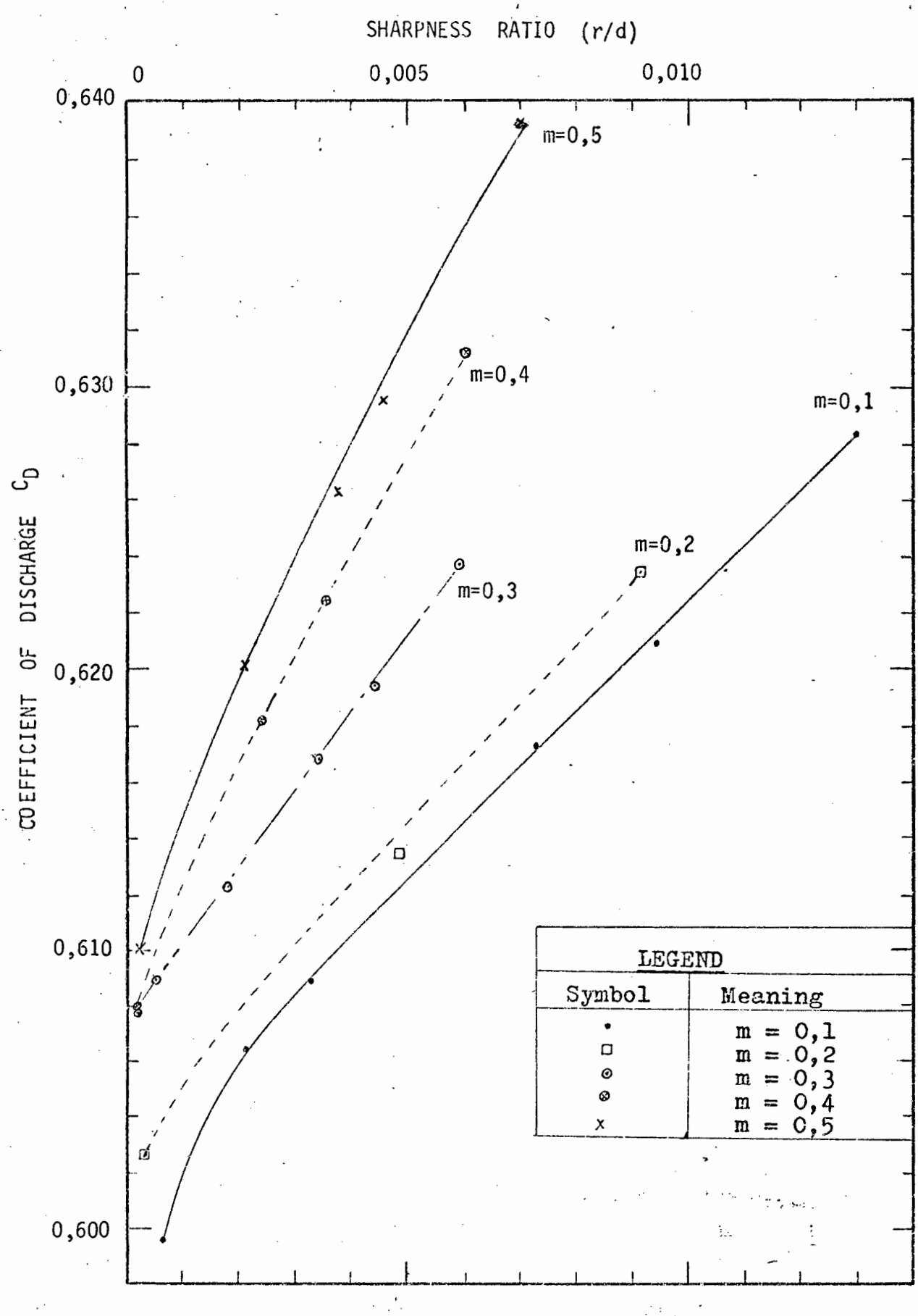

Fig.59. The Effect on the Coefficient of Discharge of Orifice Plates of Increasing the Sharpness Ratio of a Plate

Fig. 60. The Percentage Change in the Coefficient of Discharge of Orifice Plates with Increasing Edge Radii

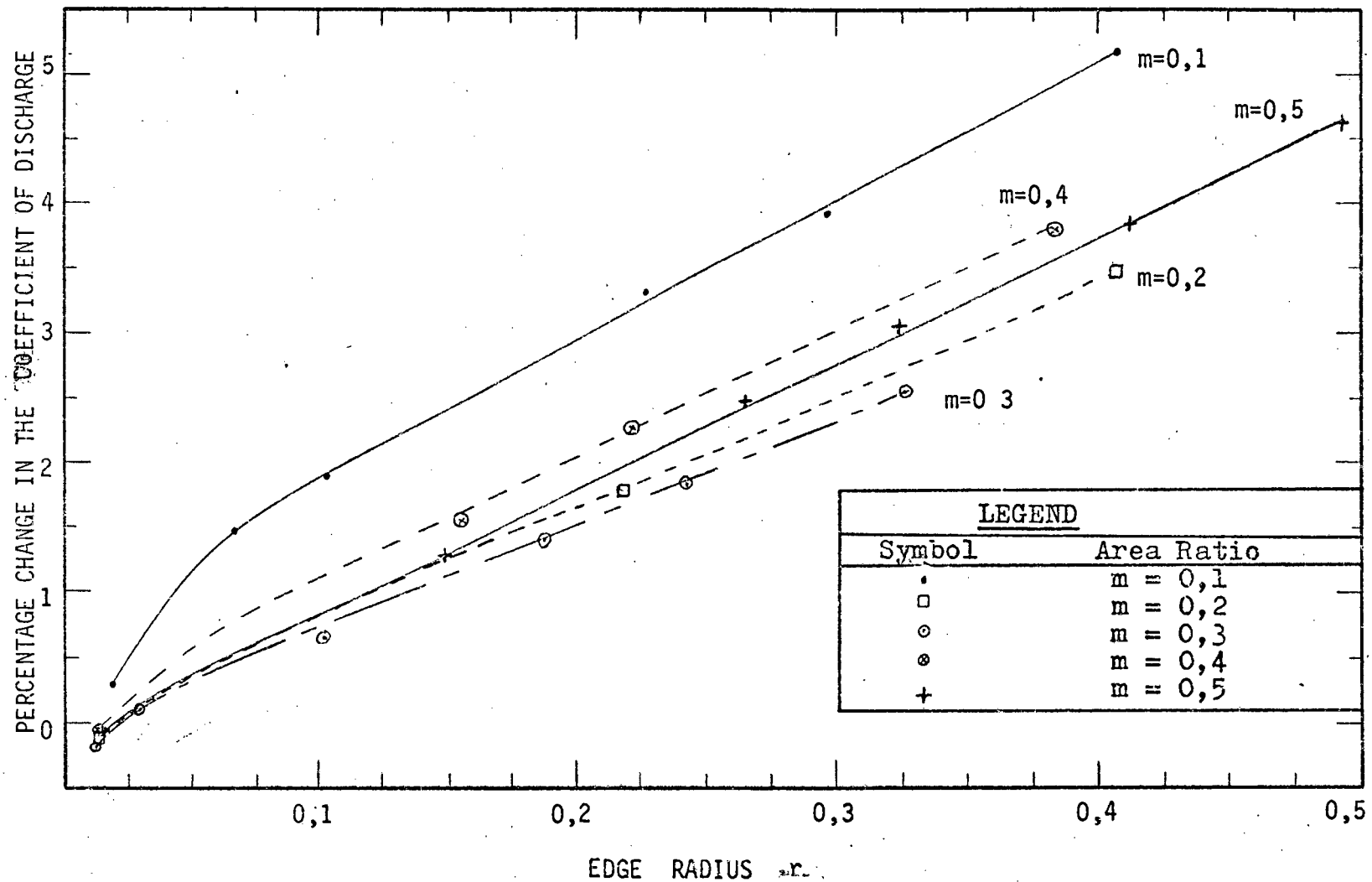

Fig.61 *The Percentage Change in the Coefficient of Discharge of Orifice Plates with Increasing Sharpness Ratio*

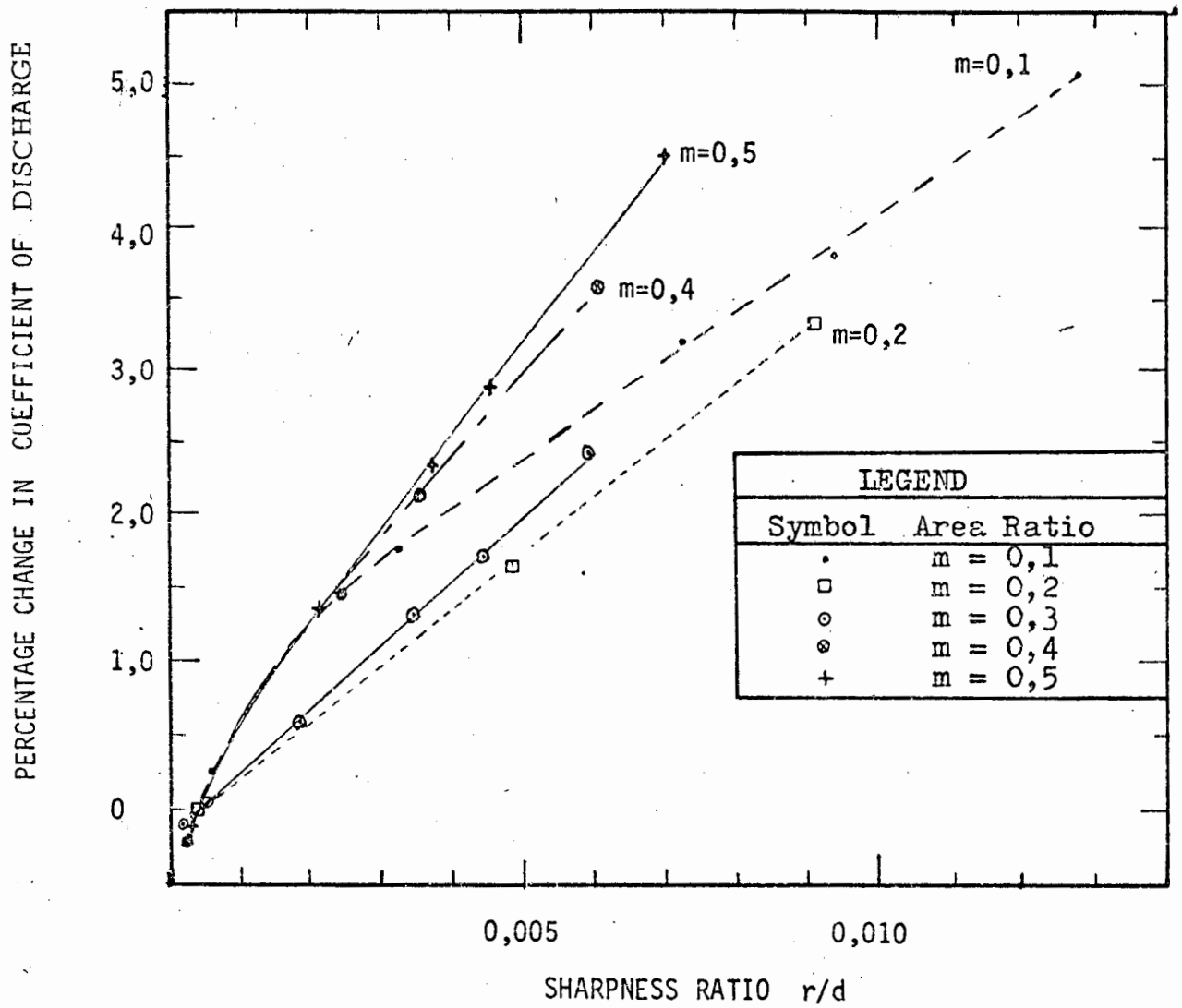

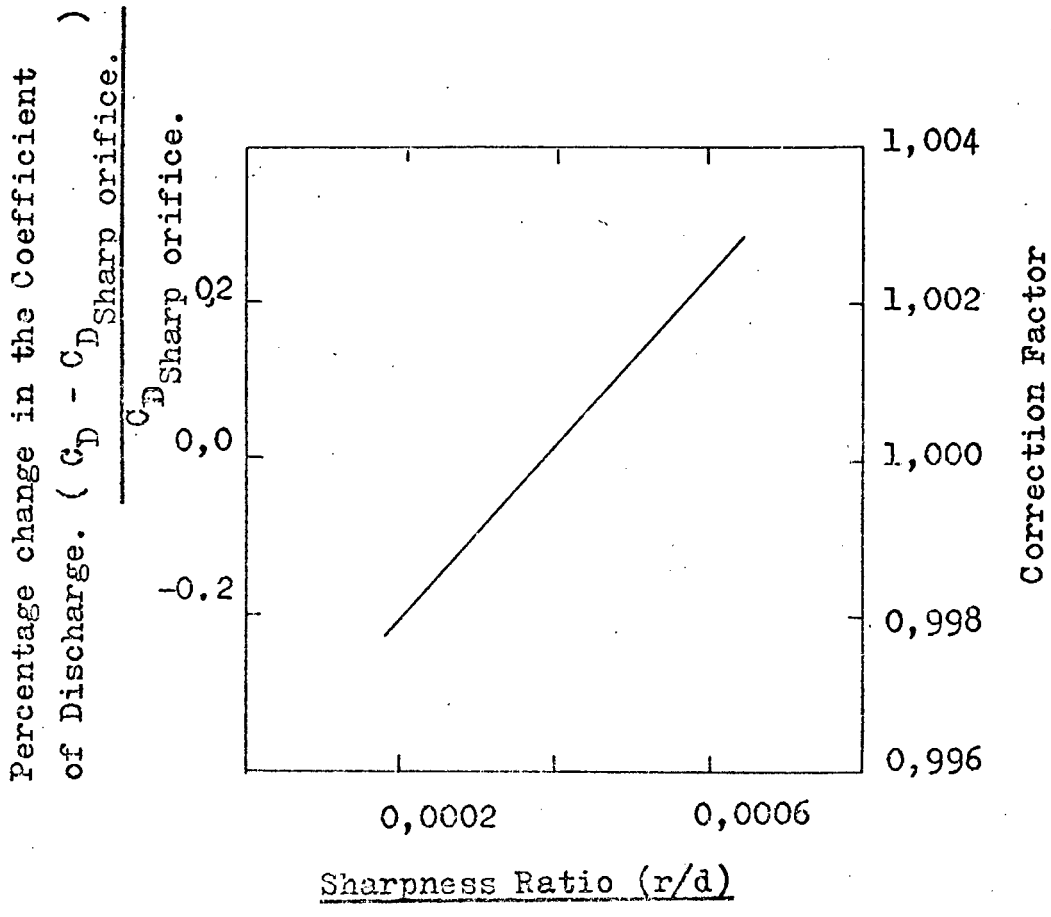

Fig. 62. The recommended correction factors to be applied to Orifice Plates whose sharpness ratio varies between 0,0002 - 0,0006

CHAPTER FIVE

D I S C U S S I O N

5.1 METHOD OF CALIBRATION AND GENERAL RESULTS.

In Chapter Four it was shown that the repeatability of the coefficient of discharge increased with increasing Reynolds number, which in turn increased with increasing flow rate. The accuracy of the pressure difference readings also increased with increasing flow rate. From the above information it was concluded that the change in the repeatability of the coefficient of discharge with flow rate was mainly due to the change in the accuracy of the pressure measurement. The reason for the large difference between the accuracy of the pressure difference reading and the repeatability of the coefficient of discharge at high flow rates was due to the decrease in the repeatability of the reference meter reading with increasing flow rate. Therefore the repeatability of the reference meter and the accuracy of the pressure difference reading influenced mainly the repeatability of a single calibration.

5.2 RESULTS OBTAINED FOR THE SHARP ORIFICE PLATES.

It was found that the sharpness ratio (r/d) of the orifice plates varied even though the edge radius of each plate was approximately equal. The variation in the sharpness ratio from 0,0004 caused a significant increase or decrease in the discharge coefficient. (see section 5.5).
Thus to determine the relationship between coefficient of discharge and area ratio of orifice plates tested, the coefficient of discharge of each concentric plate had to be corrected for sharpness ratio.

The coefficient of discharge of the orifice plates with area ratios of 0,15; 0,45; and 0,55 was about 0,5 per cent higher than expected.
This difference can only be attributed to a minor change in the apparatus used to calibrate these orifice plates. The modification was introduced because special flanges were required which allowed for varying the eccentricity of the orifice plates without having to remove the plates.
For the edge sharpness experiments, the upstream and downstream tappings were positioned at a distance of 100mm and 49mm respectively. With the new flanges, these distances changed to 104 and 55 millimetres respectively. The position of the tappings in each case satisfied the British Standards specifications for D and D/2 tappings but in the latter case, the position of the downstream tap was D/2 + 0,047D which was close to the maximum allowable limit of D/2 + 0,5D. Since the British Standard Specifications were adhered to, the change in the position of the downstream pressure tap was considered acceptable . This increase in the distance of the downstream pressure tap caused the increase in the value of the coefficient of discharge of the orifice plates with area ratios of 0,45 and 0,55.

The distance of the vena contracta from the orifice plates of area ratios of 0,45 and 0,55 was 0,48 and 0,41 pipe diameters respectively. Moving the downstream tapping further away from the orifice plate resulted in a lower pressure drop for the same flow rate than would have occurred with the taps in the initial position. The coefficient of discharge therefore increased.

The sharpness ratio of these plates was 0,0003 and 0,0002 respectively. If an orifice plate was considered to be sharp when it had a sharpness ratio of 0,0004, then these plates could have been considered oversharp and as a result their coefficients were lower than for sharp plates. For the orifice plates with the area ratios of 0,45 and 0,55 the effect of moving the downstream pressure tap further away from the upstream face of the orifice plate was opposed by the oversharpness of these plates. The net result was a coefficient which was slightly higher than expected for these orifice plates.

The actual correction factor for these plates was not known as the relationship between the position of the pressure taps and the coefficient of discharge was unknown. The above results demonstrated the necessity for the accurate location of the downstream taps and highlighted the need for stringent specifications if hign accuracy was required.

The plate with the area ratio of 0,15 was found to have a sharpness ratio of 0,0007 and this roundness of its edge caused an increase in its coefficient of approximately 0,4 per cent. The findings of Spencer, Calame and Singer substantiate the above statement. They found that for orifice plates with small area ratios, a substantial increase in the coefficient of discharge occurred as a result of microscopic imperfections in the edge.

5.3. COMPARISON OF THE EXPERIMENTAL RESULTS FOR SHARP CONCENTRIC ORIFICE PLATES AGAINST VARIOUS STANDARDS

a). The British Standards.

The coefficients of discharge determined experimentally at a Reynolds number of 100 000 and 200 000 for the sharp orifice plates tested and the coefficient of discharge specified by the British standards at these Reynolds numbers was plotted against the area ratio (figure 63 & 64).

From figures 63 and 64 it is evident that the experimentally determined coefficients of discharge are well within the tolerance limits of the British Standards. The largest difference between the experimentally determined coefficient of discharge and the British Standard coefficient of discharge at a Reynolds number of 200 000 is for the orifice plate with area ratio of 0,4, and this difference is 0,49%. Therefore it can be concluded that if the British Standards were used to determine the coefficient of discharge of the orifice plates tested, then the largest error that would occur would be equal to 0,49%.

If the correction factor determined in section 4.4.2 for orifice plates whose sharpness ratio was not 0,0004 was applied to the coefficient of discharge of the orifice plates tested, then the British Standard coefficients would be in agreement with the experimental ones to within ± 0,35 per cent. This shows that improvement in the tolerance limit specified by the British Standard could be achieved by including a correction factor for the sharpness of the upstream edge of the orifice plates.

It is also evident that the closest agreement between the British Standard coefficients and the uncorrected experimental one is for the orifice plates whose area ratios are greater than 0,45. This is contrary to expectations as the tolerance limit on the coefficient of discharge of the orifice plates with area ratios less than 0,4 is constant at ± 0,75% while for the plates with area ratios greater than 0,4 this tolerance increases with increasing area ratio. As a result of the above it was expected that the specified standard coefficient for low area ratio orifice plates would be in closer agreement with the experimental results than the coefficients for the large area ratio plates. The explanation for this occurrence seems to be that the effect of upstream edge roundness is greater for the small area ratio plates than for the larger ones. This explanation is substantiated by the notable improvement in agreement between the British

Standard and the experimental results which were corrected for edge sharpness effect. This improvement was especially notable for the low area ratio orifice plates.

Similar results are achieved at a Reynolds number of 100 000, but the difference between the British Standard coefficient and the experimental one is larger for both the corrected and uncorrected coefficients.

b) A.S.M.E.

The experimentally determined coefficient of discharge for sharp orifice plates was compared with the American Standards in figure 65 where the respective coefficients of discharge determined at a Reynolds number of 200 000 are plotted against the area ratio. This comparison shows that the experimentally determined coefficients of discharge of the orifice plates with area ratios of 0,15; 0,40 and 0,50 are outside the tolerance limits specified by ASME. The largest difference between the ASME and experimental coefficient is for the orifice plate with area ratio of 0,15 and this difference is equal to 0,89 per cent.
If the experimental coefficients are corrected for edge sharpness, then this difference decreases to 0,65 per cent. This shows clearly that the experimental results are closer to the British Standard coefficients than to the ASME ones. Furthermore ASME coefficients are supposed to apply within a lower tolerance limit ($\pm$ 0,50%) than the British ones ($\pm$ 0,75%). The experimental results clearly indicate that ASME coefficients are high for large area ratio plates ($m > 0,3$) and low for plates whose area ratio is less than 0,3. The only orifice plate whose experimental coefficient is equal to that specified by ASME is the one with area ratio of 0,3.

c). I.S.O.

I.S.O. does not specify the coefficients of discharge of orifice plates with D & D/2 taps, but specifies the coefficients of

discharge of orifice plates with vena contracta taps. The coefficients specified by I.S.O. should be correct within a tolerance limit of $\pm$ 0,25 per cent for orifice plates with area ratios ranging between 0,15 and 0,45, as the I.S.O. specifications for the vena contracta are adhered to by a D/2 tapping for these orifice plates.

In figure 66 the experimentally determined discharge coefficients were compared with the I.S.O. coefficients. The coefficients of discharge were determined at a Reynolds number of 200 000. The results show that contrary to expectations, only the coefficients of discharge of the orifice plates with area ratios of 0,4 and 0,5 are within the tolerance limit specified by I.S.O. The coefficients of all the other orifice plates are too high. The actual percentage difference between the coefficients specified by the I.S.O, A.S.M.E. and British Standards as compared with the experimental coefficients, as stated in Table 8.

The experimental coefficients of discharge were corrected for edge sharpness and these coefficients were compared with the I.S.O. coefficients. This results in a reduction in the maximum difference between the experimental coefficients and the I.S.O. coefficients from 1,26 per cent to 0,79 per cent.

From these results one can conclude that the I.S.O. specifications regarding either the position of the vena contracta or the tolerance limit on its coefficients are in need of revision.

TABLE 8

Comparison between the values quoted for the discharge coefficient by the various standards and by researchers with the values obtained experimentally.

Area Ratio of Orifice Plate	PERCENTAGE DIFFERENCE BETWEEN THE STANDARD AND EXPERIMENTAL RESULTS AT A REYNOLDS NUMBER OF 200 000				
	B S	ASME	ISO	Buckinghams Equation	Dowell & Yullin Chen Equation
0,1	-0,30	-0,30	-0,78	-0,30	0,17
0,15	-0,45	-0,89	-1,26	-0,89	-0,13
0,2	0,50	-0,15	-0,60	-0,15	0,30
0,3	0,54	-0,03	-0,49	-0,03	0,12
0,4	0,49	0,84	0,23	-0,84	0,39
0,45	-0,38	0,20	-0,31	0,20	0,10
0,5	0,07	0,79	0,18	0,79	0,72
0,55	-0,29	0,34	-0,39	0,34	0,44

NOTE: ISO VALUES ARE FOR VENA CONTRACTA TAPS AND NOT D & D/2 taps.

d) Dowell & Yo-Lin Chen's proposed coefficients

Comparing the experimental results with Dowell and Yu-Lin Chen's proposed coefficients shows agreement within 0,3 per cent for the orifice plates with area ratios lower than 0,3 and at worst, of 0,72 per cent for orifice plates with area ratios greater than 0,3 (Fig. 67). This shows that there is good agreement between the author's results and the coefficients proposed by Dowell and Yu-Lin Chen for orifice plates with area ratios less than 0,3. Dowell and Yu-Lin Chen's proposed equation results in coefficients which are too high for plates with area ratios greater than 0,3.

If the experimental results are corrected for upstream edge sharpness, then the maximum difference between Dowell and Yu-Lin Chen's proposed coefficients and the experimentally determined ones, decreases to 0,50 per cent.

From these comparisons, it is evident that the experimentally determined coefficients are in the closest agreement with the British Standard; then with Dowell and Yu-Lin Chen's coefficients, followed by A.S.M.E. and lastly I.S.O. The results also show that the agreement between the experimental results and any of the standards can be improved by introducing a correction factor for upstream edge sharpness.

It must be noted that the author's experiments were conducted in a 100 millimetre pipe and therefore the above analysis applies to this pipe size only. To try and extend it for other pipe diameters, reliable results on pipe size effects must be used.

Figure 63. Comparison between the experimentally determined coefficient of discharge and the ones specified by the British Standard for the orifice plates tested.(Comparison at a Reynolds Number of 100 000)

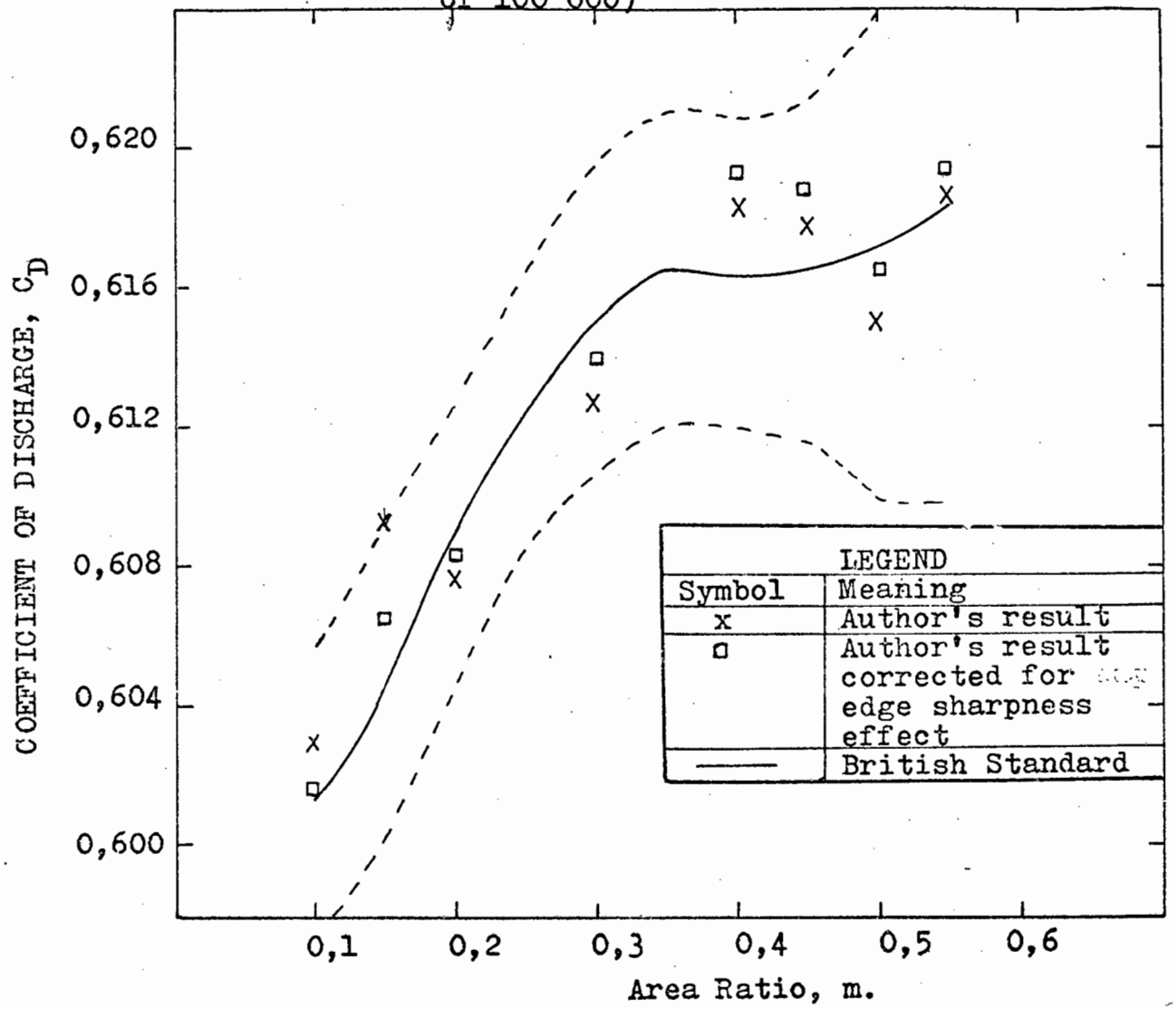

Figure 64. Comparison between experimentally determined coefficients of discharge and the ones specified by the British Standard for the orifice plates tested. (Comparison at a Reynolds number of 200 000).

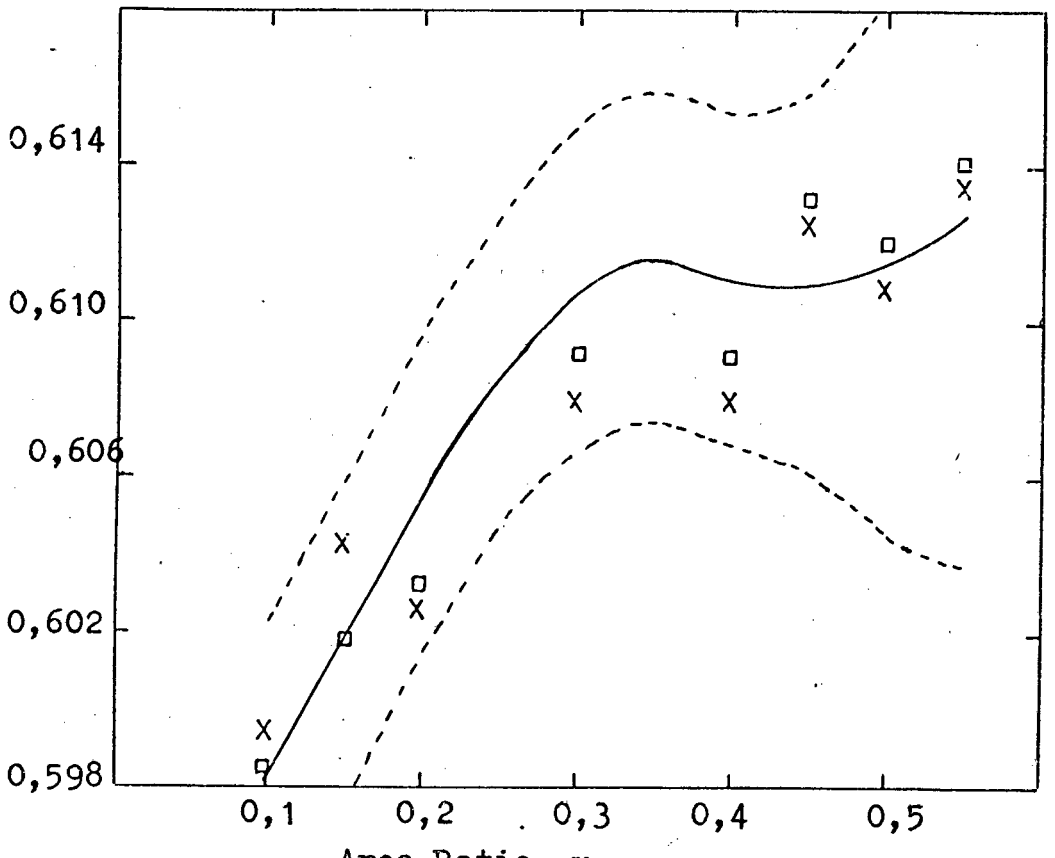

LEGEND	
Symbol	Meaning
x	experimentally determined coefficients of discharge
□	experimentally determined coefficients of discharge corrected for edge sharpness
——	British Standard coefficients of discharge
- - -	Tolerance on the British Standard coefficient as specified by this standard.

Figure 65. Comparison between experimentally determined coefficients of discharge and the ones specified by A.S.M.E.for the orifice plates tested. (Comparison at a Reynolds number of 200 000.)

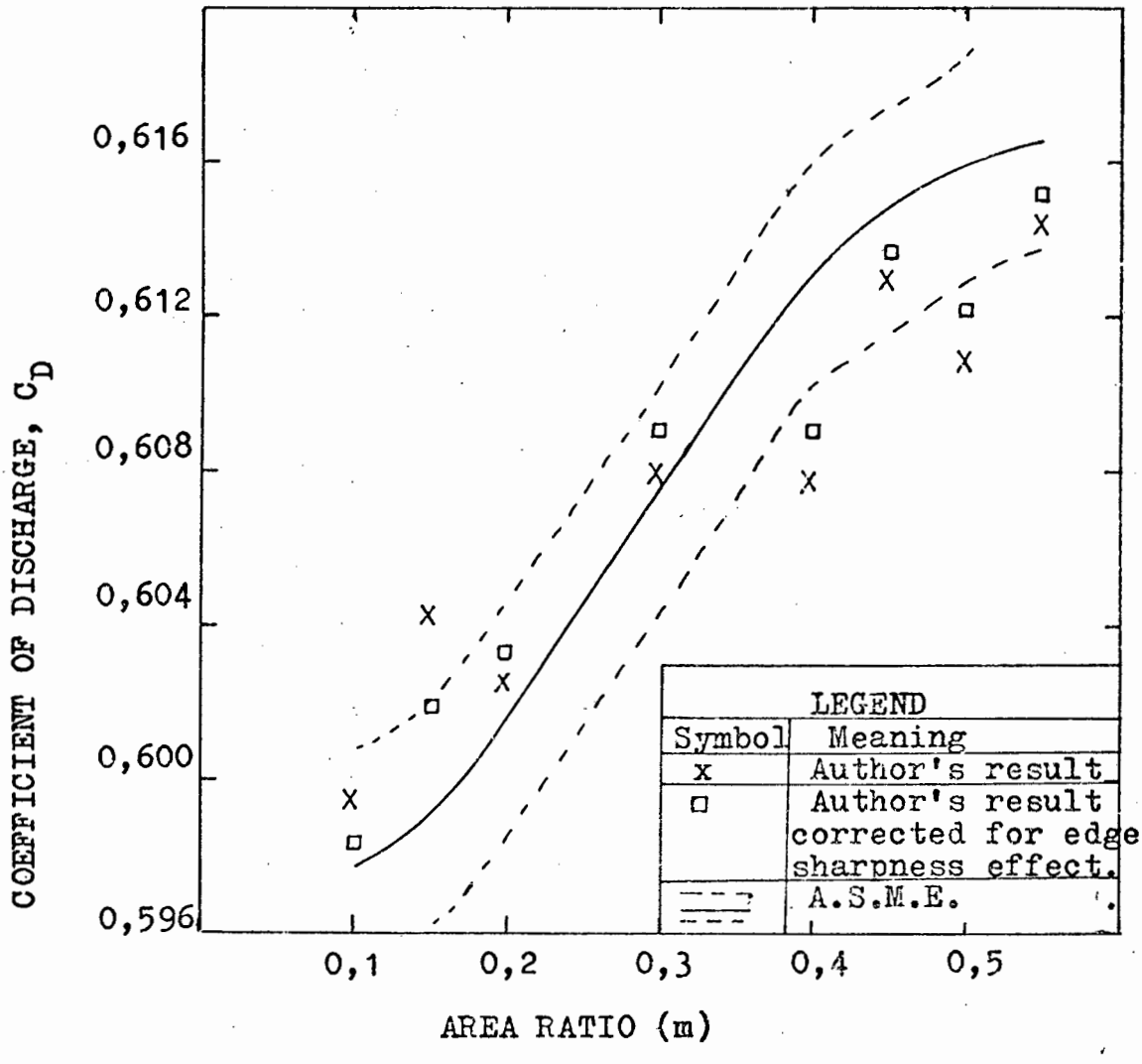

Figure 66. Comparison between experimentally determined coefficients of discharge and the ones specified by I.S.O. for the orifice plates tested. (Comparison at a Reynolds number of 200 000).

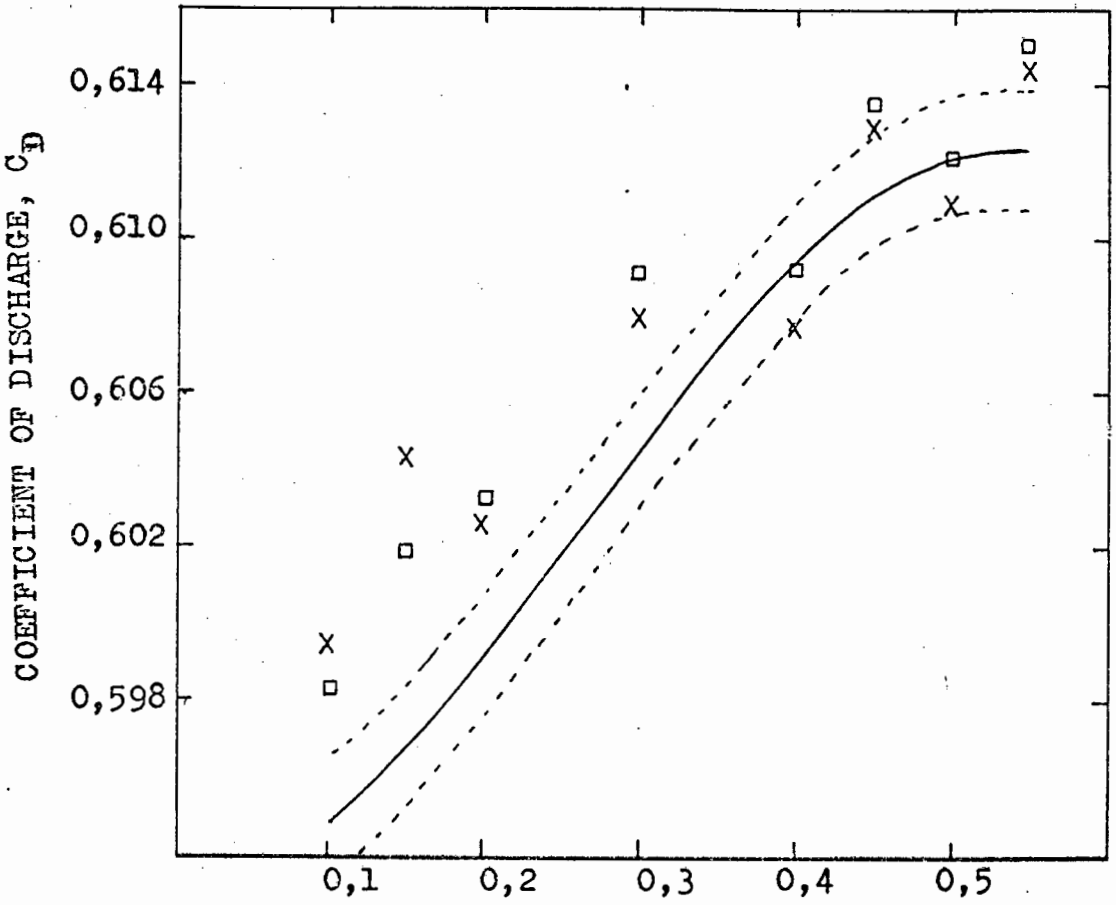

LEGEND Symbol	Meaning
x	Author's result
□	Author's result corrected for edge sharpness effect
———	I.S.O. coefficients of discharge
- - - -	Tolerance on the I.S.O. coefficient as specified by this standard.

Figure 67. Comparison between experimentally determined coefficients of discharge and the ones specified by Yu lin Chenfor the orifice plates tested. (Comparison at a Reynolds number of 200 000)

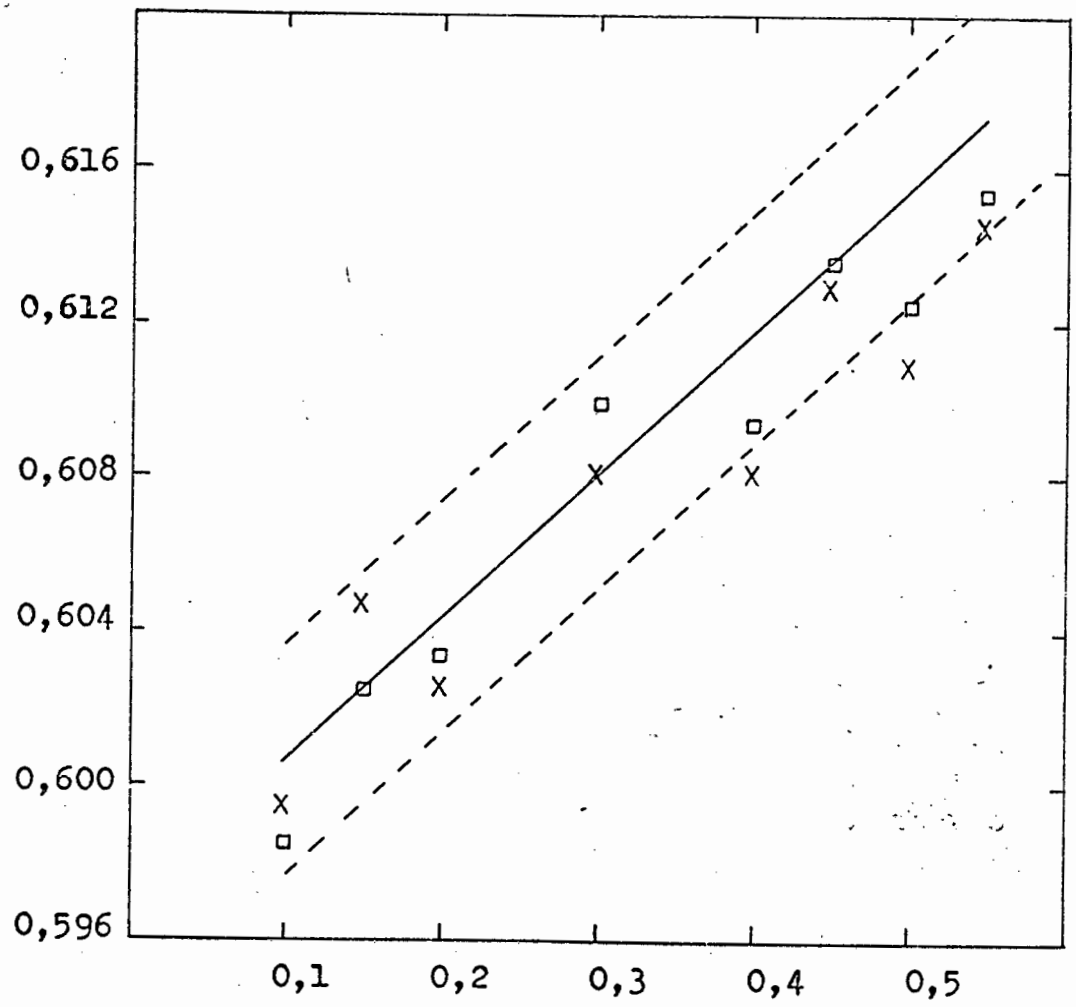

LEGEND	
Symbol	Meaning
x	Author's result
	Author's result corrected for edge sharpness effect
	Dowell and Yu-Lin Chen's proposed coefficient

5.4 THE EFFECT OF ECCENTRICITY.

a) Relationship between discharge coefficient and eccentricity

Three orifice plates were tested and a logarithmic relationship between the coefficient of discharge and eccentricity was obtained.

The initial small increase in the coefficient of discharge with increasing eccentricity was expected as similar findings were reported by Miller and Kneisel after the completion of their experiments. Miller and Kneisel did not find a readily discernible relationship between eccentricity and the coefficient of discharge. Although their findings differed from the results obtained in this experiment, the difference was due only to the fact that they did not test for larger eccentricities than 7,5 millimetres. An examination of their results showed that if they would have continued to increase the eccentricity, results similar to those found in this paper would have been obtained (See figure 68).

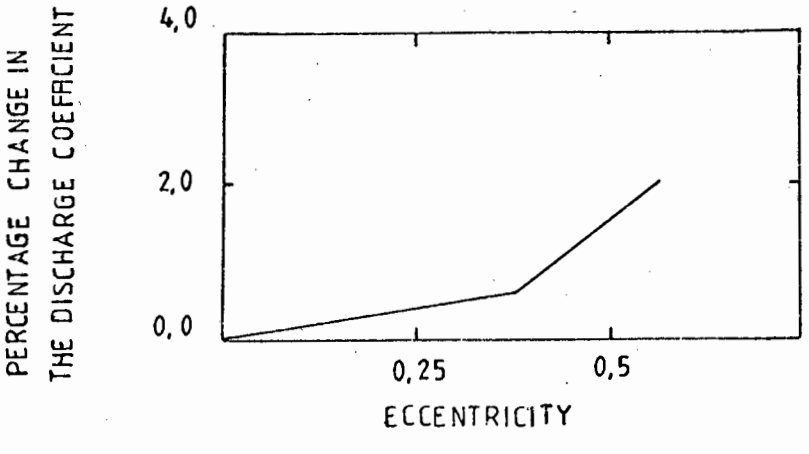

Fig. 68 Typical Results obtained by Miller & Kneisel

For small eccentricity ratios the work done by Hinz, Scofield, Edwards and Casale was in agreement with the experimental findings.
The results obtained by Hinz and his fellow researchers are shown in figure 69.

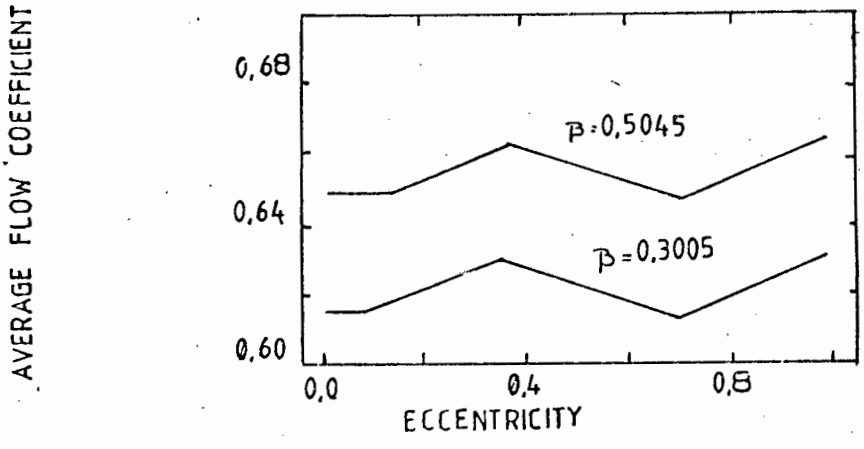

Fig. 69. The Results obtained by Hinz and Fellow Researchers.

For eccentricity ratios greater than 0,35 differences between the findings of Hinz and co-authors and those of the author exist.

One of the reasons why their results did not agree with the author's findings was that their experiments were conducted in a 25,4 millimetre pipe. The author's results were applicable to flow in one hundred millmeter pipes only, and thus could not be compared with those of Hinz and his fellow researchers. Furthermore the change in the trend of the flow coefficient with eccentricity ratio as determined by them could not be explained. Even Hinz states that:- "the author feels that the data in this region may be less reliable than in the other regions". He refers to the second region where the eccentricity ratio varies from 0,35 to 0,7.

The experimental results showed that the coefficient of discharge was related to the magnitude of the eccentricity and to the diameter ratio.

The above findings were substantiated by statements found in the standards, and by the findings of Miller and Kneisel.

The effect of eccentricity on the coefficient of discharge increased with increasing area ratio. They have found that the coefficient of discharge was also related to the direction of the eccentricity with respect to the pressure taps. Multiple tappings were used in the experiments conducted by the author and thus no relevant comment could be made on the above statement. With the use of multiple tappings, directional influences were neither expected nor detected.

All other researchers studying the effect of eccentricity found an initial increase in the pressure fluctuations and a subsequent decrease with increasing eccentricity. The recordings taken with the pressure differential transducer of the fluctuations in pressure with increasing eccentricity, clearly illustrated this point.

b) Determination of the maximum error in the coefficient of discharge of standard orifice plates as a result of eccentricity specifications.

From the specifications of the various standards the maximum allowable eccentricity for various area ratio plates was determined. From these values, the maximum allowable eccentricity ratio for each orifice plate was determined. From figure 54, the percentage change in the coefficient of discharge of concentric orifice plates due to eccentricity of these plates was obtained. The results obtained for the various engineering standards are tabulated in table 9 on the following page.

TABLE 9

The percentage error in the coefficient of discharge, as specified by the various standards, which arises when the orifice plate is positioned at the limit of the eccentricity specifications of the standard concerned.

ENGINEERING STANDARD	PERCENTAGE ERROR IN THE COEFFICIENT OF DISCHARGE AT AN AREA RATIO OF		
	0,15	0,45	0,55
B.S.	0,20	0,35	0,4
A.S.M.E.	0,05	0,08	0,12
A.G.A.	0,16	0,85	1,4
I.S.O.	0,12	0,08	0,08
BEANS SUGGESTION	0,08	0,08	0,10

From table 9 it is evident that adhering to the British standard specifications for maximum allowable eccentricity can cause errors greater than 0,4 per cent. Considering that the tolerance limit quoted by the British Standard on its coefficient is 0,75 per cent for orifice plates with area ratios below 0,4, the error introduced by eccentricity alone is very high.

A.S.M.E. specifications for eccentricity of the plate are more stringent than those of the British Standard and consequently the error due to the maximum allowed eccentricity is very low. Only orifice plates with area ratios greater than 0,55 will have errors in their coefficients which are greater than 0, 1 per cent.

The I.S.O. specifications are less stringent than the A.S.M.E. ones for small area ratio plates but they are more stringent for large area ratio plates. The manner in which I.S.O. specifies the maximum allowable eccentricity is therefore better, as it does not call for over stringent specifications where it is not required. (i.e. small area ratio plates). The maximum error in the coefficient of discharge due to eccentricity will not exceed 0,12 per cent if I.S.O. specifications are adhered to.

A.G.A., similarly to ASME, specifies a constant maximum allowable eccentricity irrespective of the area ratio, but contrary to ASME its specifications are so slack that errors of over 1,4 per cent can occur.
These errors can place the coefficient of discharge outside the tolerance limit quoted by A.G.A.
Bean's suggestion for maximum allowable eccentricity results in the smallest errors. The maximum error due to eccentricity will not exceed 0,1 per cent.

c) The author's suggestion for maximum allowable eccentricity.

The experimental results show that initially large changes in eccentricity cause small errors in the discharge coefficient, and that further increases in eccentricity result in large errors in the discharge coefficient. (see Figure 54)
As a result of these findings, and because of the need to improve on the accuracy of the standard coefficients, the author feels that specifications which will limit the maximum error in the coefficient of discharge due to eccentricity to below 0,1 per cent, are justifiable and also possible to achieve.

To limit the error in the coefficient of discharge due to eccentricity to 0,1 per cent, the maximum allowable eccentricity can be calculated from the following equation:

$$\frac{100\ E}{D-d} = 3{,}55 - 1{,}69\ m \quad \ldots\ldots\ldots \quad (1)$$

d) Comparison with ASME for fully eccentric orifice plates.

The experimental results could not be compared with the ASME coefficients for fully eccentric orifices as the coefficients specified in ASME were for vena contracta taps. Since the distance of the vena contracta from the orifice plate increased with increasing eccentricity, the experimental tests, which were obtained with D and D/2 tappings, resulted in coefficients which were higher than those quoted in ASME.
An indication of the difference between these coefficients is given in table 10.

TABLE 10

The difference between the coefficients of discharge determined experimentally with D & D/2 taps and those quoted by ASME for vena contracta taps for fully eccentric orifice plates.

Area Ratio	Experimental coeff.	ASME coeff.	% difference
0,15	0,632	0,621	1,74
0,45	0,657	0,640	2,59
0,55	0,665	0,645	3,01

5.5. THE EFFECT OF EDGE SHARPNESS.

5.5.1 General findings.

The author's experimental results showed that the coefficient of discharge of every orifice plate tested increased considerably with increasing edge radius, but the shape of the curve portraying the relationship between sharpness ratio and change in coefficient

of discharge varied for the different area ratio plates. These curves were similar, but the curve for the orifice plate with area ratio of 0,3 was almost linear. Furthermore, the change in the coefficient of discharge with increasing edge radius was greatest for the orifice plate with area ratio of 0,1.

5.5.2 Comparison with Hernings results for orifice plates with area ratios of 0,1 and 0,3.

The results obtained by the author and Herning for orifice plates with area ratios of 0,1 and 0,3 are compared in figure 70 and 71 respectively.
It is evident from this comparison that close agreement exists between Herning's and the author's results. These figures indicate clearly the similarity between the experimentally determined curves and those determined by Herning. They show that the coefficient of discharge of the orifice plate with area ratio of 0,1 is more affected by a variation in the edge radius than the plate with area ratio of 0,3.
The coefficients of discharge determined by Herning for an orifice plate with area ratio of 0,1 are higher than those determined by the author. The reason for this discrepancy is that Herning determined his coefficients at a Reynolds number of 70 000 while the author determined his coefficients at a Reynolds number of 200 000. Since the discharge coefficient decreases with increasing Reynolds numbers, the experimental coefficient had to be lower than Hernings. The results for the orifice plates with area ratio of 0,3 correlate with each other to within 0,2 per cent. This difference in the results is understandable, as the repeatability of a calibration as performed by the author is $\pm$ 0,1 per cent and the measurement of the orifice edge radius is $\pm$ 2%.

Figure.70. Comparison between author's results and Herning's results for effect of edge sharpness on the coefficient of discharge of orifice plates with area ratio of 0,1

□ Author's results ———

X Herning's results - - - -

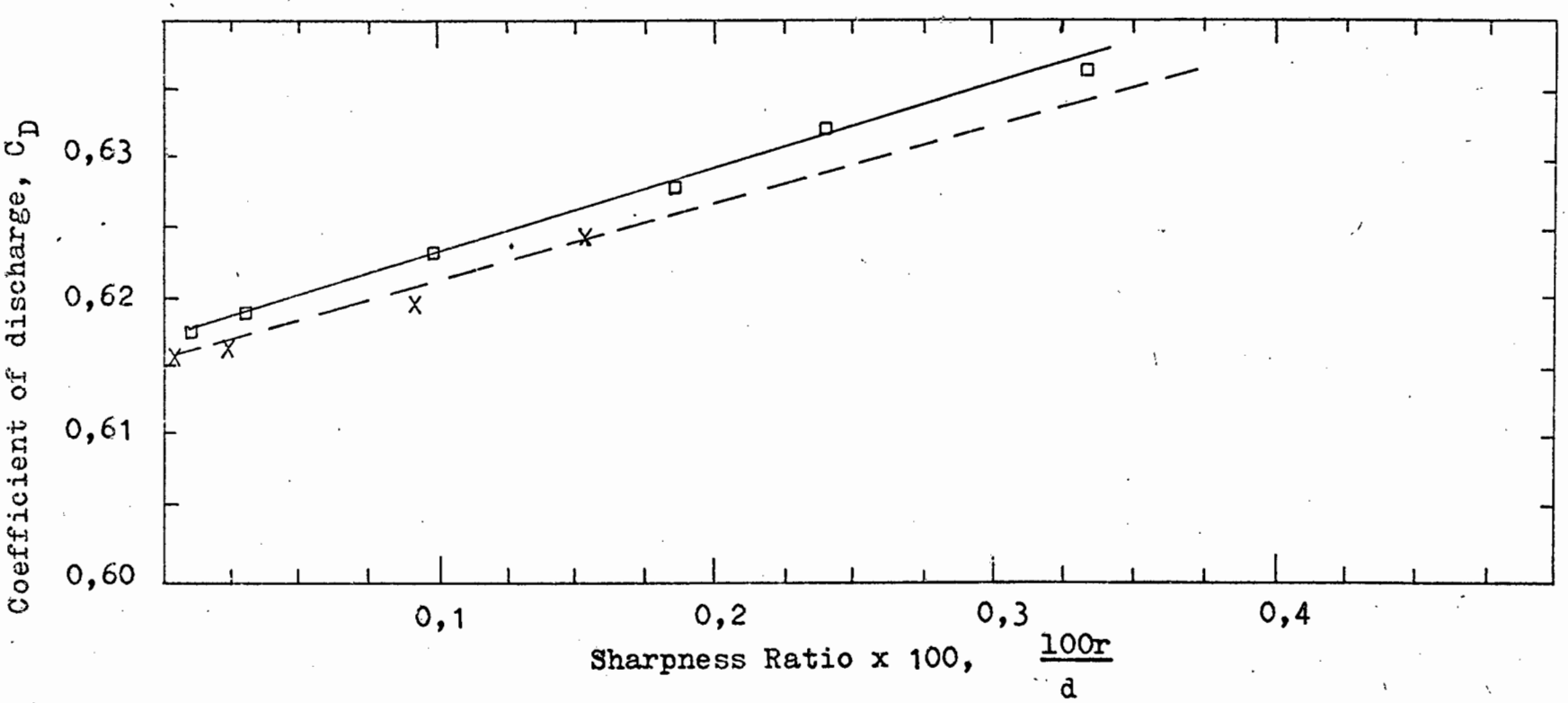

Figure 71. COMPARISON between AUTHOR'S results and HERNING'S results for effect of edge sharpness on the coefficient of discharge of orifice plates with area ratio of 0,3.

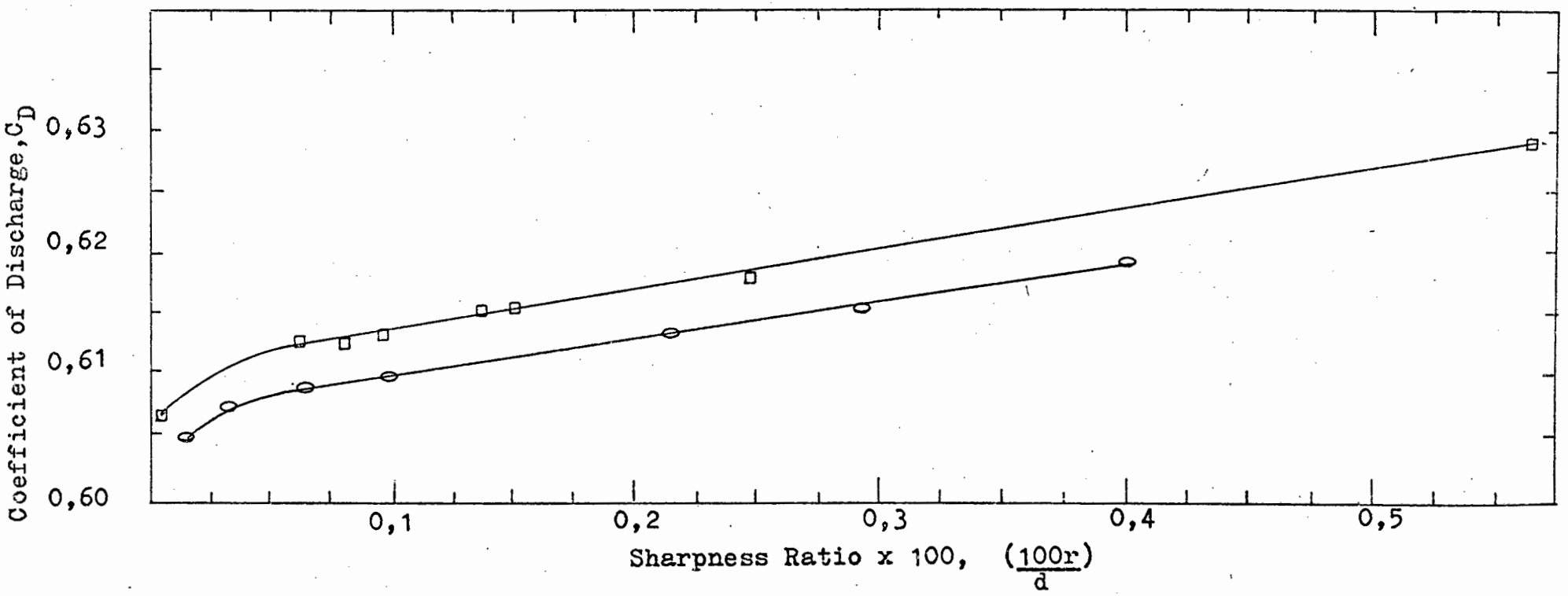

This result showed that measurements obtained with orifice plates are highly repeatable.

5.5.3 Analysis of the results.

From the results obtained the author determined the percentage change in the coefficient of discharge of orifice plates whose sharpness ratio was not equal to 0,0004. This change in the coefficient of discharge was then plotted against the sharpness ratio. The resultant data was then studied by the author and he came to the conclusion that from this data reliable correction curves for the effect of edge sharpness on the coefficient of discharge can be deduced.

Initially a single correction curve for the effect of edge sharpness on the coefficient of discharge of any orifice plate was determined. (see figure 72). Such a correction curve was considered useful as the deduced correction factor would be dependent on the value of the sharpness ratio only, and therefore the coefficient of discharge of any orifice plate could be corrected for edge sharpness effects. If the proposed correction curve is used, then the tolerance on the corrected coefficient of discharge will be in the order of $\pm$ 1,0 per cent.

Herning and Wolowski also determined such a correction curve, but the tolerance in the coefficient of discharge corrected by their curve is only $\pm$ 0,75 per cent. The author compared his correction curve with that of Herning and Wolowski in figure 73. From this figure it is evident that the correction factors proposed by the author are at most 0,3 per cent lower than those presented by Herning and Wolowski. For small sharpness ratio plates, agreement to within 0,1 per cent exists.

To enhance the validity of the proposed correction curve, the author decided to use his own results and those of Herning to derive a final proposed correction curve(see figure 73)

The tolerance on the coefficient of discharge corrected by use of this correction curve is in the order of $\pm$ 0,9 per cent. Because of this high tolerance on the corrected coefficient of discharge, this correction curve is not acceptable if highly accurate measurements are required.

To reduce the tolerance on the corrected discharge coefficient, the author decided to take into account the effect of area ratio on the coefficient of discharge of orifice plates with rounded upstream edge radii. It was found that the percentage change in the coefficient of discharge of all the orifice plates which had area ratios equal to or greater than 0,2 was independent of area ratio, and was dependent on the sharpness ratio only. As a result of the above findings, it was decided to propose two correction curves; one for the orifice plates with area ratios equal to or greater than 0,2, and the other for orifice plates with area ratios equal to 0,1. These two correction curves are shown in Figure 73.

From Figure 73 it is evident that if the general correction curve is applied to orifice plates with area ratios greater than 0,2, then the tolerance on the corrected coefficient of discharge is in the order of $\pm$ 0,4 per cent. For the orifice plate with area ratio equal to 0,1, the tolerance on the corrected coefficient of discharge is equal to $\pm$ 0,1 per cent.

The tolerance limit on the correction coefficient is reduced considerably by this approach, but care must be taken on how these correction curves are used. This is due to the fact that the experimental results were obtained for orifice plates with area ratios of 0,1 0,2, 0,3, 0,4 and 0,5 only and the effect of edge roundness on the discharge coefficient of orifice plates with area ratios smaller than 0,2 is not known, with the exception of the plates with area ratios equal to 0,10. Due to the above, the correction curve for orifice plates with area ratios equal to or greater than 0,2 should be corrected for edge sharpness effects by the use of the proposed correction factor, while for orifice plates with area ratios less than 0,2 the

correction factor proposed in Figure 72 should be used.

Although the correction factors deduced in figures 72 and 73 are useful, lower tolerance on the correction coefficient of discharge of orifice plates with sharpness ratios varying from 0,0002 to 0,0006 can be achieved. Such a correction curve was presented in chapter 4 and the tolerance on the corrected coefficient is in the order of ± 0,1 per cent. Most orifice plates in use should have sharpness ratios smaller than 0,0006 as an orifice plate bored out on a lathe has a sharpness ratio which varies from 0,0002 to 0,0006 and therefore the proposed correction factor in figure 62 could be used in most cases.

The author tried to compare his results for small sharpness ratio plates with those of Herning, of Benedict, Wyler and Brandt and those of Crocket and Upp. He found that such a comparison was not possible as the Reynolds numbers at which their results were given was diffferent from the range over which the author tested his plates. Furthermore, to determine the percentage change in coefficient of discharge, the different researchers used different standard coefficients as the reference coefficient. For example Upp and Crocket and Benedict, Wyler and Brandt based their comparison on the A.S.M.E. standard coefficient. It is interesting that in both these references the difference between the standard coefficient and their experimentally determined ones, for sharp orifice plates exceeds the tolerance limit specified by ASME.

Herning used the I.S.O. and the DIN coefficients as a basic coefficient and he compared all his results with the specifications of these standards. Although the basic coefficient used for comparison by Herning is different from the author's, close agreement between their results exist for small sharpness ratio plates. (see figure 74). For orifice plates with sharpness ratios varying from

0,0002 to 0,0006 the largest difference between the proposed correction factors is 0,15 per cent.

Herning had found that the same correction factor for edge roundness applied irrespective of the pipe diameter. Since the experimental results were for one hundred millimetre pipes only, no comment was made on the above finding. If it is assumed that Herning's findings are correct and the author's results prove this, then the proposed correction factor could be used for pipes of all sizes.

Based on the above discussion the author makes the following recommendations:

1. If any orifice plate with area ratio less than 0,2 and sharpness ratio greater than 0,0006 is used, then the correction factor proposed in figure 72 should be used.

2. For any orifice plate with area ratio greater than 0,2 and sharpness ratio greater than 0,0006, the correction curve proposed in figure 73 should be used.

3. For any orifice plate with sharpness ratio varying between 0,0002 and 0,0006 the correction factor proposed in figure 62 should be used.

5.5.4 Analysis of the Engineering standards regarding edge sharpness

From figures 67 and 68 it was evident that the effect of rounding the edge of an orifice plate caused substantial increases in the discharge coefficient. For example, increasing the sharpness ratio of an orifice plate with an area ratio of 0,5 from 0,0002 to 0,0003 caused an increase in the coefficient of discharge of 0,16 per cent. Thus an orifice plate which had a sharpness ratio smaller than 0,0004 and was referred to

as 'oversharp' in this thesis, would have a similar error in its coefficient as a plate whose edge was slightly rounded. As a result of the above findings, the validity of the definitions of the various standards was examined.

1. ASME and I.S.O.

Small changes in the sharpness ratio were not detectable by a mere visual inspection, thus illustrating the fact that the ASME and I.S.O. specifications for the condition of the upstream edge of an orifice plate were inadequate and thus the specifications of these standards were in need of revision.

2. British and German Standards.

The British and the DIN standards on flow measurement specified that the sharpness ratio had to be equal to or less than 0,0004 for an orifice plate to be considered sharp. For highly accurate measurements this specification was also inadequate as two plates, both conforming to the above specification but differing in sharpness ratio, could have coefficients of discharge differing by as much as 0,5 per cent.

5.5.5 The validity of the experimental results.

The two factors which affected the validity of the experimental results were firstly the variation in the shape and size of the upstream edge of the orifice around its circumference, and secondly the uncertainty in the measurement of its edge sharpness. The problem of the varying radii along the edge of a single orifice plate could have been overcome by designing a special tool which could have been used to increase the edge radius of each plate. Since the increases in the edge radii were small, the tool had to be very accurate and therefore it would have been

expensive. Such a tool was not warranted because of the low repeatability in the measurement of the edge radius and because of the high cost involved.

Using the average edge radius as obtained from six measurements around the circumference of an orifice plate caused errors in the results obtained, but these results nevertheless gave a good indication of the effect of varying the edge radius of an orifice plate. The close agreement between these results and those of Herning seem to substantiate their validity.

Figure 72. The recommended correction factor for any orifice plate as given by author and by Herning

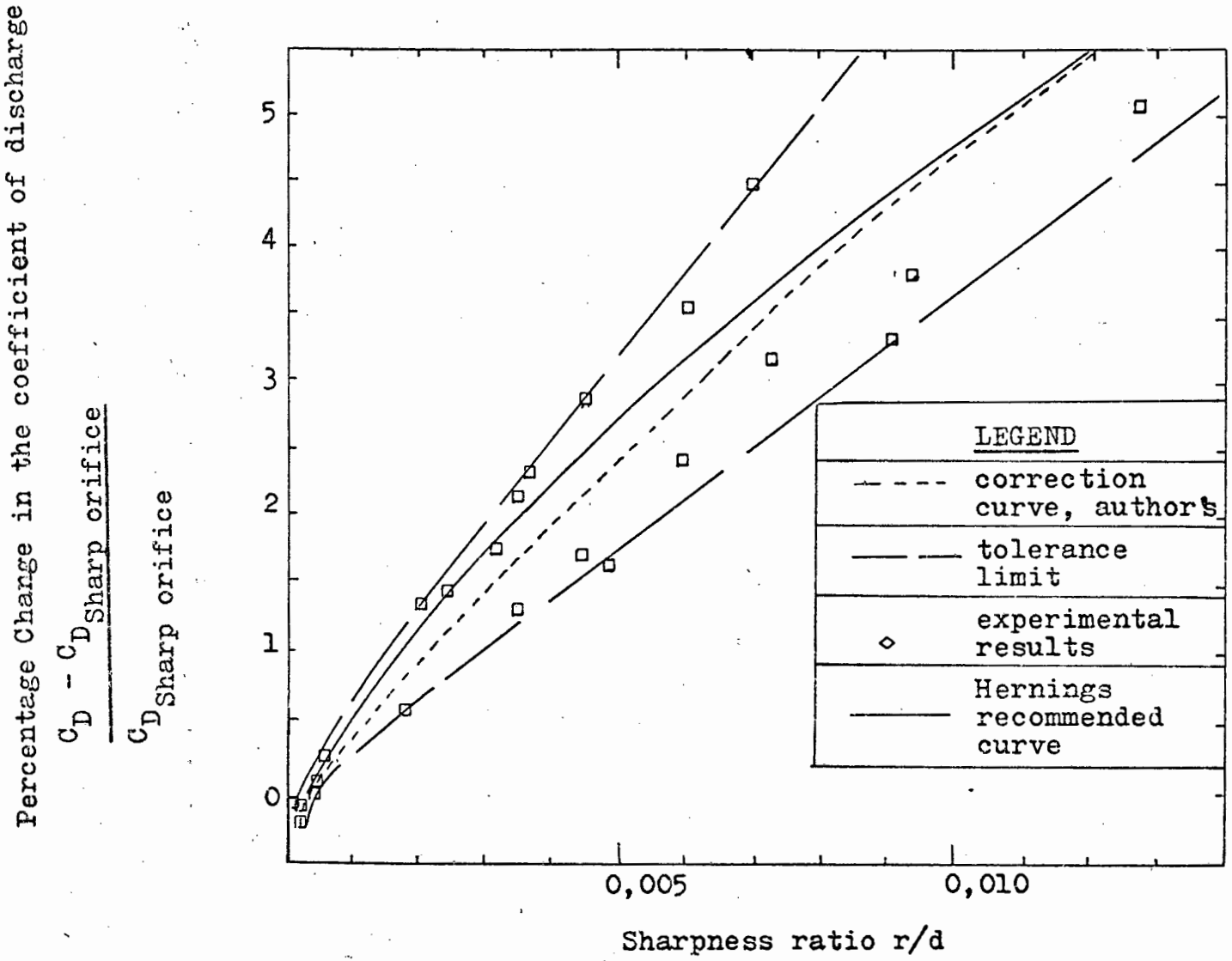

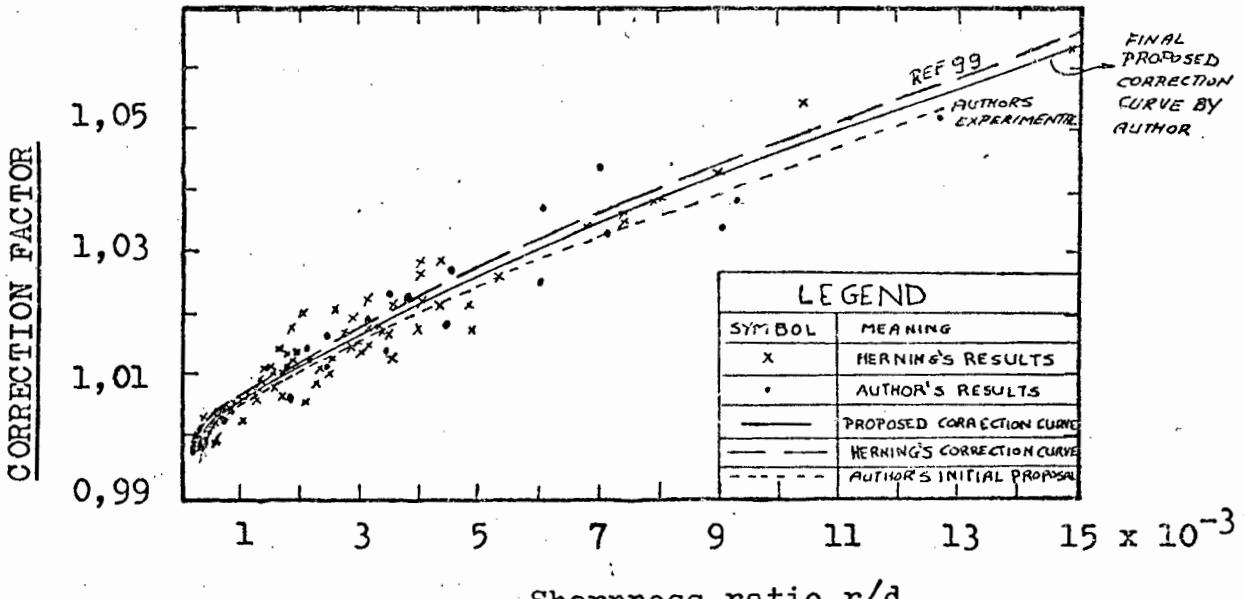

Sharpness ratio r/d

Figure 73. Comparison between author's correction curve for effect of edge sharpness and Hernings

Figure 74. Correction curves for change in the edge radius for orifice plates with area ratios 1. equal to 0,1
2. greater than 0,2

⊙ m = 0,1

x m ⩾ 0,2

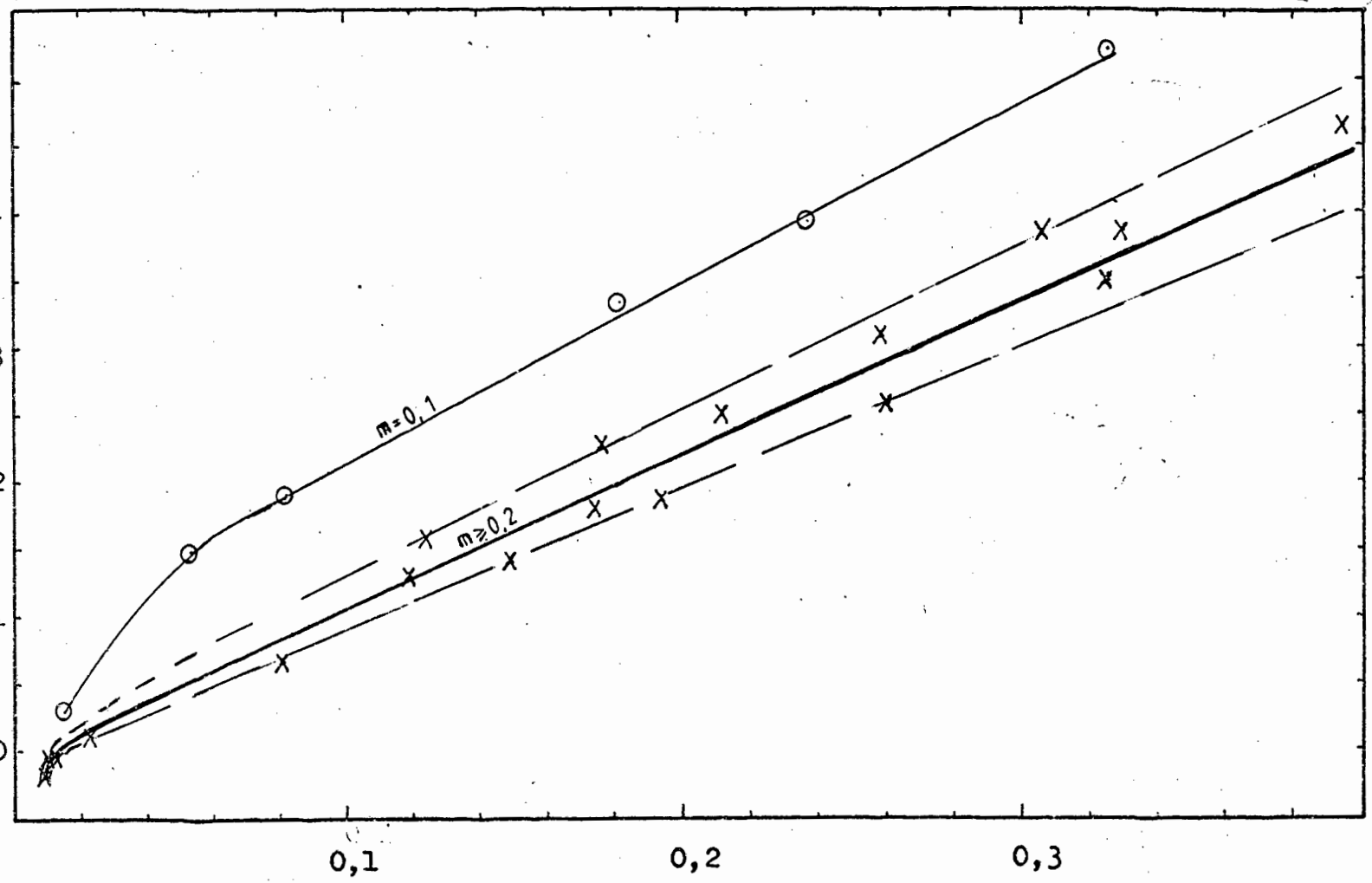

Percentage change in the Coefficient of Discharge. $\left(\frac{C_D - C_{D_{Sharp\ orifice.}}}{C_{D_{Sharp\ orifice}}}\right)$

Edge radius r in millimetres

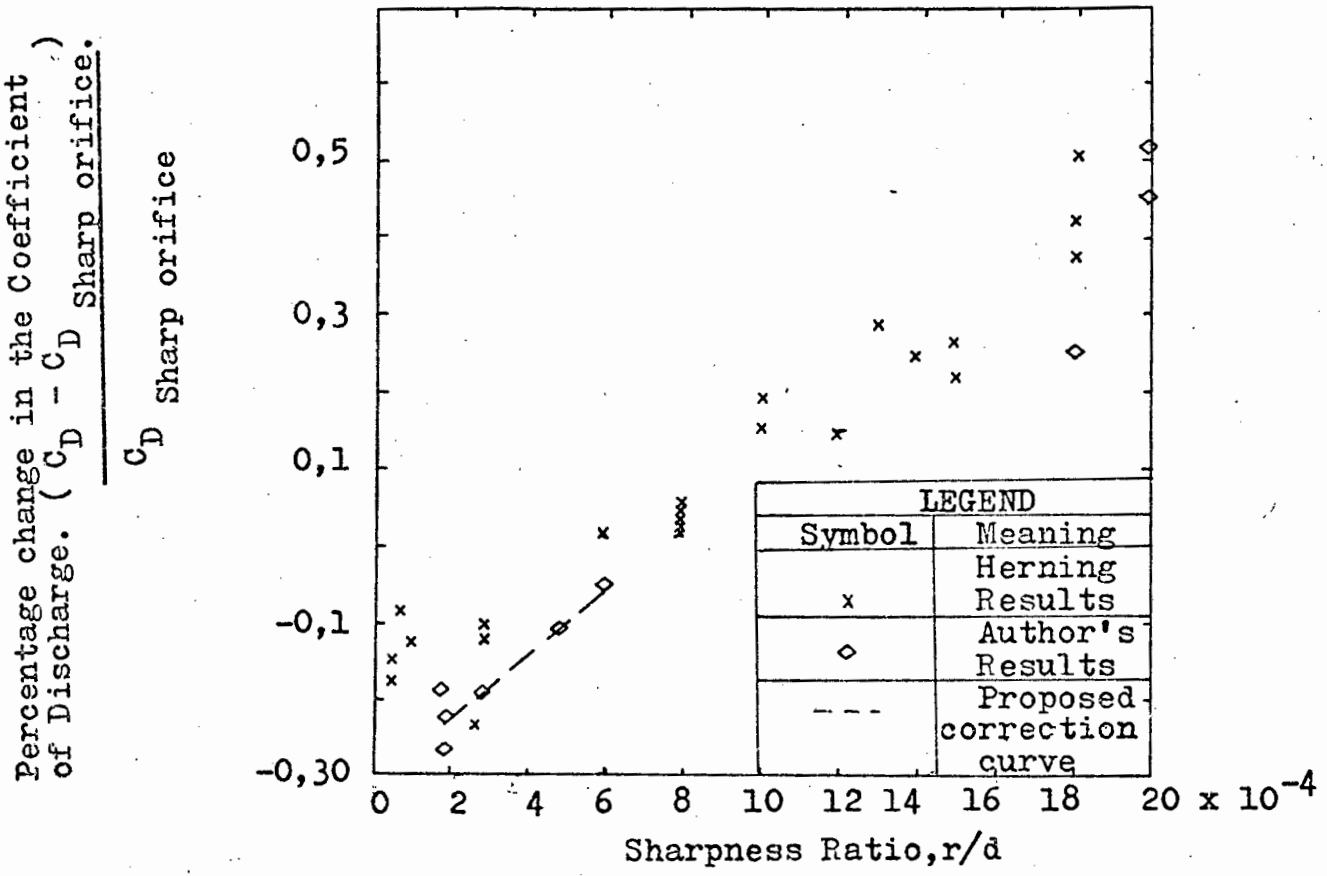

Fig. 75. Comparison between Hernings and Author's results for orifice plates with small sharpness ratios.

CHAPTER 6

C O N C L U S I O N

The author found that the experimental results were accurate within $\pm$ 0,1 per cent. These results, when compared with the various standards, showed that some of the experimentally determined coefficients were outside the limit of some of these standards. The experimental results were within the tolerance limits of the British Standard but outside those of ASME and I.S.O. The comparisons showed that best agreement existed between the British Standard and the experimental results. The next best agreement was between the experimental results and Yu Lin Chen's proposed coefficients. This was followed by ASME and then I.S.O. In all cases, when the experimental coefficients were corrected for effect of edge sharpness, better agreement between the experimental results and the standards was achieved thus proving that such a correction factor would be useful.

An increase in the coefficient of discharge arises as a result of an increase in eccentricity of an orifice plate. The effect of eccentricity was not only dependent on the magnitude of the eccentricity but also on the area ratio of the orifice plates. The larger the area ratio, the greater was the effect of eccentricity on the discharge coefficient. Adherence to the specifications for maximum allowable eccentricity, as given by the various engineering standards, was found not to cause such an error in the value of the specified coefficients that they would lie outside their tolerance limits. It was also found that improvement in the accuracy of the standard coefficients would result if the specifications for maximum allowable eccentricity would be as given in equation 1.

$$\frac{100\,E}{D-d} < 3{,}55 - 1{,}69\,m \quad \ldots\ldots\ldots(1)$$

This specification can be adhered to without any difficulty and the error in the coefficient of discharge due to eccentricity of the plate would be reduced to below 0,1%.

It was found that small increases in the edge sharpness resulted in large increases in the value of the discharge coefficient. As a result of this the specifications of ASME and I.S.O. regarding edge sharpness are in need of revision. The specifications of both the German and the British standards are satisfactory only if errors in the coefficient of discharge of $\pm$ 0,5 per cent are acceptable.

Correction curves for the effect of edge sharpness are proposed, which will reduce the error caused by edge roundness. These correction curves are based on the authors and Herning's results.

7. REFERENCES:

1. J.T. Filban - "ORIFICE METERING" - Journal of the S.C.M.A. - Instruments and Control Systems, Volume 33, January 1960, pg 116 - 119.

2. K. Kendall - "ORIFICE FLOW" - Journal of the S.C.M.A. - Instruments and Control Systems, Volume 37, December 1964, pg 115-118.

3. Thos. R. Weymouth - Measurement of natural gas. Transactions of ASME, 1912, page 1921.

4. E.O. Hickstein - Flow of air through Thin-Plate Orifices. Transactions of ASME. 1915, Vol 37, page 765.

5. H. Judd - Experiments in water flow through pipe orifices. Presented at Spring Meeting, New Orleans, Louisiana, April, 1916. ASME paper no. 1538.

6. S.R. Beitler - Determination of discharge coefficients of sharp edged orifices in pipes from one to fourteen inches in diameter. Instruments Vol. 7,pages 3 - 8 (1934).

7. S.R. Beitler - Flow of water through orifices (a study in 1 inch, 1,5 in, 2 in, 3 in, 6 in, 10 in, and 14 in. Lines). Ohio State University Engineering Experiment Station, Bulletin no. 89 (1935).

8. Joint A.G.A. - A.S.M.E. Committee on Orifice Coefficients. Report on the joint A.G.A. - A.S.M.E. Committee on orifice coefficients 1935. (History of orifice meters and the calibration, construction and operation of orifices for metering). New York , American Gas Association and American Society of Mechanical Engineers (1935).

9. A.S.M.E. Special Research Committee on Fluid Meters. Report of the A.S.M.E. Special Research Committee on Fluid Meters, Part 1. (Fluid Meters, their theory and application). 4th Edition, New York. American Society of Mechanical Engineers (1937).

10. A.S.M.E. Special Research Committee on Fluid Meters. Report of the A.S.M.E. Special Research Committee on Fluid Meters, Part 1 (Fluid Meters their theory and application 5th Edition. New York, American Society of Mechanical Engineers.

11. A.S.M.E. Special Research Committee on Fluid Meters. - "Report of the A.S.M.E. Special Research Committee on Fluid Meters, Part 1 (Fluid Meters their theory and application)" 6th Edition. New York: American Society of Mechanical Engineers (1971).

12. A.G.A. Gas Measurement Committee - "Gas Measurement Committee report No. 2. New York: American Gas Association May (1935).

13. A.G.A. Gas Measurement Committee - "Gas Measurement Committee report No. 3. New York: American Gas Association April 1955.

14. Report of Joint A.G.A. - A.S.M.E. Committee on orifice Coefficients "Investigation into orifice meter requirements"- Interim Research Report No. 1. (MARCH 1951) and No.2. (JANUARY 1954).

15. R. Witte. - "Durchflussbeiwerte Der I.G. - Messmündungen für Wasser, Öl, Dampf Und Gas". - Zeitschrift Des Vereines Deutscher Ingenieure, Vol. 72 pp 1493-1502 (1928).

16. R. Witte. - "Durchflusszahlen Von Düsen Und Stauröndern"- Technische Mechanik Und Thermodynamik - Jan, Feb, March, 1930, Vol 1, pg 34.

17. R. Witte.- "Neuere Mengenstrommessungen Zür Normung Von Düsen Und Blenden" - Forschung Auf Dem Gebiete Des Ingenieurwesens, Vol 8, pg 192-202 (1937).

18. Technical Committee I.S.A. 30- "ISA Bulletin 9 (Rules for measuring the flow of fluids by means of nozzles and orifice plates. ARTS. 1,2,3,4 & 5 - preliminary reccomendations)" 1st edition. Basle: Internation Federation of the National Standardization Associations (1935).

19. Technical Committee I.S.A. 30- "ISA Bulletin 12 (Rules for measuring the flow of fluids by means of nozzles and orifice plates. Arts 6 & 7, preliminary reccomendations) 1st edition. Basle: International Federation of the National Standardization Association (1936).

20. Technical Committee I.S.O./R541 - (1967).

21. STRÖMUNGSMESSERAUSSCHUSS DES VEREINES DEUTSCHER INGENIEURE. "DIN 1952 (Regeln für die DURCHFLUSSMESSUNG MIT GENORMTEN DÜSEN UND BLENDEN)" 1st Edition Berlin: VDI Verslag (1930).

22. STRÖMUNGSMESSERAUSSCHUSS DES VEREINES DEUTSCHER INGENIEURE. "DIN 1952 (Regeln für die DURCHFLUSSMESSUNG MIT GENORMTEN DÜSEN UND BLENDEN UND VENTURIDÜSEN)" 6th edition Berlin VDI Verslag 1948.

23. S.R. Beitler and D.J. Masson - Calibration of Eccentric & Segmental orifices in 4 & 6 inch Pipe Lines - Transactions of A.S.M.E. October 1949. vol 71.

24. H.G. GIESE - "MENGENMESSUNG MIT DÜSEN UND BLENDEN BEI KLEINEN REYNOLDSSCHEN ZAHLEN". FORSCHUNG. JAN-FEB 1933.

25. W. KOENNECKE - "MESSDÜSENFORMEN FÜR KLEINERE UND MITTLERE REYNOLDSZAHLEN" - ZEITSCHRIFT V.D.I. MARCH 1939.

26. W. KOENNECKE-"Neue Düsenformen für Kleinere Und Mittlere Reynoldszahlen" - Forschung. May - June 1938.

27. M.V. RAMAMOORTHY & K. SEETHARAMIAH - "Quadrant - Edge orifice & performance at very high Reynolds Numbers". Journal of Basic Engineering, Transactions of ASME, Series D. March 1966, pg. 9-13.

28. M.V. RAMAMOORTHY & K. SEETHARAMIAH - "Quadrant - Edge orifice - modification for better performance" - La Houille Blanche No:3 1966, pg 313-318.

29. A.R. Howell, - "A note on R.A.E. Annular Airflow Orifices - Aeronotical Research Committee Reports and Memoranda. No. 1934, London, Britain, November 1939.

30. E.A. Spencer - Current practice in fluid flow measurement. Proceedings of the International Conference held at Harwell, pages 13 - 21.

31. B.J. Caldwell- Flow measurement in the fuel gas industry. Flow Measurement Symposium, Pittsburgh, Pennsylvania. September 26 - 28, 1966. Edited by K.C. Cotton, published by ASME, 1966, pages 69-76.

32. E.L. Upp - World-wide trends in petroleum fluid flow measurement - Conference on fluid flow measurement in the mid 1970's 8 -10 April, 1975. Held at the Birnichill Institute, National Engineering Laboratory, East Kilbride

33. C.G. Clayton and G.V. Evans - Industrial demands for flow measurement. Modern developement in flow measurement - Proceedings of the International conference held at Harwell, 21-23 September, 1971. Pages 1-13, P.P.L Conference Publication 10, 1972.

34. E.A. Spencer - Flow Measurement at the National Engineering Laboratory, Process Engineering, August, 1968.

35. I.S.O. Technical Committee. TC.30/WGL.

#36. T.H. Redding - "Flowrate measurements with orifice plates. An assessment of standard orifice forms" - Part 1, Instrument Practice, 15,8, pp 988-955 (August, 1961). - Part 2, Instrument Practice, 15,9, pp 1126-1129. (September 1961) - Part 3, Instrument Practice, 15, 10 pp 1266-1270. (October 1961).

37. International Standards Organization, ISO Recommendation R.541 "Measurement of Fluid flow by means of orifice plates and nozzles." 1st Edition 1967.

38. E.A. Spencer and P. Harrison - "Flow measurement by orifice plates of precision manufacture" - NEL Report No: 14 November 1961.

39. L.A. West - "The Calibration and use of flowmeters for performance testing" - Transactions of the S.A. Institution of Mechanical Engineers Vol 21, No: 3 April 1971.

40. F.V.A. Engel - "New Interpretations of the discharge characteristics of measuring orifices - An approach to improved accuracy", A.S.M.E. Paper 62 - WA - 237 New York, 1962.

41. F.V.A. Engel & A.J. Davies - "Velocity Profiles and flow of fluids through a contracted pipe line", The Engineer, Dec 30, 1938, Vol 166 pp 720-723.

42. F.V.A. Engel & W. Stainsby - "Discharge Coefficient Characteristics of Orifices", The Engineer, 31 July, 1964 pg 161-168.

43. F.V.A. Engel & J.W.E. French - "Orifices for flow measurement" - Engineering, Oct 16, 1936, Vol 142.

44. F.V.A. Engel - "Some problems of Fluid flow measuring devices" - Engineering, July 3, 1953, Vol 176 pg 6-9 & 35-37.

45. W.S. Pardoe - "Effects of installation on coefficients of Venturi Meters"- Transactions of A.S.M.E. Hydraulic Section, November 1936, Vol 58, No 8 pg 677 - Concluded in transactions of A.S.M.E. 1943, page 337.

46. V.L. Streeter - "The Kinetic energy and momentum correction for pipes and for open channels of great width". Civil Engineering April 1942, Vol 12, No. 4 page 212.

47. J.W. Murdock, C.J. Falt & C. Gregory - "Effect of a globe valve in approach piping on orifice meter accuracy") A.S.M.E. Paper No. 54-A-122 6 pp (December 1954).

48. M. Sasiadek - "The influence of the straight pipe line section of the measuring orifice". - Proc. International Measurement Conference 3, pp 41-49 (1958) N.E.L. Translation 1550.

49. F. Herning & H. Bellenberg - "New experiments with standard orifice plates". - Brennstoff - Wärme - Kraft, 12,3, March, 1960, pg 89-96.

50. R.E. Sprenkle and N.S. Courtright, - "Straightening vanes for flow measurement". - A.S.M.E. Paper 57-A-76 December 1957, 3 pp.

51. K.J. Zanker - "The development of a flow straightener for use with orifice plates flowmeters in disturbed flows". Flow measurement in Closed Conduits, Paper D-2 N.E.L. Symposium (September, 1960).

52. S.R. Beitler - "The Flow of Water through Orifices. A study in 1 in., 2 in., 3 in., 6 in., 10 in., and 14 in. Lines" - Ohio State University Engineering Experiment Station Bulletin, Vol IV, No. 89, No. 3, May 1935.

53. G. Ruppel - "Die Durchflusszamlen von Normblenden und IHRE ABHÄNGIGHEIT VON DER KANTENLANGE" - ZEITSCHRIFT VDI, Vol 80, 1936, pp 1381-1387.

54. L.W. Thrasher, & R.C. Binder, - "Effect of edge thickness on small orifice meters. - Instruments and Automation, 27 November 1954 pg 1810-1811.

* 55. L.S. Marks, - "Mechanical Engineers' Handbook", McGraw Hill Book Company, New York, 3rd edition 1930.

56. Grace & Lapple - "Discharge coefficients of small-diameter orifices and Flow Nozzles", A.S.M.E. Paper 50-A-64. November 1950, pp 5.

* 57. R.E. Rayle, - "Influence of orifice geometry on static pressure measurements." A.S.M.E. paper 59-A-234, pp 3 (December 1959)

58. K.J. Zanker and L. Fellerman - "Some experiments with orifice plate flow meters". - B.H.R.A. - N.E.L. Joint Report No. 2 (December, 1961), pp 12.

59. P.H. Oosthuizen - "An approximate method for predicting the effect of small changes in the initial velocity profile on the coefficient of discharge of an orifice plate". - The South African Mechanical Engineer, 13,9, April, 1964 pg 238 -243.

60. A. Schlag - "The influence of roughness on the discharge coefficient of inferential meters" - Revue Universelle des Mines, 9, 3, March 1953.

61. S. Abramaritz, - "Effect of pipe roughness on fluid meter discharge coefficient" - Power, Engineering and Management Section, 101, 8 August, 1957 pg 75-77.

* 62. W.J. Clark and R.C. Stephens - "Flow measurement by square-edged orifice plates: pipe roughness effects". Proceedings of the Institution of Mechanical Engineers 171, 33, 1957 pg 895-904.

63. G. Thibessard - Influence of pipe roughness on the flow coefficient of standard orifices with corner taps". N.E.L. Translation 1660 - Brennstoff - Wärme - Kraft, 17,1, January, 1965, pg 26-29.

64. F. Herning & E. Wolowski - "Influence of pipe friction on the discharge coefficient of standard orifices with vena contracta tappings" - BRENNSTOFF - WÄRME - KRAFT, 18, 2, February 1966, pg 61-67.

65. E.A. Spencer, H. Calame and J. Singer - "Edge sharpness and pipe roughness Effects on Orifice Plate Discharge Coefficients." - N.E.L. Report No. 427 August 1969, 18 pages, 31 figures.

66. H.E. Dall - "The effect of roughness of the orice plate on the discharge coefficient" - Instrument Engineer 2,5, April, 1958 pg 91-92.

67. British Standards Institution - "Method for the measurement of fluid flows in pipes - Part 1: Orifice plates, Nozzles and Venturi tubes"". B.S.S. 1042. Part 1, 224 pp (1964).

68. E.A. Spencer - "Flow measurement practices in GREAT BRITAIN". Pipe Line Industry, April, 1967.

69. F.V.A. Engel - "New Interpretations of the discharge Characteristics of measuring Orifices - An approach to improved accuracy", ASME Paper 62-WA-237 New York, 1962.

70. S.R. Beitler - "The flow of water through Orifices. A study in 1 in., 2 in., 3 in., 6 in., 10 in., and 14 in. Lines" - Ohio State University Engineering Experiment Station Bulletin, Vol IV, No. 89., No. 3, May 1935.

71. F.C. Johansen - "Flow through pipe orifices at Low Reynolds Numbers" - Aeronautical Research Committee, Great Britain, Reports and Memoranda, No. 1252, June 1929.

72. J. Rotta, - "Experimenteller für Enstellung turbulenter Strömung im Rohr" - Ingenieur - Archiv, Vol 24, 1956 pp 258-281.

73. H.W. Iverson - "Orifice coefficients for Reynolds Numbers from 4 to 50000" - Transactions of A.S.M.E., February 1956 pg 359-364.

74. R.P. Millar and I.V. Nemecek - "Coefficients of discharge of short pipe orifices for incompressible flow at Reynolds number less than one." - ASME Paper No. 58-A-106, 7 pages (December, 1958).

75. H.G. Giese - "Mengenmessung mit Düssen und Blenden bei kleinen Reynoldsschen Zahlen". Forschung Jan Feb, 1933.

76. G.A. Marxman and H. Burlage - "Expansion coefficients for orifice meters in pipes less than one inch in diameter". Transactions of A.S.M.E. 83, Series D, 2, pp 289-298 June 1961.

77. R. Witte - "Durchflussbeiwerte Der IG. - Messmundungen für Wasser, DL DAMPF und Gas". - Zeitschrift VDI, Vol 72, 1928 pg 1493.

78. S.R. Beitler - "The flow of Water through Orifices. A study in 1 in., 2 in., 3 in, 6 in., 10 in., and 14 in Lines"- Ohio State University Engineering Experiment Station Bulletin, Vol 1V, No. 89, no. 3, May 1935.

79. H.S. Bean - "Formulation of Equations for orifice coefficients"- Transactions of ASME, Vol 93, Series D, No. 2, June 1971, pp 97-98.

80. M. Marchetti - "I Boccagli E I Diaframmi Normalizzati Inseriti Nelle Condotte Forzate" - L'Energia Elettrica, Vol. 12, Nov, 1935, pp 789-811.

81. M. Marchetti, - "La Misura Delle Portate Fluide A. Mezzo Die Diaframmi - L'energia Elettrica, Vol. 14, January 1937, pp 61-67.

82. H.S. Bean- Formulation of equations for orifice coefficients - Transactions of ASME, Vol 93, Series D, No. 2, June 1971, pg 97-98.

83. E. Buckingham - "Notes on some recently published experiments on Orifice Meters" - Transactions of ASME, 78, 2, pp 379-387. (February 1956).

84. M. Marchetti - "Coefficienti di effusso dei diaframmi unificati. Formule di coordinamento dei valori sperimentali per bassi numeri di Reynolds".(Coordination and Formulation of the Variation of experimental Values of the Coefficient of Discharge of Standard Orifices with Reynolds Number), L'ENERGIA ELETTRICA, Vol. 15, Apr. 1938, pp 229-244.

85. R.B. Dowell, & Yu-Lin Chen - "A statistical approach to the prediction of discharge coefficients for concentric Orifice Plates"- Transactions of ASME, Journal of Basic Engineering, Vol 92, series D, 1, December 1970 pp 752-765.

86. E. Scimemi - "Prove Su Boccagli Diaphrammi Normalizzati Inscrite in Condotte da 200 mm." - L'Energia Elettrica, Vol 13, 1936, pp 359-369.

87. H.S. Bean., M.E. Benesh, & E. Buckingham - "Experiments on Metering Large Volumes of Air,"- NB of S Journal of Resh., Vol 7-1, July 1931, RP 335 p 93.

88. H.S. Bean, E. Buckingham & P.S. Murphy - "Discharge Coefficients of Square-Edged Orifices for Measuring the Flow of Air." NB of S Journal of Resh., Vol 2-3, March 1929, RP 49 page 561.

89. S.R. Beitler and D.J. Masson - "Calibration of Eccentric and segmental orifices in 4 and 6 inch Pipe Lines". - Transactions of A.S.M.E. , Vol 71, October 1949 (Also presented at the Annual Meeting of the American Society of Mechanical Engineers, New York , November 28 - December 3, 1948. Paper No. 48-A-49).

90. R.W. Miller and O. Kneisel - "Experimental Study of the effects of orifice plate eccentricity on flow coefficients" ASME paper No. 68-WA/FM-1 December 1968, 11 pages.

91. R.W. Miller and O. Kneisel - "Experimental Study of the effects of orifice plate eccentricity on flow coefficients" Journal of Basic Engineering, 91, 1 pp 121-131 March (1969).

92. G.A. Hinz., G.A. Scofield., J.A. Casale and C.L. Edwards - "Empirical Evaluation of the Eccentric Orifice in Small - Diameter Pipes"- The Petroleum Mechanical Engineering Conference, Philadelphia, Pa., September 17-20, 1967 ASME Publication 67 - PET-21. 4 Pages.

93. H.S. Bean - "Indications of an Orifice Meter" - American Gas Association Monthly, July-August 1947, pg 340.

94. R.G. West - "Developments of flow metering by means of orifice plates" - Proceedings National Engineering Laboratory, 1960, Vol 1, Paper B3.

95. L.K. Spink - "Principles and Practice of Flow Meter Engineering". The Foxboro Company, 9th Edition, 1967.

96. R.A. Collacott - "Discharge coefficients of Chamfered Orifices and Nozzles". - Aircraft Engineering, 20, April 1948 pg. 112-113.

97. The Foxboro Company, 9th Edition, 1967.

98. Fr Herning - "Untersuchungen zum Problem der Kantenunschärfe bei Normblenden und bei Segmentblenden"(Investigation on the bluntness of the entrance edge of standard orifices and segmental orifices) - Brennstoff - Wärme - Kraft, 14, 3, March 1962 pg 119-126.

99. Fr. Herning and E. Wolowski - "Die Kantenunschärfe von Normblenden und Segmentblenden und das Ähnlichkeitsgesetz" (The edge radius of standard and segment orifice plates and the similarity law). - Brennstoff - Wärme - Kraft, 15, 1, January, 1963, pg. 26-30.

100. H.S. Bean - "Effect of Rounding, Inlet Corner of Orifice" chart in "Developments in the Application of Orifice Meters to the measurement of fluids, especially gases". - Pennsylvania State College Bulletin.

101. K.A. Crockett and E.L. Upp, - "The measurement and effects of Edge sharpness on the flow coefficients of Standard Orifices" - Transactions of A.S.M.E., Journal of Fluids Engineering, June 1973 pg 271-274.

102. E.A. Spencer, H. Calame, J. Singer - "Edge Sharpness and pipe roughness Effects on Orifice Plate Discharge Coefficients" - N.E.L. Report No. 427 August 1969 18 pages, 31 figures.

103. L.A. West - "The Calibration and use of flowmeters for performance testing" - Transactions of the S.A. Institution of Mechanical Engineers Vol 21, No: 3 April 1971.

104. G.R. Gallacher - "Measuring edge sharpness of orifice plates"- Engineer 1968, 225, (5860), 17 May, 1968 pages 783-785

105. R.P. Benedict, J.S. Wyler and G.B. Brandt - "The effect of edge sharpness on the discharge coefficient of an Orifice" Transactions of A.S.M.E., Journal of Engineering for Power October 1975, pg 576-580.

106. V.P. Head - "The effect of edge sharpness on the discharge coefficient of an Orifice". Transactions of A.S.M.E., Journal of Engineering for Power, October 1975, pg 581.

107. E.T. Leigh and J.A. Leys - "Experiments on Metering Orifices for use at Low Reynolds numbers" - Instrument Practice, Vol.4 No. 6 Published in London.

108. K.A. Crocket and E.L. Upp, - "The measurement and effects of Edge Sharpness on the flow coefficients of Standard Orifices"- Transactions of A.S.M.E., Journal of Fluids Engineering, June 1973.

109. P. Jepson and E.P. Johnson - "A method of measuring orifice edge sharpness" - Gas Council Engineering Research Station. Technical Report No. ERST 415 CICC 91 Newcastle Upon Tyne: Gas Council Engineering Research Station, 1971.

110. T.J.S. Brain and J. Reid - "Measurement of orifice plate edge sharpness". - Measurement and Control, Vol 6, September 1973. pg 377-383.

#111. E.A. Spencer & A.T.J. Hayward - "The accurate calibration of flow meters with water", Transactions of the Society of Instrument Technology, March, 1957 Pg 1-12.

112. R.K. Dutkiewicz, L.A. West & L.D. Meyer - "An installation for accurate calibration of flow measuring devices" - The transactions of the S.A. Institute of Mechanical Engineers, March 1971.

113. "Handbook of Noise and Vibration Control". 3rd Edition, published by Trade & Technical Press Ltd., Morden, Surrey, England. pg 620.

114. B.S.Massey - "Mechanics of Fluids" - 2nd Edition, Reinhold Company, London, 1972 pg 94 & 95.

115. L.K. Spink, - Principles and practice of flow meter engineering The Foxboro Company, Foxboro, Massachusetts, U.S.A. eighth edition, 1961 pg 50-51.

116. W.S. Pardoe - "Effects of installation on coefficients of Venturi Meters" - Transactions of A.S.M.E. Hydraulic Section, November 1936, Vol 58, No 8 pages 677 - concluded in transactions of A.S.M.E. 1943 page 337.

117. V.L. Streeter "The Kinetic Energy and Momentum Correction for Pipes and for open Channels of Great Width." Civil Engineering, April 1942, Vol. 12, no. 4 pg 212.

118. South African Bureau of Standards - Metrication in the fan, ventilation, refrigeration and compressed air industries.

APPENDIX A

DERIVATION OF THE THEORETICAL HYDRAULIC EQUATION FOR ORIFICE PLATES

The theoretical hydraulic equation can be derived in a number of ways, depending on the assumptions made.

Method 1.

The flow pattern through an orifice is as shown in figure 76.

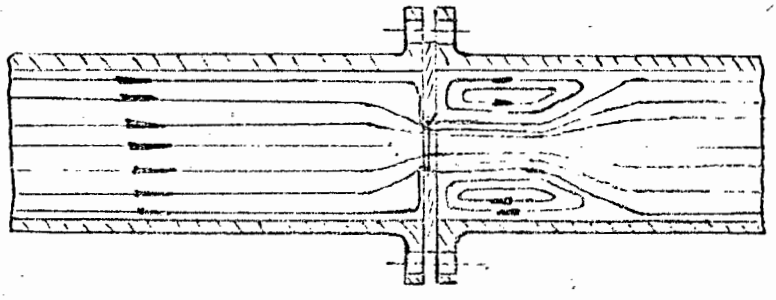

Figure 76 - General flow pattern through an orifice.

Application of Bernoulli's equation between point (1) upstream of the orifice and the vena contracta (2) for an ideal fluid and uniform velocity distribution gives

$$\frac{P_1}{\rho g} + \frac{V_1^2}{2g} + Z_1 = \frac{P_2}{\rho g} + \frac{V_2^2}{2g} + Z_2 \qquad \ldots\ldots\ldots\ldots 1$$

Assume pipe is horizontal, i.e. $Z_1 = Z_2$

$$\therefore \quad \frac{P_1 - P_2}{\rho g} = \frac{V_2^2 - V_1^2}{2g}$$

$$\therefore \quad V_2^2 - V_1^2 = \frac{2\,(P_1 - P_2)}{\rho} \qquad \ldots\ldots\ldots\ldots 2$$

Assuming steady state, no loss or gain of heat energy, no friction losses and applying the continuity equation gives:

$$q_1 = q_2 = \rho_2 V_2 A_2 = \rho_1 V_1 A_1 \quad \ldots\ldots\ldots\ldots\ldots\ldots \quad 3$$

Assume the fluid to be incompressible

$$\therefore \quad \rho_1 = \rho_2$$

and $$V_2 A_2 = V_1 A_1$$

$$\therefore \quad V_1 = \frac{V_2 A_2}{A_1} \quad \ldots\ldots\ldots\ldots\ldots\ldots\ldots\ldots \quad 4$$

and $$V_2 = \frac{q}{\rho A_2} \quad \ldots\ldots\ldots\ldots\ldots\ldots\ldots \quad 5$$

substituting the value of V_1 from equation 4 into 2 gives

$$V_2^2 - \frac{V_2^2 A_2^2}{A_1^2} = \frac{2(P_1 - P_2)}{\rho} \quad \ldots\ldots\ldots \quad 6$$

$$\therefore \quad V_2 = \frac{\sqrt{\frac{2(P_1 - P_2)}{\rho}}}{\sqrt{1 - \left(\frac{A_2}{A_1}\right)^2}} \quad \ldots\ldots\ldots\ldots\ldots \quad 7$$

Substituting the value of V_2 from equation 5 into 7 gives,

$$\frac{q}{\rho A_2} = \frac{\sqrt{\frac{2(P_1 - P_2)}{\rho}}}{\sqrt{1 - \left(\frac{A_2}{A_1}\right)^2}}$$

$$\therefore \quad q = \frac{A_2 \sqrt{2\rho (P_1 - P_2)}}{\sqrt{1 - \left(\frac{A_2}{A_1}\right)^2}} \quad \ldots\ldots\ldots \quad 8$$

The area of the jet at the vena contracta is difficult to measure and therefore for practical considerations it is assumed that the velocity at the downstream pressure tap is related to that at the upstream pressure tap, as the area of the orifice to that of the inlet pipe.

Equation 8 can then be written as

$$q = \frac{\pi d^2}{4} \left(\frac{[2\rho \ (P_1 - P_2)]}{[\ 1 - \left(\frac{d}{D}\right)^4\ ]} \right)^{\frac{1}{2}} \quad \ldots\ldots\ldots\ 9$$

The flowrate determined experimentally does not agree with that computed from equation 9. To correct equation 9 the right hand side is multiplied by the coefficient of discharge, C_D.

$$\therefore \quad q = C_D \cdot \left(\frac{\pi d^2}{4}\right) \left(\frac{[2\rho \ (P_1 - P_2)]}{[\ 1 - \left(\frac{d}{D}\right)^4\ ]} \right)^{\frac{1}{2}} \quad \ldots\ldots\ldots\ 10$$

The overall coefficient of discharge, K, includes the velocity of approach factor, $1 - \left(\frac{d}{D}\right)^4$.

$$\therefore \quad q = K. \left(\frac{\pi d^2}{4}\right) [2\rho \ (P_1 - P_2)]^{\frac{1}{2}} \quad \ldots\ldots\ldots\ 11$$

If the fluid is compressible then a coefficient of expansion, Y, is introduced and equation 11 becomes

$$q = Y.K. \left(\frac{\pi d^2}{4}\right) [2\rho \ (P_1 - P_2)]^{\frac{1}{2}} \quad \ldots\ldots\ldots\ 12$$

Equation 12 is used by all the standards to determine the flowrate when orifice plates are used.

Method 2.

In this case a real fluid is assumed. Applying Bernoulli's equation gives

$$V_2 = C_v \left[2g\left(h_1 - h_2 + \frac{V_1^2}{2g}\right)\right]^{\frac{1}{2}} \quad \ldots\ldots\ldots\ldots\ldots\ldots \quad 13$$

where C_v is the coefficient of velocity (114).

The ratio of the area of the jet at the vena contracta to the area of the orifice is equal to the coefficient of contraction, C_c.

Applying the continuity equation and expressing the area at the vena contracta in terms of the coefficient of contraction and orifice area gives,

$$V_1 A_1 = V_2 A_2 = V_2 C_c A_o \quad \ldots\ldots\ldots\ldots\ldots\ldots \quad 14$$

$$\therefore \quad V_1 = \frac{V_2 C_c A_o}{A_1} \quad \ldots\ldots\ldots\ldots\ldots\ldots\ldots \quad 15$$

and $$V_2 = \frac{q}{C_c \rho A_o} \quad \ldots\ldots\ldots\ldots\ldots\ldots\ldots\ldots \quad 16$$

Substitute value of V_1 from equation 15 into 13.

$$\therefore \quad V_2 = C_v \left(\frac{[2g\ (h_1 - h_2)\ ]}{\left\{1 - C_v^{\,2} C_c^{\,2} \left(\frac{Ao}{A_1}\right)^2\right\}}\right)^{\frac{1}{2}} \quad \ldots\ldots\ldots\ldots\ldots \quad 17$$

Substituting for V_2 in equation 17 gives,

$$\frac{q}{C_c A_o \rho} = C_v \left(\frac{[\ 2g\ (h_1 - h_2)]}{\left\{1 - C_v^{\,2} C_c^{\,2} \left(\frac{A_o}{A_1}\right)^2\right\}}\right)^{\frac{1}{2}} \quad \ldots\ldots\ldots\ldots\ldots \quad 18$$

$$\therefore \quad q = C_c . C_v . A_o . \rho \left(\frac{[2g(h_1 - h_2)]}{\left\{1 - C_v^{\,2} C_c^{\,2} \left(\frac{A_o}{A_1}\right)^2\right\}}\right)^{\frac{1}{2}} \quad \ldots\ldots\ldots\ldots\ldots \quad 19$$

Let $$K = \frac{C_c C_v}{[1 - C_c^{\,2} C_v^{\,2} (\frac{d}{D})^4]^{\frac{1}{2}}} \quad \ldots\ldots\ldots\ldots\ldots\ldots\ldots\ldots \quad 20$$

$\therefore$ Equation 19 is identical to equation 11.

Method 3.

In this analysis a size coefficient η is introduced. The derivation is the same as in method 2 but the overall coefficient of discharge can be expressed as

$$K = \frac{\bar{\alpha}\,\bar{\mu}}{\left\{1 - \frac{\bar{\alpha}^2\bar{\mu}^2}{\eta}\left(\frac{d}{D}\right)^4\right\}^{\frac{1}{2}}} \qquad \ldots\ldots\ldots\ldots\ldots\ldots \quad 21$$

Method 4.

Spinks (115) derives the theoretical flow equation by using the equation for power.

The total power at point1 for a variable velocity profile is

$$\int_0^{A_1} \left[\frac{\rho V_1^3}{2} + \rho Z_1 V_1 + \frac{P_1 V_1}{g}\right]\delta A_1 \quad \text{and at point 2 is}$$

$$\int_0^{A_2} \left[\frac{\rho V_2^3}{2} + \rho Z_2 V_2 + \frac{P_2 V_2}{g}\right]\delta A_2$$

The total hydraulic power at point 1 must be equal to that at point 2 if no gain or loss of power is assumed.

$$\therefore \quad \int_0^{A_1} \left[\frac{\rho V_1^3}{2} + \rho Z_1 V_1 + \frac{P_1 V_1}{g}\right]\delta A_1 = \int_0^{A_2} \left[\frac{\rho V_2^3}{2g} + \rho Z_2 V_2 + \frac{P_2 V_2}{g_{22}}\right]\delta A_2$$

In a circular pipe with a symmetrical velocity profile, the velocity can be expressed as a function of the distance, a., and $\delta A = \pi a \delta a$.

Pardoe (116) and Streeter (117) have used this equation to analyse the effect of pipe roughness and that of other disturbances which are related to the velocity profile.

If a constant velocity profile is assumed then equation 22 yields

$$\frac{\rho_1 V_1^3 A_1}{2} + \rho Z_1 A_1 V_1 + \frac{P_1 V_1 A_1}{g} = \frac{\rho V_2^3 A_2}{2} + \rho Z_2 A_2 V_2 + \frac{P_2 V_2 A_2}{g} \quad \ldots\ldots\ldots\ldots \quad 23$$

The final flow equation is identical in form to equation 12 and no benefit is derived from this complex derivation.

APPENDIX B

THE DESIGN OF THE EXPERIMENTAL EQUIPMENT

1. ORIFICE PLATE CALIBRATING EQUIPMENT

The tolerance on the final measurement of the flow rate is in the order of +/- 1½ percent if the orifice plate is made and installed strictly to the specifications of any Standard Code. This includes the coefficient tolerance, errors in the determination of the density of the fluid, the area ratio of the plate and the manometric differential pressure. If the rate of flow of the fluid in the pipeline is to be known to an accuracy greater than 1½ percent, the plate has to be calibrated.

To calibrate an orifice plate, constant flow in a pipeline is measured with the orifice plate and with a reference meter whose accuracy and repeatability is well known. The readings are compared and the orifice plate coefficient is determined. The accuracy of the overall system is slightly lower than that of the reference meter.

It was required to design an orifice plate calibrating unit which would satisfy the following criteria.

a) an overall accuracy of +/- 0,2 percent
b) in accordance with the specifications of BS 1042 : 1964
c) for water as a working fluid
d) to suit a 100mm pipeline installation
e) to enable the testing of any orifice plate with the following differing parameters:
   (i) orifice diameter less than 100mm
   (ii) orifice edge sharpness
   (iii) orifice eccentricity
f) to maintain a constant flowrate during a test.

A wide variety of methods are used for calibrating orifice plates, some of the more popular methods are described below:

A. VOLUMETRIC OR GRAVIMETRIC TANK USED IN THE STANDING-START AND FINISH MODE

A simple calibrating system of this type is shown in figure 77. Before

the pump is started the pipeline has to be full of water from the pump to the hose of the tank. The pump is started with the stop valve closed and the dial of the meter set to zero. The volume or the weight of the tank is noted (dependent on the system used). The valve is rapidly opened. When the tank is nearly full the valve is rapidly closed and the volume or the weight of the tank noted. The total volume passed through the meter is then compared with that added to the tank. The gravimetric system is preferred where metering water or a viscous oil, while the volumetric method is used for low viscosity hydrocarbons. This method is suited for the calibration of quantity meters rather than rate meters.

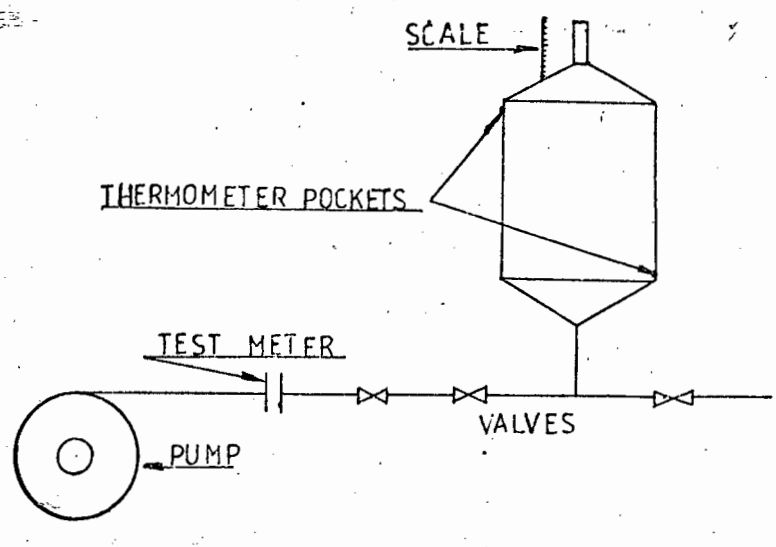

Figure 77- Volumetric tank, standing-start and finish.

B. GRAVIMETRIC FLYING START AND FINISH METHOD WITH STATIC WEIGHING

This method of calibration is used successfully at N.E.L., and ESCOM. In both cases an accuracy of +/- o,1 percent is claimed. In this system the fluid passes through the meter, a control valve and then a fishtail, from where it emerges as a fan shaped jet. Figure 78 shows the diverter which then diverts the fluid into a reservoir (sump) or into a weigh tank. A switch connected to an electronic timer is operated by the diverter plate. This allows for the measurement of the time during which the weightank is being filled.

This method is widely used when flowrate meters have to be calibrated with water.

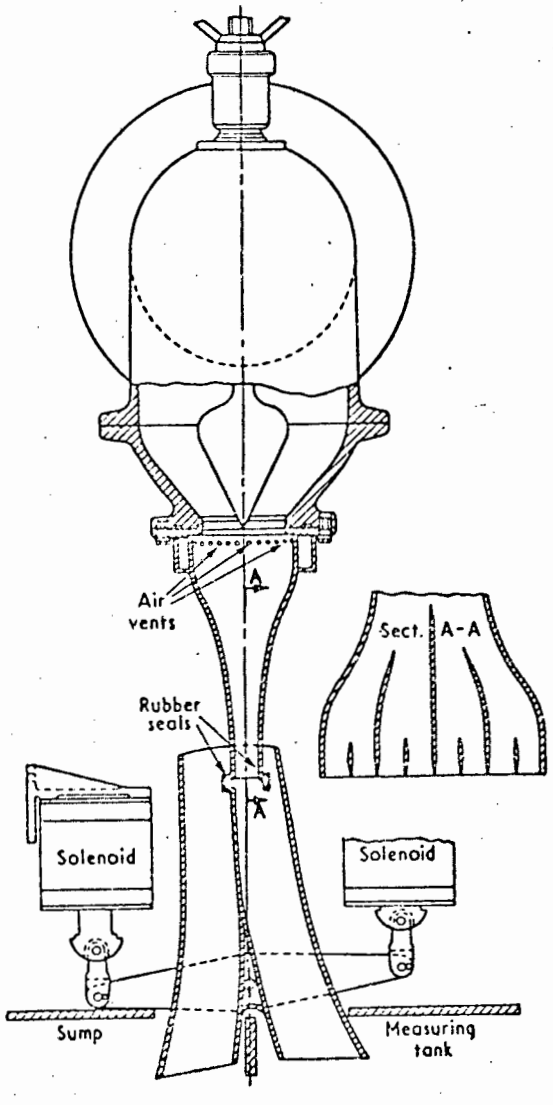

Fig. 78. Control Valve, Fishtail and Diverter in Pilot System found at NEL. This Figure is a Replica from Reference (112).

C. GRAVIMETRIC FLYING START AND FINISH METHOD WITH DYNAMIC WEIGHING

The fluid passes through the meter and then into a weightank and out through a dump valve at its base. When calibrating, the dump valve is suddenly closed and when the water reaches a certain weight a timer is set into operation. When another preset weight is reached the timer is switched

off and the valve reopened again after a few seconds. This method is suitable for moderate flowrates but with large flowrates inertia effects cause errors.

D. PIPE PROVERS

Pipe provers are used to obtain a reference measurement on site. They are expensive to install but once installed are reliable, rapid in operation, have low operating cost and are highly accurate to +/- 0,1 percent.

In this type of meter a hollow sphere of synthetic rubber is filled with water at high pressure so that its diameter is about 2 percent larger than that of the pipe from which the prover is constructed. The sphere is forced into the pipe. It then acts as a seal and as a piston which can travel round corners. The fluid, after passing through the meter which is being calibrated, can either flow through the prover or bypass it, depending upon the manipulation of shut-off valves. When calibrating, it flows through the prover and takes the sphere from one end of the prover to the other. The time taken over a specified distance is recorded and the flow rate is calculated. In order to obtain a high degree of accuracy, tests in both directions are performed so that directional effects in the sphere detectors are eliminated.

E. OTHER METHODS

Any meter whose accuracy and repeatability is well known can be used as a reference meter and be installed in series with the orifice plate. The disadvantage is that two meters are used simultaneously and that both are affected by wear and dirt deposits.

CALIBRATING METHOD ADOPTED

The chosen calibrating system is similar to the one used at ESCOM and at N.E.L. (method B above). The calibration circuit is illustrated schematically in figure 79. The water from the sump is delivered by a suction pump to the constant head supply tank. The excess water is returned via an overflow to the sump. A pipe connects the test line to the constant head tank. Into this line a medium and a fine meshed strainer are introduced. The orifice plate is installed into the test line between specially designed flanges.

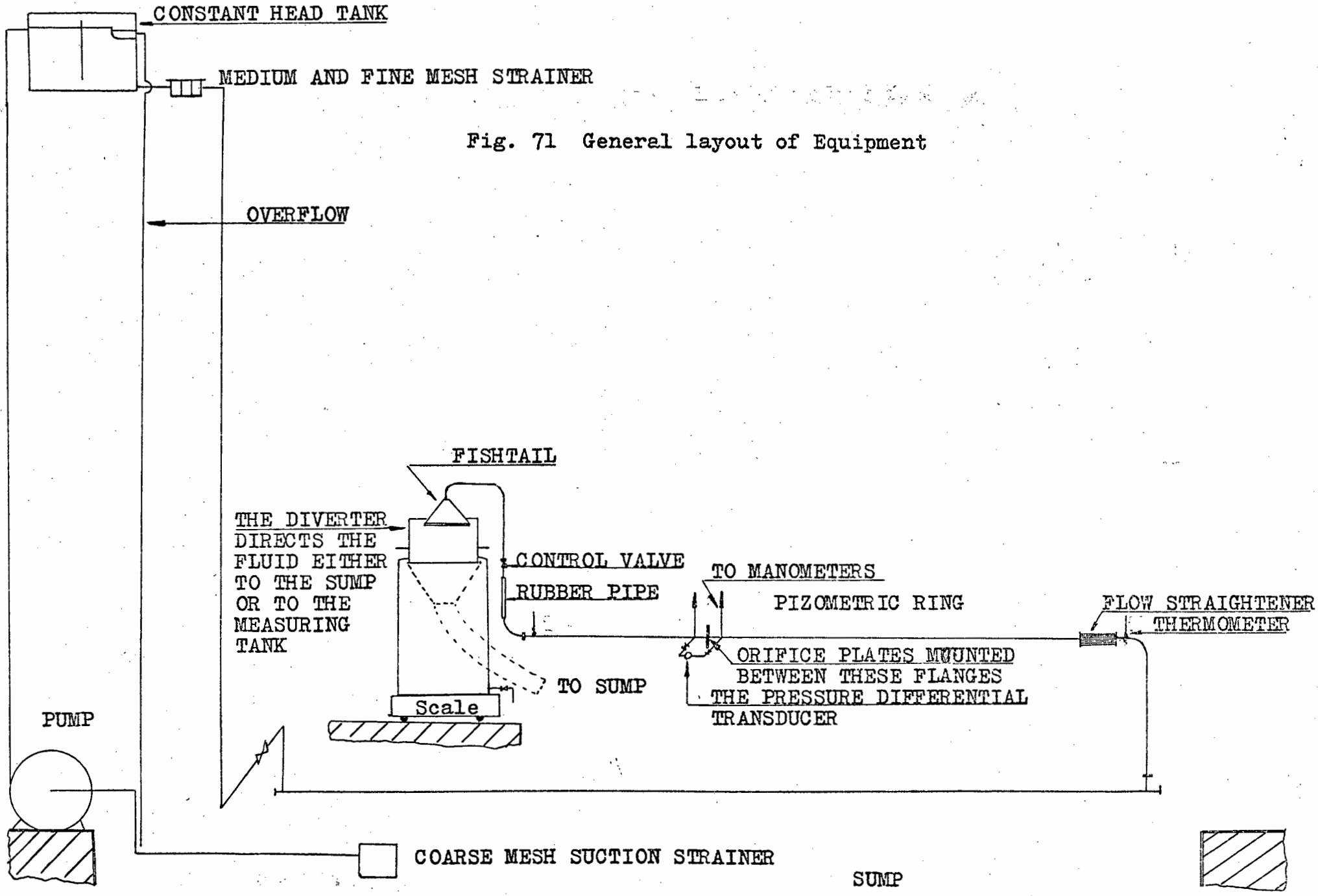

Fig. 71 General layout of Equipment

The straight length of pipe upstream of the orifice plate is preceded by a flow straightener and a 90 degree bend. The flow rate is controlled by a 50mm valve which is inserted into the pipeline which connects the fishtail to the test line. Immediately before the valve a short length of rubber piping is used so that vibrations due to the quick change over in the diverter position will not be transmitted to the test line. The water flows through the fishtail into the diverter. The diverter frame is pivoted above its centre of gravity so that it can direct the water to the measuring tank or to the collecting trough which allows the water to flow into the sump. The diverter is actuated pneumatically. The compressed air is supplied to the pneumatic cylinder by a 'Hydrovane' compressor. The air is kept dry by passing it through an air receiver before the pneumatic cylinder. The diverter actuates a crystal-controlled timer which times the diversion interval. The measuring tank is placed onto a scale and its mass is measured before and after the diversion. The pressure difference across the orifice plate is measured with a mercury manometer or a water manometer (depending on the magnitude) and a pressure differential transducer. The output from the transducer is amplified and then it is read off directly from a voltmeter or a graphical plot is obtained by using an Ultra-Violet recorder. D and D/2 pressure tappings connected to a ring chamber are used. The temperature of the water is measured upstream and downstream of the orifice plate with mercury thermometers.

A detailed description of the individual components of the calibrating system follows:

(i) The Sump (figure 80)

The sump is positioned below the test line. It is made from cement and its capacity of 13m^3 (13000ℓ) ensures that no excessive rise in the temperature of the water occurs during the period of a test. It is 1.3 metres deep thus ensuring that no vortex entrainment occurs through the pump into the system. It is sufficiently long to ensure that the air bubbles, introduced into the sump at the point where the water from the system is discharged into the sump, are not carried back into the system by the pump.

(ii) Coarse meshed suction strainer

The frame is made from light gauge angle-iron. A coarse wire mesh is bolted to the frame. Large foreign matter in the water is kept in the sump, thus the pump is protected and the tank is kept clean.

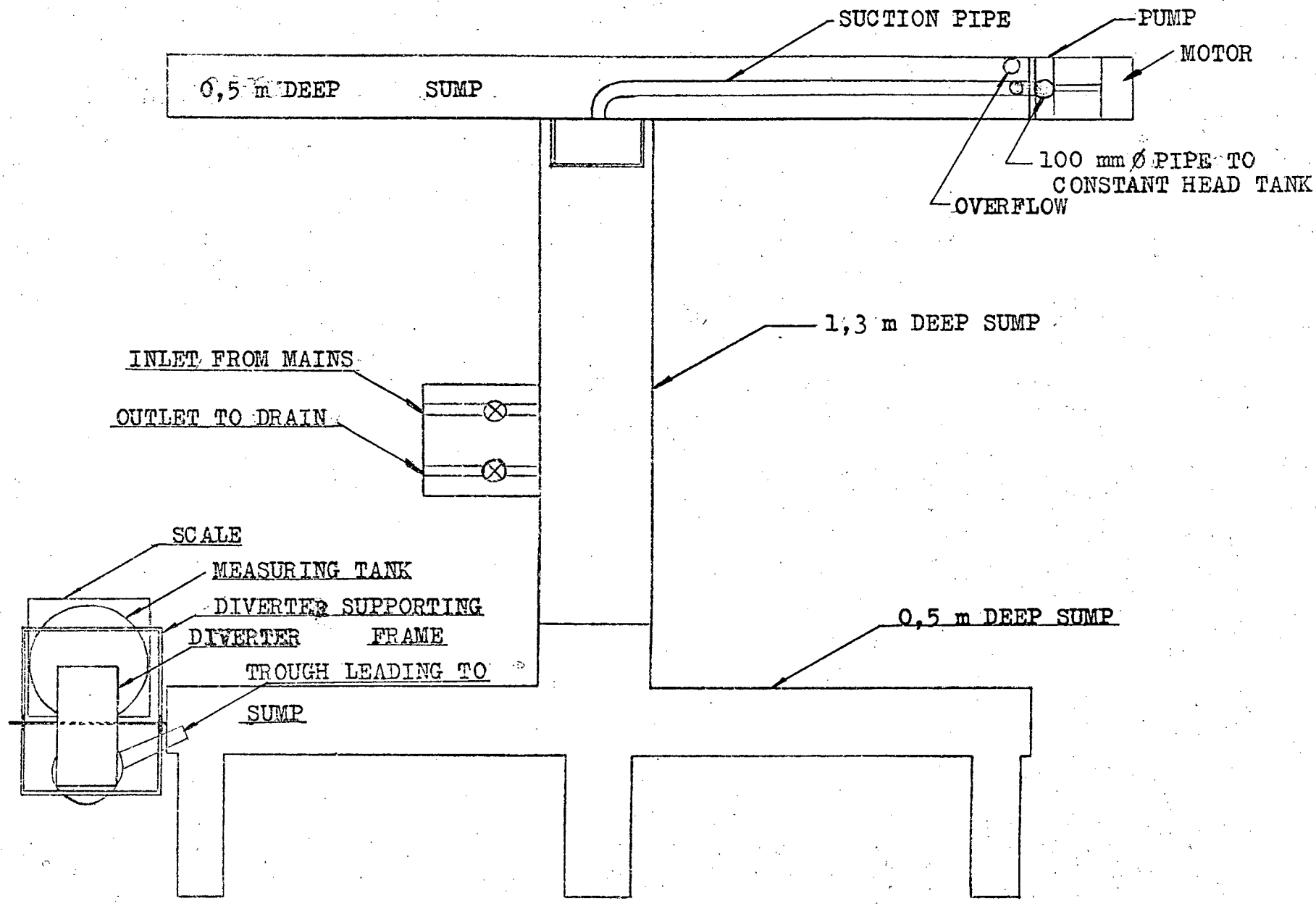

Fig.80. Sump and General Layout of the Equipment
Note: The Test Piping and Piping from the Constant Head Tank are not shown.

(iii) Constant Head Tank (figure 81)

A constant head supply tank is used so as to ensure a steady flowrate through the test section. The tank is fabricated from 6mm mild steel plates. It is 1,82m long by 1,22m wide and 1,22m high. The capacity of the tank is 2,6m^3 (2600ℓ). The tank has a dividing section which ensures that no air bubbles and large fluctuations in the pump discharge are transmitted to the calibrating section. The tank is fitted with a weir so that no large fluctuations in the height of the free surface occur. The water flows over the weir and down the overflow pipe to the sump while a separate pipe leads to the test section. Small variations in the height of the free surface occurs with varying flow over the weir, resulting in a variation of the quantity of flow which passes through the test line. To eliminate this variation, the supply rate to the tank is controlled.

The tank is mounted on the roof of the building so that the free surface of water is approximately 25 metres above the test pipe centre line. Under operating conditions the variation of the free surface of water did not exceed 10 mm resulting in a maximum pressure fluctuation in the test line of 0,04 percent.

(iv) The Medium and Fine Meshed Strainer

The strainer is introduced into the supply line, about twenty pipe diameters after the tank. The strainer is fabricated from six millimetre mild steel plate. After fabrication the whole unit was galvanised. A two millimetre wire mesh filter precedes the 0,8mm one. Quick replacement or cleaning of the filters is possible.

Before the introduction of this strainer, clogging up of the flow straightener occurred and the frequent cleaning of the straightener was required. The introduction of this strainer solved the above problem.

(v) The Flow Straightener

The flow straightener was introduced to reduce the swirl and the eddying which occurs straight after a 90 degree bend. The use of a flow straightener reduces the straight length of pipe required for fully developed flow to occur.

Figure 82 shows the construction of the flow straightener. The wire mesh

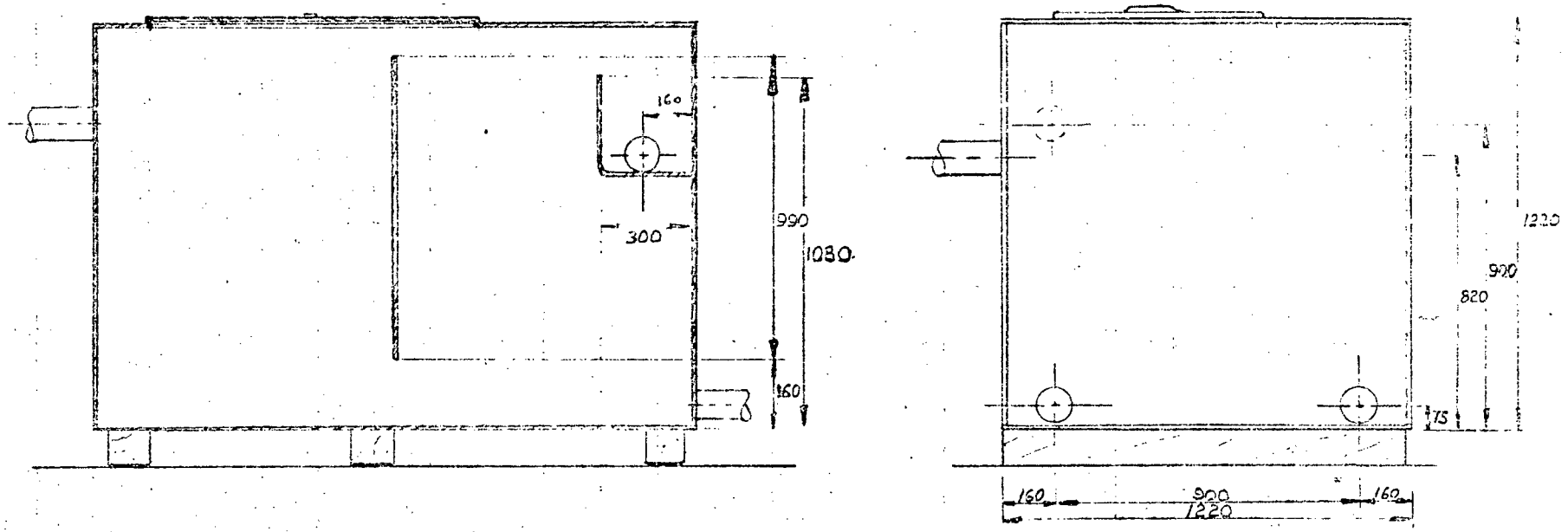

Fig. 82 *Constant Head Tank.*

Note: Fabricated from 10 mm mild steel plate.
Pipes are 100 mm in diameter.

SCALE : 1 : 20

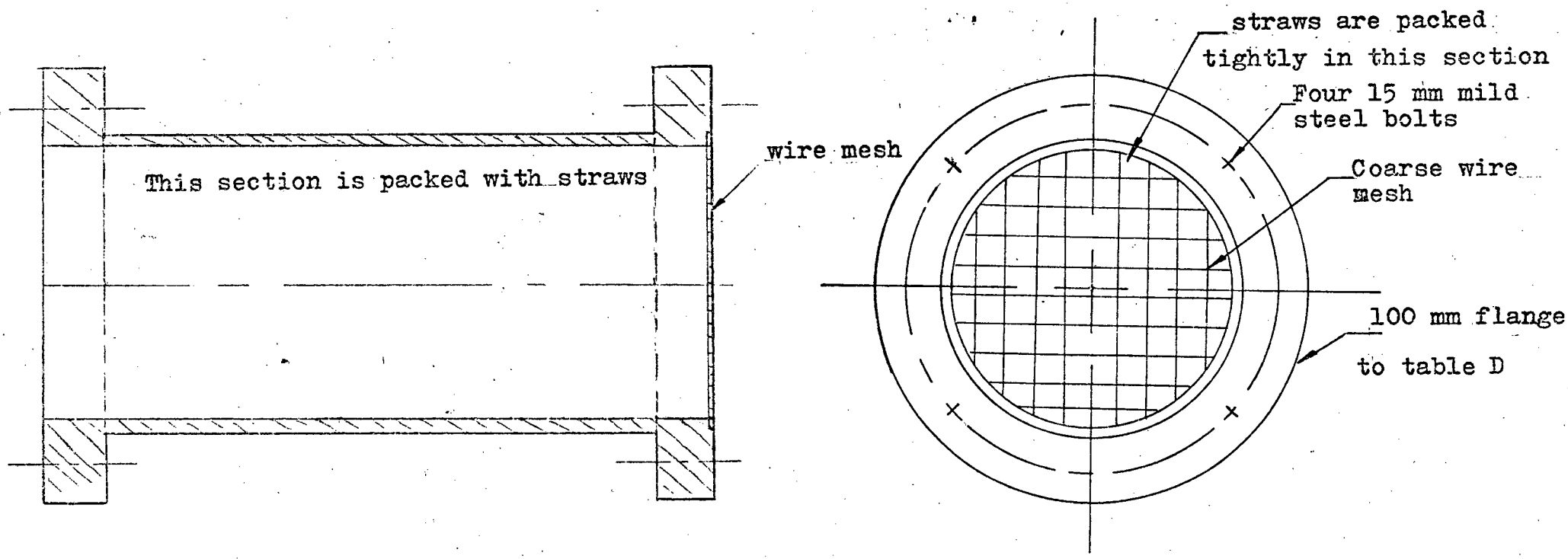

Fig82. The Flow Straightener

at the discharge end ensures that the straws are not swept away by the flow. The straws can easily be replaced when required.

(vi) The Straight Test Section

As already pointed out in chapters 1 and 2, an orifice plate will give inaccurate readings if the streamlines of the flow approaching the plate are not parallel to the axis, or if asymmetric velocity distribution across the diameter occurs or if the flow is not fully developed. The need for long, straight piping free from encrustations is essential for accurate readings. The British Standard calls for 40 pipe diameters before and 7 after the plate for orifice plates with area ratios less than 0,55. The test section is straight and circular for a distance of 47 pipe diameters upstream from the plate and 15 pipe diameters downstream from it. The 100mm P.V.C. pipe was specially selected and it has all the requirements specified by BS 1042 : 1964.

(vii) The Control Valve

The flow is controlled by a 50mm gate valve specially suited for P.V.C. piping. It is located in the pipe which connects the test section to the diverter.

(viii) The Diverter System

Due to the high calibrating accuracy required, the reference meter has to be very accurate. The most accurate method of measuring the flow rate is achieved by measuring the time taken for a quantity of fluid to flow into a container. To achieve this the jet of the fluid has to be diverted from the recirculating system into the measuring tank for a period of time.

Figure 83 shows the diverter. The central plate moves across the jet at a high speed and diverts the flow into the sump or the measuring tank. The diverter frame is pivoted above its centre of gravity. A point above the pivoting point and on the line of the axis of symetry of the diverter is connected to a double acting pneumatic cylinder. When the piston is at one end of the cylinder the "diverter" directs the water to the collecting trough as shown in figure 83, while with the piston at the other end the water is directed to the measuring tank. To avoid splashing, to ensure a finite jet and an even distribution of the water in the diverter, the circular jet issuing from the pipe is changed into a narrow rectangular one by a "fishtail" fitted at the end of the circular pipe and just above the

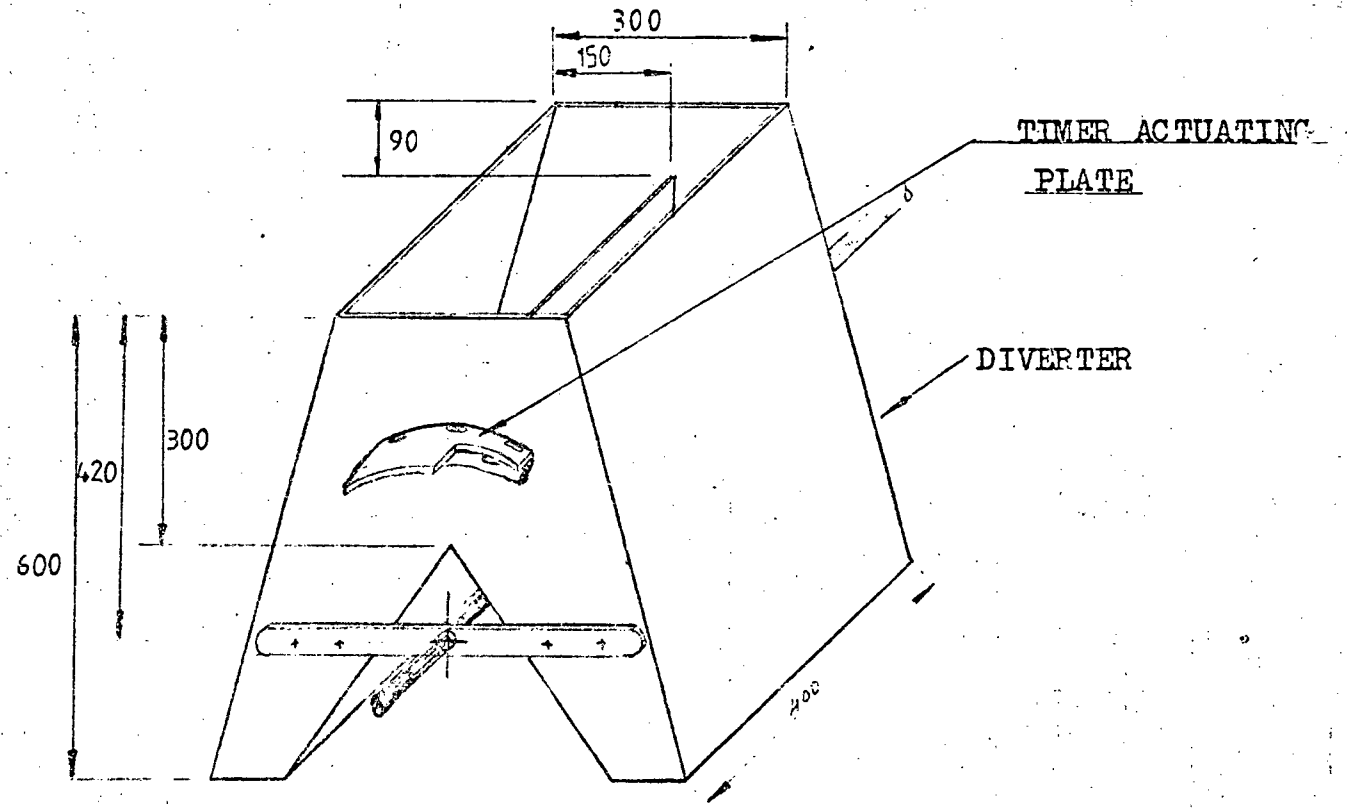

Fig. 83. The Diverter

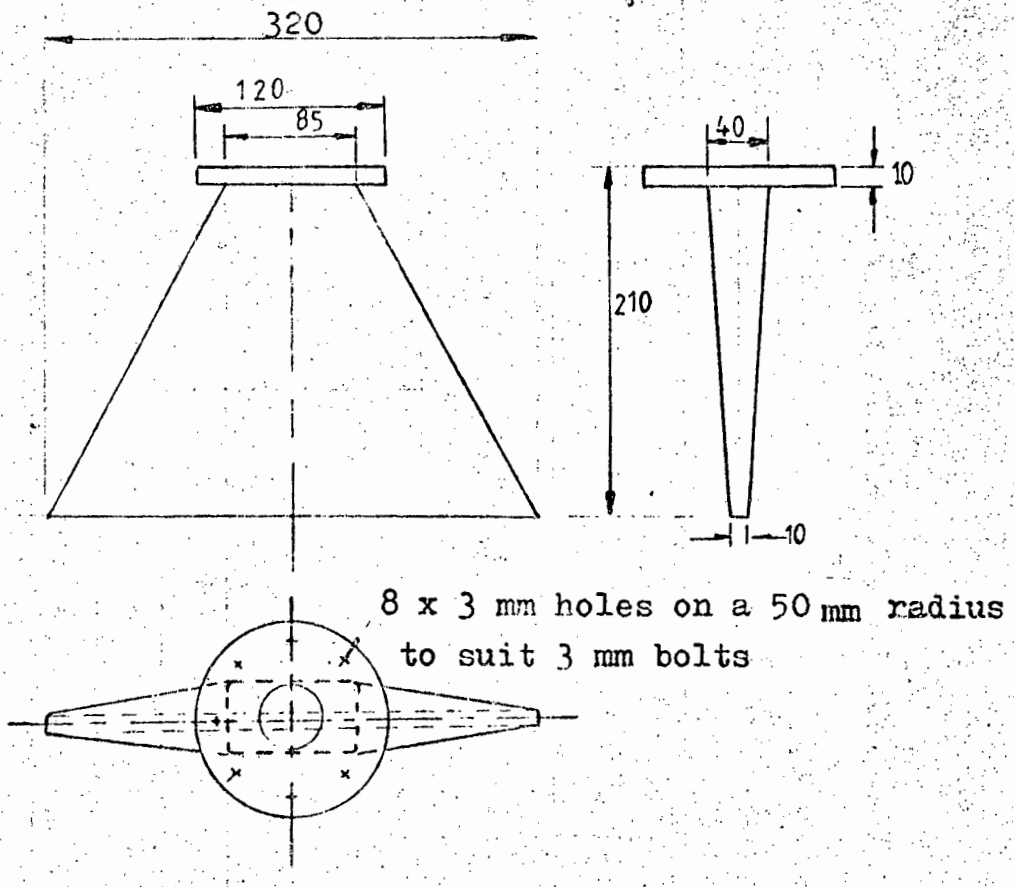

*Fig.*84. *The Fishtail*

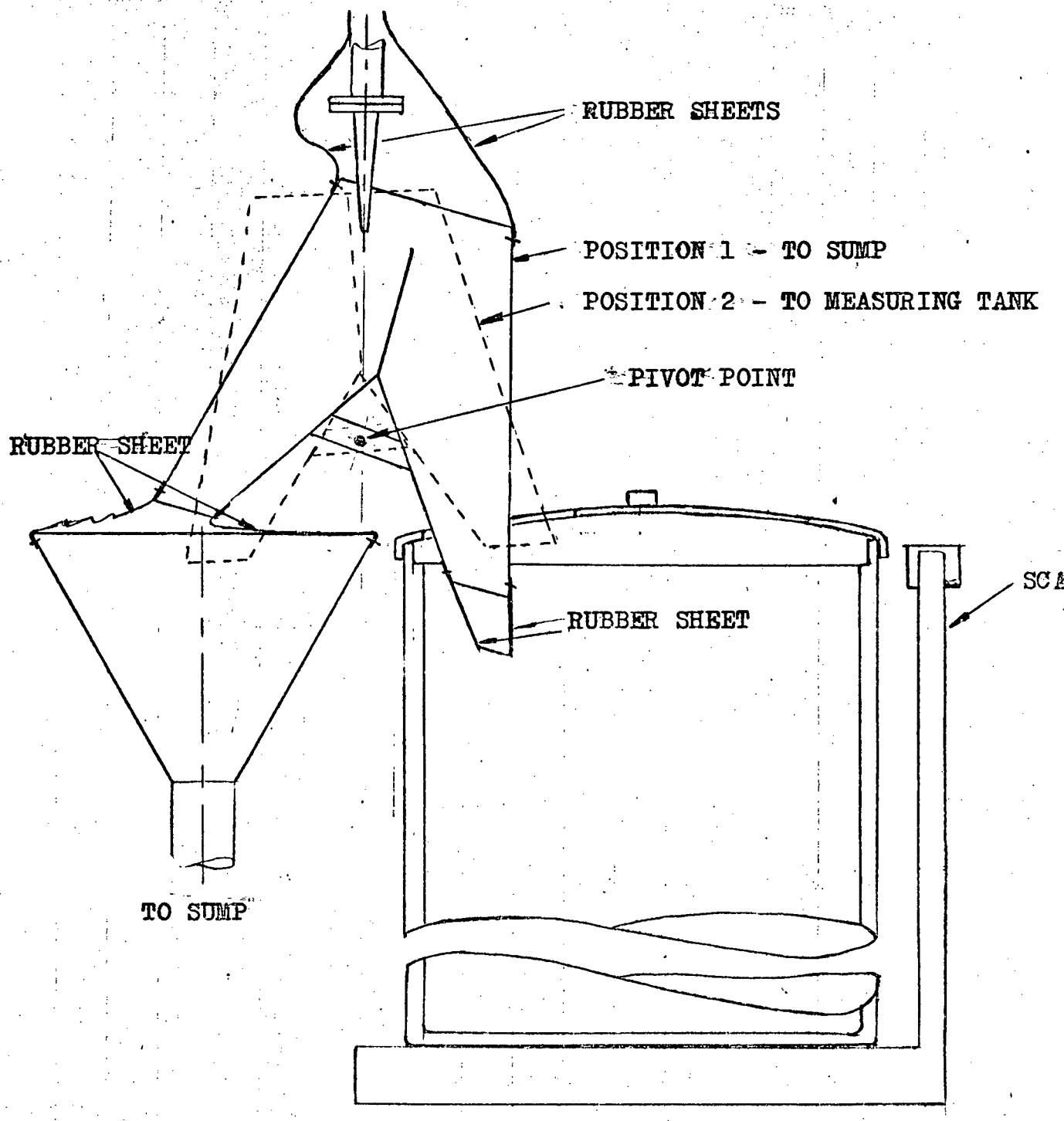

Figure 85.: Positions of the Diverter.

diverter. To ensure no splashing at high flowrates the diverter top and bottom arms are covered, as shown in figure 85, with rubber sheeting.

A brass plate is mounted at the rear of the diverter. A photo-diode and a light source are mounted onto a box as shown in figure 86.

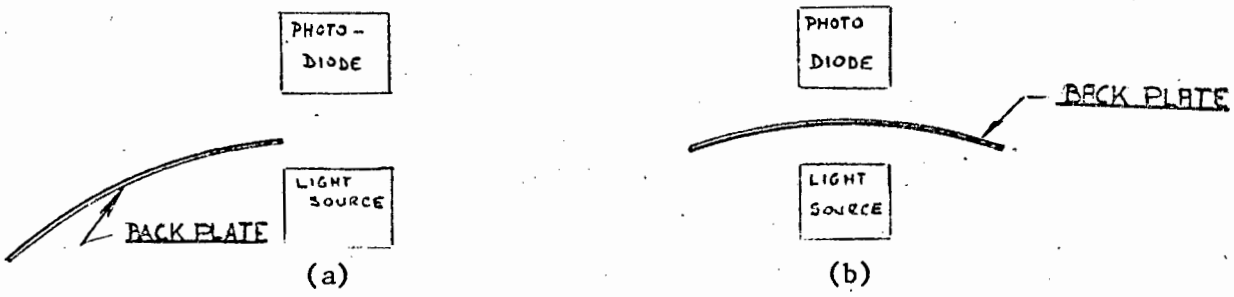

Figure 86 - Actuator on the Digital Counter

(a) Water is directed to the sump - Counter is off

(b) Water is directed to the measuring tank - Counter is on

When the water is diverted into the sump the light from the bulb is detected by the photo-diode and the electronic counter is not registering. When the water is directed into the measuring tank the back plate is in the position shown in figure 86b, the beam of light is cut by the back plate and the electronic counter is registering. The time during which the measuring tank is filled is thus recorded.

The jet of water issuing from the "fishtail" is of finite thickness and it takes a finite time to cross the dividing plate. To overcome the problem posed by the above fact a high and equal velocity of traverse is maintained in either direction. The velocity of traverse can be varied by changing the constant compressor delivery pressure. During the experiment the compressor pressure was maintained at 100 lbf/in^2. To achieve equal velocity of traverse in either direction the time interval between the time taken by a small back plate to cross and recross the mid-point of the jet is measured. The small plate is mounted centrally, in line with the diverter plate. The diversion time is controlled by using a restrictor to control the air flow to the double acting pneumatic cylinder and by monitoring the time taken for the small back plate to traverse the light source in either direction.

✳ (ix) The Timer

To ensure accurate calibration with limited random errors the electronic timer is actuated automatically by the movement of the diverter. The actual method of actuation was described in Section (viii) above.

Figure 87 shows the electronic circuit used to activate the electronic timer.

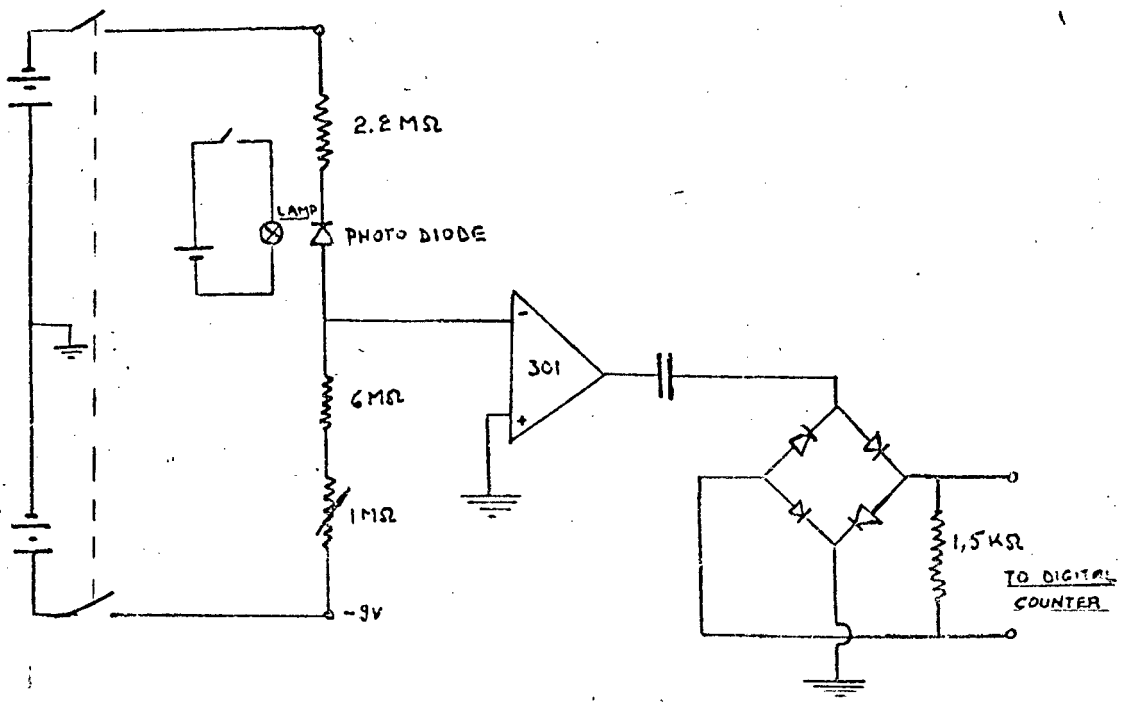

Figure 87 - The electronic circuit used to actuate the electronic timer

The light falling on the photo-diode overbalances the divider. The op-amp compares the input signal with the ground. Its output is rectified to give specific pulses which actuate the electronic timer.

The electronic timer has a quartz crystal frequency generator passing pulses to a digital counter. The counter thus measured the time, in milliseconds, during which the measuring tank is being filled. It is important to ensure that the timer starts and stops counting when the diverter is in mid travel and therefore the back plate has to be carefully positioned. Since the jet is of finite thickness, when the first diversion into the weigh tank occurs

some water passes into the sump and into the tank while the timer is actuated. The same procedure is repeated during the second diversion. If the plate is correctly positioned the error occurring during the first diversion is compensated by the one recurring during the second diversion.

(x) The Pneumatic Circuit

The diverter is actuated by a double acting pneumatic cylinder. The air flow diagram is illustrated in figure 88.

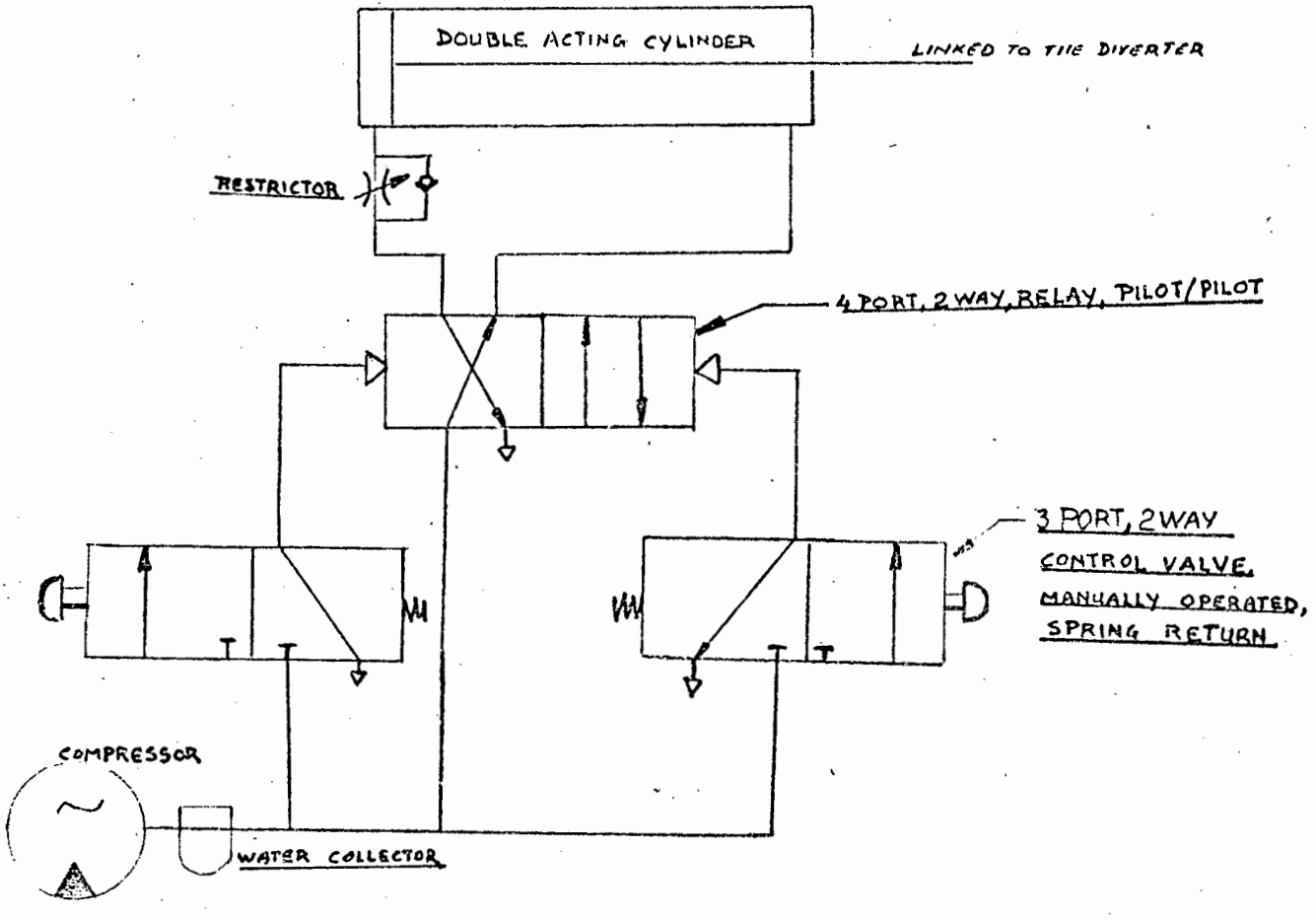

Figure 88 - Pneumatic Circuit

The "Hydrovane" compressor supplies air at constant pressure to the double acting cylinder. The cylinder is actuated by two manually operated spring return control valves. By selecting the correct switch the diverter is actuated.

The water collector was introduced due to the excessive amount of water collecting in the cylinder which caused a decrease in the change-over speed.

The cylinder, the relay and the control valves are standard "Festo" equipment. The model 9 PU "Hydrovane" compressor is capable of delivering air at a maximum constant pressure of 1020 kPa. It is driven by a 1,5kW, 220 volt, 50 Hertz motor. The water collector is made from brass. Its dimensions and shape is as shown in figure 89.

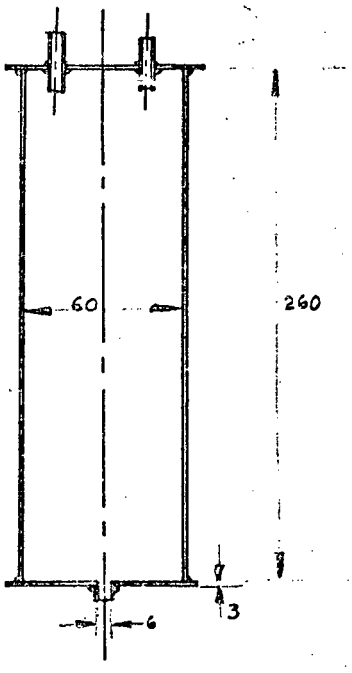

Figure 89.- The water collector.

(xi) Orifice plate mounting flanges

The orifice plate is mounted between specially designed flanges. The following factors must be borne in mind in designing the flanges:

1) Orifice plates with varying edge radii, and area ratios but with constant outside diameter and thickness are to be tested.
2) The flanges must allow for eccentric positioning of the orifice plate. The amount of eccentricity has to be known to 0,01mm. It must be possible to vary the eccentricity of the plate while water is flowing through the system, without altering any of the other prevailing conditions.
3) When assembled the flanges must always be in the same position relative to each other.

4) Changing of plates must be simple and quick to perform. One person should be able to change the plates without any assistance.

The design of the flanges is illustrated in figures 90 and 91. The round orifice plates used to determine the effect of rounding the upstream edge of an orifice plate are placed into the recess provided. Two five millimetre dowels, one on either side of the plate, are fitted into one of the flanges. The other flange has holes drilled in the appropriate places to ensure correct matting of the flanges. O-rings on either side of the orifice plate, mounted in the flanges ensured sealing. Six specially designed shouldered bolts are used to fasten the flanges together. Two six millimetre bolts are secured into the flanges. These bolts are tightened for quick and easy removal of the orifice plates. The flanges were mounted concentrically with the pipe. This was achieved with the use of a mandril.

The orifice plates used for the determination of the effect of eccentric location on the coefficient of discharge are rectangular. The orifice hole of these plates is circular with its centre coinciding with the midpoint of the rectangle. A small location hole is drilled into every orifice plate. A dowel, fitting this hole within a tolerance of +/- ,005 mm locates the orifice plate relative to the flange and the axis of the pipe. The plate can be moved vertically up and down by turning handle A. The movement is measured with a dial gauge.

The position of the plate can be varied if required under test conditions.

(xii) The Temperature Measurement

The water in the system is slowly warmed up during the day due to friction losses in the pipes and pump. The atmospheric temperature varied during the day and this affected the temperature of the water and of the mercury in the manometer.

Mercury thermometers were used to measure the temperature of the water upstream and downstream of the orifice plates. The thermometer pockets were made from brass. A small quantity of oil was placed into them. The thermometers were calibrated. They were used to measure the temperature of the water to within 0,1° C. The siting of the thermometers in the pipes conformed to the requirements of BS 1042. By measuring the temperature up-

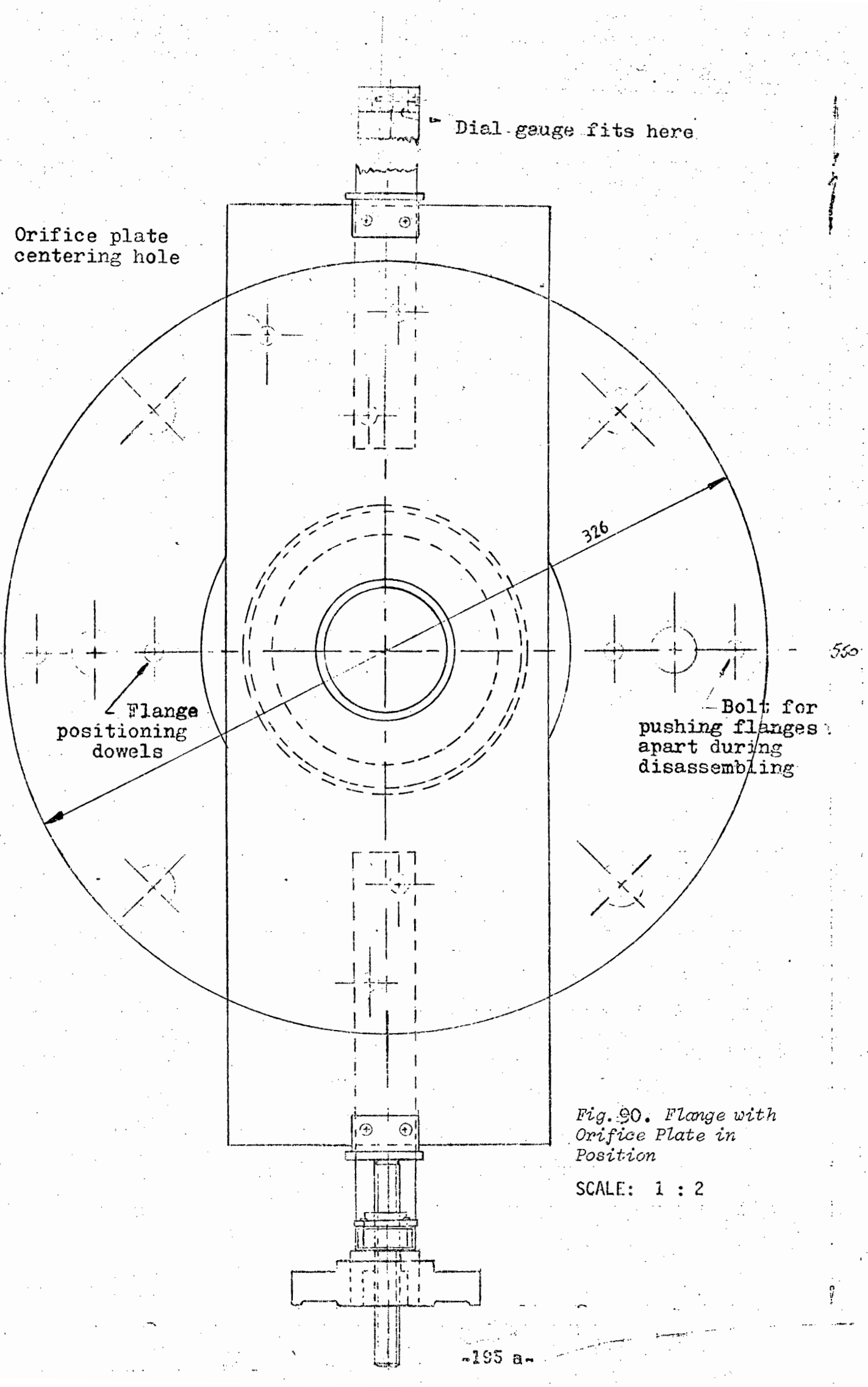

Fig. 90. Flange with Orifice Plate in Position

SCALE: 1 : 2

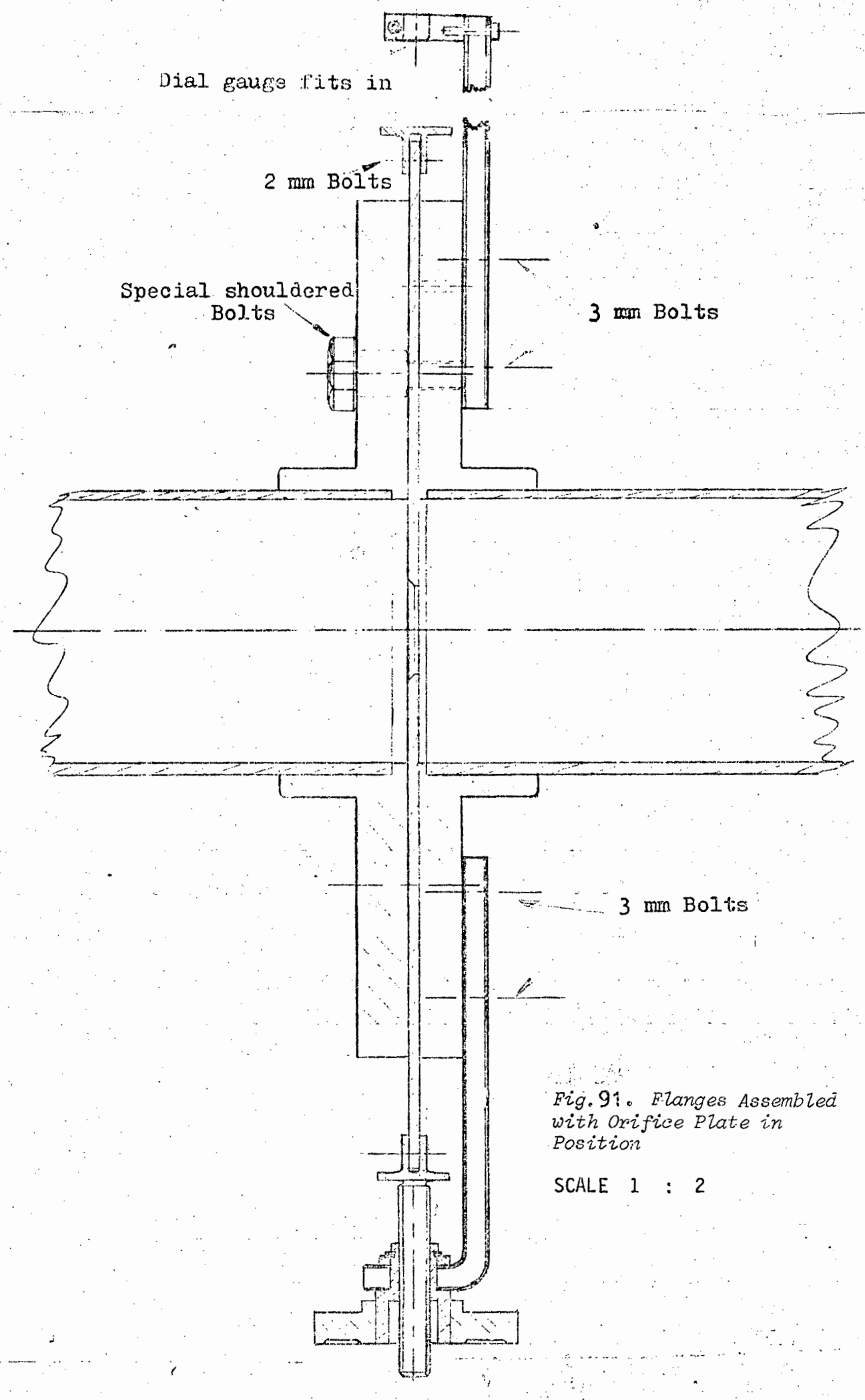

Fig.91. Flanges Assembled with Orifice Plate in Position

SCALE 1 : 2

stream and downstream of the plate, any variations in the temperature of the water were detected. A mercury thermometer was lowered into the measuring tank so as to measure the temperature of the water in the tank. The local atmospheric temperature was measured to within 0,1°C. All the thermometers were calibrated against standard thermometers.

(xiii) Pressure-differential Measurement

The pressure drop across the orifice plate was measured with U-tube manometers and with a pressure-differential transducer. Pressure fluctuations due to turbulence occur and therefore the accurate measurement of the pressure differential is difficult to obtain. The flow straightener helps to improve the flow regime but fluctuations in the pressure differential still occur.

To overcome the above, the manometers designed were fitted with special valves so that instantaneous pressure difference could be measured to within 0,05mm of mercury at high flowrates and 0,5mm of water at low flowrates. A number of readings at one flowrate were taken. The average of these readings was used for the calculations. It was found that if twelve readings or more at maximum flowrate (condition of greatest pressure fluctuations) were taken the average calculated pressure did not vary by more than +/- 0,05 mm of mercury. Therefore 12 pressure differential readings were taken at each flowrate.

The D and D/2 pressure tappings conform to the stipulations of BS 1042. The piezometric ring joins the four pressure taps. The average pressure at the taps is therefore measured. The undamped pressure leads connect the piezometric rings to the manometers. The pressure difference can be read on either the water-mercury manometer or the water-air inverted manometer and the output from the pressure transducer can be recorded on the U.V. recorder.

Figure 92 illustrates the manometers, the amplifier and the U.V. recorder. The water-mercury U-tube manometer can be used to measure a maximum pressure difference of five hundred millimetres of mercury. The pressure difference can be measured within +/- 0,05 millimetres of mercury. The operation of this manometer is as follows:

Valves A and B are closed and the upper measuring unit is moved approximately in line with the meniscus . Screw C is tightened. The meniscus is sighted through the eye-piece and screw D is turned till the hair line

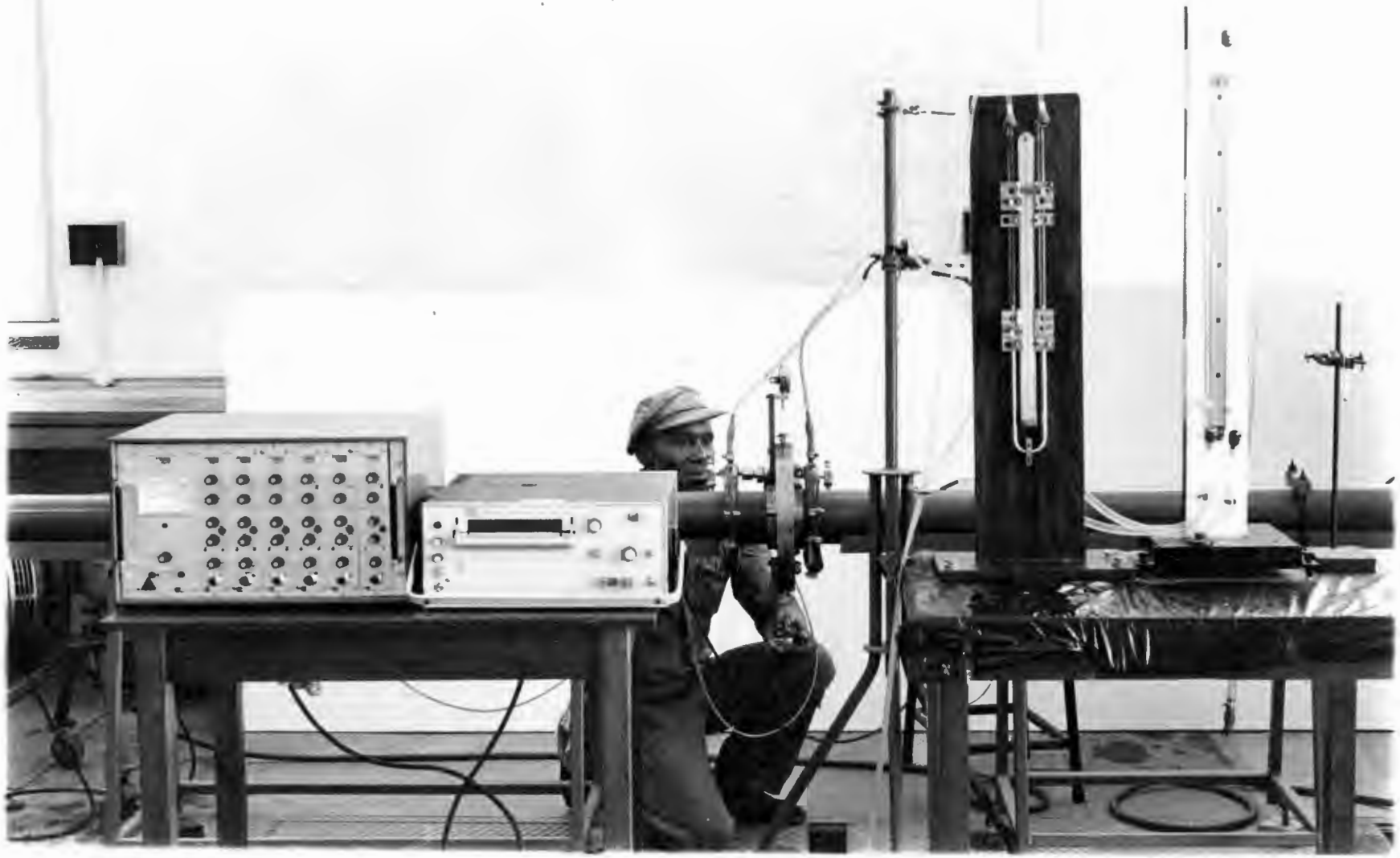

Fig. 92 The Pressure Tappings, the Mercury and the Water Manometer, the Pressure Differential Transducer and the U.V. Recorder

of the eye piece lines up perfrectly with the meniscus. The height of the meniscusis then read from the rule and the vernier. scale. Similar procedure is adopted using the other measuring unit to measure the height of the meniscus in the other leg of the manometer. One must remember to level the manometer before testing starts, to purge the air from the line and to check that the same readings are obtained from both the upper and lower measuring units. At no flow the reading obtained using any of the measuring units should be the same in both legs of the manometer.

The water-air manometer is used to measure the pressure difference up to eight hundred millimeters of water. The manometer can be read to within +/- 0,5 millimetres of water. The shape and size of the manometer can be seen in figure 92 Initially the manometer was filled with water. With all these valves open compressed air was blown in through the top tube. When the water was at the right level (i.e. the level at about midpoint of the rule) valve C at the top was closed. The U tube is made from 12mm glass tube. The steel rule is calibrated accurately to within 0,5mm at $20^{o}C$.

The pressure transducer is used to monitor the instantaneous pressure difference. The fluctuations in the instantaneous pressure difference can be measured. The transducer, voltmeter on the amplifier and the U.V. recorder were calibrated against a dead weight pressure gauge calibrater.

(xiv) The Measuring Tank

The plastic measuring tank is 1,1 metres high with an internal diameter of 0,74 meters and has a capacity of $0,5m^3$ (500 ℓ). The tank has a removable plastic cover. A sight glass is installed on the side of the tank. The 50mm P.V.C. outlet pipe is fitted with a butterfly valve and the water from the outlet pipe is directed to the sump.

(xv) The Weight Measurement

The mass of the tank before and after diversion is measured using an "AVERY" weighing scale. The scale is graduated in 0,1 kg divisions up to 500 kilograms. The scale was calibrated by using assized 20 lb. mass weights.

(xvi) The Orifice Plates

The orifice plates used conform to BS 1042. They are made from cold rolled brass plates. The plate thickness is 3mm, the edge thickness is 1,2mm and the bevel angle is 45 degrees. The surface finish of the plates was measured with a "Talysurf" surface roughness meter. The edge sharpness, flatness and diameter of each orifice place was recorded. In order that the plates would not get damaged they were kept in a special box.

The size of the orifice plates used is given in Table 11

TABLE 11.

The size of the orifice plates used.

TYPE OF PLATE	PLATE NO	ORIFICE DIAMETER	PIPE DIAMETER	AREA RATIO
ROUND PLATES	1	31,55	100,51	0,099
	2	44,75	100,51	0,198
	3	54,61	100,51	0,295
	4	63,00	100,51	0,393
	5	70,99	100,51	0,499
RECTANGULAR PLATES	15	38,93	100,51	0,150
	45	67,42	100,51	0,450
	55	74,54	100,51	0,550

NOTE: The orifice and the pipe diameter are given in table 11 in millimetres.

The Edge Radius Measurement

Little work has been done on the effect of edge sharpness of the orifice plates due to the difficulty of measuring the sharpness of the edge without destroying the plate. Researchers in this field knew that the edge sharp ness did affect the flow coefficient, but to what extent was not known. Lately a number of ways have been developed for measuring the edge sharpness of orifice plates. These are:

1) the casting method
2) the lead foil method
3) the optical method.

1. THE CASTING METHOD

This method was developed by Gallacher. The plate is thoroughly cleaned and an impression of the orifice edge is obtained by forming a negative casting within a region defined by a wax boundary cup. The negative casting is made from a yellow coloured cold forming plastic known as Technovit. Once the casting has hardened it is removed from the plate. A positive casting is then made in a second wax cup formed around the negative casting. Epikote 816, a transparent epoxy resin is used to form the positive casting. This positive casting is sliced and polished prior to viewing and measuring the edge sharpness. During casting care must be taken for air bubble formation within the casting and for shrinkage during the setting of the casting material.

The advantage of this process is excellent following of the edge profile resulting in accurate measurement of the edge radius and in the determination of the shape of the re-entrant profile. The disadvantages of this method are:

a) the requirement for great skill to produce a good casting.
b) the duration to complete a measurement is over twenty-four hours.

2. THE LEAD FOIL METHOD

Professor Herning was the first researcher to use this method. The apparatus designed by Herning was improved upon by Upp and more recently Johnson and Jepson.

An impression of the upstream edge of the orifice is obtained by pressing a very thin lead foil onto it. The indentation in the foil is magnified and the edge radius measured using a template. Brain and Reid compared this method with the optical and the casting ones. Their results showed that the value obtained for the edge radius by the casting method and by the lead foil method approach one another closely. Upp found that a repeatability of 2 percent can be achieved using this method. The lead foil method is quick but skill is required for accurate measurements. Often a fragment of lead juts out into the radius of the remaining impression and measurement is rendered impossible.

3. THE OPTICAL METHOD

This method was suggested by A. Aschenbrenner. The projection of a fine beam of light directed onto the orifice edge is observed and photographed. The profile of the distorted image of the upstream edge is measured with a reticle. By using geometric equations the edge radius of the orifice plate is obtained.

Brain and Reid state that this method is the least reliable but affords the quickest results from the three mentioned. They suggest the use of this method for examining large diameter plates for burrs and for excessive rounding of their edges.

The designed apparatus for measuring the edge roundness of the orifice plates.

Taking into consideration the findings of Brain and Reid it was decided to use either the casting method or the lead foil one. Measurements were taken using both these methods. The description of the method used and the conclusions drawn are as follows:

1. Casting Method

The cold forming plastic called Technovit was not available and silastic was used instead to form the negative casting. Further procedure was the same as suggested by Gallagher. The resultant cast followed the shape of the edge well. Difficulty was found in measuring the edge, as to cut a straight and thin section required great skill. When measured under the microscope a double edge was visible. To complete a measurement takes over twenty-four hours.

2. The Lead Foil Method

Initially the following crude method was tried to give an indication of the usefulness of this method. The lead foil was clamped in a holder and then pressed onto the edge. This method was quick and easy to use. Reasonable repeatability was achieved and no difficulty was experienced in measuring the edge. This method was therefore adopted and a special lead foil holder was designed.

To use this method successfully the lead foil holder must be designed so that:

1) the orifice plate will be clamped in such a position that the line of travel of the lead foil will be along the appropriate marked diameter on the plate.

2) the orifice plate will be perpendicular to the holder and simultaneously the approach of the lead foil will be at 45^{o} to the upstream face of the plate.

3) the depth of the impression is the same for every measurement.

If the above are fulfilled, then accurate, undistorted measurements can be obtained which can be used to compare realistically the edge radii. A photograph of the apparatus designed can be seen in figure 31 in the main text. (Chapter 3).

Method of using Apparatus

Clamp orifice plate onto holder as shown in figure 93. Place main body of apparatus onto the rails and slide till pins A & B just touch circumference of orifice. Tighten screw C. Figure 31 shows the apparatus at this stage of the procedure. The micrometer screw is turned until the lead foil just touches the orifice edge. The fine control of the micrometer is turned until the lead is pressed onto the edge until the indentation in the lead is 0,2 mm deep. The lead foil is then retracted by turning the micrometer screw in the opposite direction. By keeping to this procedure no change in the indentation occurs during the removal of the lead foil from the orifice edge. The lead foil is removed from apparatus by loosening screw D. It is then placed onto a transparent film which has accurate half millimetre graduations on it. The film is placed into a slide holder and viewed with a microscope. If the microscope is equipped with measuring apparatus, the radius can be measured directly. Since such a microscope was not available, the slide was placed into an enlarger and the image photographed. The image from the photographic negative was further enlarged. The correct magnification could be determined from the scale. A template was used to measure the edge radius. Typical photographs of the edge radius of an orifice plate and the method of measurement is shown in figure 94.

Tests for repeatability of measurement were carried out. Two orifice plates were used and 2 positions on each plate were selected. At each position six imprints were taken. The image of the imprint was magnified 50 times

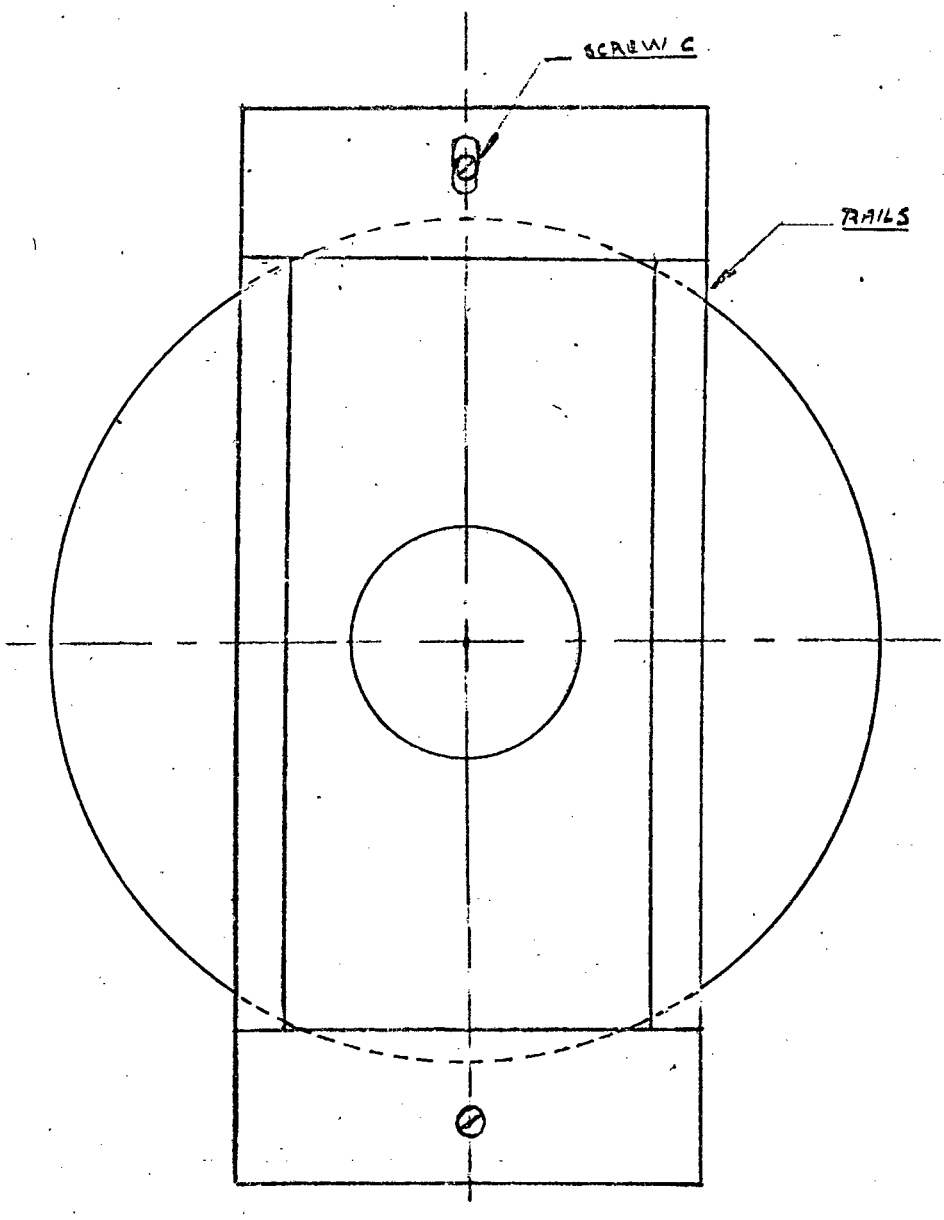

Figure 93 - Orifice plate clamped into holder

and 300 times respectively. The following results were obtained in the best case. The same edge radius measured on six occasions was equal to 0,320mm in four of the measurements while the remaining two measurements were equal to 0,330mm. Maximum deviation of the reading was therefore +/- 2 percent from the mean. The edge radius in this case was large and therefore low magnification of the imprint was required. For very sharp edges a magnification of 300 was used. In the worst case the maximum range of a reading was +/- 5 percent.

During experimentation the edge radius of each plate was measured in six

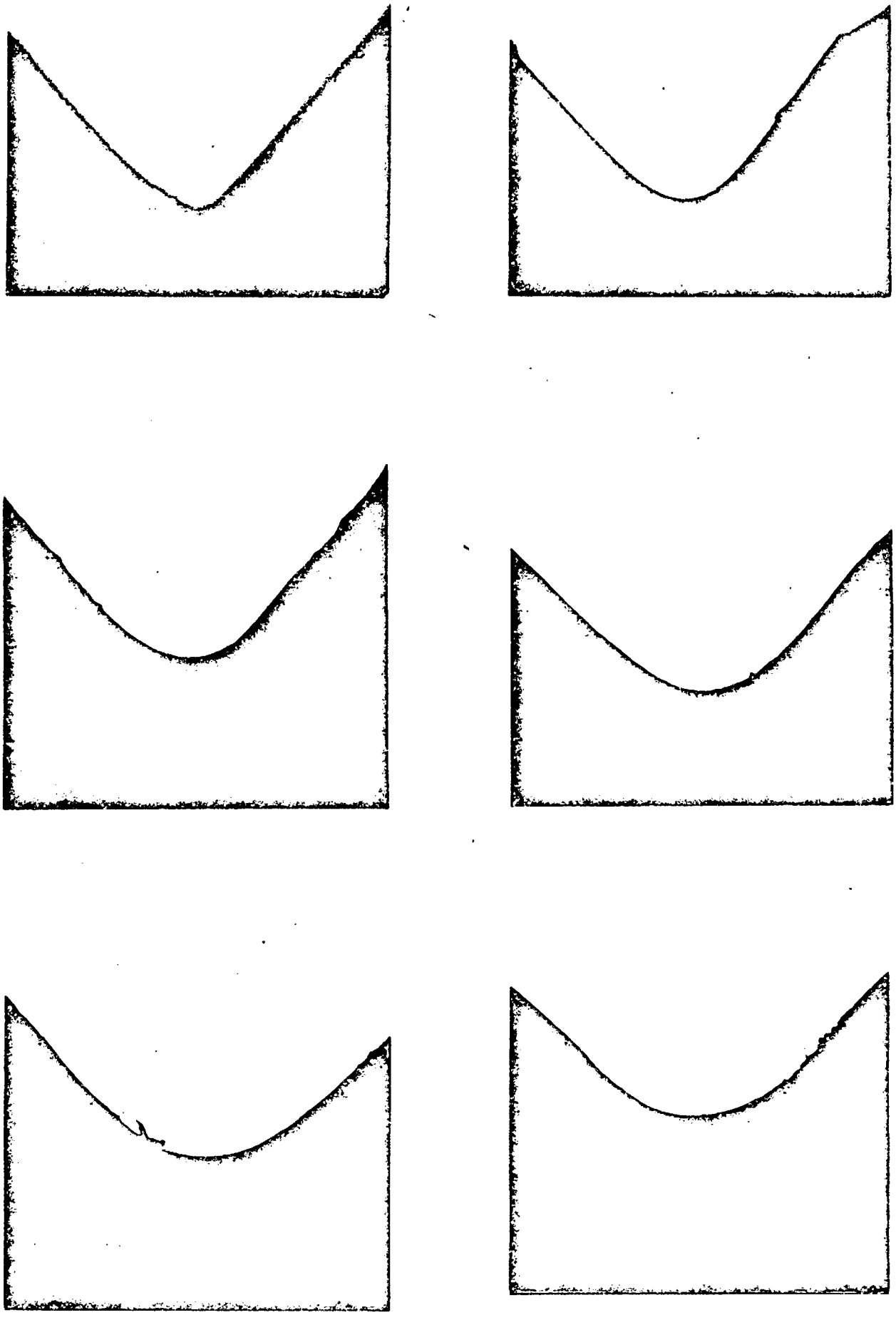

Fig. 94 Photographs obtained of the Edge Radius of an Orifice Plate using the Lead Foil Method (Magnification 100)

different positions (see figure 95).

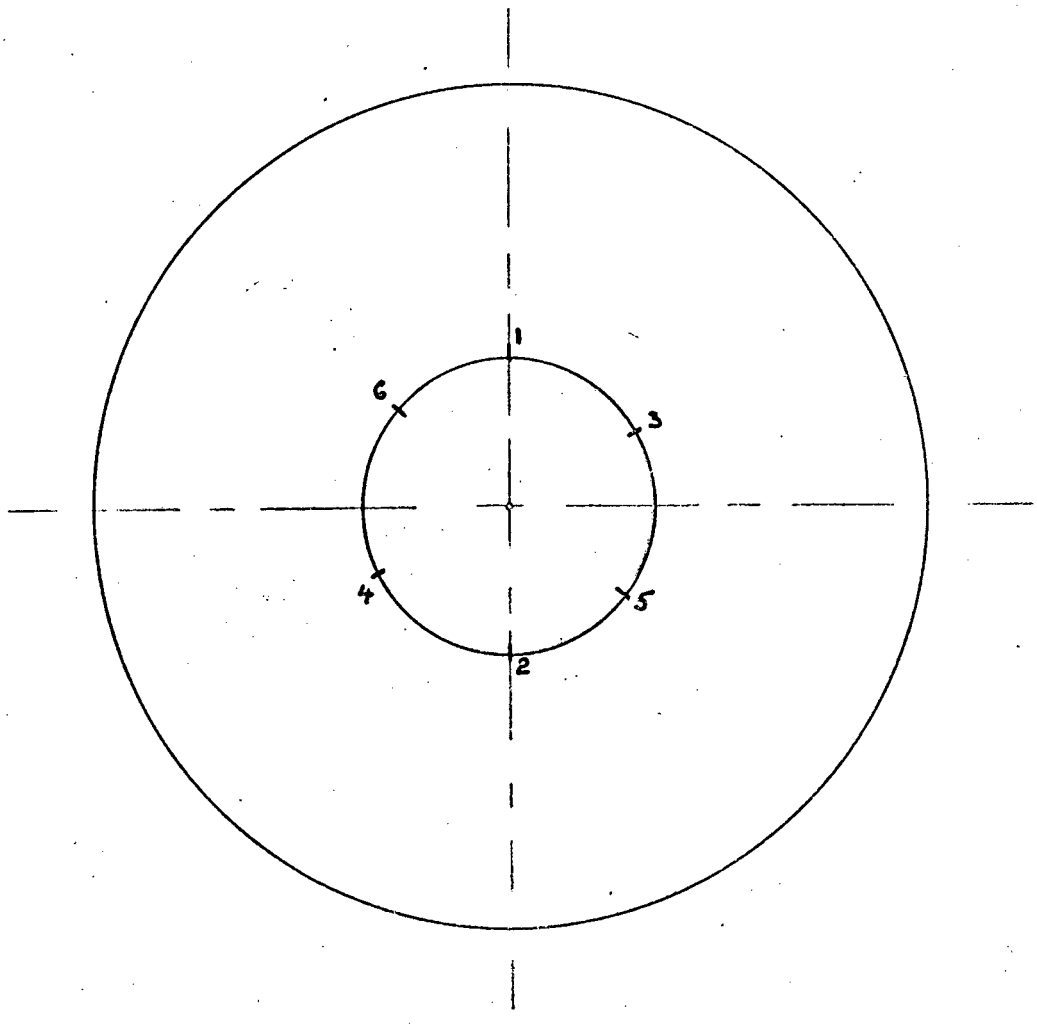

Figure 95 - Position for measuring the edge sharpness of a plate.

The average edge radius of a plate was determined.

The upstream edge radius of the orifice plate was increased by using emery paper while the plate was rotated in a lathe. Because this operation was not accurately controlled, the edge radius of the plate varied along its circumference. For the edge radius to be equal around the entire circumference would have necessitated the design and manufacture of a special tool. Since the increases required in the edge radius were only in the order of 0,1 millimetre, such a tool would have been costly. As the variations in the edge radius around the orifice circumference did not exceed 2,5 percent and because the repeatability of an edge measurement

reading was only +/- 2 percent, the expense of the above tool was not warranted.

The measuring of the edge radius with the template is subject to personal interpretation. To overcome this bias two independent persons were asked to measure the edge radius. The value of the size of the edge radius of one plate at a specific point as measured by the different persons varied by +/- 1 percent from the average reading at that point. The average radius measured by these people was then used for further analysis.

The following problems occurred during measurement of the edge sharpness:

1) On a number of occasions fragments of lead jutted out into the radius making it impossible to measure it.
2) Sometimes a double edge or an undefined edge was observed.

These problems occurred mainly when very sharp edges were measured. In all these cases new imprints were taken. Figure 33e shows some examples of problematic prints. Upp found similar difficulties using the lead foil method.

It can be concluded that the edge radius of an orifice plate can be measured with the designed apparatus and a repeatability in the readings of +/- 5 percent can be achieved. Brain and Reid found that the edge radius measured by the casting method and the lead foil method were in good agreement. The work done by the author similarly agrees with the results obtained by the aforementioned researchers.

APPENDIX C

THE DETERMINATION OF THE DENSITY OF THE WATER

To achieve the required overall accuracy for the calibration of an orifice plate, the density of the water has to be determined to within +/- 0,01 percent. To obtain this degree of accuracy the following instruments were used.

1) A specific gravity bottle whose volume is accurately known to +/- 0,004 percent.
2) A chemical balance capable of measuring to within +/- 0,1 mg.
3) Standard assized masses.
4) Calibrated mercury thermometer.

Monthly and/or each time the water in the sump was changed samples of it were taken. The water was heated to different temperatures in beakers. The specific gravity bottle was cleaned and dried using low pressure compressed air. The empty specific gravity bottle was weighed on the chemical balance. The bottle was then filled with the sample water from one of the beakers. The mass of the bottle and water was measured. The temperature of the water in the bottle was measured to within +/- 0,1^{o}C. The density of the water was calculated from the readings and it was determined at a number of different temperatures, and a graph was drawn showing density versus temperature. See Table 14 for results obtained. As the density of the water was likely to change over a period of time as a result of the accumulation of dust and dirt in the sump and the constant head tank, it was necessary to determine its density periodically. At monthly inspections it was found that the density of the water had not changed as a result of the above causes.

During the calibration experiments only the temperature of the water in the pipe and tank was used. The correct density of the fluid was determined from the plotted graph.

An error analysis of the results was done. It was found that the uncertainty of any single measurement of the density at a specific temperature was +/- 0,004 percent.

Error Analysis

$$\rho = \frac{M}{V}$$

$$\therefore \quad W\rho = \left[\left(\frac{\delta\rho}{\delta m} W_m\right)^2 + \left(\frac{\delta\rho}{\delta V} Wv\right)^2\right]^{\frac{1}{2}} \qquad \frac{\delta\rho}{\delta m} = \frac{1}{V}$$

$$\therefore \quad W\rho = \left[\left(\frac{10^{-7}}{50{,}032 \times 10^{-6}}\right)^2 + \left(\frac{49{,}7267 \times 10^{-3} \times 2 \times 10}{(50{,}032 \times 10^{-6})^2}\right)^2\right]^{\frac{1}{2}}$$

$$\frac{\delta\rho}{\delta V} = \frac{M}{V^2}$$

$W\rho = +/- \ 3.98 \times 10^{-2} \ kg/m^3$

$\therefore \quad \rho = 993{,}90 +/- 0{,}0398 \ kg/m^3$

or $\quad \rho = 993{,}90 +/- \underline{0{,}004\%} \rightarrow$

$Wm = 1 \times 10^{-7} \ kg$

$Wv = 0{,}002 \times 10^{-6} \ m^3$

$M = 49{,}7267 \times 10^{-3} \ kg$

$V = 50{,}032 \times 10^{-6} \ m^3$

TABLE 12

The variation in the density of the water with temperature

°C	0,0	0,1	0,2	0,3	0,4	0,5	0,6	0,7	0,8	0,9
9,0	1,00030	1,00029	1,00028	1,00027	1,00026	1,00025	1,00024	1,00023	1,00022	1,00021
10,0	1,00020	1,00019	1,00017	1,00016	1,00014	1,00013	1,00012	1,00010	1,00009	1,00007
11,0	1,00006	1,00005	1,00003	1,00002	1,00000	0,99999	0,99998	0,99996	0,99995	0,99993
12,0	0,99992	0,99991	0,99989	0,99988	0,99986	0,99985	0,99983	0,99982	0,99980	0,99979
13,0	0,99977	0,99975	0,99974	0,99972	0,99971	0,99969	0,99967	0,99966	0,99964	0,99963
14,0	0,99961	0,99959	0,99957	0,99956	0,99954	0,99952	0,99950	0,99948	0,99947	0,99945
15,0	0,99943	0,99941	0,99939	0,99937	0,99935	0,99933	0,99931	0,99929	0,99927	0,99925
16,0	0,99923	0,99921	0,99919	0,99917	0,99915	0,99913	0,99910	0,99908	0,99906	0,99904
17,0	0,99902	0,99900	0,99897	0,99895	0,99892	0,99890	0,99888	0,99885	0,99883	0,99880
18,0	0,99878	0,99876	0,99873	0,99871	0,99868	0,99866	0,99864	0,99861	0,00959	0,99856
19,0	0,99854	0,99852	0,99849	0,99847	0,99844	0,99842	0,99840	0,99837	0,99835	0,99832
20,0	0,99830	0,99827	0,99824	0,99822	0,99819	0,99816	0,99813	0,99810	0,99808	0,99805
21,0	0,99802	0,99799	0,99796	0,99792	0,99789	0,99786	0,99783	0,99780	0,99776	0,99773
22,0	0,99770	0,99766	0,99763	0,99759	0,99756	0,99752	0,99748	0,99745	0,99741	0,99738
23,0	0,99734	0,99730	0,99726	0,99722	0,99718	0,99715	0,99711	0,99707	0,99703	0,99699
24,0	0,99695	0,99690	0,99685	0,99680						

SAMPLE CALCULATION:

To determine the coefficient of discharge of an orifice plate at various Reynolds numbers the following procedure was followed:

$$C_D = \frac{\text{The actual mass rate of flow}}{\text{Theoretical mass rate of flow}} \quad \ldots\ldots\ldots\ldots\ldots 1$$

The actual mass flow rate was determined in this experiment with the reference meter. The first set of data given in Table 15 was used for the sample calculation.

The experimental data

Initial Mass of the measuring tank	36,20 kg
Final Mass of the measuring tank	478,85 kg
Time taken to fill the measuring tank	260,436 seconds
Temperature of the atmosphere	16,9°C
Temperature of the water in the test section	16.2°C
The pressure difference across the orifice plate	52,30mm of Hg
Orifice diameter	31,55mm
Pipe diameter	100,51mm
Atmospheric Pressure	759,45mm Hg

The Calculation

The mass of water added to the tank in 260,436 seconds was

$$\text{Final Mass} - \text{Initial Mass}$$
$$478,85 \quad - \quad 36,20 \quad = \quad \underline{442,65}$$

The mass of the air displaced from the tank was calculated from the following equations:

$$\text{Volume of air displaced, } V = \frac{M_w}{\rho_w} \quad \ldots\ldots\ldots\ldots\ldots\ldots 2$$

$$\text{Mass of the air displaced, } M_a = \frac{\rho_a M_w}{\rho_w} \quad \ldots\ldots\ldots\ldots\ldots 3$$

Where M_a is the mass of the air displaced from the tank
M_w is the mass of water added to the tank
ρ_a is the density of the air
ρ_w is the density of the water

From table 12 the density of the water at 16,2°C is 999,19 kg/m³. From

table 60 the density of the air at a pressure of 760mm of mercury and a temperature of 16,9°C is 1,216 kg/m³.

The density of the air at a pressure of 759,45mm of mercury can be calculated by using equation 4 which is derived as follows:

$$\frac{P_a}{\rho_a} = RT_a$$

Since R is a constant and $T_1 = T_2$, the density of the air at pressure P_2 is given by:

$$\frac{Pa_1}{\rho a_1} = \frac{Pa_2}{\rho a_2}$$

$$\therefore \quad \rho_{a_2} = \frac{Pa_2}{Pa_1} \times \rho_{a_1} \qquad \ldots\ldots\ldots\ldots\ldots\ldots \quad 4$$

$\therefore$ at a pressure of 759,45mm of mercury the density of the air is:

$$\rho_{a_2} = \frac{759,45}{760} \times 1,216$$

$$\therefore \quad \rho_{a_2} = \underline{1,215 \text{ kg/m}^3} \rightarrow$$

and the mass of the air displaced is

$$M = \frac{1,215 \times 442,65}{999,19}$$

$$= \underline{0,54\text{kg}} \rightarrow$$

$\therefore$ the net mass of the water was equal to

$$442,65 - 0,54 = \underline{442,11 \text{ kg}} \rightarrow$$

The actual mass rate of flow was calculated from equation 5.

$$q = \frac{\text{Net mass of water added}}{\text{Time Taken}} \qquad \ldots\ldots\ldots\ldots\ldots\ldots \quad 5$$

$$\therefore \quad q = \frac{442,11}{260,436}$$

$$= \underline{1,6975 \text{ kg/s}} \rightarrow$$

The theoretical mass rate of flow was calculated from equation 6

$$q = \frac{\pi d^2}{4} \left(\frac{2\rho(P_1 - P_2)}{1 - (\frac{d}{D})^4} \right)^{\frac{1}{2}} \quad \ldots\ldots\ldots\ldots 6$$

where $P = \rho_w g h_w$ 7

and $h_w = \frac{h_m (\rho_m - \rho_w)}{\rho_w}$ ..... 8 Valid, see Douglas p 41-2

where h_w is the pressure difference in millimetres of water
h_m is the pressure difference in millimetres of mercury
and ρ_m is the densiry of the mercury in the manometer

The temperature of the mercury was assumed to be equal to that of the atmosphere. From table 59 the density of the mercury at 16,9°C is 13,553 kg/m³. Substituting these values into equation 8 gave

$$h_w = \frac{52,30\ (13533 - 999,19)}{999,19}$$

$$= \underline{657,10\text{mm of water}} \rightarrow$$

The orifice diameter had to be corrected for contraction due to its temperature being lower than when measured. It was measured at 18°C.

The coefficient of expansion of brass is 10×10^{-6} mm/mm °C

The diameter of the orifice at 16,2°C was calculated by using equation 9.

$$d_{t_1} = d(1 - k \Delta T) \quad \ldots\ldots\ldots\ldots 9$$
$$= 31,55\ [1 - 19 \times 10^{-6} \times (18 - 16,2)]$$
$$= \underline{31,55\text{mm}} \rightarrow$$

Substituting the appropriate data into equation 6 yielded

$$q = \frac{\pi \times (31,55 \times 10^{-3})^2}{4} \left[\frac{2 \times 999,19\ (999,19 \times 9,7965 \times 657,10 \times 10^{-3})}{1 - \left(\frac{31,55}{100,51}\right)^4} \right]^{\frac{1}{2}}$$

$\therefore$ $q = \underline{2,8166\text{ kg/sec}} \rightarrow$

The coefficient of discharge was then computed from equation 1.

$$C_D = \frac{1,6975}{2,8166}$$

$$= \underline{0,6027} \rightarrow$$

The Reynolds number was calculated with the aid of equation 10:

$$Re_d = \frac{\rho V d}{\mu}$$

and $$q = \rho V A$$

$$\therefore \quad Re_d = \frac{q d}{A \mu} \qquad \ldots\ldots\ldots\ldots\ldots\ldots 10$$

Where Re_d is the Reynolds number based on the orifice diameter, μ is the viscosity of the water in the test section. From table 61 at 16,2°C the viscosity of the water was given as 1,1160 centipoises.

Substituting into equation 10

$$Re_d = \frac{1,6975 \times 31,55 \times 10^{-3}}{1,1160 \times 10^{-3} \times \frac{\pi \times (31,55 \times 10^{-3})^2}{4}}$$

$$\therefore \quad Re_d = \underline{61384} \rightarrow$$

Similarly the coefficient of discharge of each plate and the Reynolds number at which the coefficient of discharge was determined, was calculated from the available data.

APPENDIX E

EXPERIMENTAL DATA

READINGS FOR PLATE NO. 1

orifice diameter .... 31.55 mm.
edge radius ..... 0.0255 mm.
area ratio 0.099
Atmospheric Pressure ..... 759,45 mm Hg

TABLE NO. 13

Readings for the calibration of the test orifice plate

Air temp. deg. C	Water temp. deg. C	Init. mass kg.	Final mass kg.	Time seconds	Press. dif. mm. Hg.
16.9	16.2	36.20	478.85	260.436	52.30
16.9	16.4	37.70	467.60	201.373	82.65
16.7	16.6	38.10	469.70	180.595	103.85
16.7	16.9	37.45	467.15	157.294	135.65
16.7	17.0	37.90	475.95	142.751	171.50
16.8	17.2	37.70	475.70	129.788	207.60
16.9	17.4	37.95	465.50	117.910	240.00
16.7	18.3	36.45	471.35	113.858	266.55
16.9	18.4	37.85	476.35	108.283	299.65
17.0	18.4	37.20	470.60	103.577	319.90
16.9	18.6	36.55	468.65	97.983	355.35
17.1	18.7	37.70	468.10	95.602	370.85
17.2	18.7	38.00	466.55	93.976	380.55
17.3	18.8	37.80	469.05	92.002	401.90
17.8	18.8	37.50	469.60	88.355	437.10
17.9	18.8	38.80	467.00	86.104	452.20
17.9	18.9	39.80	466.75	84.442	467.15
17.9	18.4	36.15	470.10	85.426	471.05
17.9	18.4	38.10	464.20	93.812	377.55
17.9	18.4	40.05	470.90	111.617	272.20
16.8	16.5	38.55	466.70	127.608	205.80
16.8	16.6	38.90	469.35	139.234	174.90
16.9	17.1	37.85	476.00	408.500	21.10
16.9	17.1	36.45	472.25	233.998	63.40

NOTE: For the last eight readings the atmospheric pressure was 748,95 mm Hg.

READINGS FOR PLATE NO. 1

orifice diameter .... 31.55 mm.
edge radius ..... 0.0794 mm.
area ratio 0.099
Atmospheric Pressure ...750.80 mm. Hg

TABLE NO. 14

Readings for the calibration of the test orifice plate

Air temp. deg. C	Water temp. deg. C	Init. mass kg.	Final mass kg.	Time seconds	Press. dif. mm. Hg.
15.5	16.2	38.30	478.35	291.017	40.65
15.8	16.7	36.80	478.10	246.705	57.05
15.7	16.9	37.15	474.25	206.209	80.15
15.5	17.1	36.40	467.85	185.865	95.55
15.8	17.2	37.70	476.50	160.927	131.90
15.9	17.2	37.90	478.95	143.977	167.60
15.8	17.2	37.60	475.80	133.820	191.35
15.8	17.3	37.90	480.30	124.411	225.15
15.8	17.4	37.05	476.80	115.068	260.30
15.9	17.4	38.55	479.40	109.304	290.10
15.9	17.4	38.10	468.10	101.911	318.80
15.7	17.4	37.55	467.70	96.732	352.80
15.7	17.4	37.40	477.45	95.099	374.15
16.0	17.4	38.65	467.65	90.708	399.20
16.1	17.5	39.30	473.60	90.810	408.80
16.0	17.5	39.45	466.20	88.057	419.35
16.9	17.5	39.20	469.85	85.612	452.10
15.0	15.4	36.20	470.00	84.570	469.75
15.3	15.7	37.60	472.45	96.398	363.50
15.5	15.9	37.80	466.05	116.961	239.00
15.6	15.9	36.30	472.35	142.240	167.85
15.9	18.0	37.30	473.90	159.206	134.45
16.1	18.1	38.35	472.40	188.051	95.15
15.9	18.2	38.20	476.00	303.745	36.90

READINGS FOR PLATE NO. 1

orifice diameter .... 31.55 mm.
edge radius ..... 0.1025 mm.
area ratio 0.099
Atmospheric Pressure ... 760.50 mm Hg.

TABLE NO. 15

Readings for the calibration of the test orifice plate

Air temp. deg. C	Water temp. deg. C	Init. mass kg.	Final mass kg.	Time seconds	Press. dif. mm. Hg.
15.8	16.7	36.35	471.10	275.279	43.95
15.4	16.9	38.30	463.55	220.190	65.45
15.4	16.9	37.75	467.05	188.635	91.20
15.4	17.1	38.60	462.40	159.345	126.20
15.4	17.2	37.70	464.95	140.818	162.60
15.4	17.3	37.65	468.10	131.051	190.60
15.4	17.3	37.95	469.30	123.478	216.45
15.3	17.3	38.55	468.70	115.816	244.95
16.4	17.4	39.40	466.25	109.446	269.60
15.5	17.4	37.85	465.75	102.885	307.10
14.9	15.8	39.50	465.30	103.729	299.55
15.5	16.0	37.70	468.90	99.064	336.35
14.9	16.1	38.15	464.20	95.079	355.80
14.9	16.2	39.35	467.65	92.672	379.35
15.0	16.3	39.35	468.20	88.347	418.65
15.4	16.6	39.35	472.60	85.809	445.85
15.1	16.7	39.30	465.20	81.678	481.85
15.8	16.9	42.10	469.85	79.959	508.10
15.2	16.9	38.90	470.55	80.041	514.30
15.0	17.1	39.70	467.40	94.513	363.15
15.1	17.7	38.40	471.45	119.255	234.60
15.1	17.8	37.85	475.45	138.430	177.45
15.2	17.9	37.75	472.55	185.500	97.65
15.2	17.9	38.10	467.70	104.735	299.00

READINGS FOR PLATE NO. 1

orifice diameter .... 31.55 mm.
edge radius ..... 0.2133 mm.
area ratio 0.099
Atmospheric Pressure ... 754.40 mm. Hg

TABLE NO. 16

Readings for the calibration of the test orifice plate

Air temp. deg. C	Water temp. deg. C	Init. mass kg.	Final mass kg.	Time seconds	Press. dif. mm. Hg.
15.3	17.0	38.80	464.60	297.496	35.10
15.3	17.3	37.20	463.05	203.515	74.65
15.5	17.4	37.15	471.80	189.630	89.65
14.1	15.3	36.20	465.65	168.847	110.40
14.1	15.5	38.20	470.55	152.591	136.85
14.1	15.7	38.25	472.15	140.158	164.25
14.3	15.8	38.10	471.50	128.865	193.85
14.2	16.2	38.50	468.95	118.153	227.40
14.2	16.9	38.25	455.35	109.146	251.25
14.3	17.1	38.60	475.10	108.003	280.25
14.4	17.1	38.40	469.85	100.996	313.40
13.5	15.0	36.20	459.60	95.607	336.30
13.7	15.4	37.15	462.05	94.396	348.60
13.9	15.8	37.25	474.80	95.362	360.90
13.9	16.0	39.45	472.05	91.781	380.45
14.1	16.2	38.15	470.30	89.927	396.65
14.1	16.4	38.60	484.00	91.475	406.50
13.9	15.5	36.10	461.50	84.684	433.45
14.1	15.8	37.95	468.60	84.388	447.40
14.3	16.0	38.50	465.60	82.153	464.45
14.4	16.3	38.10	470.65	82.191	476.60
14.6	16.5	38.60	464.00	79.792	488.90
14.7	16.8	37.80	462.65	79.425	492.55
14.7	16.9	37.80	462.00	86.945	409.20

READINGS FOR PLATE NO. 1

orifice diameter .... 31.55 mm.
edge radius ..... 0.2867 mm.
area ratio 0.099
Atmospheric Pressure ... 759.20 mm. Hg

TABLE NO. 17

Readings for the calibration of the test orifice plate

Air temp. deg. C	Water temp. deg. C	Init. mass kg.	Final mass kg.	Time seconds	Press. dif. mm. Hg.
15.5	18.9	36.00	472.30	265.538	45.25
15.5	19.1	37.00	466.60	208.223	71.65
15.5	19.2	37.15	465.90	182.626	93.30
15.3	19.3	36.80	470.20	161.323	122.40
14.8	16.6	36.00	466.40	144.619	150.05
15.3	16.8	36.45	462.45	134.706	169.55
15.7	17.1	37.65	469.35	130.274	186.65
15.7	17.7	37.85	463.90	123.591	202.00
15.9	18.0	37.65	463.10	118.990	217.20
16.2	18.3	37.20	472.20	115.826	239.75
16.5	18.7	37.90	467.50	110.902	255.45
16.5	18.8	38.50	466.95	104.484	286.75
16.3	19.0	37.60	469.10	101.633	307.15
16.4	19.7	36.50	467.15	99.048	322.80
16.5	19.8	37.50	465.60	94.551	349.65
16.8	20.0	76.30	946.95	190.603	355.90
16.8	20.2	39.55	453.20	89.025	367.95
16.8	20.2	39.05	460.80	88.263	388.75
16.9	20.3	38.40	453.65	85.440	402.60
16.9	20.4	36.85	463.35	86.023	419.00
16.9	20.4	38.90	456.45	83.154	429.50
16.9	20.4	38.75	456.05	81.176	450.10
16.9	20.4	38.80	461.70	80.387	471.50
16.9	20.4	39.30	456.50	77.468	494.20

NOTE: For the last twenty readings the atmospheric pressure was 764.55 mm Hg.

READINGS FOR PLATE NO. 1

orifice diameter .... 31.55 mm.
edge radius ..... 0.4100 mm.
area ratio 0.099
Atmospheric pressure .... 754.90 mm. Hg.

TABLE NO. 18

Readings for the calibration of the test orifice plate

Air temp. deg. C	Water temp. deg. C	Init. mass kg.	Final mass kg.	Time seconds	Press. dif. mm. Hg.
17.4	19.3	36.25	465.80	278.632	39.00
18.0	20.7	39.60	461.95	203.356	73.90
18.4	21.0	39.10	461.55	167.271	105.50
18.3	21.4	39.40	467.25	153.721	128.15
18.5	21.9	39.80	449.85	133.164	157.30
18.7	22.2	39.60	470.75	131.758	177.60
18.8	22.9	36.75	470.20	123.773	203.80
18.9	23.1	38.90	466.20	115.386	227.60
18.9	23.2	38.90	466.45	109.208	254.80
19.1	23.4	38.85	470.05	104.726	282.35
18.9	23.5	39.05	463.65	98.437	309.70
18.9	23.6	38.95	462.95	94.644	333.80
19.0	23.7	38.40	466.50	93.191	351.45
19.0	23.8	37.00	466.40	90.878	371.45
19.0	23.8	39.25	465.85	86.894	401.40
19.0	23.8	38.60	464.55	84.093	427.60
17.3	18.1	36.05	469.60	81.103	475.80
17.4	18.2	37.85	462.70	77.873	495.05
17.5	18.2	38.50	462.25	77.000	505.05
17.5	18.2	38.55	463.00	80.227	466.15
17.5	18.2	38.60	451.70	83.341	408.80
17.5	18.2	38.05	453.50	100.905	281.75
17.6	18.3	37.20	467.80	128.361	186.55
17.6	18.4	37.50	461.30	189.349	82.75

READINGS FOR PLATE NO. 2

orifice diameter ..... 44.75 mm.
edge radius ..... 0.02 mm.
area ratio 0.198
Atmospheric Pressure ..... 747.50 mm Hg.

TABLE NO. 19

Readings for the calibration of the test orifice plate

Air temp. deg. C	Water temp. deg. C	Init. mass kg.	Final mass kg.	Time seconds	Press. dif. mm. Hg.
16.9	16.1	37.20	470.90	150.591	35.15
17.2	16.4	37.35	470.55	123.346	52.85
17.4	16.7	40.15	469.50	103.270	74.20
17,5	17.1	38.15	464.00	91.023	94.35
17.5	17.4	37.70	465.50	80.834	120.85
17.7	17.7	37.55	469.80	74.254	146.55
17.7	18.1	37.10	471.75	66.214	186.60
17.7	18.8	36.55	471.15	62.517	209.45
17.7	18.9	37.50	477.00	58.912	241.60
17.7	19.0	37.55	465.55	54.179	270.80
17.7	19.1	37.35	466.35	52.240	293.25
17.5	19.3	36.80	470.95	51.198	312.45
17.7	19.3	78.65	932.75	97.653	332.05
17.7	19.3	80.15	935.15	95.520	348.75
17.7	19.4	80.25	940.50	93.357	369.05
17.7	19.5	77.40	934.30	91.668	380.15
16.4	16.0	76.05	930.10	90.104	390.35
16.5	16.6	75.75	930.25	88.743	402.85
16.8	16.8	78.45	937.95	86.314	431.30
16.9	17.4	76.20	930.60	84.515	444.65
16.9	17.5	78.90	917.05	80.604	470.25
16.9	17.5	38.60	463.85	51.486	296.85
16.8	17.6	37.15	466.00	66.103	182.50
16.5	17.4	37.15	466.40	96.661	85.40

READINGS FOR PLATE NO. 2

orifice diameter ..... 44.75 mm.
edge radius ..... 0.26 mm.
area ratio 0.198
Atmospheric Pressure ..... 759.45 mm Hg.

TABLE NO. 20

Readings for the calibration of the test orifice plate

Air temp. deg. C	Water temp. deg. C	Init. mass kg.	Final mass kg.	Time seconds	Press. dif. mm. Hg.
15.3	18.0	36.05	474.85	157.901	32.30
15.5	18.3	38.45	464.60	134.864	41.20
15.7	18.5	38.55	467.75	121.968	51.05
15.7	18.7	37.40	465+85	111.126	61.65
15.8	18.9	38.75	469.15	102.663	72.80
15.8	18.0	37.45	468.15	95.689	83.95
15.8	19.1	37.35	470.00	87.767	101.05
15.9	19.1	37.25	467.05	81.904	114.70
15.9	19.2	37.35	464.35	75.386	133.90
15.9	19.2	37.35	458.95	70.035	151.20
15.7	16.2	36.10	464.40	65.588	177.90
15.7	17.0	36.75	469.60	63.209	195.45
15.6	17.2	37.05	461.70	59.029	215.15
15.5	17.5	37.00	463.05	56.787	235.50
15.5	17.7	37.15	460.00	54.151	255.70
15.7	18.2	36.55	462.30	53.034	269.80
15.8	18.3	37.10	458.90	51.383	282.35
15.9	18.5	75.15	908.10	97.864	303.60
15.9	18.7	76.95	918.35	95.379	326.35
16.1	19.1	75.35	930.05	93.491	350.65
16.1	19.2	78.25	908.50	89.417	360.80
16.2	19.3	77.30	916.65	87.314	388.30
16.2	19.4	77.55	919.45	85.320	409.05
16.2	19.4	76.90	907.50	76.634	493.25

READINGS FOR PLATE NO. 2

orifice diameter ..... 44.75 mm.
edge radius ..... 0.40 mm.
area ratio 0.198
Atmospheric Pressure ..... 758.20 mm Hg.

TABLE NO. 21

Readings for the calibration of the test orifice plate

Air temp. deg. C	Water temp. deg. C	Init. mass kg.	Final mass kg.	Time seconds	Press. dif. mm. Hg.
17.9	20.9	20.65	472.35	133.685	45.45
17.9	21.0	36.75	464.45	114.982	55.35
17.9	21.0	37.25	465.80	103.982	68.10
17.9	21.0	37.20	465.95	97.685	77.45
17.9	21.0	37.25	465.90	90.402	90.30
17.9	21.0	37.20	459.05	85.000	99.25
17.9	21.0	37.25	462.25	80.434	112.40
17.5	18.7	36.10	469.95	75.849	132.20
17.5	19.4	39.65	457.40	67.487	154.45
17.6	19.7	39.05	460.90	64.951	170.40
17.8	19.9	39.60	455.80	59.981	195.40
17.8	20.1	37.80	462.75	58.573	211.40
17.9	20.4	39.40	449.40	54.573	228.90
17.9	20.7	39.40	452.35	53.108	245.35
17.9	20.9	30.65	448.65	50.930	262.60
17.9	21.1	39.60	452.75	50.077	275.80
17.9	21.8	75.60	903.15	95.093	308.15
17.9	21.9	79.60	919.80	93.686	326.65
18.0	22.0	78.95	921.70	91.585	344.05
18.0	22.1	79.25	905.40	86.731	368.60
18.0	22.2	76.50	921.25	86.334	389.55
18.0	22.2	78.40	892.15	79.016	430.65
17.9	22.2	79.00	900.40	78.596	446.15
17.9	22.2	79.30	921.30	78.564	466.10

READINGS FOR PLATE NO. 3

orifice diameter ..... 54.61 mm.
edge radius ..... 0.02 mm.
area ratio 0.295
Atmospheric Pressure ..... 761.50 mm. Hg.

TABLE NO. 22

Readings for the calibration of the test orifice plate

Air temp. deg. C	Water temp. deg. C	Init. mass kg.	Final mass kg.	Time seconds	Press. dif. mm. Hg.
19.8	21.5	36.90	449.15	39.190	203.30
19.8	22.0	38.65	434.50	32.706	270.05
19.8	22.1	39.50	439.55	31.879	289.70
19.8	22.2	36.85	450.35	32.328	301.10
20.1	20.7	35.95	464.95	99.536	33.65
20.1	21.3	36.85	454.60	59.778	88.75
20.1	22.1	36.95	455.30	58.723	92.20
20.1	23.2	36.40	461.30	46.718	151.65
20.1	23.4	37.15	454.95	58.137	94.40
20.1	23.7	38.65	450.10	39.057	203.90
20.1	23.8	75.85	886.25	63.430	301.05
20.1	23.9	74.30	883.75	70.196	244.95
17.3	18.5	38.70	451.75	102.275	29.40
17.5	13.9	38.70	434.90	64.857	68.10
17.7	19.3	77.25	887.90	89.037	151.15
17.7	19.8	74.95	871.80	75.372	205.15
17.7	19.9	80.85	854.25	60.250	303.40
18.0	20.1	77.85	883.00	71.031	236.50
16.7	18.3	38.20	443.60	73.931	54.70
16.9	19.0	36.65	443.65	58.947	86.70
17.0	19.1	37.00	444.30	50.618	118.05
17.7	19.2	77.55	891.75	84.376	169.85
17.8	19.3	78.05	909.10	74.961	225.30
17.1	19.5	76.50	874.10	62.459	299.95

NOTE: For last six readings the atmospheric pressure was equal to 756.50 mm Hg.

READINGS FOR PLATE NO. 3

orifice diameter ..... 54.61 mm.

edge radius ..... 0.03 mm.

area ratio 0.295

Atmospheric Pressure ..... 750.80 mm Hg.

TABLE NO. 23

Readings for the calibration of the test orifice plate

Air temp. deg. C	Water temp. deg. C	Init. mass kg.	Final mass kg.	Time seconds	Press. dif. mm. Hg.
15.3	16.9	36.60	469.25	104.702	31.05
15.5	17.1	37.60	468.55	96.484	36.05
15.4	18.1	36.35	471.60	89.827	42.35
15.5	18.2	37.80	474.35	82.687	50.35
15.7	18.3	37.90	468.90	75.198	59.50
15.8	18.4	37.65	473.25	70.934	68.30
15.8	18.4	39.70	475.25	64.135	83.65
16.0	18.5	39.95	477.20	61.399	91.80
15.8	18.5	40.10	473.65	58.688	99.20
15.9	18.6	38.70	465.95	54.217	112.90
15.9	18.6	37.75	462.15	50.754	127.15
16.0	18.6	38.00	466.85	49.703	135.15
15.9	18.6	37.80	459.65	46.828	147.35
16.1	18.7	78.00	929.00	92.091	155.35
15.1	16.1	77.25	946.70	91.147	165.30
15.5	16.4	76.05	944.20	88.301	175.90
15.8	16.8	78.00	926.20	83.693	186.90
15.8	17.0	77.75	946.05	83.078	199.00
15.4	14.9	75.30	945.20	84.279	194.50
15.7	15.1	77.40	940.55	75.835	236.40
15.5	15.6	79.40	921.55	71.399	253.95
16.1	15.8	78.80	902.50	68.488	263.55
15.9	15.9	78.95	923.95	69.528	269.65
16.1	16.0	79.20	924.80	69.211	272.15

READINGS FOR PLATE NO. 3

orifice diameter ..... 54.61 mm.
edge radius ..... 0.10 mm.
area ratio 0.295
Atmospheric Pressure ..... 763.50 mm Hg.

TABLE NO. 24

Readings for the calibration of the test orifice plate

Air temp. deg. C	Water temp. deg. C	Init. mass kg.	Final mass kg.	Time seconds	Press. dif. mm. Hg.
14.9	15.1	36.50	470.50	121.115	22.90
15.0	15.2	37.80	467.30	110.397	26.70
14.0	14.2	36.50	472.80	106.267	29.80
14.8	14.8	38.90	473.30	98.671	34.15
15.0	15.0	37.55	473.60	93.188	38.55
14.8	18.2	37.60	475.25	87.369	44.40
15.0	15.9	37.50	469.55	78.851	53.05
15.0	16.0	37.90	468.85	74.342	59.20
15.0	16.8	36.45	477.65	71.581	67.55
15.0	16.9	37.40	473.05	67.436	74.10
15.0	17.0	37.85	467.40	62.793	83.50
15.0	17.0	37.75	471.10	60.305	92.55
15.5	17.1	39.15	468.25	58.039	98.00
15.0	17.1	36.75	454.55	54.207	106.45
14.9	17.1	37.90	469.85	54.175	113.80
15.0	17.1	37.50	468.05	51.914	123.20
15.2	17.2	37.25	464.40	49.962	131.10
15.3	17.2	76.65	923.20	92.475	150.80
15.5	17.2	79.40	918.65	86.574	168.90
17.3	14.7	78.90	907.95	82.519	181.95
15.3	15.4	78.00	921.95	80.704	196.60
13.5	14.2	77.45	912.25	75.677	219.65
15.5	14.7	75.95	928.10	73.981	239.50
16.1	16.1	76.60	887.40	68.531	252.70

READINGS FOR PLATE NO. 3

orifice diameter ..... 54.61 mm.
edge radius ..... 0.22 mm.
area ratio 0.295
Atmospheric Pressure ..... 755.90 mm Hg.

TABLE NO. 25

Readings for the calibration of the test orifice plate

Air temp. deg. C	Water temp. deg. C	Init. mass kg.	Final mass kg.	Time seconds	Press. dif. mm. Hg.
15.7	17.8	39.30	466.70	105.698	28.55
15.7	17.9	38.40	475.05	101.004	32.50
14.7	15.5	38.55	472.70	93.380	37.85
15.0	16.1	40.35	466.35	86.188	42.55
15.1	16.3	38.35	463.75	79.994	49.35
15.3	16.5	38.05	462.35	76.070	54.10
15.3	16.6	37.05	467.05	73.156	60.15
15.3	16.5	37.15	460.40	68.002	67.75
15.3	16.1	38.85	463.75	64.742	75.80
15.3	16.2	38.40	457.40	61.078	82.75
15.3	16.4.	38.55	462.90	58.757	91.80
15.2	16.6	38.70	460.25	56.287	98.40
15.4	16.9	38.00	454.60	53.511	106.75
15.4	16.9	37.35	454.90	52.096	113.40
15.4	17.0	37.35	458.55	51.111	120.00
14.8	15.5	36.15	452.50	48.647	129.75
14.9	15.7	76.70	913.30	93.382	142.55
15.4	15.9	77.80	916.35	90.263	153.40
15.4	17.2	75.45	923.70	88.562	162.55
15.8	17.4	77.40	930.25	85.954	174.20
15.9	17.5	79.00	907.60	79.913	190.80
15.9	17.7	77.30	924.50	79.581	200.85
15.9	17.8	77.00	909.10	71.540	240.25
15.9	18.0	78.35	924.20	71.075	251.85

READINGS FOR PLATE NO. 3

orifice diameter ..... 54.61 mm.
edge radius ..... 0.27 mm.
area ratio 0.295
Atmospheric Pressure ..... 759.20 mm.

TABLE NO. 26

Readings for the calibration of the test orifice plate

Air temp. deg. C	Water temp. deg. C	Init. mass kg.	Final mass kg.	Time seconds	Press. dif. mm. Hg.
15.1	16.1	39.00	462.20	107.565	26.90
15.1	16.8	37.65	461.55	98.423	32.10
14.8	16.9	39.10	467.55	93.173	36.50
14.8	17.1	39.15	461.15	85.169	42.40
14.9	17.2	37.25	455.40	79.027	48.35
13.3	15.6	38.15	450.20	72.378	56.25
19.6	17.9	35.95	468.40	82.954	47.00
19.6	18.1	37.00	457.50	71.042	61.00
19.8	18.4	37.25	459.15	66.784	69.55
19.8	18.7	37.15	465.00	64.433	76.95
19.4	19.4	36.50	463.40	60.979	85.60
19.4	19.6	37.10	462.70	56.999	97.80
19.6	19.7	36.45	462.40	54.299	107.50
19.7	19.9	37.25	449.50	50.653	116.40
19.1	20.0	37.40	461.60	50.441	124.40
17.9	18.9	36.10	458.05	48.009	136.20
18.2	19.5	74.90	936.45	95.075	144.45
18.3	19.8	76.50	906.90	87.807	157.45
18.3	20.1	76.70	894.25	83.136	169.95
18.5	20.3	77.40	910.25	82.139	180.90
18.5	20.6	76.80	906.75	79.866	190.50
18.6	21.3	74.40	899.30	77.739	198.25
18.7	21.5	76.55	892.20	70.739	235.10
18.7	21.6	76.85	909.00	70.000	249.75

READINGS FOR PLATE NO. 3

orifice diameter ..... 54.61 mm.

edge radius ..... 0.30 mm.

area ratio 0.295

Atmospheric Pressure ..... 757.95 mm Hg.

TABLE NO. 27

Readings for the calibration of the test orifice plate

Air temp. deg. C	Water temp. deg. C	Init. mass kg.	Final mass kg.	Time seconds	Press. dif. mm. Hg.
17.5	19.6	36.10	472.35	113.516	25.45
17.7	19.8	36.85	472.15	99.724	32.65
19.9	20.2	37.35	472.00	92.066	38.15
17.8	20.3	37.70	468.10	83.203	45.80
17.8	20.3	37.70	471.20	77.305	53.90
17.3	19.4	38.30	462.70	59.565	87.45
17.5	19.9	36.55	448.15	54.743	97.75
17.5	21.0	36.45	465.65	52.791	114.30
18.1	21.5	36.50	453.90	49.176	124.65
17.7	21.6	37.55	463.25	48.644	132.50
16.2	17.4	75.25	913.25	90.246	149.25
16.4	17.6	76.95	918.05	86.244	164.90
16.4	18.0	76.45	917.10	83.396	176.30
16.6	18.3	77.70	931.45	81.593	190.25
16.7	18.6	79.15	915.60	77.853	200.45
16.9	18.2	75.10	909.75	70.588	243.05
16.9	18.6	77.35	890.70	67.298	254.20
16.9	18.6	75.25	885.85	66.511	259.30
17.1	18.6	37.10	461.30	53.813	108.10
17.3	20.5	36.60	469.00	60.604	88.40
17.5	20.7	37.35	461.55	56.954	96.15
17.5	20.9	37.25	466.65	63.458	79.25
17.5	21.9	36.45	465.85	70.417	64.25
17.1	19.4	37.60	455.35	50.721	117.95

NOTE: For last nineteen readings the atmospheric pressure was equal to 755.40 mm Hg.

READINGS FOR PLATE NO. 4

orifice diameter ..... 63.00 mm.

edge radius ..... 0.02 mm.

area ratio 0.393

Atmospheric Pressure ..... 758.00 mm Hg.

TABLE NO. 28

Readings for the calibration of the test orifice plate

Air temp. deg. C	Water temp. deg. C	Init. mass kg.	Final mass kg.	Time seconds	Press. dif. mm. Hg.
17.0	17.0	36.35	464.25	92.097	19.95
17.0	17.4	37.00	470.00	63.441	43.60
17.1	18.7	36.70	464.35	52.441	63.45
17.1	18.8	37.25	452.45	45.105	81.15
17.3	19.2	37.05	446.25	37.575	113.25
17.3	19.3	76.80	918.15	71.331	133.25
17.3	19.4	77.45	915.10	64.684	160.35
16.1	17.3	38.85	465.45	78.520	27.45
16.5	17.7	36.75	453.20	50.585	64.60
16.7	18.6	76.05	914.45	84.372	94.10
16.5	17.8	85.35	928.75	84.094	96.00
16.9	19.0	74.75	905.85	72.832	124.35
16.9	19.3	78.65	911.10	69.284	137.85
18.4	28.6	40.80	470.45	86.183	23.05
18.8	19.0	36.95	457.65	57.373	50.65
18.9	19.2	78.30	932.35	63.822	171.15
18.3	18.9	36.15	465.75	110.677	13.90
18.5	19.5	36.50	461.85	55.518	55.20
18.7	19.8	37.45	454.85	47.397	74.05
18.9	19.9	77.25	926.20	90.045	85.00
19.0	20.1	79.15	915.20	80.273	103.45
19.1	20.3	77.25	902.95	72.996	122.20
19.3	20.5	75.95	904.80	64.366	158.35
19.1	20.8	38.35	467.40	72.817	32.65

READINGS FOR PLATE NO. 4

orifice diameter ..... 63.00 mm.
edge radius ..... 0.18 mm.
area ratio 0.393
Atmospheric Pressure..... 754.40 mm Hg.

TABLE NO. 29

Readings for the calibration of the test orifice plate

Air temp. deg. C	Water temp. deg. C	Init. mass kg.	Final mass kg.	Time seconds	Press. dif. mm. Hg.
16.6	18.0	36.00	474.65	112.024	13.80
16.6	18.2	37.15	459.05	98.549	16.53
16.7	18.4	37.60	463.00	93.326	18.80
16.8	18.6	38.30	463.30	87.676	21.15
16.9	18.8	38.10	467.60	83.511	23.90
16.9	18.9	38.25	467.90	78.990	26.85
16.9	19.1	37.25	465.55	73.732	30.65
17.3	20.0	37.65	464.20	67.845	35.85
17.4	20.0	37.50	466.85	63.889	41.25
17.3	20.2	36.60	458.35	58.565	47.30
17.3	20.2	37.10	454.30	54.682	53.40
17.3	20.3	37.10	457.40	52.682	58.35
17.3	20.3	37.30	460.40	50.611	64.10
17.3	20.3	37.40	451.25	47.780	69.00
17.3	20.4	37.35	459.95	46.638	75.90
15.7	17.2	36.10	464.50	61.268	44.80
15.9	17.4	74.05	896.05	84.861	86.50
15.9	17.8	75.50	906.00	81.955	94.70
15.9	18.0	75.90	907.95	78.956	102.45
15.9	18.2	76.90	901.75	75.331	110.75
15.9	19.0	74.45	896.75	73.239	116.60
15.9	19.3	76.40	887.45	65.696	141.00
15.9	19.4	76.65	893.60	67.771	134.70
15.9	19.5	75.15	891.65	63.574	152.60

READINGS FOR PLATE NO. 4

orifice diameter ..... 63.00 mm.
edge radius ..... 0.23 mm.
area ratio 0.393
Atmospheric Pressure ..... 755.40 mm Hg.

TABLE NO. 30

Readings for the calibration of the test orifice plate

Air temp. deg. C	Water temp. deg. C	Init. mass kg.	Final mass kg.	Time seconds	Press. dif. mm. Hg.
15.9	17.8	36.35	469.65	106.774	14.80
15.9	17.9	37.40	470.95	99.913	16.85
15.9	18.0	37.55	466.70	89.784	20.30
16.1	18.1	37.75	473.30	85.742	23.00
16.1	18.1	37.85	467.90	78.976	26.60
16.1	18.2	37.70	461.70	72.904	30.25
14.5	16.0	36.15	465.45	67.456	36.30
14.8	16.5	36.85	464.90	63.128	41.10
14.9	16.8	38.30	462.75	60.775	43.65
14.9	17.0	37.05	461.30	58.593	47.10
15.0	17.2	37.30	460.20	56.196	50.90
15.1	17.4	38.25	453.85	53.686	54.00
15.3	17.5	38.50	464.00	53.176	57.80
15.3	17.8	36.80	455.05	50.803	61.00
15.2	17.8	37.35	452.15	48.107	67.20
15.3	18.0	38.20	457.60	47.416	70.55
15.1	18.1	75.95	889.60	88.974	75.75
15.8	17.5	73.40	893.10	82.710	89.55
16.0	18.2	75.35	898.65	81.502	93.10
16.0	18.5	75.00	901.70	78.661	100.55
15.3	17.4	73.70	905.05	76.933	106.45
15.6	17.9	76.15	883.80	71.740	115.55
15.7	18.4	75.65	890.80	65.985	139.35
15.7	18.7	76.75	879.55	62.861	148.65

READINGS FOR PLATE NO. 4

orifice diameter ..... 63.00 mm.
edge radius ..... 0.37 mm.
area ratio 0.393
Atmospheric Pressure..... 757.95 mm Hg.

TABLE NO. 31

Readings for the calibration of the test orifice plate

Air temp. deg. C	Water temp. deg. C	Init. mass kg.	Final mass kg.	Time seconds	Press. dif. mm. Hg.
16.3	18.4	36.05	471.90	109.270	14.00
16.3	18.6	37.45	466.70	99.723	16.05
16.3	18.8	37.55	468.90	92.437	18.90
16.5	19.2	37.80	469.15	85.707	22.00
16.5	19.2	37.60	466.25	78.114	26.00
16.6	19.5	38.35	459.30	72.253	29.35
16.6	19.5	37.95	467.40	69.072	33.35
16.7	19.6	37.25	458.85	64.539	37.00
16.7	19.7	37.25	456.30	61.935	39.85
16.9	18.2	39.50	462.30	58.697	45.45
16.9	18.8	36.60	459.45	56.104	49.85
16.9	19.0	37.20	455.40	52.804	55.15
17.1	19.2	37.75	461.40	51.064	60.45
17.1	19.4	37.80	455.65	49.050	63.90
17.1	19.5	38.00	457.15	47.712	67.95
17.1	19.6	39.60	446.60	45.299	71.25
17.1	19.8	78.25	912.90	88.058	79.45
17.4	20.2	76.15	890.85	82.175	87.05
17.5	20.4	78.25	897.60	79.399	94.35
17.5	20.5	79.25	898.30	76.460	101.85
17.5	20.5	76.50	901.65	74.488	109.00
17.9	19.5	74.00	917.25	70.362	127.50
17.9	19.8	76.10	890.45	66.530	133.25
17.9	20.3	76.10	889.80	64.397	142.10

NOTE: For last fifteen readings the atmospheric pressure was equal to 756.90 mm Hg.

READINGS FOR PLATE NO. 5

orifice diameter ..... 71.00 mm.
edge radius ..... 0.01 mm.
area ratio 0.499
Atmospheric Pressure ..... 751.65 mm Hg.

TABLE NO. 32

Readings for the calibration of the test orifice plate

Air temp. deg. C	Water temp. deg. C	Init. mass kg.	Final mass kg.	Time seconds	Press. dif. mm. Hg.
22.9	26.2	36.65	475.15	83.669	w 179.25
22.9	26.2	39.70	472.20	168.627	w 43.25
22.9	26.2	39.75	473.55	126.099	w 77.00
22.9	26.2	39.55	475.20	108.094	w 106.50
22.8	26.2	37.70	469.60	92.665	w 140.50
22.8	26.2	39.60	469.10	74.673	w 215.75
22.8	26.2	39.35	468.15	68.113	w 260.00
22.8	26.2	40.00	471.00	64.190	w 295.75
22.8	26.2	39.65	463.55	59.454	w 333.00
22.8	26.2	39.65	465.80	56.123	w 378.25
22.8	26.2	39.65	460.45	52.870	w 415.25
22.8	26.2	39.35	468.80	51.776	w 451.00
22.8	26.2	39.30	459.45	48.795	w 486.50
22.8	26.2	39.10	460.50	47.288	w 521.00
22.7	26.2	38.60	466.30	46.736	w 550.25
22.7	26.2	38.65	452.10	43.894	46.35
21.8	23.4	75.40	924.70	88.078	48.50
22.2	23.7	75.35	919.55	85.612	50.90
22.6	24.3	79.40	917.35	81.940	54.50
22.6	24.6	79.65	917.35	79.505	57.75
22.6	24.8	79.35	919.15	77.184	61.65
22.8	25.0	79.85	916.80	75.155	64.35
22.8	25.3	79.65	915.95	73.594	66.95
22.8	25.5	79.80	922.20	72.938	69.80

w: pressure difference in millimetres of water

READINGS FOR PLATE NO. 5

orifice diameter ..... 71.00 mm.
edge radius ..... 0.15 mm.
area ratio 0.499
Atmospheric Pressure .... 755.80 mm Hg.

TABLE NO. 33

Readings for the calibration of the test orifice plate

Air temp. deg. C	Water temp. deg. C	Init. mass kg.	Final mass kg.	Time seconds	Press. dif. mm. Hg.
21.2	24.0	36.75	472.85	167.224	42.50
21.2	24.0	39.60	468.20	125.318	72.50
21.4	24.1	39.65	475.70	109.744	98.25
21.4	24.0	40.10	470.90	94.610	128.75
21.4	24.0	39.80	470.55	83.286	166.00
21.4	24.0	39.95	470.40	74.856	205.75
21.4	24.0	38.75	476.40	69.990	244.00
21.4	24.0	39.95	470.90	63.983	282.25
21.4	24.0	39.70	466.20	59.666	318.50
20.7	21.6	36.30	467.10	56.945	357.25
20.8	21.7	39.20	463.80	53.706	390.50
20.9	21.8	38.95	464.15	51.506	425.50
21.2	22.0	39.15	464.70	49.679	458.25
21.2	22.1	39.00	461.30	47.750	489.50
21.0	22.5	36.95	464.95	46.957	519.75
21.0	22.5	39.10	463.40	45.554	540.75
20.5	22.6	79.95	926.15	88.584	45.55
20.5	22.8	76.75	912.20	83.525	49.80
20.7	23.1	78.75	925.60	81.858	53.00
20.7	23.2	79.55	923.55	79.484	55.75
20.7	23.3	80.05	916.20	77.028	58.35
20.7	23.4	79.75	909.85	74.755	61.05
20.9	23.7	76.85	917.95	73.626	64.75
20.8	23.8	79.65	912.05	72.024	66.40

READINGS FOR PLATE NO. 5

orifice diameter ..... 71.00 mm.

edge radius ..... 0.26 mm.

area ratio 0.499

Atmospheric Pressure ..... 754.30 mm Hg.

TABLE NO. 34

Readings for the calibration of the test orifice plate

Air temp. deg. C	Water temp. deg. C	Init. mass kg.	Final mass kg.	Time seconds	Press. dif. mm. Hg.
23.4	26.4	36.65	473.65	167.024	43.75
23.4	26.5	39.55	471.90	153.788	50.25
23.3	26.7	37.10	474.15	126.479	75.75
23.3	26.7	38.95	472.95	106.975	104.50
23.3	26.7	39.40	468.50	92.725	136.00
20.5	21.8	36.05	475.20	88.504	156.25
21.4	21.8	38.50	473.85	83.767	170.75
21.4	22.0	38.60	463.25	73.759	209.75
21.3	22.6	37.05	467.95	68.511	250.50
21.4	22.9	39.85	464.20	62.661	291.00
21.5	23.0	39.80	459.60	58.505	327.25
21.5	23.1	39.80	466.50	56.163	366.25
20.9	23.2	39.70	469.80	54.095	402.75
21.0	23.3	39.30	461.30	50.983	436.25
21.3	23.4	39.95	454.95	48.522	465.75
21.4	23.5	39.90	458.90	47.278	500.75
21.6	23.6	78.95	925.50	92.935	528.00
20.9	24.3	76.70	884.45	86.288	44.45
20.6	24.4	79.75	922.10	86.035	48.40
20.9	24.4	79.75	940.10	84.716	52.15
20.9	24.5	79.70	923.75	80.612	55.40
20.7	24.5	79.60	920.90	77.912	58.90
20.5	24.5	79.40	930.30	76.490	62.55
20.9	24.5	76.75	914.90	73.198	66.45

READINGS FOR PLATE NO. 5

orifice diameter ..... 71.00 mm.
edge radius ..... 0.37 mm.
area ratio 0.499
Atmospheric Pressure ..... 756.10 mm Hg.

TABLE NO. 35

Readings for the calibration of the test orifice plate

Air temp. deg. C	Water temp. deg. C	Init. mass kg.	Final mass kg.	Time seconds	Press. dif. mm. Hg.
21.0	23.5	36.70	470.00	167.206	w 41.00
21.1	23.5	39.80	476.80	156.209	w 47.75
21.1	23.5	39.60	474.65	125.197	w 74.00
21.1	23.5	39.80	474.25	106.924	w 101.25
21.1	23.5	39.80	474.50	93.934	w 131.25
21.2	23.6	40.10	474.15	82.601	w 169.50
21.2	23.6	39.15	477.60	75.669	w 206.00
21.2	23.6	40.00	469.95	68.032	w 245.50
21.2	23.6	39.40	466.70	63.241	w 281.25
21.2	23.6	39.70	469.00	59.939	w 318.25
21.2	23.6	40.00	461.00	55.267	w 357.75
21.2	23.6	40.15	459.75	52.842	w 388.75
21.2	23.6	39.20	461.10	50.765	w 425.50
21.1	23.6	39.15	458.65	48.511	w 460.50
21.1	23.6	38.60	461.85	47.309	w 493.75
20.9	23.6	37.95	459.10	45.844	w 520.00
20.9	23.6	79.25	925.70	89.560	w 552.50
20.1	20.9	76.00	923.70	85.602	48.20
20.1	21.1	78.50	912.85	81.432	51.60
20.5	21.6	75.05	919.15	79.757	55.10
20.5	21.8	78.85	929.55	78.587	57.35
20.5	21.9	78.20	913.75	75.703	59.75
20.3	21.9	80.35	906.30	72.672	63.35
20.2	21.9	78.85	921.75	72.674	65.95

w: pressure difference in millimetres of water

READINGS FOR PLATE NO. 5

orifice diameter ..... 71.00 mm.
edge radius ..... 0.49 mm.
area ratio 0.499
Atmospheric Pressure ..... 749.05 mm Hg.

TABLE NO. 36

Readings for the calibration of the test orifice plate

Air temp. deg. C	Water temp. deg. C	Init. mass kg.	Final mass kg.	Time seconds	Press. dif. mm. Hg.
20.1	19.7	36.35	472.95	168.082	w 40.25
20.1	19.7	39.55	473.80	156.396	w 45.50
20.2	19.8	40.10	469.75	123.225	w 72.25
20.2	19.9	40.00	473.45	106.775	w 98.25
20.2	20.4	36.65	475.20	95.042	w 126.25
20.2	20.6	38.95	465.15	81.532	w 163.00
20.2	20.6	39.20	467.75	73.952	w 200.00
20.3	20.6	39.75	467.55	67.955	w 236.00
20.3	20.7	39.40	461.45	62.073	w 276.25
20.3	20.8	40.15	469.70	59.604	w 310.25
20.5	20.9	39.70	463.30	55.482	w 348.75
20.5	20.9	38.75	459.65	52.463	w 384.75
20.4	21.2	36.85	466.30	51.382	w 417.25
20.3	21.4	37.20	460.75	48.748	w 450.75
20.4	21.4	38.20	458.30	46.787	w 481.50
20.5	21.4	40.00	470.85	46.698	w 509.00
20.5	21.4	78.10	924.80	89.264	w 538.00
20.5	21.5	77.00	935.10	86.335	46.95
20.1	20.0	76.15	921.60	80.612	52.40
20.2	20.3	79.55	932.25	79.230	55.15
20.3	20.6	79.65	917.95	77.017	56.45
20.3	20.9	79.15	926.45	75.687	59.65
21.0	22.5	76.95	909.00	72.567	62.60
21.1	22.7	79.05	924.95	72.448	64.80

w: pressure difference in millimetres of water

READINGS FOR PLATE NO. 15

orifice diameter ..... 38.86 mm.
plate eccentricity ..... 0.00 mm.
area ratio 0.150
Atmospheric Pressure ..... 755.40 mm Hg.

TABLE NO. 37

Readings for the calibration of the test orifice plate

Air temp. deg.C	Water temp. deg. C	Init.mass kg.	Final mass kg.	Time seconds	Press.dif. mm. Hg.
18.3	18.7	38.90	467.70	254.228	21.50
18.2	19.0	38.95	467.65	194.400	36.90
18.2	19.5	36.65	470.75	172.304	48.35
18.3	19.7	37.45	467.15	146.619	65.65
18.3	20.0	38.75	464.85	131.531	80.30
18.2	20.2	37.70	463.90	119.146	97.95
18.3	20.3	37.15	463.25	108.308	119.20
18.5	20.5	37.30	466.85	100.146	141.60
18.5	20.6	37.20	465.20	92.507	164.75
18.5	20.7	37.35	461.50	84.400	195.05
18.1	19.8	36.25	466.15	76.827	241.75
18.3	20.1	37.30	462.80	72.952	262.20
18.5	20.5	37.40	458.45	68.896	288.40
18.7	20.9	37.10	463.60	67.415	308.65
19.0	21.3	37.20	460.65	64.996	327.40
19.2	22.1	36.60	464.30	63.441	350.45
19.2	22.2	38.95	457.00	60.340	371.05
19.3	22.8	38.15	458.20	59.019	391.70
19.3	22.9	38.50	459.30	57.712	409.85
19.3	23.3	36.75	461.90	56.959	430.50
19.3	23.3	38.85	455.45	54.825	445.90
19.3	23.3	38.50	458.65	54.372	461.25
19.3	23.3	78.05	909.15	105.867	475.60
19.3	23.4	76.95	913.75	103.463	504.75

READINGS FOR PLATE NO. 15

orifice diameter ..... 38.86 mm.

plate eccentricity ... 0.05 mm.

area ratio 0.150

Atmospheric Pressure ..... 755.90 mm Hg.

TABLE NO. 38

Readings for the calibration of the test orifice plate

Air temp. deg. C	Water temp. deg. C	Init. mass kg.	Final mass kg.	Time seconds	Press. dif. mm. Hg.
19.3	23.3	36.85	469.95	234.623	25.65
19.2	23.3	37.80	472.65	198.062	36.60
19.2	23.4	37.85	467.80	171.296	47.65
18.2	20.5	36.40	466.60	157.892	56.60
18.2	20.7	37.70	467.15	138.748	73.00
18.3	20.9	37.75	469.00	124.809	91.45
18.3	21.1	37.45	467.25	113.478	110.25
18.4	21.3	37.55	469.05	100.884	140.80
18.4	21.5	37.80	467.15	93.248	163.35
18.5	22.2	36.65	464.25	87.413	184.10
18.6	22.4	37.60	463.90	80.753	214.40
18.6	22.5	37.60	458.45	75.085	242.35
18.6	22.6	37.65	462.20	71.304	273.40
18.7	22.7	37.65	468.65	69.353	298.30
18.8	23.0	38.65	461.75	64.768	329.95
18.8	23.1	38.90	464.60	62.767	354.75
18.9	23.1	38.50	459.90	60.164	378.95
18.9	23.1	38.60	462.35	58.733	402.05
18.9	23.1	38.60	456.65	56.320	425.70
18.9	23.1	38.40	464.30	56.447	440.15
18.9	23.0	39.15	458.45	54.110	463.75
18.9	23.0	38.75	456.50	52.887	482.50
18.9	23.0	77.45	910.75	103.849	498.25
17.2	18.0	76.10	919.15	103.845	508.35

READINGS FOR PLATE NO. 15

orifice diameter ..... 38.86 mm.
plate eccentricity ... 0.15 mm.
area ratio 0.150
Atmospheric Pressure ..... 753.10 mm Hg.

TABLE NO. 39

Readings for the calibration of the test orifice plate

Air temp. deg. C	Water temp. deg. C	Init. mass kg.	Final mass kg.	Time seconds	Press. dif. mm. Hg.
17.3	18.8	38.90	465.50	257.205	20.70
17.5	18.9	39.00	462.75	197.597	34.85
17.6	18.9	39.00	461.00	169.667	47.00
17.6	19.0	38.85	461.10	148.723	61.25
17.6	19.2	38.30	463.30	132.864	78.40
17.8	19.4	38.95	459.60	117.656	98.20
17.8	19.6	37.85	461.15	110.510	112.75
17.8	20.9	36.60	461.30	101.008	136.05
6.2	18.4	38.70	470.25	95.096	158.45
16.4	18.6	37.55	466.15	86.904	186.80
16.5	18.8	37.50	467.00	82.517	208.25
16.7	19.0	37.70	465.35	77.015	237.65
16.8	19.1	38.50	461.15	71.005	273.20
16.8	19.3	38.95	458.00	67.194	299.85
16.8	19.4	38.90	468.95	66.258	324.90
16.6	19.6	36.70	453.85	62.013	349.45
16.6	19.7	39.10	456.70	59.684	377.70
16.6	19.7	39.80	453.40	57.740	395.50
16.6	19.8	39.85	457.40	56.791	416.75
16.6	19.8	39.90	453.65	55.054	436.20
16.7	19.9	39.80	461.25	54.898	455.05
16.8	20.0	39.70	455.15	53.235	471.00
16.9	20.2	77.45	910.40	104.679	488.60
17.0	20.3	79.45	912.50	103.041	504.25

READINGS FOR PLATE NO. 15

orifice diameter ..... 38.86 mm.
plate eccentricity ..... 0.30 mm.
area ratio 0.150
Atmospheric Pressure ..... 750.30 mm Hg.

TABLE NO. 40

Readings for the calibration of the test orifice plate

Air temp. deg. C	Water temp. deg. C	Init. mass kg.	Final mass kg.	Time seconds	Press. dif. mm. Hg.
16.3	17.8	35.95	470.40	228.949	27.05
16.3	18.1	37.30	469.50	186.692	40.30
16.5	18.2	37.50	471.15	164.147	52.75
16.5	18.3	37.15	462.45	139.921	70.15
15.5	16.5	36.25	467.15	127.834	86.70
15.8	16.7	38.90	464.25	114.839	104.60
15.8	17.4	36.85	461.15	104.763	125.40
15.9	17.6	38.90	457.15	96.050	145.50
16.1	17.9	38.95	464.80	92.352	163.00
16.2	18.1	38.90	463.15	87.029	182.55
16.2	18.3	38.95	464.55	81.929	207.15
16.3	18.4	39.00	463.65	76.622	236.40
16.4	18.6	38.90	458.50	71.040	268.45
16.5	19.5	36.65	458.85	67.756	298.55
16.7	19.8	38.90	464.15	64.896	330.70
16.7	19.8	38.90	461.40	62.163	355.80
16.6	19.9	38.80	457.75	59.589	380.55
16.6	20.0	38.95	460.40	57.927	407.90
16.6	20.1	38.90	455.90	56.381	422.00
16.6	20.2	38.95	459.60	55.604	441.80
16.6	20.3	39.30	455.70	54.064	457.65
16.4	20.5	37.00	454.10	53.051	476.20
16.6	20.5	77.60	923.50	106.396	487.65
16.6	20.6	78.30	915.55	102.951	509.85

READINGS FOR PLATE NO. 15

orifice diameter ..... 38.86 mm.

plate eccentricity .... 0.60 mm.

area ratio 0.150

Atmospheric Pressure ..... 756.40 mm Hg.

TABLE NO. 41

Readings for the calibration of the test orifice plate

Air temp. deg. C	Water temp. deg. C	Init. mass kg.	Final mass kg.	Time seconds	Press. dif. mm. Hg.
16.6	20.6	37.00	468.00	227.558	27.00
16.3	20.6	38.40	470.65	200.076	35.00
16.6	20.6	37.65	471.85	164.630	52.75
16.8	20.6	37.55	467.55	145.687	66.05
16.9	20.6	37.55	468.60	128.339	86.20
16.9	20.6	37.60	468.75	117.086	103.85
16.0	16.9	36.20	467.25	105.564	128.00
16.3	17.4	38.90	469.15	98.572	146.05
16.3	17.7	38.85	466.10	89.854	173.35
16.3	18.0	37.85	469.70	85.040	197.90
16.5	18.4	37.35	469.75	79.821	225.70
16.5	18.7	37.35	469.80	75.289	254.20
16.5	19.0	37.50	465.20	70.561	283.00
16.7	20.1	36.70	464.65	67.170	312.50
16.7	20.3	37.30	461.95	64.029	339.00
16.7	20.3	37.70	465.50	62.192	363.85
16.7	20.3	39.15	461.10	59.695	385.85
16.7	20.6	39.20	467.55	59.025	406.55
16.7	20.6	39.00	463.50	56.875	428.50
16.8	21.0	36.80	457.80	54.895	453.50
16.7	21.1	36.95	464.35	54.537	471.50
16.8	21.1	78.60	923.30	106.490	484.70
16.8	21.1	78.70	929.50	104.674	508.70
16.8	21.1	39.10	465.65	55.214	461.10

READINGS FOR PLATE NO. 15

orifice diameter ..... 38.86 mm.

plate eccentricity ..... 1.20 mm.

area ratio 0.150

Atmospheric Pressure ..... 763.10 mm Hg.

TABLE NO. 42

Readings for the calibration of the test orifice plate

Air temp. deg.C	Water temp. deg. C	Init.mass kg.	Final mass kg.	Time seconds	Press.dif. mm. Hg.
16.8	21.0	36.80	471.30	238.788	25.35
16.8	21.0	37.75	467.80	194.187	37.10
16.8	21.0	38.35	466.45	164.386	51.25
16.8	21.0	37.50	468.85	145.301	66.95
16.8	21.0	37.40	471.25	130.217	84.65
16.8	21.0	37.55	469.55	119.771	99.30
16.7	19.3	36.20	469.45	107.360	124.90
16.9	19.5	38.95	467.75	96.572	151.25
17.1	19.7	38.95	469.10	90.102	174.90
17.1	20.0	38.95	468.65	83.869	201.65
17.1	20.2	38.95	467.70	78.993	225.85
17.5	21.2	36.65	471.00	75.841	252.45
17.5	21.4	37.45	464.15	70.747	279.75
17.5	21.6	37.50	462.00	66.940	310.10
17.8	21.7	38.90	461.30	64.015	335.95
17.8	21.8	38.85	464.90	62.465	358.10
17.8	21.9	38.65	464.10	60.328	383.15
17.9	22.0	38.25	468.45	59.113	406.85
17.9	22.2	37.00	463.95	57.095	430.75
17.9	22.3	39.30	463.50	55.490	450.50
17.9	22.3	39.45	467.55	55.580	458.55
17.9	22.3	38.75	462.75	54.654	463.80
18.1	21.0	75.20	935.75	107.758	491.60
18.1	21.2	77.75	923.50	104.251	507.20

READINGS FOR PLATE NO. 15

orifice diameter ..... 38.86 mm.
plate eccentricity ..... 5.00 mm.
area ratio 0.150
Atmospheric Pressure ..... 754.60 mm Hg.

TABLE NO. 43

Readings for the calibration of the test orifice plate

Air temp. deg. C	Water temp. deg.C	Init. mass kg.	Final mass kg.	Time seconds	Press. dif. mm. Hg.
17.4	19.6	36.10	465.40	234.413	25.30
17.4	19.9	38.80	467.20	198.079	34.95
17.9	21.3	36.60	467.15	161.260	53.80
18.0	21.5	38.90	467.30	139.807	71.55
18.3	21.5	38.90	468.00	128.054	85.30
17.9	20.3	36.25	475.60	118.882	104.15
17.9	21.8	36.50	471.65	105.628	129.25
17.8	20.9	36.25	463.80	95.391	152.85
17.8	20.9	37.05	471.25	87.340	188.95
17.8	20.9	37.20	475.60	82.190	217.80
17.8	20.9	37.30	465.40	76.448	239.70
17.8	20.9	37.25	466.40	72.852	266.00
17.8	20.9	36.90	468.25	70.361	286.10
17.8	20.9	37.35	465.50	67.613	307.40
17.8	20.9	37.30	465.95	66.004	323.85
17.7	18.9	36.15	470.55	66.823	322.55
17.8	19.2	37.70	468.30	63.900	346.05
17.9	19.5	37.70	462.85	61.302	366.15
18.0	20.0	39.40	467.30	60.611	382.25
18.2	20.5	37.65	466.10	59.352	396.12
18.5	21.4	36.75	465.00	58.368	411.35
18.5	21.6	38.95	467.35	57.642	424.31
18.5	21.7	78.85	932.40	109.850	463.00
18.5	21.9	78.35	926.80	104.765	499.35

READINGS FOR PLATE NO. 15

orifice diameter ..... 38.86 mm.
plate eccentricity .... 10.00 mm.
area ratio 0.150
Atmospheric Pressure ..... 756.95 mm Hg.

TABLE NO. 44

Readings for the calibration of the test orifice plate

Air temp. deg. C	Water temp. deg. C	Init. mass kg.	Final mass kg.	Time seconds	Press. dif. mm. Hg.
20.5	22.4	38.85	474.05	261.250	20.65
20.7	22.7	38.95	474.40	217.282	29.70
20.9	22.9	38.80	473.00	173.388	46.10
20.9	23.2	38.95	476.85	151.814	61.45
20.5	21.8	36.25	472.20	133.773	79.05
20.7	21.9	37.50	466.30	117.154	100.35
20.7	22.2	38.90	470.30	108.762	117.45
20.7	22.4	38.85	463.90	96.775	143.90
20.9	22.5	39.00	467.45	89.078	172.25
21.1	22.7	38.90	466.30	84.048	193.20
21.1	22.8	38.90	472.75	80.911	213.65
21.0	23.3	36.70	472.80	75.313	251.15
21.1	23.4	37.25	465.30	71.000	273.30
21.1	23.5	37.65	470.60	69.073	293.10
21.2	23.8	36.80	471.45	67.385	310.25
21.1	23.8	38.30	468.55	64.523	333.95
21.8	23.9	36.65	464.75	61.899	356.85
21.5	23.9	37.45	466.75	60.600	375.40
21.5	23.9	38.60	465.60	59.333	390.00
20.7	22.7	36.25	468.95	59.056	402.70
20.8	22.7	38.95	461.20	56.327	417.80
20.8	22.7	39.10	461.60	55.469	432.60
20.8	22.8	41.40	461.45	53.988	453.55
20.8	22.8	39.90	458.70	51.184	498.25

READINGS FOR PLATE NO. 45

orifice diameter ..... 67.51 mm.
plate eccentricity .... 0.00 mm.
area ratio 0.450
Atmospheric Pressure ... .. 748.90 mm Hg.

TABLE NO. 45

Readings for the calibration of the test orifice plate

Air temp. deg. C	Water temp. deg. C	Init. mass kg.	Final mass kg.	Time seconds	Press. dif. mm. Hg.
21.2	22.3	36.20	476.60	160.104	w 63.00
21.3	22.4	39.20	468.85	126.030	w 96.75
21.3	22.4	37.15	468.20	108.327	w 132.25
21.2	22.6	36.85	462.45	93.479	w 173.50
21.1	22.7	36.95	457.25	82.225	w 218.75
21.0	22.8	37.10	470.45	76.789	w 267.25
20.9	22.8	37.15	467.30	70.692	w 310.50
20.6	22.9	37.20	464.75	65.549	w 359.75
21.1	21.2	36.35	472.75	62.549	w 406.75
21.1	21.4	37.90	463.05	58.053	w 449.25
21.2	21.6	38.90	461.90	55.134	w 492.75
21.3	21.7	39.05	458.15	52.574	w 533.25
21.6	22.8	37.05	461.75	51.259	45.95
21.7	22.9	39.95	464.50	49.691	48.95
21.8	23.1	38.90	464.80	48.392	51.90
21.9	23.3	38.35	463.10	47.577	53.50
21.9	23.5	79.80	929.15	92.396	56.75
22.1	23.7	79.75	910.60	88.661	59.10
22.1	23.8	79.25	930.10	89.167	60.95
21.7	24.5	76.20	918.20	85.160	65.85
21.7	24.7	78.80	910.45	81.895	69.30
21.9	24.7	79.45	916.35	79.607	74.15
21.8	24.9	79.50	916.15	77.914	77.35
21.8	25.0	78.95	910.55	76.550	79.00

w: pressure difference in millimetres of water

READINGS FOR PLATE NO. 45

orifice diameter ..... 67.51 mm.
plate eccentricity .... 3.50 mm.
area ratio 0.450
Atmospheric Pressure ..... 751.25 mm Hg.

TABLE NO. 46

Readings for the calibration of the test orifice plate

Air temp. deg. C	Water temp. deg. C	Init. mass kg.	Final mass kg.	Time seconds	Press. dif. mm. Hg.
21.3	25.1	36.60	472.45	154.994	w 64.60
21.4	25.0	38.80	472.80	128.278	w 93.50
21.4	25.0	39.85	470.35	107.226	w 130.50
21.5	25.0	39.60	469.20	94.125	w 171.50
21.3	25.0	39.10	475.45	84.951	w 216.25
21.3	25.0	39.35	469.50	75.875	w 264.00
21.3	25.0	39.30	470.35	69.869	w 312.50
21.3	25.0	39.65	468.45	64.855	w 361.00
21.3	24.9	39.75	462.60	59.925	w 410.00
21.3	24.9	39.65	463.10	57.407	w 449.25
21.3	24.9	39.60	467.80	55.440	w 493.00
21.4	24.9	39.80	460.95	52.483	w 532.50
21.3	23.4	36.60	466.95	51.854	45.25
21.5	23.5	38.00	466.30	49.998	48.25
21.5	23.7	37.60	465.20	48.550	50.95
21.6	23.9	37.35	461.10	46.945	53.40
21.8	24.0	77.75	922.40	91.545	56.10
21.8	24.2	78.65	914.30	88.814	58.10
21.7	24.3	78.90	919.85	87.250	61.00
21.7	24.4	79.40	931.90	86.290	64.10
21.7	24.8	76.95	905.10	81.039	68.70
21.8	24.8	79.55	909.30	78.754	72.95
21.8	25.0	79.85	901.75	76.497	75.85
22.3	25.0	80.50	902.00	75.587	77.60

w: pressure difference in millimetres of water

READINGS FOR PLATE NO. 45

orifice diameter ..... 67.52 mm.
plate eccentricity ..... 8.00 mm.
area ratio 0.450
Atmospheric Pressure ..... 750.60 mm Hg.

TABLE NO. 47

Readings for the calibration of the test orifice plate

Air temp. deg. C	Water temp. deg. C	Init. mass kg.	Final mass kg.	Time seconds	Press. dif. mm. Hg.
22.1	25.0	39.90	469.70	162.933	w 54.00
21.5	25.4	39.30	398.60	103.747	w 93.75
21.7	25.2	39.55	475.05	108.744	w 126.00
21.6	25.3	39.70	469.65	93.488	w 167.75
21.6	25.2	39.85	469.00	83.267	w 206.00
21.6	25.2	39.50	475.15	134.490	w 82.25
21.6	25.3	40.00	469.50	75.300	w 257.50
21.5	25.3	40.20	465.75	69.000	w 298.25
21.7	23.2	36.45	469.00	65.587	w 342.00
21.8	23.3	39.80	473.10	61.810	w 388.50
21.9	23.4	39.65	466.55	57.957	w 429.50
22.1	23.5	39.85	469.00	55.862	w 467.00
22.1	23.6	39.40	465.55	53.269	w 506.50
22.0	23.8	37.95	453.15	50.020	42.85
22.1	24.1	39.10	459.20	49.002	46.00
22.0	24.3	38.30	459.75	47.984	49.10
22.1	24.4	76.70	915.75	93.202	51.25
21.5	24.9	75.55	920.35	91.608	52.90
21.7	24.9	78.35	908.50	86.728	57.30
21.8	25.0	78.60	916.70	84.784	60.85
21.3	25.1	79.95	906.85	80.913	66.95
21.2	25.1	79.60	916.50	79.408	69.95
21.2	25.1	76.35	916.15	78.086	73.75
21.2	25.1	78.70	910.60	76.234	75.40

w: pressure difference in millimetres of water

READINGS FOR PLATE NO. 45

orifice diameter ..... 67.51 mm.
plate eccentricity ..... 13.00 mm.
area ratio 0.450
Atmospheric Pressure ..... 753.45 mm Hg.

TABLE NO. 48

Readings for the calibration of the test orifice plate

Air temp. deg. C	Water temp. deg. C	Init. mass kg.	Final mass kg.	Time seconds	Press. dif. mm. Hg.
21.2	20.2	35.90	474.75	172.612	w 48.75
21.2	20.5	39.40	473.60	128.474	w 85.75
21.4	20.7	39.65	466.40	107.464	w 119.75
21.4	20.9	39.85	474.50	94.238	w 160.00
21.5	21.0	39.80	471.25	83.391	w 202.00
21.6	21.2	39.45	469.00	75.541	w 244.00
21.7	21.4	39.85	467.35	69.403	w 287.25
21.8	21.5	39.90	471.40	64.780	w 336.00
21.8	21.7	40.30	467.25	60.426	w 377.75
21.8	21.8	39.85	470.00	57.730	w 420.50
21.6	22.9	36.95	463.55	54.785	w 461.50
21.6	23.0	39.90	462.15	52.021	w 501.25
21.7	23.1	39.80	466.75	51.264	w 525.50
21.5	23.2	39.85	452.60	47.377	45.85
21.5	23.2	39.80	469.20	47.862	48.60
21.3	23.3	39.25	458.65	45.562	50.90
21.4	23.3	78.20	907.55	87.931	53.60
21.1	23.8	75.30	924.00	86.494	58.30
20.0	20.5	76.00	919.50	83.109	62.10
20.0	20.8	75.65	919.10	81.012	65.90
20.2	21.5	76.65	915.55	77.887	69.90
20.3	21.7	78.75	905.00	75.252	72.60
20.3	21.9	77.05	912.55	74.952	75.30
20.5	21.9	78.05	918.70	74.519	77.30

w: pressure difference in millimetres of water

READINGS FOR PLATE NO. 45

orifice diameter ..... 67.51 mm.
plate eccentricity ..... 16.31 mm.
area ratio 0.450
Atmospheric Pressure ..... 755.55 mm Hg.

TABLE NO. 49

Readings for the calibration of the test orifice plate

Air temp. deg. C	Water temp. deg. C	Init. mass kg.	Final mass kg.	Time seconds	Press. dif. mm. Hg.
21.8	23.5	37.35	476.75	160.527	w 55.00
22.3	23.6	39.80	476.25	125.649	w 88.75
22,4	24.0	37.95	475.55	106.807	w 123.25
22,4	24.1	39.75	480.25	96.010	w 154.75
22.4	25.2	36.65	476.75	85.432	w 195.25
22.4	25.2	39.85	473.15	75.828	w 240.50
22.5	25.5	37.20	471.85	69.815	w 284.25
22.6	25.6	39.60	470.00	64.491	w 327.50
22.6	25.6	38.70	466.90	60.079	w 373.25
22.4	26.0	36.85	466.10	57.373	w 412.75
22.4	26.0	39.05	459.95	53.693	w 452.50
22.3	26.0	38.50	464.20	52.008	w 494.75
22.4	26.1	37.85	463.65	50.229	w 531.44
21.8	26.0	38.35	459.10	47.923	45.70
21.9	26.0	37.55	458.05	46.588	48.25
22.1	26.0	37.55	457.40	45.380	50.35
21.7	23.6	75.20	927.90	88.200	54.95
21.7	24.1	78.30	917.35	86.040	56.20
22.3	25.1	75.95	921.65	82.691	61.60
22.3	25.3	78.70	922.65	81.519	63.05
22.3	25.4	79.05	910.40	78.532	65.75
22.3	25.6	79.40	917.55	77.163	69.25
22.8	25.9	75.90	908.90	74.758	73.00
22.6	26.0	79.05	913.45	73.626	76.00

w: pressure difference in millimetres of water

READINGS FOR PLATE NO. 55

orifice diameter ..... 74.41 mm.
plate eccentricity ..... 0.00 mm.
area ratio 0.550
Atmospheric Pressure ..... 755.35 mm Hg.

TABLE NO. 50

Readings for the calibration of the test orifice plate

Air temp. deg.C	Water temp. deg.C	Init. mass kg.	Final mass kg.	Time seconds	Press. dif. mm. Hg.
20.4	22.1	36.40	474.50	212.118	w 21.00
20.6	22.3	38.70	473.20	176.260	w 30.00
20.6	22.8	36.40	470.65	148.787	w 42.00
20.7	22.9	39.15	474.15	122.249	w 62.50
20.7	22.9	39.10	468.70	105.870	w 81.50
20.8	23.0	38.60	473.15	94.347	w 105.50
20.7	23.0	38.55	470.05	83.372	w 133.00
20.9	23.1	38.10	470.75	75.046	w 164.75
20.8	23.1	38.60	469.20	68.162	w 198.75
20.7	23.1	38.95	473.80	64.752	w 226.00
20.6	23.1	37.25	464.00	59.125	w 259.00
20.4	23.1	37.85	464.45	56.340	w 286.25
21.3	20.6	36.15	464.95	55.822	w 294.25
21.1	20.8	38.50	466.10	54.195	w 310.75
21.0	21.0	38.60	457.20	50.921	w 337.50
20.9	21.1	37.60	459.65	49.832	w 359.00
21.2	21.4	78.95	927.50	93.227	w 415.25
21.4	22.0	76.90	919.50	88.643	w 452.25
21.4	22.3	78.85	913.85	85.114	w 482.00
21.0	23.3	75.50	928.75	82.252	42.90
21.0	23.5	79.45	885.65	74.547	46.60
21.0	23.6	79.85	906.80	72.936	51.15
21.2	23.6	77.30	904.80	71.176	53.90
20.9	23.6	80.20	891.55	68.865	55.35

w: pressure difference in millimetres of water

READINGS FOR PLATE NO. 55

orifice diameter ..... 74.41 mm.
plate eccentricity ..... 2.00 mm.
area ratio 0.550
Atmospheric Pressure ..... 753.85 mm Hg.

TABLE NO. 51

Readings for the calibration of test orifice plate

Air temp. deg. C	Water temp. deg. C	Init. mass kg.	Final mass kg.	Time seconds	Press. dif. mm. Hg.
20.1	23.6	37.15	466.05	158.853	w 35.25
20.3	23.6	39.60	478.75	126.879	w 58.25
20.5	23.6	39.70	474.30	107.744	w 79.50
20.4	23.5	39.35	475.65	92.990	w 107.75
20.4	23.5	38.70	474.55	83.747	w 132.00
20.7	21.4	38.05	468.70	80.183	w 141.25
20.8	22.1	36.85	470.95	76.776	w 155.75
20.9	24.0	36.50	471.75	71.319	w 182.00
20.9	24.0	38.85	468.85	65.594	w 210.25
20.9	24.0	38.80	466.60	61.524	w 236.00
20.9	21.1	36.05	469.25	62.733	w 233.50
20.9	21.2	38.75	461.65	58.620	w 255.00
20.9	21.4	39.30	467.40	56.798	w 278.25
21.0	21.5	38.95	466.65	54.360	w 302.75
21.1	21.6	39.20	461.60	51.767	w 326.50
21.1	21.8	39.10	463.25	50.387	w 347.50
21.1	22.5	76.05	926.35	98.181	w 368.00
21.1	22.7	79.10	913.65	91.741	w 405.75
21.1	22.8	78.80	923.25	90.944	w 424.25
21.1	23.0	79.05	914.00	87.972	w 442.75
21.0	23.5	76.60	917.05	83.875	w 495.00
21.1	23.6	79.90	919.15	80.631	w 534.75
20.9	23.6	78.35	915.25	77.291	46.20
20.9	23.7	79.25	917.50	76.871	46.80

w: pressure difference in millimetres of water

READINGS FOR PLATE NO. 55

orifice diameter ..... 74.41 mm.
plate eccentricity ..... 5.00 mm.
area ratio 0.550
Atmospheric Pressure ..... 761.20 mm Hg.

TABLE NO. 52

Readings for the calibration of the test orifice plate

Air temp. deg. C	Water temp. deg. C	Init. mass kg.	Final mass kg.	Time seconds	Press. dif. mm. Hg.
20.7	23.6	36.70	471.05	158.965	w 34.50
20.9	23.6	39.30	469.95	127.032	w 52.75
20.9	23.6	37.15	465.30	105.845	w 76.50
20.9	21.7	36.30	463.95	90.347	w 105.50
21.0	21.9	39.70	471.95	83.075	w 127.25
21.0	22.0	39.85	459.80	73.322	w 155.25
21.0	22.3	39.75	461.85	67.112	w 185.75
21.2	22.7	36.85	466.15	63.946	w 213.00
21.1	22.9	39.90	463.60	58.996	w 244.00
21.3	23.0	39.85	463.40	54.425	w 287.50
21.5	23.1	39.80	453.30	51.714	w 302.50
21.6	23.2	39.85	451.30	49.228	w 331.25
21.7	23.3	39.80	452.90	47.603	w 355.00
21.3	23.3	39.75	453.70	46.145	w 381.25
21.3	23.4	39.80	447.70	44.120	w 407.50
21.3	23.5	39.60	446.75	42.858	w 426.50
21.3	23.6	79.65	913.95	85.654	w 452.50
20.9	23.9	76.30	894.60	80.244	w 492.75
20.9	24.0	79.80	888.95	74.487	44.55
20.9	24.0	79.70	878.15	70.908	48.00
20.8	24.0	75.30	896.40	70.744	50.70
20.8	24.0	78.60	918.85	71.501	52.25
20.9	24.1	78.10	889.05	68.571	52.55
21.1	24.1	78.55	890.30	68.550	52.95

w: pressure difference in millimetres of water

READINGS FOR PLATE NO. 55

orifice diameter ..... 74.41 mm.
plate eccentricity ..... 7.25 mm.
area ratio 0.55
Atmospheric Pressure ..... 757.65 mm Hg.

TABLE NO. 53

Readings for the calibration of the test orifice plate

Air temp. deg. C	Water temp. deg. C	Init. mass kg.	Final mass kg.	Time seconds	Press. dif. mm. Hg.
22.7	22.4	38.50	467.45	155.808	w 33.50
22.9	22.6	39.85	472.50	127.430	w 51.75
22.7	23.2	39.80	474.85	108.152	w 72.75
22.8	23.3	39.45	470.00	91.764	w 98.50
22.9	23.6	39.50	471.80	82.931	w 121.50
22.8	23.7	39.70	472.75	74.717	w 150.50
23.0	23.9	39.80	465.60	67.818	w 178.50
22.3	24.0	39.70	464.50	62.140	w 211.75
23.3	24.2	39.80	460.35	57.924	w 241.00
23.2	24.3	39.55	461.50	54.880	w 270.25
23.5	25.4	39.45	461.05	52.626	w 295.00
23.5	25.4	39.80	462.25	50.449	w 318.50
23.8	26.1	38.65	464.30	48.992	w 343.25
23.8	26.1	39.25	467.15	47.509	w 371.50
23.6	26.2	39.50	463.05	45.476	w 396.25
23.4	26.2	39.50	453.75	43.389	w 417.75
23.5	26.2	78.75	921.30	85.114	w 447.75
23.5	26.2	78.95	905.70	82.751	w 459.50
23.2	26.2	80.00	915.80	76.735	43.15
23.0	26.2	78.85	904.15	73.456	46.05
22.9	26.2	79.20	894.10	70.677	48.25
21.4	23.9	79.40	900.35	69.067	51.20
21.7	23.7	79.75	898.05	68.437	52.25
21.2	23.6	76.40	891.20	68.043	52.65

w: pressure difference in millimetres of water

READINGS FOR PLATE NO. 55

orifice diameter ..... 74.41 mm.
plate eccentricity ..... 12.13 mm.
area ratio 0.550
Atmospheric Pressure ..... 759.30 mm Hg.

TABLE NO.54

Readings for the calibration of the test orifice plate

Air temp. deg. C	Water temp. deg. C	Init. mass kg.	Final mass kg.	Time seconds	Press. dif. mm. Hg.
20.1	23.2	36.00	473.35	166.313	w 29.50
20.2	23.3	39.85	475.50	124.851	w 52.50
20.5	23.3	37.30	473.90	108.308	w 69.50
20.5	23.3	39.35	473.30	92.709	w 93.75
20.6	23.3	38.70	472.60	81.959	w 119.75
20.7	23.3	39.10	471.65	74.215	w 147.00
20.6	23.3	37.50	467.05	67.378	w 174.75
20.6	23.3	38.70	469.10	62.735	w 202.75
20.6	23.2	39.00	463.95	58.121	w 230.25
20.6	23.2	39.20	462.90	54.780	w 258.50
20.6	23.2	39.10	463.15	52.077	w 286.75
20.6	23.2	39.30	465.55	50.318	w 309.75
20.6	23.2	39.60	460.90	47.764	w 336.50
20.6	23.2	39.30	460.45	46.202	w 358.25
20.6	23.2	39.30	457.40	44.357	w 384.25
20.6	23.1	39.50	457.05	43.129	w 403.75
20.6	23.1	79.05	916.75	84.528	w 423.25
20.5	23.1	79.40	909.45	82.096	w 441.00
20.0	23.5	76.95	920.80	82.218	36.15
20.2	23.6	79.15	915.90	78.396	39.15
19.7	23.7	78.60	916.95	76.208	41.65
20.1	23.7	75.70	913.70	74.864	43.00
20.0	23.7	75.75	910.70	73.958	43.55
19.9	23.7	77.90	912.90	73.799	44.00

w: pressure difference in millimetres of water

READINGS FOR PLATE NO. 55

orifice diameter ..... 74.41 mm.

area ratio 0.550

Atmospheric Pressure ..... 754.60 mm.

TABLE NO. 55

Tests for repeatability of a reading

Air temp. deg.C	Water temp. deg. C	Init. mass kg.	Final mass kg.	Time seconds	Press. dif. mm. Hg.
21.6	23.6	39.85	477.05	134.057	w 52.50
21.7	23.8	40.80	478.20	126.539	w 59.00
21.7	23.9	40.75	476.90	107.867	w 81.25
21.7	23.9	39.35	476.10	93.615	w 108.00
21.8	24.0	40.30	475.00	82.990	w 136.75
21.7	24.1	38.90	475.30	75.087	w 168.25
21.6	24.1	40.30	473.80	68.361	w 200.50
21.6	24.2	39.75	469.05	62.772	w 233.75
21.6	24.3	36.85	468.95	59.831	w 260.75
21.7	24.3	40.20	469.70	56.131	w 292.75
21.7	24.3	40.20	456.20	51.737	w 324.00
21.6	24.3	40.20	472.55	51.544	w 351.25
21.7	24.3	40.30	470.05	49.293	w 380.25
21.6	24.3	40.30	461.05	46.592	w 407.90
21.7	24.4	40.35	470.45	46.273	w 431.50
21.7	24.3	40.25	464.00	44.325	w 457.75
21.7	24.2	78.95	911.30	85.172	w 478.50
21.7	24.8	76.55	935.70	86.043	w 499.50
21.7	24.8	79.75	934.80	82.294	w 540.75
21.7	24.9	79.30	910.75	76.795	46.55
22.0	25.0	80.10	926.80	75.258	50.30
22.1	25.0	80.05	933.20	73.992	52.80
22.1	25.0	80.50	924.90	72.194	54.50
22.1	25.0	80.05	918.45	71.226	55.25

w: pressure difference in millimetres of water

READINGS FOR PLATE NO. 55

orifice diameter ..... 74.41 mm.

area ratio 0.550

Atmospheric Pressure ..... 755.60 mm Hg.

TABLE NO. 56

Tests for repeatability of a reading

Air temp. deg. C	Water temp. deg. C	Init. mass kg.	Final mass kg.	Time seconds	Press. dif. mm. Hg.
21.6	23.4	36.40	475.55	169.986	w 33.00
21.6	23.5	39.60	472.70	155.573	w 38.25
21.8	23.6	40.35	478.00	126.758	w 59.25
21.9	23.6	40.30	477.65	107.822	w 81.50
22.0	23.7	40.30	480.10	94.417	w 107.75
22.2	23.8	40.30	476.40	83.316	w 136.50
22.2	23.8	40.30	467.80	73.553	w 168.75
22.2	23.9	40.20	475.00	68.951	w 198.25
22.2	24.0	40.40	468.80	63.029	w 230.50
22.2	24.0	40.30	473.75	59.844	w 261.75
22.2	24.0	40.20	470.15	55.949	w 294.75
22.3	24.1	40.30	472.70	53.664	w 324.00
22.3	24.1	40.30	467.80	50.857	w 352.75
22.3	24.2	39.50	462.65	48.363	w 382.75
22.4	24.5	37.00	463.00	47.151	w 408.50
22.5	24.5	40.30	467.70	45.924	w 432.25
22.5	24.6	80.60	924.65	88.162	w 459.00
22.7	24.8	80.60	929.50	85.924	w 488.00
22.7	24.8	80.35	929.20	82.220	w 532.75
22.7	25.0	80.10	931.60	78.423	46.80
22.7	25.0	79.90	921.00	75.089	49.80
22.7	25.2	77.35	920.95	73.224	52.95
22.7	25.3	80.10	928.55	72.471	54.50
22.7	25.3	76.95	919.25	70.816	56.10

w: pressure difference in millimetres of water

READINGS FOR PLATE NO. 55

orifice diameter ..... 74.41 mm.

area ratio 0.550

Atmospheric Pressure ..... 756.10 mm Hg.

TABLE NO. 57

Tests for repeatability of a reading

Air temp. deg. C	Water temp. deg. C	Init. mass kg.	Final mass kg.	Time seconds	Press. dif. mm. Hg.
22.7	25.6	36.80	479.40	172.509	w 32.50
22.7	25.6	40.15	479.10	138.743	w 49.50
22.7	25.6	40.30	479.65	126.904	w 59.50
22.7	25.6	39.80	475.35	108.143	w 80.75
22.7	25.6	39.80	472.60	93.059	w 107.75
22.7	25.6	39.80	478.80	84.116	w 135.75
22.7	25.6	39.25	470.60	72.749	w 174.75
22.7	25.6	40.15	471.10	67.856	w 200.75
22.7	25.6	39.80	466.10	62.345	w 233.50
22.5	23.4	36.50	476.25	60.567	w 262.50
22.5	24.5	40.00	468.40	55.873	w 293.75
22.5	23.6	40.20	475.00	53.883	w 324.25
22.6	23.7	40.10	472.50	51.269	w 354.75
22.6	23.8	40.10	468.60	48.971	w 382.25
22.6	23.8	40.15	467.60	47.259	w 408.50
22.6	24.2	37.15	465.70	46.019	w 433.25
22.6	24.3	80.15	935.00	87.259	w 479.25
22.7	24.3	80.05	924.30	82.610	w 522.50
22.4	24.4	80.70	925.50	80.710	w 548.75
22.7	24.4	81.55	912.15	75.564	48.00
22.7	24.6	41.20	459.10	37.035	50.70
22.7	24.8	82.55	910.95	71.743	53.20
22.7	25.2	78.10	911.25	70.988	54.75
22.8	25.4	82.55	920.05	70.985	55.30

w: pressure difference in millimetres of water

APPENDIX F

ERROR ANALYSIS OF THE FLOW MEASUREMENT WITH THE EXPERIMENTAL EQUIPMENT

1. MEASUREMENT WITH THE REFERENCE METER

Mass flow rate $q = \frac{\text{Mass of the water accumulated in the tank}}{\text{Time taken}}$

$$\therefore \quad q = \frac{M_{FINAL} - M_{INITIAL}}{\text{Time}}$$

and
$$W_q = \left[\left(\frac{\delta q}{M} W_M\right)^2 + \left(\frac{\delta q}{T} W_T\right)^2\right]^{\frac{1}{2}}$$

$$\frac{\delta Q}{\delta M} = \frac{1}{T} \quad \text{and} \quad \frac{\delta q}{\delta T} = \frac{M}{T^2}$$

where W_q is the uncertainty in the mass flow rate
W_M is the UNCERTAINTY IN THE MASS OF THE WATER
W_T is the uncertainty in the time taken

At maximum flow rate the final mass minus the initial mass was 430 kg on the average and the uncertainty in the measurement was +/- 0,5 kg. The time taken was 29 seconds and the uncertainty in the time measurement was 0,01 seconds. The high uncertainty in the measurement of the water was due to spilage.

$$\therefore \quad W_q = \left[\left(\frac{0,5}{29}\right)^2 + \left(\frac{430 \times 0,01}{29 \times 29}\right)^2\right]^{\frac{1}{2}}$$

$$= \quad +/- \quad 0,0180 \text{kg/s}$$

$$\therefore \quad q = 14,8276 +/- 0,0180 \text{ kg/s}$$

or $q = \underline{14,8276 +/- 0,12\%}$

At low flow rates the mass of water added to the tank on the average was 430kg and the uncertainty in the measurement was +/- 0,2kg. The time taken for this mass of water to accumulate was 280 seconds and the uncertainty in the time measurement was +/- 0,01 seconds.

$$\therefore \quad W_q = \left[\left(\frac{0,2}{280} \right)^2 + \left(\frac{430 \times 0,01}{280 \times 280} \right)^2 \right]^{\frac{1}{2}}$$

$$= \quad 0,0007 \text{ kg/s}$$

$$\therefore \quad q = \quad 1,5357 \text{ +/- } 0,0007 \text{ kg/s}$$

$$\text{or} \quad q = \quad 1,5357 \text{ +/- } 0,05\%$$

2. MEASUREMENT WITH THE ORIFICE PLATE

Uncertainty in the calculated flow rate can be calculated by using equation 1.

$$W_{q_c} = \left[\left(\frac{2Wd}{1 - m^2} \right)^2 + \left(\frac{2m^2 W_D}{1 - m^2} \right)^2 + \left(\tfrac{1}{2} W\rho_w \right)^2 + \left(\tfrac{1}{2} W_h \right)^2 \right]^{\frac{1}{2}} \quad \ldots\ldots\ldots\ldots \quad 1$$

Equation 1 is derived in British Standard, BS 1042:1964 on page 72 and 73.

For example, the measurements taken and the tolerances on them for an orifice plate with area ratio of 0,15 are given below:

orifice diameter, d = 38,93 +/- 0,025 mm
pipe diameter, D = 100,51 +/- 0,025 mm
pressure differential, h = 500 +/- 0,05mm Hg
density of the water ρ_w = 999,19 +/- 0,04 kg/m^3
area ratio, m = 0,15

The uncertainty in the calculated flow rate is calculated as shown in Table 58. At high flow rate for the orifice plate with area ratio of 0,15 the overall tolerance on the flow rate measurement is +/- 0,129% and the accuracy of the measurement is +/- 0,062%.

Similar calculations have yielded the following results:

AREA RATIO	PRESSURE DIFFERENCE in mm Hg	ACCURACY	OVERALL TOLERANCE
0,15	27	+/- 0,113%	+/- 0,167%
0,55	21	+/- 0,50%	+/- 0,58%
0,55	40	+/- 0,08%	+/- 0.18%

Similarly, the uncertainty in any of the measurements can be calculated.

3. THE TOLERANCE ON THE COEFFICIENT OF DISCHARGE C_D

The coefficient of discharge C_D = $\frac{\text{Measured Mass Flow Rate}}{\text{Calculated Mass Flow Rate}}$

$$\therefore \quad C_D = \frac{q_m}{q_c}$$

$$\therefore \quad W_{C_D} = \left[\left(\frac{\delta C_D}{\delta q_m} \; W q_m \right)^2 + \left(\frac{\delta C_D}{\delta q_c} \; W_{q_c} \right)^2 \right]^{\frac{1}{2}}$$

$$\therefore \quad W_{C_D} = \left[\left(\frac{W_{q_m}}{Q_c} \right)^2 + \left(\frac{Q_m \times W_{q_c}}{Q_c^2} \right)^2 \right]^{\frac{1}{2}}$$

Example $\quad m = 0,1 \qquad h = 52,30 \pm 0,05$ mm Hg

$$W_{C_D} = \left[\frac{0,0007}{2,8173}^2 + \frac{1,6975 \times 0,0002}{(2,8173)^2}^2 \right]^{\frac{1}{2}}$$

$$W_{C_D} = \pm 0,0005$$

$$\therefore C_D = 0,6025 \pm 0,0005$$

$$C_D = 0,6025 \pm 0,08\%$$

Similar calculations were conducted to determine the greatest uncertainty in the coefficient. It was found that the overall tolerance on the coefficient should not exceed $\pm$ 0,1 percent. Only when very low pressure difference (below 30mm of mercury) did the tolerance on the coefficient exceed $\pm$ 0,1 percent In these cases the water manometer was used to measure the pressure difference.

TABLE NO. 58

CALCULATION OF THE UNCERTAINTY IN THE CALCULATED FLOWRATE. AREA RATIO OF ORIFICE PLATE IS 0.15

Factor involved	Symbol	Percentage tolerance on factor				% Tolerance on flow		
		Symbol	Random error	Systematic error	Total	Effect	Accuracy	Total
Orifice diameter	d	ω_d	0.05	0.03	0.058	$\frac{2\omega_d}{1 - m^2}$	0.061	0.119
Pipe diameter	D	ω_D	0.05	0.025	0.056	$\frac{2m^2\omega_D}{1 - m^2}$	0.001	0.003
Pressure difference	h	ω_h	0.01	0.01	0.014	$\frac{1}{2}\omega_h$	0.005	0.007
Density of water	ρ_ω	ω_{ρ_w}	0.004	0.004	0.004	$\frac{1}{2}\omega_{\rho_w}$	0.002	0.004
Density of Hg	ρ_m	ω_{ρ_m}	-	-	-	-	-	-
							± 0.062	± 0.129

APPENDIX G

CALIBRATION TABLES

TABLE NO. 59

DENSITY OF THE MERCURY

Temp. °C	0.0	0.1	0.2	0.3	0.4	0.5	0.6	0.7	0.8	0.9
9.0	13.573	13.573	13.573	13.572	13.572	13.572	13.572	13.571	13.571	13.571
10.0	13.571	13.570	13.570	13.570	13.570	13.569	13.569	13.569	13.569	13.568
11.0	13.568	13.568	13.568	13.567	13.567	13.567	13.567	13.566	13.566	13.566
12.0	13.566	13.565	13.565	13.565	13.565	13.564	13.564	13.564	13.564	13.563
13.0	13.563	13.563	13.563	13.562	13.562	13.562	13.562	13.561	13.561	13.561
14.0	13.561	13.560	13.560	13.560	13.560	13.559	13.559	13.559	13.559	13.558
15.0	13.558	13.558	13.558	13.557	13.557	13.557	13.557	13.556	13.556	13.556
16.0	13.556	13.556	13.555	13.555	13.555	13.554	13.554	13.554	13.554	13.553
17.0	13.553	13.553	13.553	13.552	13.552	13.552	13.552	13.551	13.551	13.551
18.0	13.551	13.550	13.550	13.550	13.550	13.550	13.549	13.549	13.549	13.549
19.0	13.549	13.548	13.548	13.548	13.548	13.548	13.547	13.547	13.547	13.547
20.0	13.546	13.546	13.546	13.546	13.545	13.545	13.545	13.545	13.544	13.544
21.0	13.544	13.544	13.543	13.543	13.543	13.543	13.542	13.542	13.542	13.542
22.0	13.541	13.541	13.541	13.541	13.541	13.540	13.540	13.540	13.539	13.539
23.0	13.539	13.539	13.538	13.538	13.538	13.538	13.537	13.537	13.537	13.537
24.0	13.436	13.536	13.536	13.536	13.535	13.535	13.535	13.535	13.534	13.534
25.0	13.534	13.534	13.533	13.533	13.533	13.533	13.532	13.532	13.532	13.532

NOTE: The density of the mercury in table 59 is in g/cm^3

TABLE NO. 60

DENSITY OF THE AIR

Temp. °C	0.0	0.1	0.2	0.3	0.4	0.5	0.6	0.7	0.8	0.9
9.0	1.250	1.250	1.249	1.249	1.248	1.248	1.247	1.247	1.247	1.246
10.0	1.246	1.245	1.245	1.244	1.244	1.244	1.243	1.243	1.242	1.242
11.0	1.241	1.241	1.241	1.240	1.240	1.239	1.239	1.238	1.238	1.238
12.0	1.237	1.237	1.236	1.236	1.235	1.235	1.235	1.234	1.234	1.233
13.0	1.233	1.232	1.232	1.232	1.231	1.231	1.230	1.230	1.229	1.229
14.0	1.229	1.228	1.228	1.227	1.227	1.226	1.226	1.226	1.225	1.225
15.0	1.224	1.224	1.223	1.223	1.223	1.222	1.222	1.221	1.221	1.220
16.0	1.220	1.220	1.219	1.219	1.218	1.218	1.217	1.217	1.217	1.216
17.0	1.216	1.215	1.215	1.214	1.214	1.214	1.213	1.213	1.212	1.212
18.0	1.211	1.211	1.211	1.210	1.210	1.209	1.209	1.208	1.208	1.208
19.0	1.207	1.207	1.206	1.206	1.205	1.205	1.205	1.204	1.204	1.203
20.0	1.203	1.202	1.202	1.202	1.201	1.201	1.200	1.200	1.199	1.199
21.0	1.199	1.198	1.198	1.197	1.197	1.197	1.196	1.196	1.195	1.195
22.0	1.194	1.194	1.194	1.193	1.193	1.192	1.192	1.191	1.191	1.191
23.0	1.190	1.190	1.189	1.189	1.188	1.188	1.188	1.187	1.187	1.186
24.0	1.186	1.185	1.185	1.185	1.185	1.184	1.184	1.183	1.182	1.182
25.0	11.82	1.181	1.181	1.180	1.180	1.179	1.179	1.179	1.178	1.178

NOTE: DENSITY IN kg/m^3 at a pressure of 760 millimetres of mercury.

TABLE NO. 61

VISCOSITY OF THE WATER

Temp. °C	0.0	0.1	0.2	0.3	0.4	0.5	0.6	0.7	0.8	0.9
9.0	1.3508	1.3455	1.3407	1.3359	1.3311	1.3263	1.3214	1.3166	1.3118	1.3070
10.0	1.3022	1.2992	1.2962	1.2932	1.2902	1.2872	1.2842	1.2812	1.2782	1.2752
11.0	1.2722	1.2692	1.2662	1.2632	1.2602	1.2572	1.2542	1.2511	1.2481	1.2451
12.0	1.2421	1,2391	1.2361	1.2331	1.2301	1.2271	1.2241	1.2211	1.2181	1.2151
13.0	1.2121	1.2091	1.2061	1.2031	1.2001	1.1971	1.1941	1.1911	1.1881	1.1851
14.0	1.1821	1.1791	1.1761	1.1731	1.1701	1.1671	1.1641	1.1611	1.1581	1.1551
15.0	1.1521	1.1490	1.1460	1.1430	1.1400	1.1370	1.1340	1.1310	1.1280	1.1250
16.0	1.1220	1.1190	1.1160	1.1130	1.1100	1.1070	1.1040	1.1010	1.0980	1.0950
17.0	1.0920	1.0890	1.0860	1.0830	1.0800	1.0770	1.0740	1.0710	1.0680	1.0650
18.0	1.0620	1.0590	1.0560	1.0530	1.0500	1.0470	1.0440	1.0410	1.0380	1.0350
19.0	1.0319	1.0289	1.0259	1.0229	1.0199	1.0169	1.0139	1.0109	1.0079	1.0049
20.0	1.0019	0.9999	0.9979	0.9958	0.9938	0.9918	0.9898	0.9878	0.9857	0.9837
21.0	0.9817	0.9797	0.9777	0.9756	0.9736	0.9716	0.9696	0.9676	0.9655	0.9635
22.0	0.9614	0.9594	0.9574	0.9553	0.9533	0.9513	0.9493	0.9473	0.9452	0.9432
23.0	0.9411	0.9391	0.9371	0.9350	0.9330	0.9310	0.9290	0.9270	0.9249	0.9229
24.0	0.9209	0.9188	0.9169	0.9148	0.9128	0.9108	0.9088	0.9068	0.9047	0.9027
25.0	0.9007	0.8987	0.8967	0.8946	0.8926	0.806	0.8886	0.8866	0.8845	0.8825

NOTE: They dynamic viscosity in table is in centipoise

TABLE NO. 62

READINGS TO DETERMINE THE PIPE DIAMETER D

Upstream from orifice plate	Downstram from orifice plate
Diameter of pipe in inches	Diameter of pipe in inches
3.966	3.958
3.970	3.953
3.971	3.952
3.963	3.940
3.977	3.957
3.970	3.970
3.955	3.946
3.973	3.957
3.978	3.954
3.973	3.959
3.936	
3.933	
3.943	
3.952	
3.933	
3.949	
Average 3.959	Average 3.955

Pipe diameter, D = 3.957 inches

The pipe diameter is therefore 100.51 mm.→

TABLE NO. 63

CALIBRATION OF THE THERMOMETERS

Temp. on standard thermometer	Thermometer A	Thermometer B	Thermometer C	Thermometer D
20.7 °C	20.6	20.6	20.8	20.9
23.1 °C	23.0	23.1	23.2	23.3
25.1 °C	25.1	25.1	25.2	25.3
28.4 °C	28.3	28.3	28.5	28.5
30.9 °C	30.8	30.8	30.9	31.1
32.5 °C	32.3	32.4	32.5	32.7

At a temperature of	Correction factor for Thermometer A	Thermometer B	Thermometer C	Thermometer D
21.7 °C	- 0.1	- 0.1	+ 0.1	+ 0.2
23.1 °C	- 0.1	0.0	+ 0.1	+ 0.2
25.1 °C	0.0	0.0	+ 0.1	+ 0.2
28.4 °C	- 0.1	- 0.1	+ 0.1	+ 0.1
30.9 °C	- 0.1	- 0.1	0.0	+ 0.2
32.5 °C	- 0.2	- 0.1	0.0	+ 0.2

APPENDIX H

RESULTS

TABLE NO. 64

RESULTS OBTAINED FROM EXPERIMENTAL DATA FOR VARYING THE EDGE SHARPNESS OF AN ORIFICE PLATE

Area Ratio	Edge radius in millimetres	Coefficient of discharge at a Reynolds Number of		
		100 000	150 000	200 000
0,0985	0,018	0,6009	0,5996	0,5996
	0,065	0,6072	0,6069	0,6065
	0,100	0,6090	0,6084	0,6090
	0,227	0,6201	0,6186	0,6173
	0,293	0,6231	0,6213	0,6209
	0,403	0,6302	0,6293	0,6283
0,1982	0,012	0,6057	0,6034	0,6027
	0,216	0,6167	0,6154	0,6135
	0,403	0,6288	0,6252	0,6236
0,2952	0,012	0,6108	0,6089	0,6081
	0,028	0,6120	0,6104	0,6090
	0,100	0,6188	0,6147	0,6124
	0,185	0,6223	0,6195	0,6169
	0,240	0,6247	0,6221	0,6194
	0,322	0,6275	0,6258	0,6237
0,3929	0,012	0,6165	0,6103	0,6079
	0,153	0,6246	0,6210	0,6183
	0,219	0,6286	0,6259	0,6224
	0,380	0,6388	0,6351	0,6313
0,4990	0,014	0,6132	0,6111	0,6111
	0,147	0,6215	0,6202	0,6201
	0,261	0,6277	0,6258	0,6261
	0,320	0,6312	0,6299	0,6295
	0,489	0,6406	0,6396	0,6393

TABLE NO. 65

RESULTS OBTAINED FROM EXPERIMENTAL DATA FOR VARYING THE ECCENTRICITY OF AN ORIFICE PLATE

Area ratio	Eccentricity in millimetres	Coefficient of discharge at a Reynolds Number of		
		100 000	150 000	200 000
0.1500	0.00	0.6073	0.6051	0.6044
	0.05	0.6080	0.6054	0.6046
	0.15	0.6072	0.6052	0.6046
	0.30	0.6086	0.6059	0.6051
	0.60	0.6087	0.6058	0.6049
	1.20	0.6092	0.6063	0.6050
	5.00	0.6105	0.6082	0.6073
	10.00	0.6170	0.6152	0.6140
0.45	0.00	0.6158	0.6149	0.6127
	3.50	0.6278	0.6205	0.6197
	8.00	0.6356	0.6345	0.6334
	13.00	0.6481	0.6469	0.6463
	16.31	0.6576	0.6567	0.6546
0.55	0.00	0.6168	0.6147	0.6137
	2.00	0.6216	0.6208	0.6177
	5.00	0.6333	0.6314	0.6307
	7.25	0.6478	0.6441	0.6423
	12.13	0.6630	0.6616	0.6615

FIGURE NO. 96

THE EFFECT OF ROUNDING THE UPSTREAM EDGE OF AN ORIFICE PLATE WITH AN AREA RATIO OF 0.0865 PLACED IN A SMOOTH P.V.C. LINE

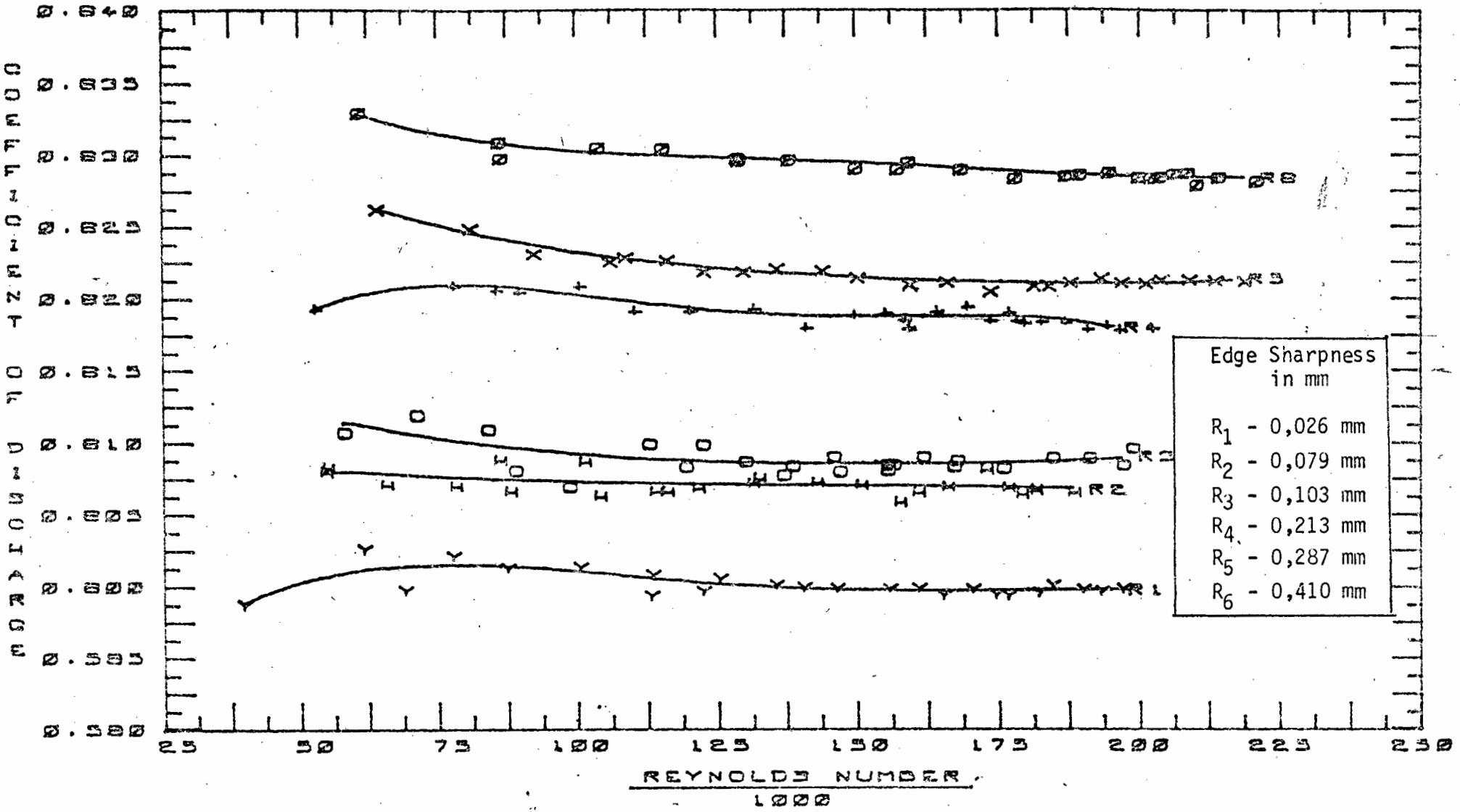

FIGURE NO 97

THE EFFECT OF ROUNDING THE UPSTREAM EDGE OF AN ORIFICE PLATE WITH AN AREA RATIO OF 0,198 PLACED IN A SMOOTH P.V.C. PIPE

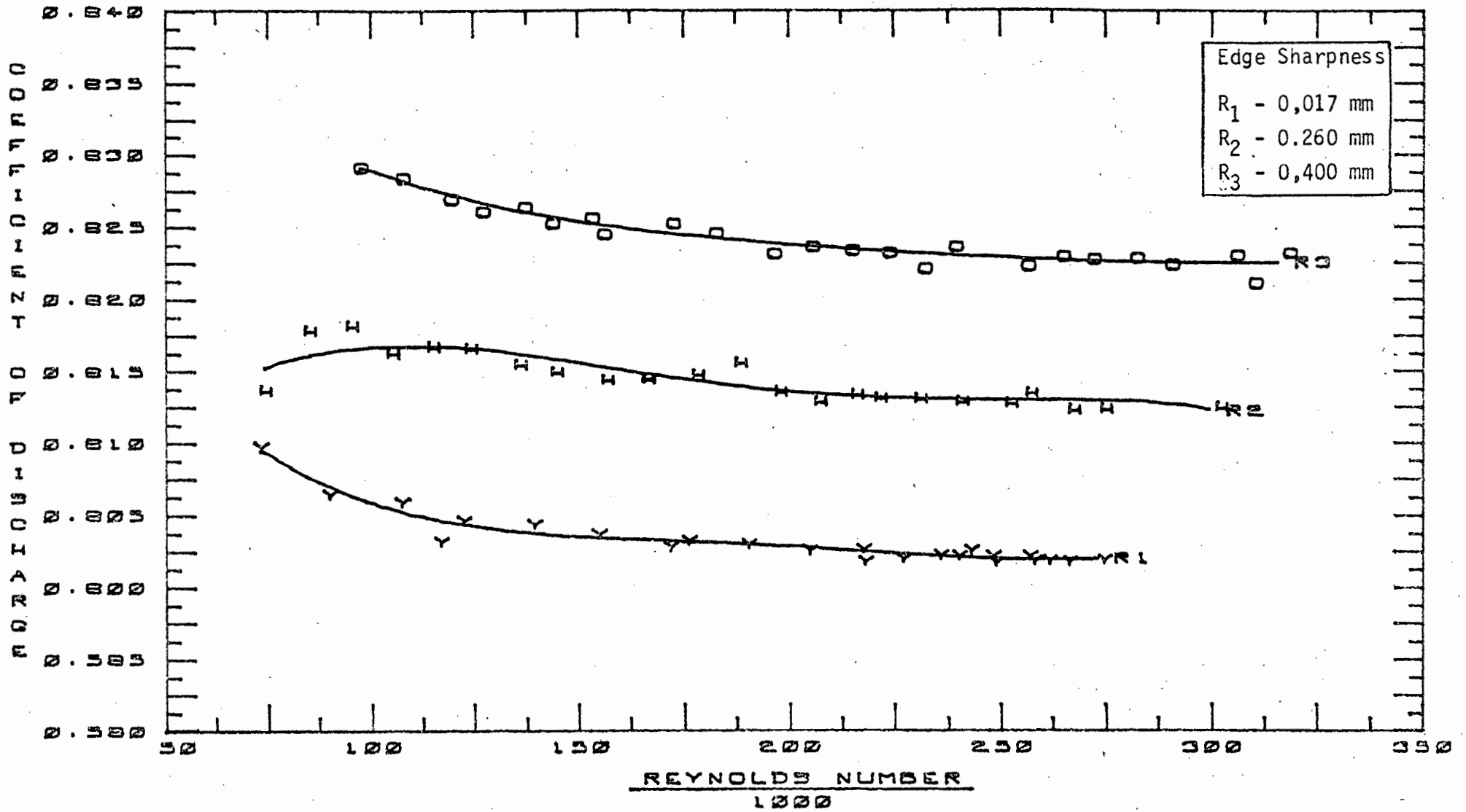

FIGURE NO. 98

THE EFFECT OF ROUNDING THE UPSTREAM EDGE OF AN ORIFICE PLATE WITH AN AREA RATIO OF 0,295 PLACED IN A SMOOTH P.V.C. PIPE

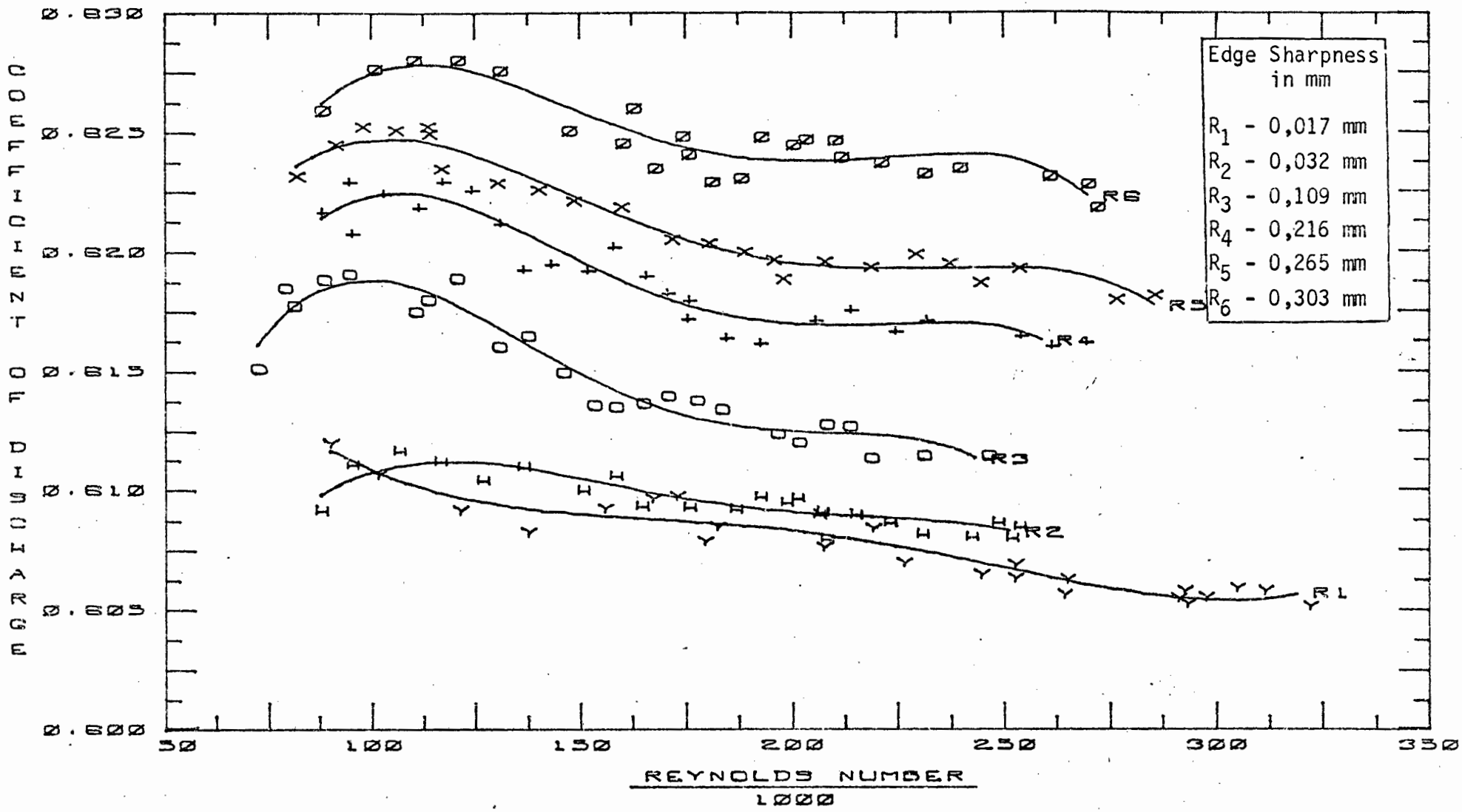

FIGURE NO. 99

THE EFFECT OF ROUNDING THE UPSTREAM EDGE OF AN ORIFICE PLATE WITH AN AREA RATIO OF 0,392 PLACED IN A SMOOTH P.V.C. PIPE

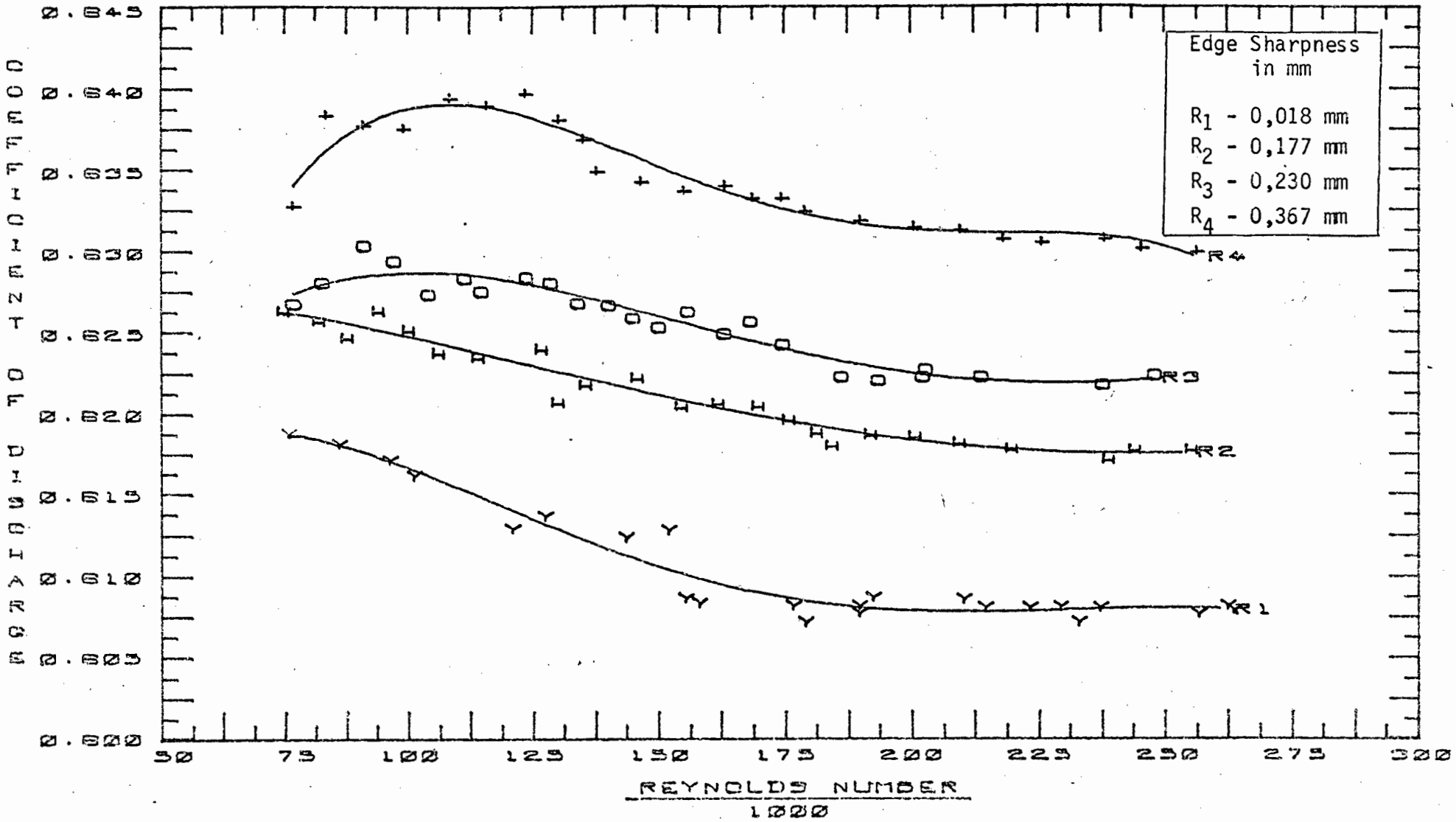

FIGURE NO. 100

THE EFFECT OF ROUNDING THE UPSTREAM EDGE OF AN ORIFICE PLATE WITH AN AREA RATIO OF 0,499 PLACED IN A SMOOTH P.V.C. PIPE